THE DESIGN AND TESTING OF A CONSTRAINED PROXIMAL HUMERAL TOTAL SHOULDER REPLACEMENT (TSR)

Gregory D. Wessels

A dissertation submitted to the Department of Mechanical Engineering, University of Cape Town, in fulfillment of the requirements for the degree of Master of Science in Engineering

Cape Town, November 2005

Abstract

Orthopedic oncology provides for a challenging field in prosthetic design, especially in proximal humeral sarcoma cases. In these cases a large volume of bone and muscle is removed as a result of the sarcoma. This leaves insufficient musculature to stabilize an un-constrained prosthesis. This report deals with the design and testing of constrained total shoulder replacements, as their inherent built-in stability compensates for lost musculature stability.

The weakest area of any shoulder replacement is the fixation of the glenoid component to the scapula. The design of an innovative glenoid attachment system was a main focus of the project. A total of three glenoid attachments were designed. The other focus was to design and analyze the link which constrains the humeral and glenoid components. This was done experimentally and analytically using finite element analysis (FEA).

The humeral fixation design has been kept standard as clinical results have shown this to be adequate, the only addition being the incorporation of modularity into the humeral neck.

Declaration

I know the meaning of plagiarism and declare that all of the work in the document, save for that which is properly acknowledged, is my own.

I have used the Harvard citation convention. Each significant contribution to, and quotation in, this thesis from the work, or works, of others has been cited and referenced.

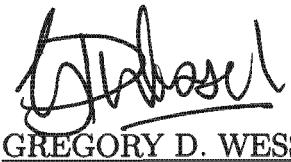

GREGORY D. WESSELS

NOVEMBER 2005

Acknowledgements

I want to thank Glen Newins and Len Watkins for their advice when it came to manufacture and designing around manufacture.

To Dr. Keith Hosking, Dr. Basil Verretos and Dr. Steve Roach all practicing at *Vincent Pallotti Hospital*, Cape Town, South Africa, thank you for your input and the opportunity to sit in on surgery. A highlight of this project has been the pleasure of interacting with you during your busy schedule.

To Prof. Launa Martin at the *University of Cape Town Forensic Pathology Department*, your help and advice in acquiring ethics approval for the use of human scapula was phenomenal.

To Dr. George Vicatos at the *University of Cape Towns Mechanical Engineering Department*, thank you for your help and I wish you all the best with *ISIQU Orthopedics*.

To Steven Rhodes, Nicholas Gordon and Karanja Kibicho, thank you for integrating me into to the Mechanical Engineering Department. I would also like to thank Steve Marais for helping me with the layout of this document.

To the most important people in my life, my family and the lady I spend as much time with as humanly possible, Mary Haw. I want to thank you for your support and patience at times when I have been highly frustrated.

Lastly to my granddad Empty Wessels, thank you for spurring my interest in the sciences and letting me know that I can still learn at 93. Your never ending enthusiasm is always a joy.

Contents

Abstract i

Declaration iii

Acknowledgements v

Contents ix

Glossary xv

Notations xix

1 Introduction 1
- 1.1 Problem Definition . . . 1
  - 1.1.1 A Typical Cancer Case . . . 2
  - 1.1.2 Design Factors . . . 3
- 1.2 Design Approach . . . 5
- 1.3 Testing Approach . . . 6

2 Literature Review 7
- 2.1 The Shoulder Joint . . . 7
  - 2.1.1 The Effects of Cancer on the Shoulder . . . 10
  - 2.1.2 Properties of Bone . . . 12
- 2.2 Classification of Shoulder Replacements . . . 13
- 2.3 Existing Constrained TSR . . . 14
- 2.4 Current Orthopedic Innovation . . . 21
  - 2.4.1 Modularity . . . 22
  - 2.4.2 Constrained Articulation . . . 23
  - 2.4.3 Fixation . . . 23
  - 2.4.4 Implant Material . . . 25
- 2.5 Standard Implant Materials . . . 26
  - 2.5.1 Titanium (Ti-6Al-4V) . . . 26

2.5.2 Cobalt Chrome Molybdenum (Co-Cr-Mo) 27
2.5.3 Ultra High Molecular Weight Polyethylene 27
2.5.4 Polymethyl Metacrylate (PMMA) Bone Cement 28
2.6 Implant Failure Modes 29
2.7 Summary 30

3 Specifications **33**

4 Final Designs **39**
4.1 Design Similarities 40
4.1.1 Ball-in-Socket System 40
4.1.2 Humeral Fixation System 41
4.1.3 Modularity 43
4.2 Quad-Point TSR 43
4.3 Hybrid-Screw TSR 45
4.4 Central-Peg TSR 49
4.5 Summary 49

5 Discussion **51**
5.1 Design Similarities 51
5.1.1 Ball-in-Socket System 51
5.1.2 Humeral Fixation System 55
5.1.3 Modularity 56
5.2 Quad-Point TSR 57
5.3 Hybrid-Screw TSR 59
5.4 Central-Peg TSR 61
5.5 Summary 62

6 Conclusions **63**
6.1 Glenoid Fixation 63
6.2 Ball-in-Socket System 63
6.3 Humeral Fixation 64

7 Recommendations **65**

8 Future Work **67**
8.1 Testing Glenoid Fixation 67
8.2 Operating Tooling 69

References **70**

Bibliography **75**

A Ball Neck Strength Calculations **A1**
A.1 Introduction A1
A.2 Method A2
A.3 Results A2
A.4 Conclusion A4

B Press-Fit Socket Report **B1**
B.1 Introduction B2
B.2 Method B3
B.2.1 Interference Fit Calculations B4
B.2.2 FEA Model B5
B.2.3 Experimental Model B6
B.3 Results B8
B.3.1 FEA Results B9
B.3.2 Experimental Results B9
B.3.3 Comparison of Results B11
B.4 Discussion B14
B.5 Conclusions B16

C Constrained Socket Report **C1**
C.1 Introduction C2
C.2 Method C3
C.2.1 Tensile Dislocation Models C3
C.2.2 Moment Dislocation Model C6
C.3 Results C7
C.4 Conclusions and Recommendations C11

D Supporting Information **D1**
D.1 Letter of Ethics Approval D2
D.2 Delta Brochure D4
D.3 Biomet Mosaic Brochure D29
D.4 Biomet Bi-Polar Brochure D35
D.5 Synthesis LCP Brochure D37
D.6 Sawbones Catalogue D39
D.7 ASTM Cortical Screw Standards D43
D.8 Material Properties D47

E Drawings **E1**
E.1 Equipment E1
E.2 Full Designs E2

List of Figures

2.1 Internal bone structure of the scapula. 8
2.2 Glenoid variability. 9
2.3 Classification of shoulder resections 11
2.4 Biopsy of the proximal humerus. 12
2.5 The three classes of shoulder replacement. 13
2.6 The first TSR by Péan in 1893. 15
2.7 Existing Constrained Total Shoulder Replacements. 16
2.8 Bickel TSR and the Liverpool TSR 17
2.9 Floating-Socket TSR. 18
2.10 The Kessel and Bayley-Walker® TSR 19
2.11 Kölbel TSR 20
2.12 The *Biomet* Mosaic^{TM} 22
2.13 The *Biomet* Bi-Polar non-constrained shoulder replacement . . 23
2.14 Showing the Delta® by *Depuy* glenoid fixation. 24
2.15 Locking compression plate (LCP) 25
2.16 Delta® failure 30

3.1 The Quad-Point TSR (a), Hybrid-Screw TSR (b) and Central-Peg TSR (c) design side views. 34

4.1 Socket assembly, *ISIQU Orthopedics*. 40
4.2 Range of motion (ROM) of the ball-in-socket. 41
4.3 Humeral fixation according to *ISIQU orthopedics*. 42
4.4 Modular humeral extension system according to *ISIQU orthopedics*. 42
4.5 The Quad-Point TSR assembly. 44
4.6 Quad-Point TSR glenoid fixation. 44
4.7 The Hybrid-Screw TSR assembly. 46
4.8 Hybrid-Screw TSR glenoid fixation. 46
4.9 The Bayley-Walker® glenoid component 47
4.10 The Central-Peg TSR assembly. 48

4.11 Central-Peg TSR glenoid fixation. 48
4.12 The difference in glenoid fixation plates. 49

8.1 Scapula fixation test rig 68

A.1 Ball and stem representations A3
A.2 Shear, moment, and deflection of beams A3
A.3 3D ABAQUS neck test model. A4

B.1 Cross section of the ball, socket and housing. B3
B.2 Press-fit socket dimensions. B4
B.3 The FEA modeling set-up. B5
B.4 Zwick compression cradle. B6
B.5 The Zwick test set-up. B7
B.6 Socket FEA results B10
B.7 Displacement vs. reaction force on the ball. B11
B.8 Reaction force for both FEA and experimental results. B12
B.9 Comparison of break out force and push in force B13
B.10 Point of ball dislocation B14
B.11 The reaction force experienced on the FEA rigid ball. B15

C.1 Axisymmetric model at the start of the simulation. C2
C.2 *In vivo* temperature effects C4
C.3 Modeling of the locking clip C5
C.4 Axisymmetric temperature model with no stress C6
C.5 Plastic yielding in tension C8
C.6 Location of Node C and maximum deformation C8
C.7 3D tensile model C9
C.8 3D moment model showing pivoting C9
C.9 Point at which plastic yielding will take place in bending . . . C10

List of Tables

2.1 The development of constrained TSR from 1893 to 2005 . . . 14

3.1 Design specifications 35

A.1 Results A4

B.1 FEA dislocation forces B8

C.1 FEA models generated. C4
C.2 Material properties. C6

Glossary

ABAQUS	finite element analysis (FEA) software
alloy	a mixture of two or more metals
arthroplasty	a surgical operation to make a movable joint
ASTM	American Society for Testing and Materials
atrophy	wasting away of tissues or organs
axillary	anatomy relating to the armpit
bioengineering	the application of engineering principles to the solution of biomedical problems
biopsy	a sample of tissue removed from the body for testing
cancellous bone	the spongy tissue of bone where trabeculae form the latticework that is surrounded by connective tissue or bone marrow
CE marking	European Union quality certification marking
Co-Cr-Mo	a cobalt alloy containing chrome and molybdenum
cortical bone	compact hard bone
CT	Computer tomography
CTSR	Constrained total shoulder replacement
Dacron®	polyester fiber
distal	furthest from the center or medial line; opposed to proximal
elastic modulus	a material property proportional to the ratio of the stress (load) required to produce a given strain (elongation)
fatigue failure	fracture that occurs as a result of cyclic or repeated loading of a device. Failure begins as a small crack on the surface and progresses through the material until the cross-sectional area is too small to sustain the load
FDA	the United States of America Food and Drug Administration
FEA	Finite element analysis

fretting corrosion	corrosion at a point where repeated rubbing of two metallic surfaces wears away the passive oxide layer
galvanic corrosion	corrosion resulting from an electrical (galvanic) cell, usually due to electrical contact between two dissimilar metals
glenohumeral joint	the shoulder joint
glenoid cavity	a shallow depression on the scapula receiving a projection from the humerus to form the shoulder joint
HA	hydroxyapatite
humerus	the bone of the upper arm
isotropic	having similar properties in all directions
in situ	in position
in vitro	in the laboratory (literally, "in glass")
in vivo	in the living body
LCP	Locking Compression Plate
medial	near the middle or center line
medulla	central or inner part of an organ
medullary	related to the marrow or the medulla
MRI	nuclear Magnetic Resonance Imaging
necrosis	death of cells or tissue
orthopedics	medical field concerned with the skeletal system
osteoarthritis	a degenerative joint disease, characterized by softening of the articular ends of bones and thickening of joints
PH	Proximal Humerus
PHS	Proximal Humeral Sarcoma
PMMA	Polymethyl Metacrylate
proximal	nearest the trunk or point of origin, opposed to distal
resection	the cutting out of tissue
resorption	the dissolution or removal of a substance
rheumatoid arthritis	chronic and progressive inflammation of the connective tissue of joints, leading to deformation and disability
ROM	Range of Motion
sarcoma	cancerous tumor
scapula	shoulder blade
sepsis	the presence of a pathological organisms, causing pus in tissue
synergistic	the cooperative action between two phenomena
tendon	a band or cord of fibrous tissue connecting muscle to bone

Ti-6Al-4V	a medical grade titanium alloy containing vanadium and aluminium
trabecula	a supporting band or bar of connective bone tissue
TSR	Total Shoulder Replacement
UCT	University of Cape Town
UHMWPE	Ultra High Molecular Weight Polyethylene
Wolff's law	the principle relating the internal structure and architecture of bone to external mechanical stimuli

Notations

E Young's Modulus
α Coefficient of thermal expansion
ν Possions Ratio
σ_p Proof stress
ρ Density

Chapter 1

Introduction

The evolution of shoulder replacements has been dramatic and a major breakthrough was reported by Neer in 1955 (Zadeh and Calvert, 1998), with the use of the first anatomical shoulder replacement. It is now widely accepted that in most patients the anatomical joint replacement is by far the best solution. The indications for the use of an anatomical joint system are in patients where the rotator cuff and deltoid muscle groups are still intact. This is, however, not the case when a patient suffers from a proximal humeral sarcoma (PHS); in most instances the rotator cuff is resected and if the axillary nerve is affected by the cancer, it will also be resected, rendering the deltoid non-functional. This leaves the surgeon in a particulary difficult situation. Twenty years ago many of the patients with a PHS would have lost their upper limb and even now amputation is still a very real possibility.

1.1 Problem Definition

Without the rotator cuff or deltoid, an anatomical joint has little or no stability. The only solution is to have an inherent stability built into the prosthesis and a constrained device is produced. The constrained joint replacement leads to forces being transmitted through the glenoid fixation and in many

instances results in failure of the constrained joint replacement. Thus designing a constrained total shoulder replacement is not an easy task as there are many design limitations to consider. To understand how some of these limitations are generated, a cancer case will be studied, from the first signs of a tumour all the way through to surgery.

1.1.1 A Typical Cancer Case

A lump on the proximal humerus (PH) is the first indication of a possible cancerous tumour. The lump is then biopsied and subjected to pathological examination to determine whether it is benign or malignant.

In this typical cancer case we have assumed that the patient has an aggressive tumour which requires immediate attention. The first step in treatment is to stop the growth of the tumour with chemotherapy or other means. This can take many weeks. The next step is to perform a joint replacement and this would be carried out by an orthopedic surgeon specializing in oncology. The extent of the tumour would be mapped using MRI or CT scans and from this information, a decision would be made to either order a custom prosthesis or to use a stock modular system.

Firstly, the surgery involves the isolation of the tumour and the first layer of musculature surrounding the tumour, including the skin around the biopsy. This is a lengthy and difficult process as it is vital that the surgeon does not pierce the sack of tissue surrounding the tumour as this would result in the cancerous cells spreading throughout the vascular system. In isolating the cancerous tissue, any nerves that are associated with the lump must also be resected and this will result in the paralysis of the muscles they supply. What remains of these muscles will need to be attached to the prosthesis in order to improve the functionality and stability of the joint replacement

Once the tumour has been removed, the usual procedure is to use bone cement for instant fixation of the prosthesis. A concern with uncemented prostheses is that in cancer patients the bone ingrowth required for its long term survival may not be immediately possible. Patients receiving chemotherapy have greatly reduced bone growth for a period after treatment and this compromises fixation. The final surgical procedure is for any remaining muscle to be stitched onto the prosthesis and the joint is then tested and the wound closed.

The patient's joint will tend to have limited active mobility as there is a minimal amount of muscle to produce movement but the patient will have the use of his/her lower arm and hand.

1.1.2 Design Factors

Using the cancer case described in this section, all the important design considerations will be highlighted and an indication of the design route is given.

Built-in-Stability

With little musculature present, a constrained shoulder replacement is the only design option, as it provides the built-in stability that is needed. Together with glenoid fixation these are the most challenging design problems. Designing a compact link between the humerus and scapula components, that provides a large range of motion (ROM) and will not fail, makes up a major part of this report, see Appendix B and C.

Glenoid Fixation

Linking the humerus to the scapula allows for the transfer of load to the glenoid fixation. The scapula provides anchor points for muscle attachments and the resulting bone structure is efficient with little volume and cortical bone. However, this does not provide a good bone structure for glenoid fixation and ultimately becomes the primary failure point of constrained shoulder replacements. The focus of this report is to improve present glenoid fixation used in cancer cases.

Instant Fixation

If instant fixation is achieved using PMMA bone cement. Loosening of the cement bone interface takes place in many cases. Which may be due to various reasons; the design of the implant, surgical technique, limitations in quantity and quality of bone for fixation, tissue reaction to particulate debris, rotator cuff deficiency with glenohumeral instability, and high patient activity levels were proposed as potential causes of loosening (Boyd et al., 1990; Wilde et al., 1984; Barrett et al., 1987; Kelly et al., 1987). To combat this, a design must incorporate components that allow for bone ingrowth. The fixation provided by the bone ingrowth would later supplement the fixation provided by the cement.

Space Constraints

There is little space to work with in designing any shoulder replacement. In cancer cases this problem is heightened, as a varying amount of skin is removed due to the biopsy. The result is less skin available to close the wound and using a skin graft is not ideal, as there is little tissue present to supply the graft with the necessary blood flow. It is thus imperative, the prosthesis

be as compact as possible.

Modular System

When dealing with cancer there are various levels of resection and to accommodate for this variability one must keep the prostheses as modular as possible. In using a modular system it is possible to move away from custom prosthesis. A major benefit of having a modular system is that the manufacturer can produce a high volume of standard components, which in turn reduces the price of the prosthesis.

Ease of Assembly

For a surgeon wearing two layers of rubber gloves the assembly of small components is difficult. In designing a small assembly this must always be kept in mind.

1.2 Design Approach

The design can be approached from three angles; the first being what is available on the market, the second being what do the surgeons want and finally, what has been done in the past. These three sources provided enough information to generate designs.

Glenoid Fixation Design

Three glenoid fixation designs were chosen for review. The final designs are given in Chapter 4 and for all the design drawings see Appendix E.

Constrained Link Design

ISIQU Orthopedics, has designed a constrained link system, which consists of a ball and cup split in two halves, similar to a ball-in-socket joint. This

design was investigate experimentally and analytically using finite element analysis (FEA). Another concept was also tested, however, it was unable to meet many of the specifications, see Appendix B.

1.3 Testing Approach

An outline of the testing is given below and for more detail on possible future experimental work, see Chapter 8.

Constrained Link Testing

Two link concepts were tested rigourously experimentally and analytically using ABAQUS, a FEA package. The results are detailed in Appendix B and C.

Glenoid Fixation Testing

A test rig was designed and built, see Appendix E. Ethics approval was gained from the research ethics committee for the use of cadaveric scapulae, see Appendix D. The cadaveric tests were not carried out as only unclaimed corpses could be used for testing and during a six month period no corpses became available. Synthetic scapulae testing was then planned, but never took place as enough work had been completed on the thesis.

Chapter 2

Literature Review

The scope of the literature review concentrates on constrained total shoulder replacements (CTSR) and the factors that influence their design. The field of CTSR is specialized, as the demand for this class of joint replacement is low and in many cases custom prostheses are implanted. It is assumed that few companies have undertaken the task of developing improved CTSR prostheses due to the small market.

A direct result of a proximal humeral sarcoma is the removal of the cancerous tissue. In the light of this, a short introduction to the shoulder joint is given, which concentrates on structures that may remain after the resection of a tumour. One also needs to understand the design limitations of materials used in orthopedic implants, the design problems that need to be solved and determine why past designs have failed.

2.1 The Shoulder Joint

The glenohumeral joint, also known as the shoulder joint, is made up of a shallow ball and socket. This allows the joint to produce not only rotational motion but also sliding and rolling motion. The combination of the above factors results in a highly mobile joint, stabilized in essence by musculature.

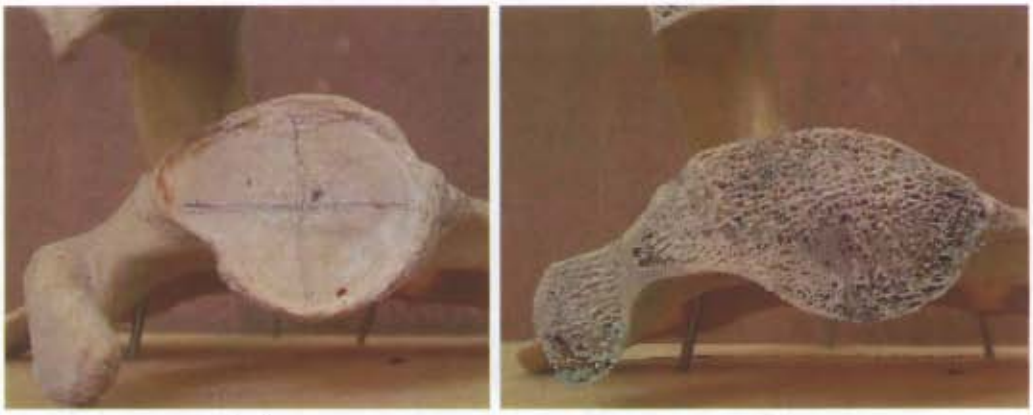

(a) (b)

Figure 2.1: The glenoid (a) and a section taken $5mm$ medial to the glenoid showing the internal bone structure (b).

The main muscles that take up this stabilizing function are the rotator cuff group which consists of four muscles and the deltoid muscle.

The glenohumeral joint links the scapula and humerus. The scapula needs only minimal structure (Fig. 2.1), as applied loads are mainly supported by musculature. This lack of cortical bone is a prosthesis designer's greatest challenge. The humerus on the other hand has good bone stock.

The shoulder generates its mobility from two sources; the glenohumeral and scapulothoracic joints. Scapulohumeral rhythm is defined as the ratio of motion produced by both joints when working synergistically. This is a complex interaction with an overall glenohumeral to scapulothoracic motion ratio of 2:1. A 4:1 ratio is produced in the first 25 degrees of elevation followed by a 5:4 rotation ratio for subsequent elevation (Poppen and Walker, 1976).

When designing around the human body, one of the prominent design issues is variability; the size, shape and quality of a specific bone structure is unique for every individual. This thesis deals with two important structures located

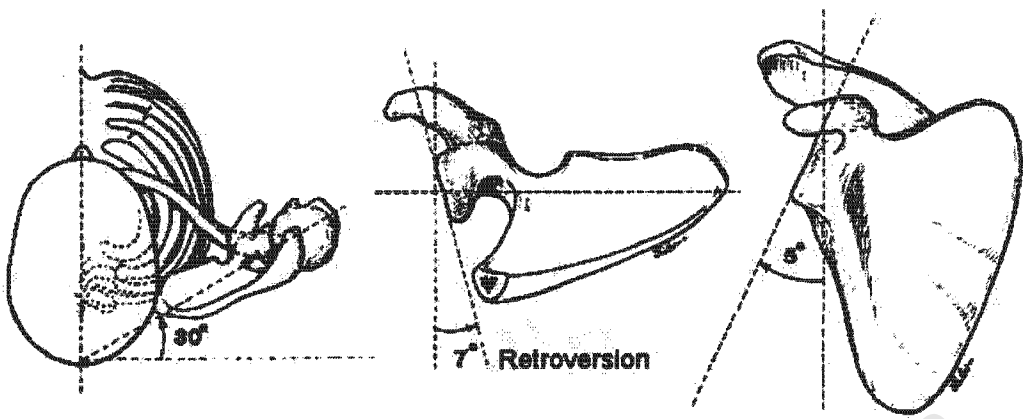

(a) (b) (c)

Figure 2.2: The anatomical location of the scapula on the thorax (a), glenoid version (b) and glenoid inclination(c), www.orthoteers.com.

on the scapula, the glenoid and coracoid process. An extensive study carried out by Churchill et al. (2001), showed the average male glenoid width and height to be 27.8mm and 37.5mm, respectively. The average female glenoid width and height was reported as 23.6mm and 32.6mm, respectively. Glenoid inclination varied from -7 to 15.8 degrees. By convention, a negative number corresponds to an inferiorly directed glenoid and a positive number indicates a superiorly directed glenoid (Fig. 2.2(c)). The range of glenoid version was -9.5 to 10.5 degrees with an average of 1.23 degrees of retroversion (Fig. 2.2(b)). The coracoid process sits at an angle to the vertical axis of the glenoid. No studies on the variability of its location and size were found.

Located on the axillary border of the scapula is a strong strut of bone that runs at an angle down to the base of the scapula. Utilizing this bone stock is important in the design of a CTSR. The shoulder is a complex joint and for a detailed description of the shoulder, Rockwood Jr. and Matsen III (1998a) is recommended.

To give an idea of the standard already set by the human body, McKee (1966) quoted:

> Wear and tear is not a problem with the natural joint. The wear products are readily removed, and the cartilage bearing surface is automatically replaced by the growth of fresh cartilage. The natural joint is also lubricated so efficiently that no artificial bearing surfaces have been designed with a lower coefficient of friction.

This makes for a highly efficient system that may never be replicated by human efforts.

2.1.1 The Effects of Cancer on the Shoulder

A typical cancer case is highlighted in Section 1.1.1. The classification of shoulder resections range from the resection of the proximal humerus to the resection of both the proximal humerus and the scapula (Fig. 2.3). A prosthesis designed for a scapulohumeral resection is not as prone to failure as a CTSR used in proximal humeral resections, as there are no fixation issues with the glenoid. The prostheses given in this report are designed to accommodate proximal humeral resection and possibly extended proximal humeral resections only. A further sub-classification of proximal humeral resections is when the deltoid muscle is preserved (type A) and type B is indicated when the deltoid muscle is resected. If the deltoid is preserved there is the option of using a reverse anatomy TSR, such as the Delta® system manufactured by *Depuy* (Appendix D).

In general, a biopsy (Fig. 2.4) should be carried out by the surgeon performing the resection. In many cases this does not occur and a poor biopsy is carried out resulting in more skin having to be removed during resection to ensure

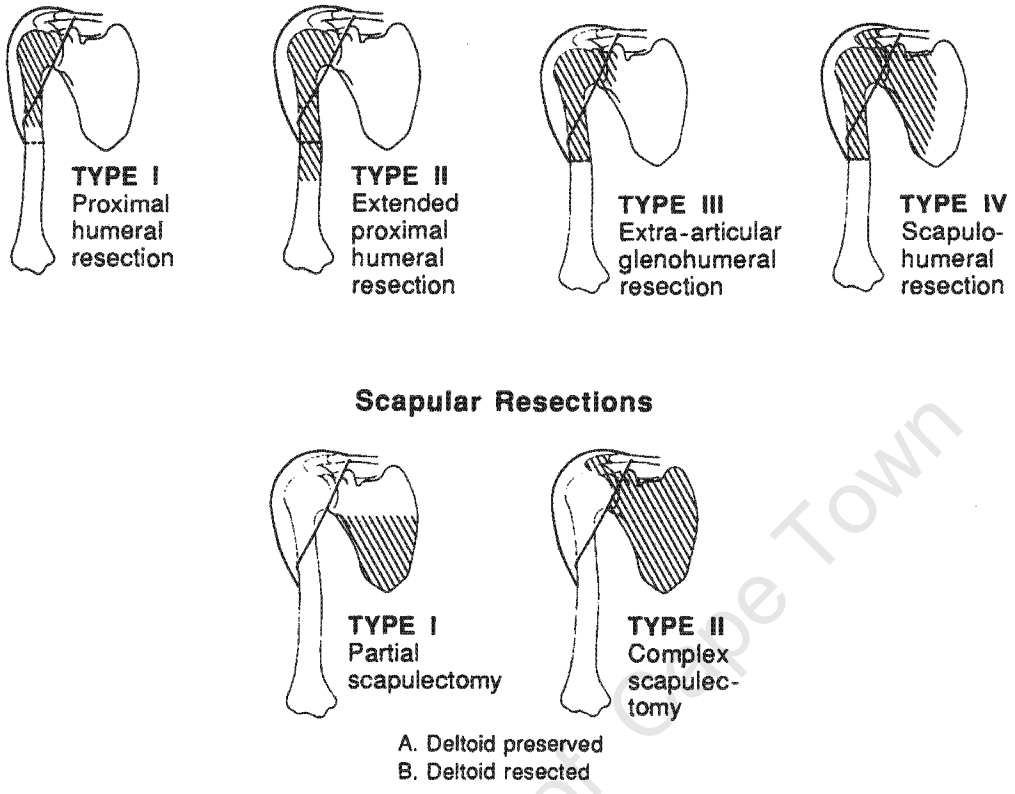

Figure 2.3: Classification of shoulder resections (Rockwood Jr. and Matsen III, 1998b, pg.1157)

that the tumour is contained. These are challenging cases as the surgeon is left with little skin to close the wound.

There are various types of cancerous lesions that effect the proximal humerus. The most severe is a high-grade bone malignancy where both postoperative and preoperative chemotherapy is necessary (Davis et al., 1994). Chemotherapy also effects the bone cells in the area, slowing bone growth which in turn reduces bone strength and the bone's ability to grow onto a prosthesis.

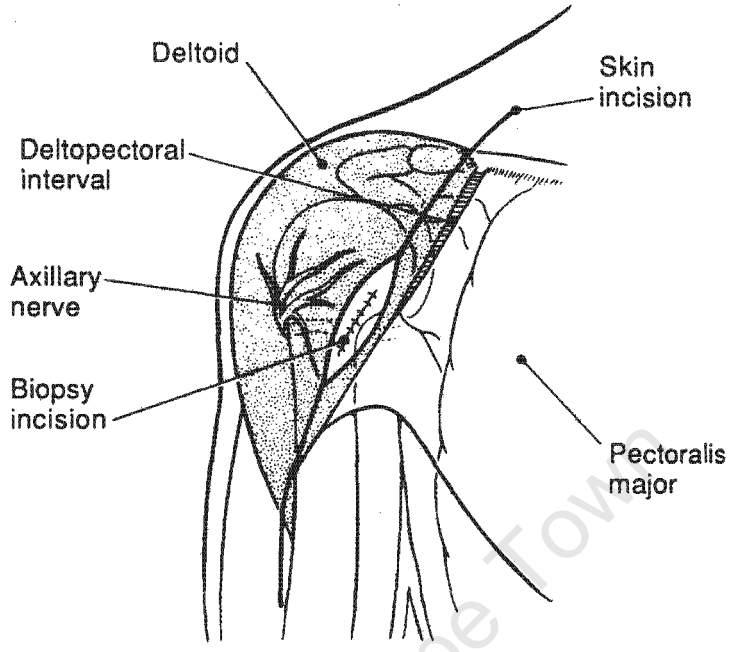

Figure 2.4: Biopsy of the proximal humerus (Rockwood Jr. and Matsen III, 1998b, pg.1152)

2.1.2 Properties of Bone

The only tissues in the body which have truly regenerative ability are epithelium, bone and liver cells (Heughan and Hunt, 1975). This is the positive that bone offers us; the negative side is that bone obeys Wolff's law, which states that *changes in the function of a bone are followed by changes in the internal structure of the bone.* Wolff's law is a major problem in all orthopedic cases where alloys are used; all bio-compatible alloys have high modulus of elasticity relative to bone. In brief, due to the implant's high elastic modulus, it absorbs most of the energy needed to stimulate bone growth. This is known as stress shielding and in addition, bone reabsorption takes place in areas of stress shielding. In many instances the result is a catastrophic failure of the bone-implant interface.

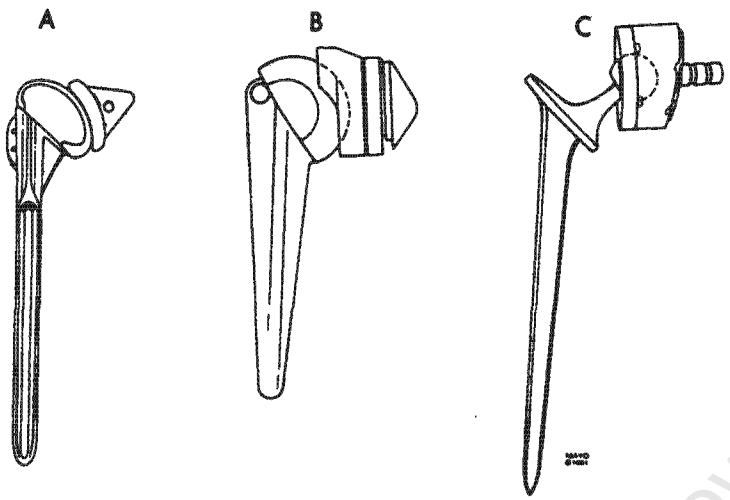

Figure 2.5: The three classes of total shoulder replacement; anatomical (unconstrained) (A), semi-constrained (B) and constrained (C), (Evarts, 1983).

2.2 Classification of Shoulder Replacements

In the past, glenohumeral joint replacement was classified as being either anatomical, semi-constrained or constrained (Fig. 2.5), (Rockwood Jr. and Matsen III, 1998b). There are two prosthetic markets; the custom and the standard production market. From a commercial point of view, only the anatomical and *Depuy's* Delta® reverse anatomy TSR have survived the standard production market.

There are many conditions that affect the glenohumeral joint both directly and indirectly. In the early developments of the 1970s and 1980s, experimentation was the order of the day. The work carried out proved that constrained devices are associated with a higher incidence of failure than unconstrained devices (Cofield, 1983). Constrained devices are not the optimal solution to the more prevalent joint conditions of rheumatoid arthritis and osteoarthritis where the rotator cuff is preserved. Thus for patients with an

intact/functional rotator cuff the unconstrained prosthesis remains the gold standard (Iannotti et al., 1992; Stewart and Kelly, 1997).

In the case of a proximal humeral sarcoma patient, the optimal solution is a sound constrained TSR and for this reason the constrained TSR is examined in detail.

2.3 Existing Constrained Total Shoulder Replacements

Understanding the history of a concept gives a greater insight into how one could improve on past designs and avoid of failed concepts. Table 2.1 shows the development of constrained shoulder replacements over the last 112 years. The only known product on the market today from Table 2.1 is the Bayley-Walker® TSR. A synopsis of the rationale behind each design is given below and when possible, the reasons why a design failed.

Table 2.1: The development of constrained TSR from 1893 to 2005

Prosthesis	Fig.	Date	Prosthesis	Fig.	Date
Péan	Fig. 2.6	1893	Wheble-Skorecki	-	1977
Gerard	-	1973	Floating-Socket	Fig. 2.9	1978
Reeves	-	1974	Kessel	Fig. 2.10(a)	1982
Fenlin	-	1975	Liverpool	Fig. 2.8(b)	1982
Zippel	Fig. 2.7(b)	1975	Trispherical	Fig. 2.7(a)	1982
Bickel	Fig. 2.8(a)	1977	Kölbel	Fig. 2.11	1987
Michael Reese	Fig. 2.7(c)	1977	Bayley-Walker®	Fig. 2.10(b)	1992
Stanmore	-	1977	Zimmer	-	-

Péan TSR 1893

The first shoulder replacement was carried out by Péan in 1893 and also happened to be a constrained TSR (Fig. 2.6). The materials used were plat-

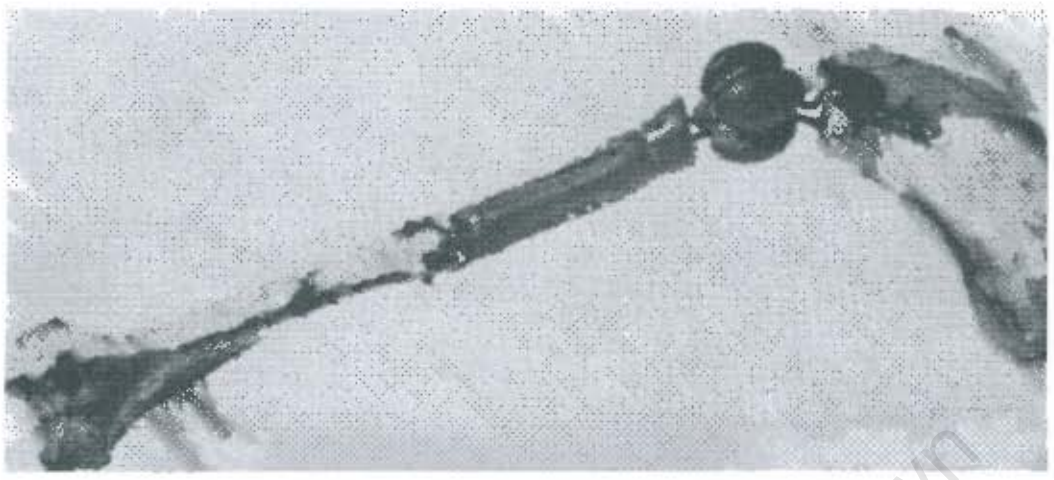

Figure 2.6: The first TSR by Péan in 1893 (Lugli, 1978).

inum and rubber and as a result the prosthesis failed due to an overwhelming tissue reaction.

Fenlin TSR 1975

The reverse ball-in-socket TSR designed by Fenlin has an uncemented wedge driven into the scapula for fixation and a rod placed down the axillary border of the scapula (Fenlin Jr, 1975). The rod appears to be placed within the medullary cavity of the axillary border. A large polyethylene (PE) ball is screwed onto the glenoid fixation and articulates with a metal cup.

Michael Reese TSR 1977

The Michael Reese total shoulder replacement was once the most widely used constrained joint system in North America (Fig. 2.5(c) and 2.7(c)). A dislocation tolerance was introduced into the the system which resulted in a controlled component dislocation to avoid glenoid fracture following trauma. Dislocation would then require open surgery and reassembly of the components. This prosthesis has been abandoned due to the high incidence of complications (Watson, 1990). The poor performance of this prosthesis is

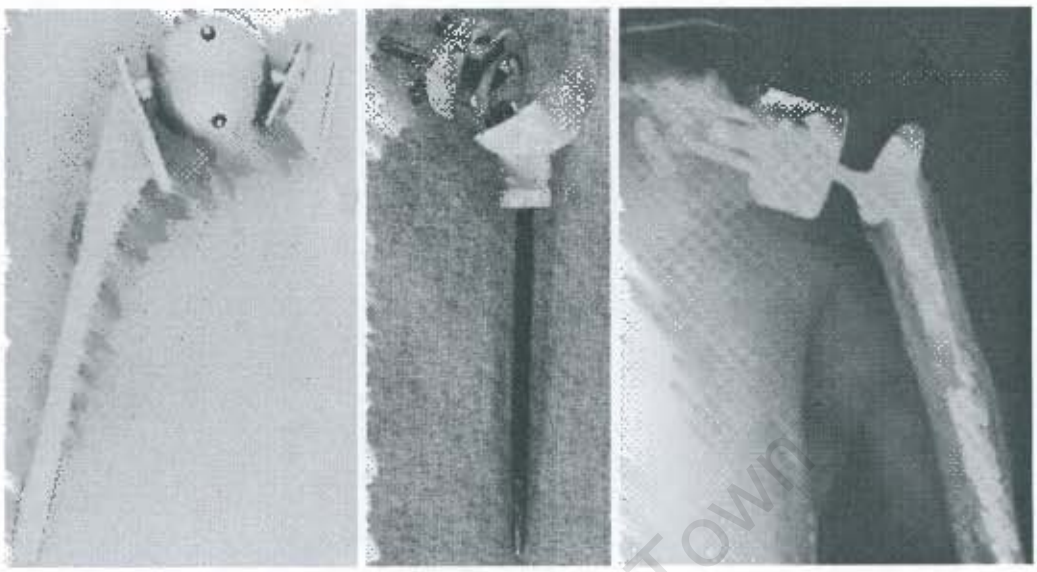

(a) (b) (c)

Figure 2.7: The trispherical TSR is designed around two spheres held captive in a spherical housing (Bayley and Kessel, 1982) (a), the model BME TSR is an early captive ball-in-socket design (Zippel, 1975) (b) and the Michael Reese TSR (Cofield, 1977) (c).

understandable as designing around a controlled dislocation is virtually impossible. As every patient is different, no surgeon can go into an operating theatre guaranteeing the quality of glenoid fixation.

Bickel TSR 1977

Cofield (1977) described the design rationale, stating that a very small ball was used to decrease the friction between components and that the glenoid component was designed to be incorporated entirely within the glenoid cavity. One of the reasons for this was to maximize the prosthesis-bone contact area (Fig. 2.8(a)). The use of a small ball increases the contact load on the PE liner which may result in increased wear. Another negative of this design is that it does not utilize enough of the available bone. The author suspects

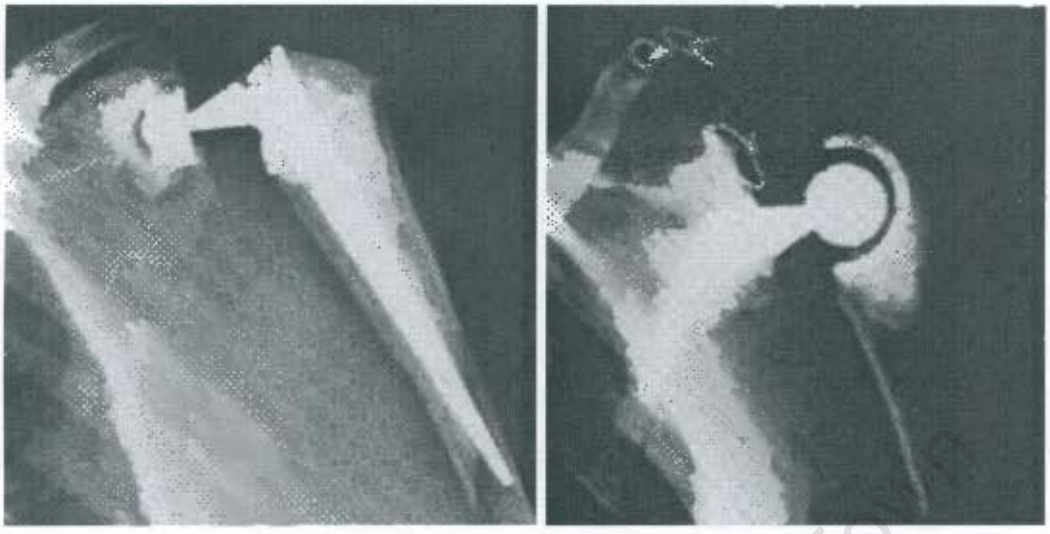

(a) (b)

Figure 2.8: The Bickel TSR (Cofield, 1977) (a) and the Liverpool TSR exhibiting the reverse ball-in-socket design (Bayley and Kessel, 1982) (b).

the design failed due to poor glenoid fixation.

Stanmore TSR 1977

The glenoid component relied solely on a large amount of polymethyl metacrylate (PMMA) for fixation (Cofield, 1977), which is a dangerous situation in the long term, as cement fixation breaks down over time. The components were snapped together after being implanted.

Floating-Socket TSR 1978

This implant contains a dual spherical bearing system (Fig. 2.9), which allows the prosthesis to have a large range of motion (ROM), (Buechel et al., 1978). The design appears to have a low dislocation threshold and no clinical results were given.

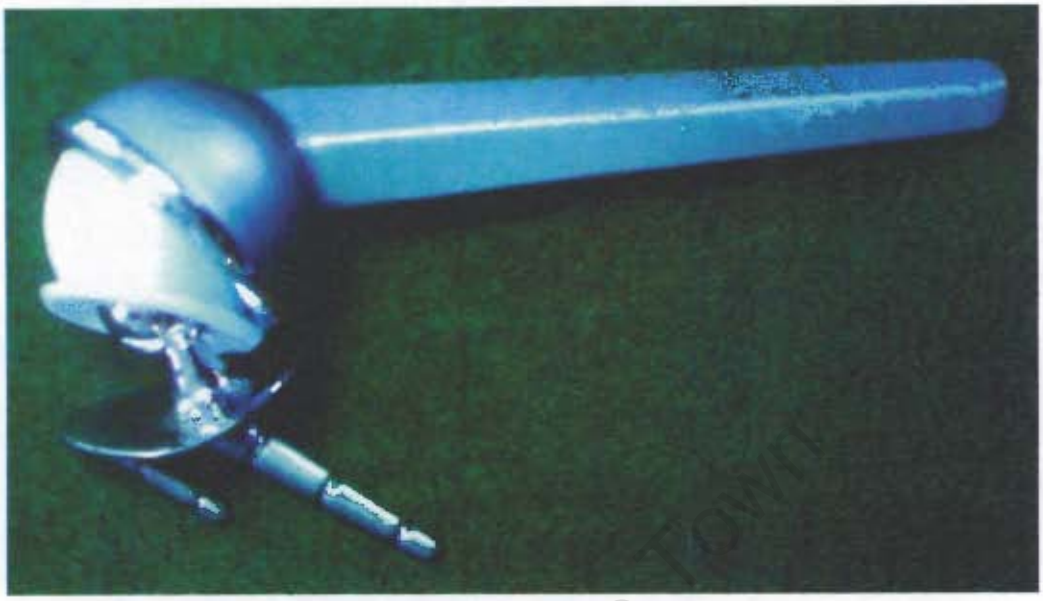

Figure 2.9: Floating-Socket TSR (Bucchel et al., 1978).

Kessel TSR 1982

The design is made up of a large 50mm screw which is first implanted into the glenoid without the use of cement. A polyethylene (PE) stem containing the socket is then cemented into the humeral canal, followed by the ball and socket being snapped together. This is known as a reverse ball-in-socket design (Fig. 2.10(a)). The Kessel prosthesis resulted in a pain-free joint but was associated with a high incidence of loosening (Brostrom et al., 1992). Bayley, in a long term review of the Kessel TSR, observed that in an original group of 31 patients there were four cases of early failure and there was only one further failure after 11 years of mean follow-up time (Zadeh and Calvert, 1998). Whether failure is defined as the need for removal or a loosening of the prosthesis is not stated. There have also been instances of the prosthesis unscrewing, particularly in the right shoulder. In a study done by Post and Haskell (1980), out of the 43 patients in the group, 15 (35%) had to undergo

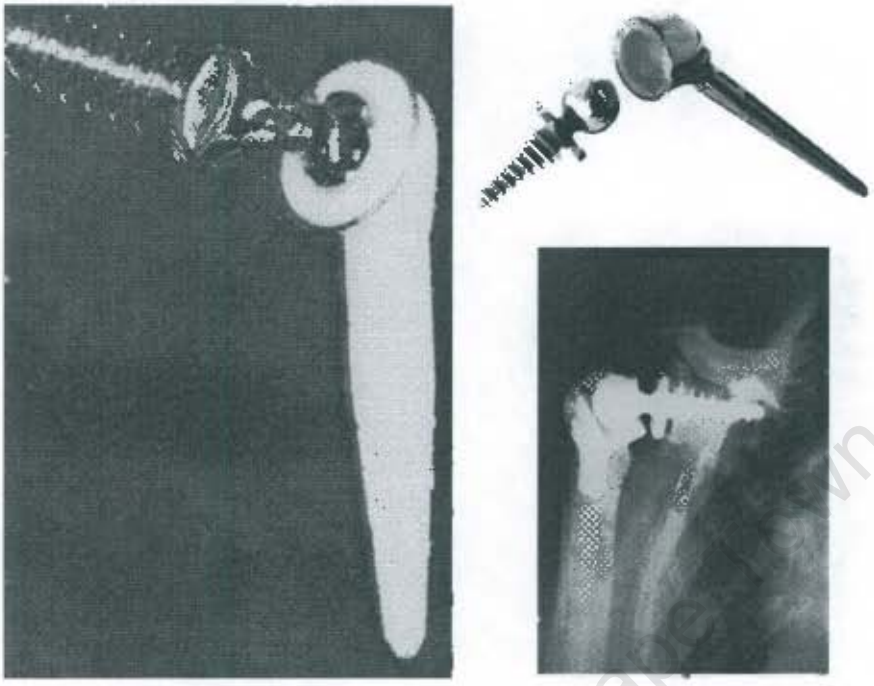

(a) (b)

Figure 2.10: The Kessel TSR is a reverse ball-in-socket design, where the glenoid component is screwed in and the humeral component is cemented in (Bayley and Kessel, 1982) (a), the design was then improved in later years and became known as the Bayley-Walker© TSR (Ahir et al., 2004) (b).

re-operation.

Liverpool TSR 1982

The only glenoid fixation the TA reverse ball-in-socket TSR has, is a stem inserted approximately 50mm down the medullary cavity of the axillary border (Fig. 2.8(b)). No clinical results were found.

Trispherical TSR 1982

Designed by Gristina, this captive system had two spheres free to rotate in a PE lining within a larger sphere, allowing for a greater range of motion (Bayley and Kessel, 1982). Notice the small keel used in the glenoid fixation

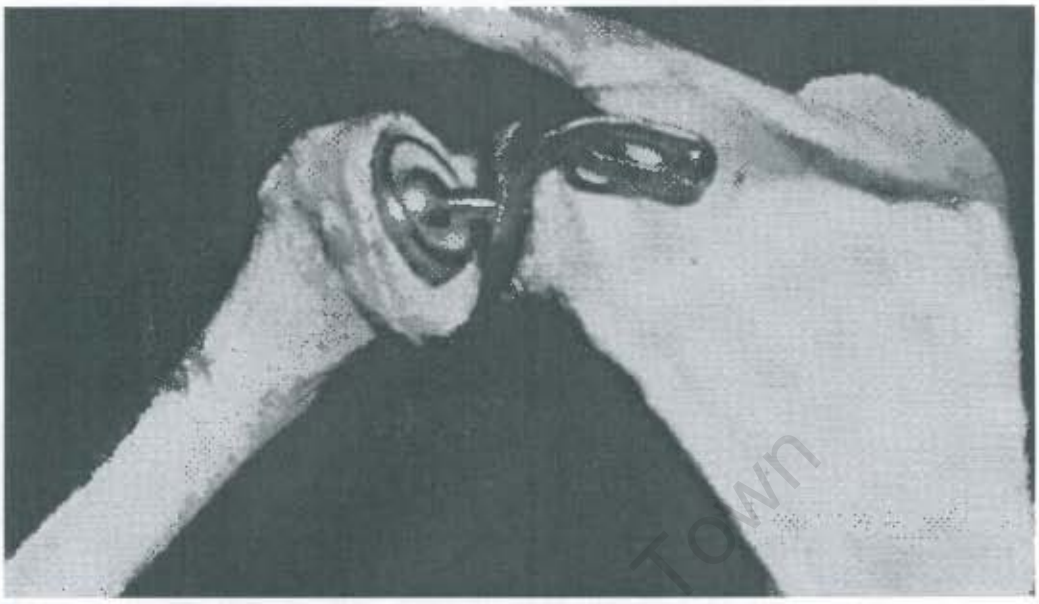

Figure 2.11: Kölbel TSR showing a flange bolted to the base of the scapula spine (Kölbel et al., 1987).

(Fig. 2.7(a)). No Clinical results were found.

Kölbel TSR 1987

Utilizing the reverse ball-in-socket design, Kölbel produced a compact prosthesis with a flange bolted to the base of the scapula's spine (Fig. 2.11), (Kölbel et al., 1987). This appears to be an excellent design, however any shoulder surgeon will ask how one gains access to the area where the screw needs to be inserted without being overly invasive.

Bayley-Walker® TSR 1992

The Bayley-Walker® is an upgraded version of the Kessel TSR and is only supplied to The Royal National Orthopedic Hospital Trust in England (Lane 2005, personal communication). The design consists of a cobalt chrome articulating head with a hydroxyapatite (HA) coated titanium screw inserted without cement (Fig. 2.10(b)). The humeral component has a titanium

stem with a polyethylene-lined socket and is cemented in place (Zadeh and Calvert, 1998). There are problems associated with the Bayley-Walker®, however reports on its clinical performance are conflicting. The majority of the praise comes directly from the designers in a paper they published together with other researchers (ref. Ahir et al., 2004). The reasons the prosthesis is not favoured by surgeons are that there is the possibility of splitting the glenoid and that large amounts of bone stock are removed. The need for less bone stock is a positive in cases of revision surgery where the screw fills the cavity left by the prosthesis. In cases of PIIS, where it is imperative remaining muscle is utilized to promote function, the surgeon requires attachment points on the prosthesis and the Bayley-Walker® does not contain any. In a personal communication with Dr. K. Hosking, his opinion was that the prosthesis does not perform.

The glenoid component utilizes the cortical bone at the vault of the glenoid by using threads which protrude through the anterior surface of the scapula. The reason the component does not utilize cement fixation is it has been shown to produce inadequate fixation of constrained devices (Ahir et al., 2004).

This is a fairly complete listing of important TSR designs used in the past and present. Many of the designs incorporated in developing the TSR in Chapter 4 are referenced to the designs mentioned above.

2.4 Current Orthopedic Innovation

In the vast field of orthopedics one must always be current with new innovations as it may be possible to apply these new concepts to the problem at hand.

An up-to-date look into the areas of modularity, constrained articulation,

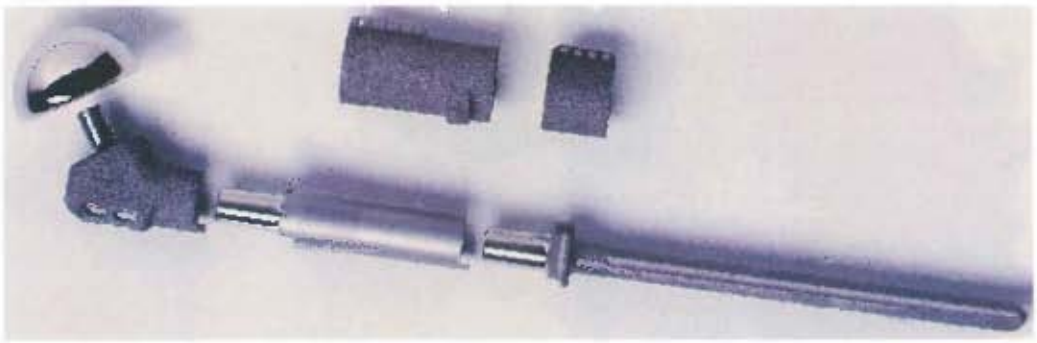

Figure 2.12: The *Biomet* Mosaic^{TM} is a limb salvage prosthesis demonstrating built in modularity.

fixation and materials is carried out in this section. All of these fields are applied to the designs generated in this report, whether directly or indirectly and should always be kept in mind for future work.

2.4.1 Modularity

A taper lock system, used to connect most modular components, is an excellent solution; the simplicity makes it easy for the surgeon to assemble and disassemble components when choosing the correct size. The connection is self locking when it is compression loaded in the axial direction. The system produces minimal surface area for corrosion to take place and there are no stress concentration points generated, unlike screw threads which may suffer from fatigue.

Shown in Fig. 2.12, is the modular system used in the *Biomet* Mosaic^{TM} limb salvage prosthesis. Notice that the two tapers on the stem have mating points where two components interlock to prevent rotation. The system comes with optional collars, which are porous coated to promote increased fixation, which in turn promotes longevity. The collars and suture holes on the proximal body are used to attach any remaining muscle to the prosthesis

(a) (b)

Figure 2.13: The *Biomet* Bi-Polar unconstrained shoulder replacement (a) and the assembly of Bi-Polar system (b).

in order to increase the functionality of the saved limb. See Appendix D for the brochure supplied by *Biomet*.

2.4.2 Constrained Articulation

An effective constrained articulation system, that provides adequate ROM and strength in both tension and bending, remains elusive. The design used in the *Biomet* Bi-Polar shoulder replacement (Fig. 2.13) is a simple yet effective system for low ROM applications. The Bi-Polar axial separation strength is over $750N$ and has a cantilever strength of over $5.1Nm$; the ROM is not given (Appendix D). A similar design was tested in this project, the results can be found in Appendix C.

2.4.3 Fixation

Fixation is the core issue of this project as the loads transferred to the glenoid are high. As a result, loosening occurs followed by failure, or simply catastrophic fracture of the glenoid. A design utilizing a novel fixation system

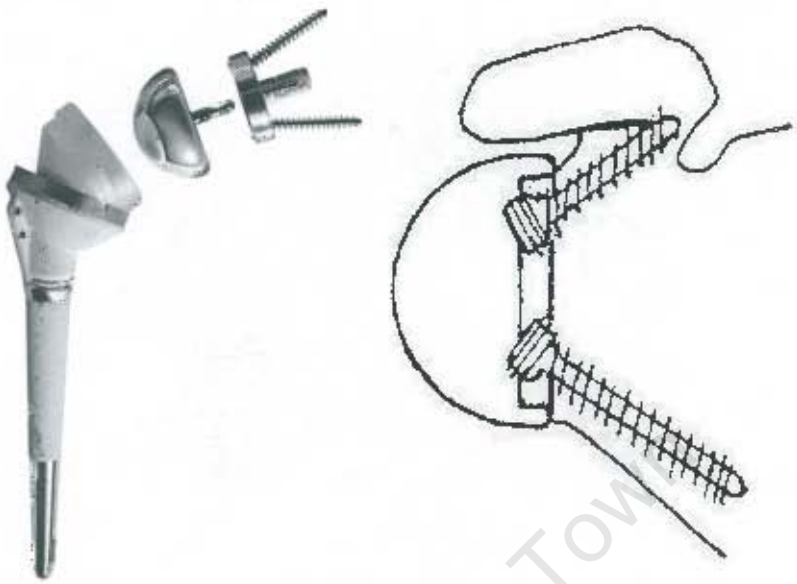

(a) (b)

Figure 2.14: The Delta® (*Depuy International Ltd*) system expanded (a), with locking inferior and superior glenoid screws shown anchoring the reversed ball (b), (Boileau et al., 2005).

with success is the Delta® manufactured by *Depuy* (Fig. 2.14). The original designer (Garmmont) found that he had many failures with cemented glenoid components and decided to generate the un-cemented concept used today. The latest model on the market is the Delta III launched in 1991 (Boileau et al., 2005). The glenoid fixation is made up of a HA coated central stem, surrounded by four cortical screws with the superior and inferior screws being locked in place by thread on the titanium base plate, the angles of which are fixed. There are two shorter cortical screws anterior and posterior of the stem and their insertion angles can vary by 15 degrees. Combined with a mediallized center of rotation this makes for a robust design. Detailed clinical results are given by Boileau et al. (2005).

The locking compression plate (LCP) shown in Fig. 2.15 is a recent development surgeons use to stabilize fractures. The plates and screws form one

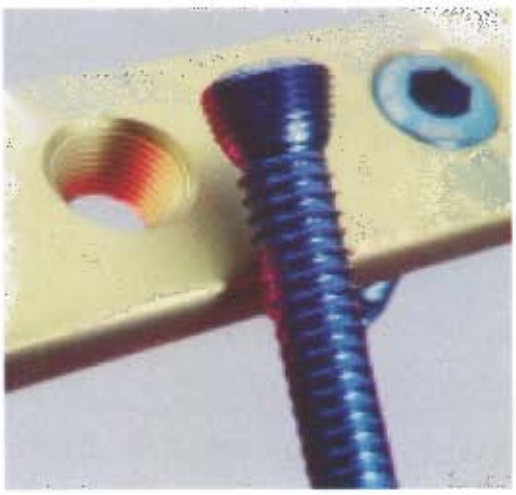

Figure 2.15: Locking compression plate (LCP) with locking screw manufactured by *Synthes*.

stable system and the stability of the fracture is dependent on the stiffness of the construct. Thus LCP's are an improvement on past systems that were not locked together. The tapered thread on the head of the screw allows the screw to lock into the compression plate even though the pitch of the cortical thread is larger than that on the LCP. The taper in essence allows a gradual meshing of the threads (Appendix D).

2.4.4 Implant Material

Implant materials promote the formation of a fibrous capsule around the material separating it from the bone (Collins, 1953). The factors that influence the thickness of the capsule are the chemical reactivity and corrosion of the implant material (Scales et al., 1970) and the size, shape, and mechanical movement of the implant (Wood et al., 1970). Even when using titanium and insuring the component has rounded corners and is rigidly fixed to the bone, a minimal capsule thickness of $1 - 10\mu m$ is produced (Hench and Ethridge, 1982). Creating an interface on which bone can bond has been a

major focal point in research; the latest offerings have been porous coated surfaces using a high temperature plasma spray technique, depositing tiny beads or wire sintered to the surface of the metal.

Hydroxyapatite (HA) coatings have also been used over the last few years, where the surface of the material is coated with this bone reactive substance. HA has been identified as a bone growth factor, stimulating the growth of new bone onto surfaces where it has been deposited. The result is the formation of a strong bone-implant interface early on in recovery. HA presently has CE approval, however the FDA has revoked its prior approval. Poor HA results have been reported by Field et al. (1997).

2.5 Standard Implant Materials

A number of proven implant materials exist and the ones applicable to this project are discussed in terms of their material properties, biocompatibility and failure modes.

2.5.1 Titanium (Ti-6Al-4V)

Titanium alloys are one of the materials of choice in orthopedics today. Titanium has the advantage of lower density and lower elastic modulus, coupled with high strength and a very low rate of corrosion (Hench and Ethridge, 1982). The lower density reduces the patients awareness of the prosthesis and the lower elastic modulus reduces stresses around the implant by flexing with the bone.

One negative in using titanium is its poor wear properties, however, recent advances in the case hardening of Ti-6Al-4V have produced 50 - 100μm wear-resistant oxide layers (Vicatos 2005, personal communication). This is

promising for wear application where fatigue is not present. Grover (1966) found the fatigue limit of a heat-treated titanium alloy to be above 50% of its tensile strength. The fatigue strengths of other biomedical materials range from 35% to 45% of their tensile strength.

Ti-6Al-4V shows two orders of magnitude less corrosion than 316L stainless steel (Aragon and Hulbert, 1972) and the latter becomes pitted while the titanium corrodes uniformly. Titanium owes its corrosive resistance to a tightly adherent oxide layer which passivates the surface. If this oxide layer is continually rubbed off by contact with another hard surface, fretting corrosion occurs. This should be avoided. Chemical sterilization appears to have no effect on corrosion rates, while dry heat and steam do affect titanium, significantly reducing the corrosion rates by producing a thicker oxide layer (Hench and Ethridge, 1982).

2.5.2 Cobalt Chrome Molybdenum (Co-Cr-Mo)

Cobalt chrome molybdenum is used in orthopedics mainly for its excellent wear resistance; in some cases it is utilized in high load applications. The material is extremely hard and is difficult to machine. The rate of corrosion is low and uniform (Hench and Ethridge, 1982).

2.5.3 Ultra High Molecular Weight Polyethylene (UHMWPE)

The *in vivo* problems associated with UHMWPE are abrasive wear, polymer degradation and cold creep. Wear particles have a large surface to volume ratio when compared to their parent material. As a result, tissue reacts more readily with the material, creating an irritation and loss of function which constitutes a failure of the prosthesis. The polymer degrades over time; up

to a 30% loss of tensile strength was reported in a 17 month *in vivo* study on polyethylene sutures (Leininger, 1965).

UHMWPE is however, the primary bearing surface used in conjunction with Co-Cr-Mo. Other innovations appearing on the market today are; metal on metal bearing surfaces and ceramic on ceramic bearing surfaces. Their manufacture is specialized and have been ruled out for use in this project.

2.5.4 Polymethyl Metacrylate (PMMA) Bone Cement

PMMA is polymerized *in situ*, creating a chemical reaction that produces thermal trauma due to the polymer reaching temperatures as high as 65°C (Lautenschlager et al., 1974). The other immediate problems are the chemical and mechanical trauma which occur when the cement is pressurized onto the bone.

Possibly the worst problem with bone cements is the deterioration of the polymer-bone or polymer-metal interface, leading to mechanical instability (Hench and Ethridge, 1982). The reasons behind this are the strength and adhesion properties of bone cements. PMMA is relatively strong in compression but weak in tension. The fatigue strength of the polymer under physiological conditions is in the order of 5 $7MPa$ (Davis et al., 1987) with Lee and Turner (1977) reporting a tensile strength of $25MPa$. This is the main reason why there is a poor long-term survival rate for glenoid components which rely heavily on bone cement for fixation.

PMMA cement has no adhesive properties and acts as a grouting between the prosthesis and bone. It merely fills space to create a ridged link between the bone and prosthesis (Hench and Ethridge, 1982). The consequence of this physical property is that undercuts, holes and furrows need to be designed

into the prosthesis. A good surgical procedure relies on the PMMA dough being pressurized between the bone and implant which results in a filling of any available cavities. This is what produces a good interlocking of PMMA with both the bone and metal surfaces with which it is in contact, creating a ridged link between the two.

2.6 Implant Failure Modes

One must remember that joint replacement is one of the most demanding of all body implant applications, because of the extent of loading, the severity of the chemical environment, and the complexity of joint function (Lisagor, 1975).

Glenoid fixation is the weakest link in any total shoulder replacement. In a FEA study done on UHMWPE linings used in an anatomical TSR, Gupta et al. (2004) showed that if subchondral bone along the longitudinal axis of the glenoid cavity is preserved, glenoid fixation strength is improved. Reasons for component loosening are the design of the implant, poor surgical technique, limitations in quality and quantity of bone for fixation, tissue reaction to debris, and high patient activity levels (Boyd et al., 1990; Wilde et al., 1984; Barrett et al., 1987; Kelly et al., 1987). The presence of one or more of the above factors may result in aseptic loosening. Boileau et al. (2005) stated that reverse ball-in-socket prostheses tend to fail because their design results in excessive torque and shear forces being applied to the glenoid component due to the center of rotation being placed outside of the scapula, as seen in Fig. 2.8(b). One must also keep in mind that the holding power of screws generally decreases with time (Hench and Ethridge, 1982).

The other major mode of failure for constrained TSR is an uncontrolled

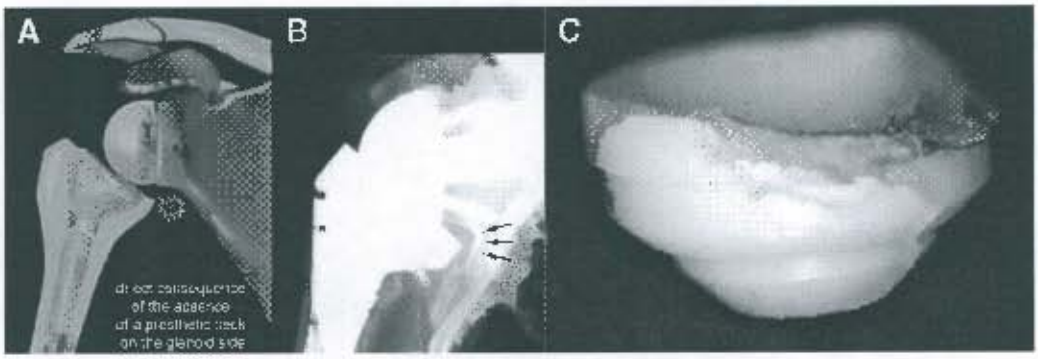

Figure 2.16: The Delta® cup is shown impinging on the lower border of the glenoid (a), a radiograph of an impingement taking place (b) and a retrieved polyethylene cup demonstrating wear (c), (Boileau et al., 2005).

dislocation of the link between the humeral and glenoid fixation components. This results in the need for revision surgery and there is a high possibility of limb amputation. One may argue the patient should take care of his/her arm and not load it excessively. Dislocation of constrained TSRs have taken place when patients have rolled on their side while asleep (Lane 2005, personal communication).

Impingement of a prosthesis on surrounding structures or itself is undesirable and falls under design failure. In orthopedics every case must be taken on merit as there are many variables to every outcome. An example of impingement is given in Fig. 2.16. Other areas of failure are corrosion and wear and these modes of failure are governed by the designer's choice of material. In this project the materials have been specified and therefore failure modes of corrosion and wear need not be discussed.

2.7 Summary

In closing, a list is given of the important points pertaining to problems that remain in the field of constrained TSR.

- Poor glenoid fixation, due to quantity and quality of bone.
- The uncontrolled dislocation of the link between the glenoid component and the humeral component.
- Space constraints as a result of less skin available to close the wound after a biopsy.
- Low mobility of the shoulder is due to resection of the abductor muscles.
- No constrained TSR with muscle attachment points available on the market.

Chapter 3

Specifications

The objective of this thesis was to generate a CTSR design. Three viable designs were generated; the Quad-Point TSR, Hybrid-Screw TSR and Central-Peg TSR (Fig. 3.1). A quantitative tabular summary of all three designs and the design target is given in this chapter.

Specifications have two functions, the first is to clarify the design problem and set a quantifiable design target, the second is to provide a means of comparing designs. The specifications have been divided up into categories based on the components that make up the final prosthesis and these components have been identified as glenoid fixation, humeral assembly and the ball-in-socket. A general and joint range of mobility (ROM) category is also given. Realistic target values have been generated for each specification when possible and are given in the column labeled 'Desired' in Table 3.1. The actual values attained by the Quad-Point, Hybrid-Screw and Central-Peg TSR designs (Fig. 3.1) are given in their respective columns (Table 3.1).

A detailed explanation of how each design functions is given in Chapter 4 and Chapter 5 will highlight the designs strengths and weaknesses.

Figure 3.1: The Quad-Point TSR (a), Hybrid-Screw TSR (b) and Central-Peg TSR (c) design side views.

Table 3.1: Design specifications

No.	Requirement	Desired	Actual Quad-Point	Actual Hybrid-Screw	Actual Central-Peg
	Glenoid Fixation				
1	Number of screw attachment points	max	3	2	1
2	Number of cemented attachment points	max	1	3	3
3	Volume of Bone removed†	min	$2.87cm^3$	$4.67cm^3$	$5.16cm^3$
4	Contact area of cement on bone†	max	$9.2mm^2$	$11.7mm^2$	$11.7mm^2$
5	Contact area of cement on prosthesis	max	$5.2mm^2$	$6.4mm^2$	$6.4mm^2$
6	Contact area of prosthesis on bone	max	$14.1mm^2$	$17.7mm^2$	$18.7mm^2$
7	Strength of the initial fixation	max	-	-	-
8	Center of rotation from glenoid face	min	$18mm$	$24mm$	$24mm$
9	Distance from humeral shaft axis to glenoid face	min	$46mm$	$41.4mm$	$41.4mm$
10	Use of both cement and bone ingrowth fixation	-	✓	✓	✓
	Humeral Assembly				
11	All tapers to be locked with a threaded section	-	✓	✓	✓
12	Minimum number of suture holes	4	5	5	5
14	Minimum diameter of suture holes	$4mm$	$3.5mm$	$3mm$	$3mm$
15	Minimum number of grooves for the attachment of *Dacron*®	2	2	2	2

† Calculated for a $1mm$ thick cement mantel.

Design specifications table *cont...*

No.	Requirement	Desired	Actual Quad-Point	Actual Hybrid-Screw	Actual Central-Peg
	Humeral Assembly cont...				
16	Diameter of grooves needed to attach *Dacron*® with wire	$2mm$	$2mm$	$2mm$	$2mm$
17	Built-in modularity	-	✓	✓	✓
	Ball-in-Socket				
18	Minimum range of motion	100°	90°	90°	90°
19	Axial force required to dislocate the gleno-humeral link	-	$1500N$	$1500N$	$1500N$
20	Axial force required to produce plastic deformation in the gleno-humeral link	$1000N$	$900N$	$900N$	$900N$
21	Moment required to separate the gleno-humeral link	-	$45Nm$	$45Nm$	$45Nm$
22	Moment required to produce plastic deformation in the socket lip	$25Nm$	$15Nm$	$15Nm$	$15Nm$
	General				
23	Only use materials Ti-6Al-4V, UHMWPE and Co-Cr-Mo	-	✓	✓	✓
24	Impingement tolerance	$2mm$	$2mm$	$2mm$	$2mm$
25	Locating window for cortical screws	20°	20°	20°	20°

Design specifications table *cont...*

No.	Requirement	Desired	Actual Quad-Point	Actual Hybrid-Screw	Actual Central-Peg
	Joint Range of Mobility (ROM)†				
25	Elevation	160°	160°	160°	160°
26	Extension	60°	60°	60°	60°
27	External rotation in Abduction	60°	52°	52°	52°
28	Internal rotation in abduction	60°	38°	38°	38°
29	Abduction*	140°	125°	125°	125°
29	Posterior reach	S1	none	none	none

† All calculations use a 7° glenoid retroversion and 5° glenoid tilt.

* Abduction includes a glenohumeral rhythm of 2:1.

Some of the specifications have been listed with either a maximum or minimum value as variability involved in the human shoulder and surgery prevents the generation of fixed target values.

A future study may use this information to help explain why a concept succeeded experimentally in the areas of the glenohumeral link and glenoid fixation.

Chapter 4

Final Designs

On the basis of the desired specifications laid out in Chapter 3, concepts were generated and analyzed. Of those concepts, three of the most promising were developed into the Quad-Point, Hybrid-Screw and the Central-Peg TSR designs. A single glenohumeral link was developed using both experimental and finite element analysis (FEA). The function and assembly of this link will be explained in this chapter together with the function and assembly of the Quad-Point, Hybrid-Screw and Central-Peg TSR designs. It is uncertain which of the three designs will have a superior glenoid fixation. To ascertain this, experimental work would have to be carried out. In Chapter 5 only the possible superiority of each designs glenoid fixation is discussed.

A list of the designs follows and all technical drawings can be found in Appendix E.

- Quad-Point TSR
- Hybrid-Screw TSR
- Central-Peg TSR

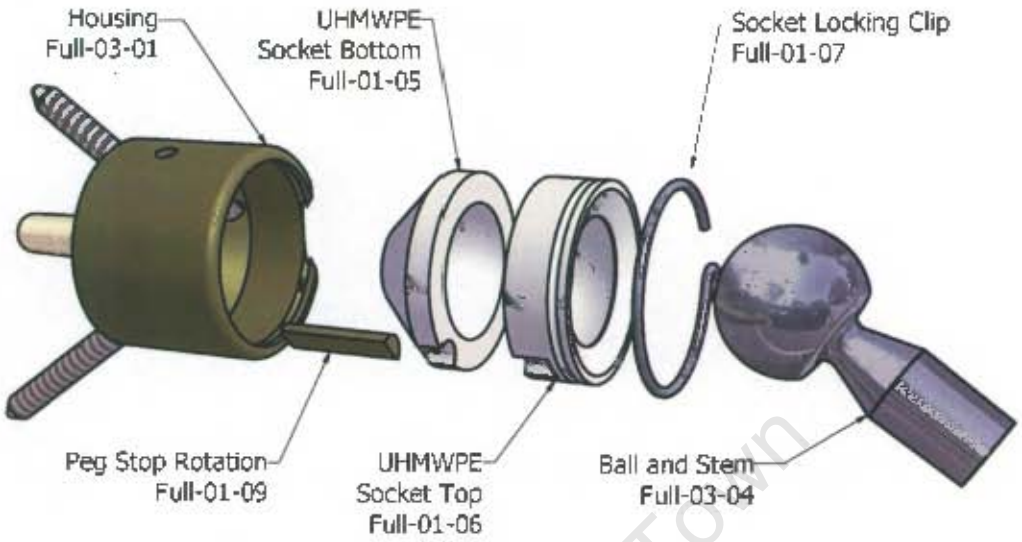

Figure 4.1: Socket assembly, *ISIQU Orthopedics*.

4.1 Design Similarities

Design similarities are first discussed, followed by a detailed explanation of each TSR's assembly and function.

4.1.1 Ball-in-Socket System

The UHMWPE socket is split in two halves to facilitate the insertion of a Co-Cr-Mo ball and stem (Fig. 4.1). However, the socket is not split on the equatorial line of the spherical cavity. This is done in order for the ball to clip into the top half of the socket. The rationale is a reduction in wear may be possible on the inside of the UHMWPE socket, as stress concentrations will not lie on the fault/split line. The bottom half of the socket is inserted into a titanium housing followed by the coupled ball and upper half of the socket. The system is then locked in place by a titanium cable placed into a groove created in both the top half of the socket and the inside of the housing. The ROM of the ball-in-socket joint is 90 degrees (Fig. 4.2). The socket

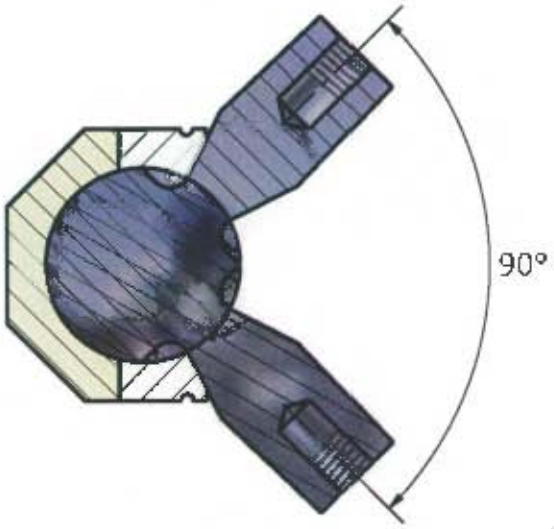

Figure 4.2: Range of motion (ROM) of the ball-in-socket.

can withstand a maximum axial force of $900N$ and a maximum cantilever force of $15Nm$. The maxima are based on the onset of plastic deformation (Appendix C).

4.1.2 Humeral Fixation System

Humeral stem fixation is robust and clinical results have shown an almost zero failure rate. The design given for all three TSR's is a standard tapered stem with three flutes (Fig. 4.3). The stem is fitted with a male taper and thread section on its proximal end, which locks together with a humeral stem extension; the thread insures that the taper will not disengage. Plates are incorporated into the distal end of the humeral stem extension (Fig. 4.3). These plates may be required in cases where an extended proximal humeral resection (Fig. 2.3) is necessary or poor bone stock is present. The surface of the plates is roughened to allow for bone ingrowth and grooves are provided for the use of surgical locking wire, thus increasing the stability of the attachment.

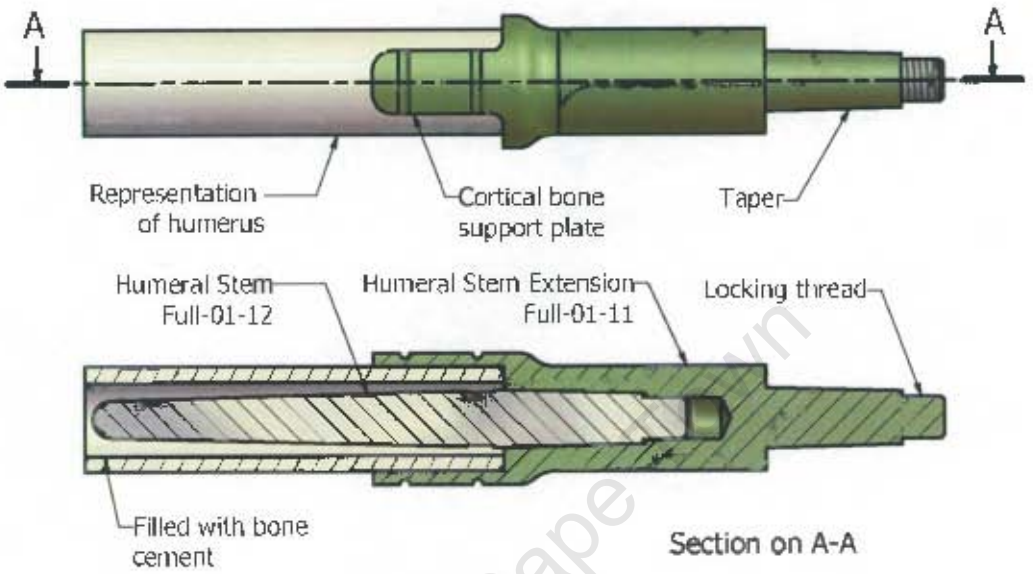

Figure 4.3: Humeral fixation according to *ISIQU orthopedics*.

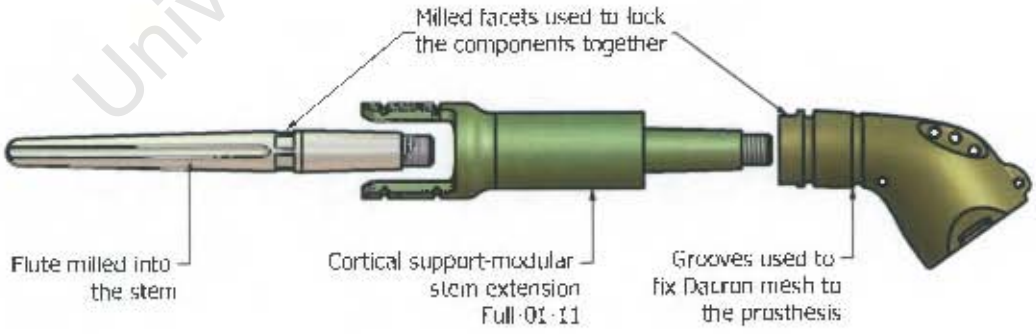

Figure 4.4: Modular humeral extension system according to *ISIQU orthopedics*.

4.1.3 Modularity

It is possible to use various length humeral stems and humeral stem extensions. The tapers in shoulder patients with large muscle loss are not under constant compression and as a result, a catastrophic unlocking of the tapers may occur. To prevent this, each taper is backed up with a threaded section (Fig. 4.3). A surgeon will normally require three sizes of each component for sizing in theatre and the mean size is chosen on the basis of a radiograph taken of the patient's humerus. Sometimes additional sizes are also supplied in cases where the resection margin is not well defined and more bone has to be resected.

4.2 Quad-Point TSR

The designs of the glenoid fixation are partly based on *Depuy's* Delta® TSR (Appendix D). Fig. 4.5 shows the Quad-Point TSR design in three views. The Quad-Point TSR central stem is cemented into the glenoid. Once the cement has fully polymerized, two cortical screws with spherical heads are inserted into the glenoid. Both screws have the flexibility of being located in a 20 degree window; the mean location angle of each screw is 35 degrees either inferiorly or superiorly (Fig. 4.6). The superior screw is shorter than the inferior screw, which is designed to locate in the medullary cavity on the axillary border of the scapula.

Once the socket housing is fixed to the glenoid, the coracoid plate can be bent into a shape that conforms with the coracoid process. The coracoid plate is then lightly screwed to the socket housing using two fine thread screws with polyethylene inserts, which insure the screws are locked in place. The plate is then permanently fixed to the coracoid process using one cortical screw.

Figure 4.5: The Quad-Point TSR assembly.

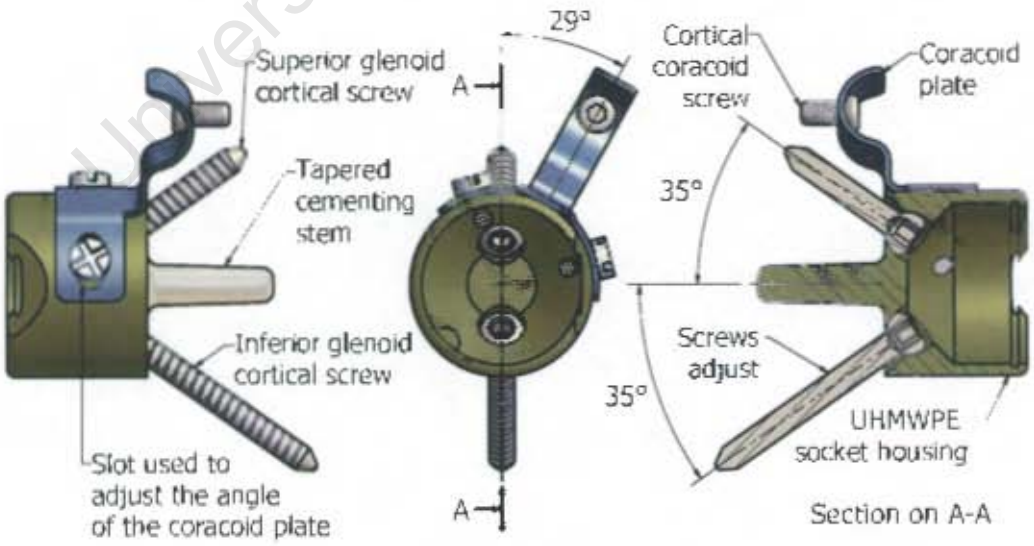

Figure 4.6: Quad-Point TSR glenoid fixation.

Once this is complete the two screws on the housing are finally tightened.

The humeral components are then assembled; first the top half of the socket is clipped onto the Co-Cr-Mo ball. The distal end of the ball has a male taper which mates with a taper on the proximal humeral component. The taper is locked in place by a screw, the thread of which is fitted with a polyethylene insert to insure permanent locking of the thread. The stem is cemented into the humeral canal and wire may also be used to fix the humeral component in place. Once this is achieved, the ball-in-socket is assembled (Section 4.1.1). The assembly of the prosthesis is now complete and the surgeon attaches as much remaining muscle as possible to the suture holes on the humeral component. A Dacron® mesh may also be used and is fixed to the humeral component using wire and the two grooves provided (Fig. 4.4). The final step is the closure of the wound.

4.3 Hybrid-Screw TSR

Kessel originally used a large un-cemented screw which filled the glenoid cavity (Fig. 2.10). The Bayley-Walker®, which is the next generation of Kessel's design, improved on the thread shape and which utilizes the cortical bone at the vault of the glenoid (Fig. 4.9). The Hybrid-Screw design has partially incorporated that design and combined it with cement fixation in a reverse ball-in-socket system (Fig. 4.7).

The glenoid fixation plate is screwed into the glenoid cavity (Fig. 4.8). Once it is tight on the glenoid, two or three of the eight threaded holes are chosen for the insertion of cemented screws (Fig. 4.12). Threaded studs will first be used to locate the position of the coracoid plate and the surgeon shapes the plate to conform with the coracoid process. The plate is then screwed

Figure 4.7: The Hybrid-Screw TSR assembly.

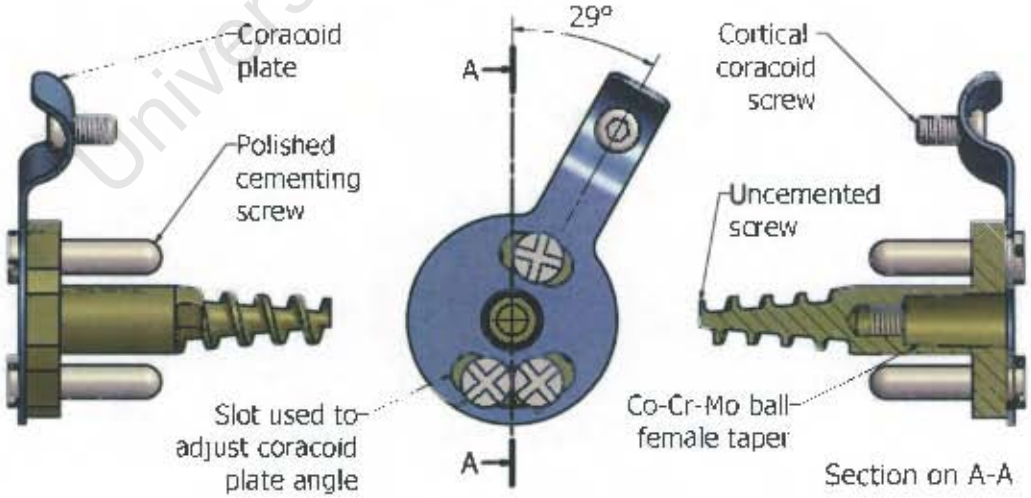

Figure 4.8: Hybrid-Screw TSR glenoid fixation.

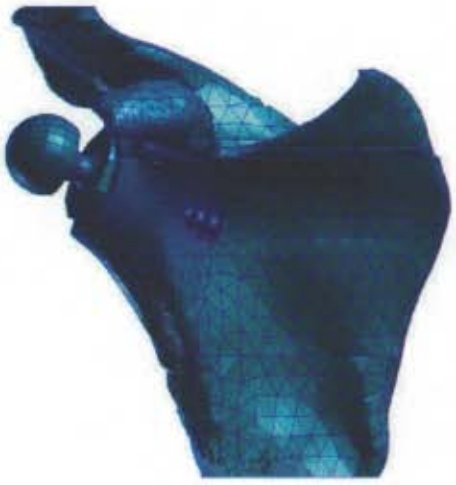

Figure 4.9: The Bayley-Walker® glenoid component implanted in the scapula (Ahir et al., 2004). Note the thread protruding through the vault of the glenoid.

into the coracoid process and the two threaded studs are removed from the glenoid fixation plate. The screws are then cemented into the glenoid, with the thread locking both the pegs and coracoid plate in position, resulting in a rigid system.

The humeral component is then assembled and cemented into the humeral canal as described in Section 5.2. The next step is to assemble the top half of the UHMWPE socket with the Co-Cr-Mo ball. Once this is complete the the taper on the proximal end of the ball is locked into place by the thread at the proximal end of the taper (Fig. 4.7). The ball-in-socket system is then assembled and locked in place with a titanium cable as described in Section 4.1.1. The surgeon follows the same procedure as undertaken in the final steps of the Quad-Point TSR implantation and finally closes the wound.

Figure 4.10: The Central-Peg TSR assembly.

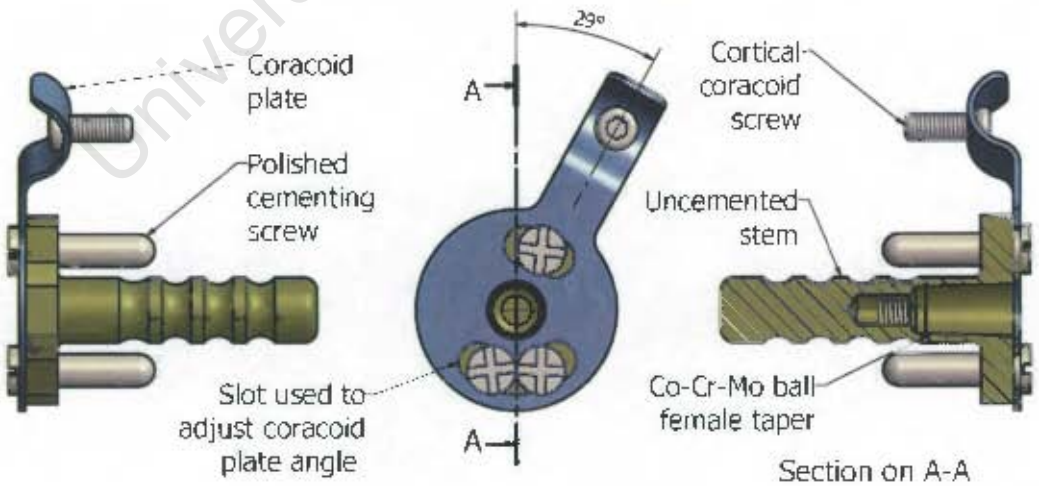

Figure 4.11: Central-Peg TSR glenoid fixation.

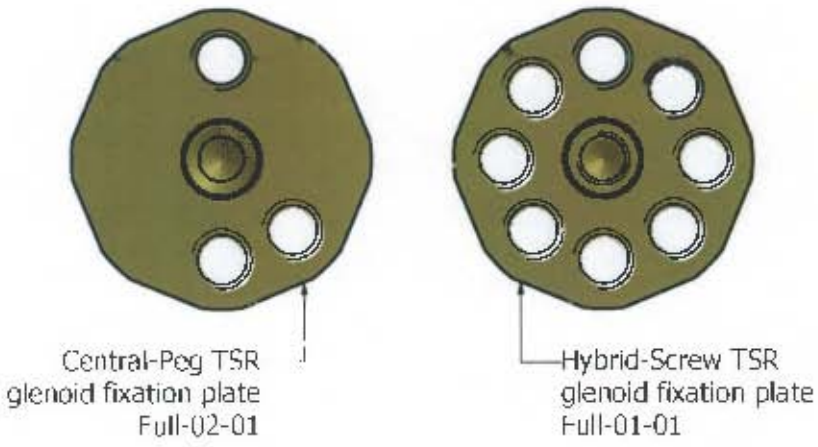

Figure 4.12: The difference in glenoid fixation plates.

4.4 Central-Peg TSR

The Central-Peg TSR (Fig. 4.10) is very similar to the Hybrid-Screw TSR in design. The only component that differs is the glenoid fixation plate where an un-cemented stem is used instead of a screw (Fig. 4.11). The result is the need for only three threaded holes on the glenoid fixation plate (Fig. 4.12), as the plate is not rotated. A central hole is drilled into the glenoid and the ridged stem is fitted into the glenoid. This is followed by the same procedure as the Hybrid-Screw TSR (Section 4.3).

4.5 Summary

In this chapter, the assembly and function of the three TSR designs have been discussed. The next chapter discusses the rationale behind the designs and the positive and negative points of each design have been highlighted.

Chapter 5

Discussion

The most important aspect of this report is to understand the rationale behind each design. Each design is discussed under the same sub headings as the previous chapter to facilitate referencing. The designs are discussed on the basis of:

- Manufacture
- Surgical Assembly
- Mobility
- Strength and Failure
- Space

5.1 Design Similarities

The ball-in-socket, humeral fixation and modularity designs are discussed first as they are used in all three TSR designs. A look at the overall TSR designs follows.

5.1.1 Ball-in-Socket System

In using a ball-in-socket, a compromise must be made between the strength versus the mobility of the system. As the mobility of the ball increases the

system becomes easier to dislocate. At the onset of the project a decision was made to investigate a press-fit ball-in-socket link using a $\varnothing 20mm$ Co-Cr-Mo ball, as this diameter offers a balance between space constraints and available mobility.

Manufacture

Cutting either an internal or an external thread on the stem of the Co-Cr-Mo ball is problematic, due to spherical accuracy. The UHMWPE socket requires a specially designed cutter to produce the undercut necessary to form the retaining lip (Appendix E, Equip-01-01).

Surgical Assembly

The assembly is locked together by a $\varnothing 1.65mm$ titanium cable fed into a mating groove, this design was generated by *ISIQU Orthopedics*. A stainless steel cable could also be used as the galvanic couple between titanium and stainless steel does not accelerate corrosion under *in vivo* conditions (Buchanan et al., 1978). The grooved assembly system proved easy to manufacture and assemble. The other benefit of this system is the ease of disassembly.

Mobility

The stem of the ball and the shape of the socket dictates the amount of mobility achieved. Incorporating these two factors, a system was designed which allowed 90 degrees of mobility. This value was chosen as it was estimated that the corresponding lip would produce the required retention force (Appendix E, Full-03-00, View B).

Strength and Failure

A press-fit ball-in-socket was first investigated. All calculations can be found in Appendix B.

The report shown in Appendix B, proves the validity of the finite element model used. In light of this, a second ball-in-socket was developed which has a split line to allow for assembly and tested using only finite element analysis (FEA). The assembly of the split ball-in-socket design is explained in Section 4.1.1. Using a socket with an entrance diameter of $18mm$ provided a $1mm$ retaining lip around the inside edge of the cup. The axial force needed for the socket lip to undergo plastic deformation was $900N$; axial separation of the ball-in-socket took place at $1500N$. The axial force necessary to produce plastic deformation is $100N$ below the target value of $1000N$. The decision was made to keep the mobility at 90 degrees and maintain a retaining force of $900N$. Going below 90 degrees of mobility is more dangerous than the $100N$ reduction in axial retention, as the risk of a dislocation due to a moment increases with reduction in mobility.

Once an acceptable axial separation strength had been attained, further analysis was carried out in the area of cantilever strength and the point at which plastic deformation takes place during the application of a moment. The point at which plastic deformation took place on the rim of the socket during a cantilever simulation was $2.5Nm$ followed by plastic deformation on the lip of the socket at $15Nm$ (Appendix C). The UHMWPE shoulder on the rim of the socket provides a shock absorption for the neck of the ball, as the ball reaches maximum ROM. If the UHMWPE shoulder were not present, metal on metal contact would occur between the Co-Cr-Mo neck and the titanium housing producing metallic wear debris. It is uncertain if this is a

major factor and whether the shoulder of the socket should be removed or increased.

Co-Cr-Mo was chosen as the material for the ball, because it has superior wear and fatigue properties. There was concern over the strength of the $\varnothing 6mm$ neck, so a FEA was carried out. The results showed that the neck would be able to support 126kg before plastic yield took place, as fatigue is not a concern due to the limb being relatively immobile. A $\varnothing 6mm$ neck was deemed safe. All calculations can be found in Appendix A.

There is a peg which spans the depth of both the socket halves and inserts into the housing. Its purpose is to stop the rotation of the socket in the housing and prevent wear on the inside of the titanium housing.

Space

Dr. G Vicatos specified that the thickness of the UHMWPE socket may not go below $4mm$. The $4mm$ wall thickness is necessary for both the dimensional stability during machining and the cushioning of the ball-in-socket interface; the wall provides the required space for the peg to stop the socket from rotating in the housing. The wall thickness in turn defined the size of the system together with the $\varnothing 20mm$ ball.

Summary

The ball-in-socket design has been optimized to produce 90 degrees of mobility at a stable axial force of $900N$. A safety factor may be incorporated into this value to make certain that the patient does not dislocate the prosthesis. However, this is unlikely as the glenoid fixation is assumed to be weaker than the ball-in-socket link. If a higher mobility or axial force is necessary, an alternative to the ball-in-socket will have to be found.

5.1.2 Humeral Fixation System

Humeral fixation is in many cases designed around the patient and the level of humeral resection. A surgeon matches the size of the prosthesis using a radiograph of the upper arm. The radiograph is also used to work out the level of resection which is dependent on the size and shape of the cancerous tumour.

Manufacture

If a Co-Cr-Mo humeral stem is used, the cutting of the locking thread becomes time consuming. There are six milled faces provided on the stem for the locking of the taper and a standard 3 degree tapered stem is used containing three flutes; see Appendix E for detailed manufacturing drawings.

Surgical Assembly

The system is easy to implant and surgeons are experienced in this procedure. There are however some cases in which the surgeon may be concerned that the condition of the humeral bone stock is poor and that the bone will not be able to support a stand alone cemented stem. In these cases, plates are fashioned at the end of the modular section (Fig. 4.3). The plates provide support and are roughened so that the remaining bone is able to grow onto the prosthesis which will strengthen the fixation.

Strength and Failure

This is not a major concern as clinical results have proven humeral fixation is by far the strongest component of a constrained TSR.

Space

The space given to this component is dictated by the anatomy of the humerus.

Summary

Humeral fixation designs are proven to be stable and engineeringly sound. Thus the testing of the standard design used in this thesis is deemed unnecessary.

5.1.3 Modularity

All tapered sections are locked with a threaded section to ensure that the taper will not release. Whether this is necessary is uncertain but without musculature present to hold the limb in place, the risk is too great not to include a locking mechanism.

Manufacture

Located at the end of the female taper is the thread used to lock the taper in position. The diameters of both the Hybrid-Screw TSR and Central-Peg TSR central screw and stem had to be increased to provide the space required to accommodate the thread cutter used in producing the internal thread.

Surgical Assembly

Taper locks are sensitive to taper angle and shaft diameter. A $2mm$ travel has been provided in which the tapers may fully engage. Two faces are milled on the proximal humeral component and six on the stem. Using two spanners, one on each set of faces, the surgeon is able to lock both tapers on the humeral replacement (Fig. 4.4).

Strength and Failure

This is a robust system that provides a simple solution for modular systems.

Space

The size of the titanium components are disproportionately large when compared to the stresses the components undergo. They are thus over designed, but are required to fill the void left by the tumour.

Summary

Modular components have been manufactured for years and there is little concern of failure, especially with the backing of a threaded section locking every taper.

5.2 Quad-Point TSR

The assembly drawing can be found in Appendix E, Drawing No. Full-03-00.

Surgical Assembly

The only foreseeable difficulty is the insertion of the socket into the housing and the insertion of the locking ring.

Mobility

When implanted on a glenoid with 7 degrees of retroversion and 5 degrees of tilt, the patient's only major reduction in mobility is posterior reach, as internal rotation of the ball-in-socket is limited. All calculated values of mobility can be found in the specifications Table 3.1, pg.35.

Strength and Failure

The cemented central stem provides the initial glenoid fixation, supported by two cortical screws. The holding power of bone screws generally decreases with time (Hench and Ethridge, 1982). To combat this, the core of the

cortical screw thread is sandblasted, to increase its roughness and promote bone ingrowth. The back of the socket housing is roughened to provide for bone ingrowth. The only problem with this design is the cortical screws are free to rotate in the housing, allowing for micro motion. There are spinal fixation products on the market which incorporate lockable screws with a 20 degree locating window. If these lockable cortical screws could be built into the available space the design would be more attractive.

Two cortical screws are used to anchor the glenoid housing, unlike the Delta® where four are used. Due to chemotherapy the bone structure is already weakened and by drilling an extra two holes into the glenoid its strength is greatly reduced. The extra fixation gained by the two cortical screws cannot justify a possible glenoid fracture.

The coracoid plate provides extra stability and can be located within a 15 degree window (Fig. 4.6). It is made of $1mm$ thick titanium plate which allows the surgeon to bend it into shape while in theatre. The flexibility of the plate is regarded as a positive quality as this allows the prosthesis to flex with the bone, preventing stress shielding and promoting bone growth. The plate is fixed in place by the coracoid screw. This dome shaped cortical screw gives the surgeon freedom to place the screw at a variety of angles .

The greatest benefit that the Quad-Point TSR offers, is that the centre of rotation is placed $18mm$ from the glenoid face. This reduces the moment transferred to the glenoid by a third, when comparing it to the other two designs. Another positive is it is possible to incorporate the Hybrid-Screw TSR and Central-Peg TSR glenoid fixation designs into the Quad-Point TSR design, this would be beneficial if one of the other glenoid fixation designs were superior and the overall Quad-Point TSR design was regarded as superior.

However, the reverse is not possible.

The other benefit the Quad-Point TSR has is that impingement does not occur. Mechanical advantage is also a benefit as the main suture holes are located $28mm$ from the center of rotation compared with the other designs' $18mm$. This will improve the patient's functionality if any muscle is attached to these suture holes.

Space

The Quad-Point TSR provides for the most space saving design out of the three designs discussed in this thesis.

Summary

The Quad-Point TSR has the following advantages; a lower moment applied to the glenoid fixation, an increase in mechanical advantage for any reattached muscle, a lower possibility of tissue impingement and the possibility to incorporate of any of the three glenoid fixation methods into the socket housing. The disadvantages are that the humeral axis lies $46mm$ from the glenoid face compared to the $41.4mm$ of the other two designs. This increases the amount of skin needed to cover the distal end of the wound.

5.3 Hybrid-Screw TSR

The assembly drawing can be found in Appendix E, Drawing No. Full-01-00.

Surgical Assembly

A possible problem during surgery is that the cement may be too viscous during the insertion of the polished cemented screws (Fig. 4.8), thus preventing the required twisting of the screws needed for the thread to lock into the

glenoid fixation plate. The surgeon will also have to be careful when locking the taper on the stem of the ball as an equal and opposite moment will have to be applied to the stem and glenoid plate.

Mobility

The mobility produced is the same as that produced for the Quad-Point TSR.

Strength and Failure

The partial central screw is promising as there are few of the worries associated with the Bayley-Walker®. Splitting of the glenoid is more difficult as the screw is only engaging at a depth of $17mm$ and the coracoid screw prevents rotation of the central screw. The benefit of having a central screw is that an interlocking of thread with cortical bone at the vault of the glenoid takes place (Fig. 4.9).

A problem with the design is it requires the removal of a large volume of bone. The cemented stems are also a concern as their focus is in the centre of the glenoid thus reducing its structural strength. If the screws are angled the design is improved. The problems that arise are; the difficulty of locking the coracoid plate to the glenoid fixation plate and the occurrence of impingement which would occur if the back of the cementing screws were to protrude any future laterally.

There are faces milled onto the Co-Cr-Mo ball's stem that interact with the edge of the socket and these may increase wear.

Space

The design forces material to be used in the anatomical position of the deltoid muscle, making closure of the wound more difficult.

Summary

The Hybrid-Screw TSR together with the Quad-Point TSR have the most promising glenoid fixation designs. The reverse ball-in-socket joint is not the optimal solution when compared to the anatomical orientation of the Quad-Point TSR. The reasons are all given in Section 5.2.

5.4 Central-Peg TSR

The assembly drawing can be found in Appendix E, Drawing No. Full-02-00. The Central-Peg TSR uses the same reverse ball-in-socket design as the Hybrid-Screw TSR, but the glenoid fixation is different. This is the weakest of all three designs.

Surgical Assembly

The implantation of this design is easier, as the surgeon does not have to line up holes when cementing outer screws into the glenoid. Also the glenoid fixation plate does not have to be screwed in.

Strength and Failure

What this design lacks in predicted long term strength it makes up in simplicity, as it is relatively easy to implant. If there is quality bone present it may be better to preserve this bone. In that case the stem would have to be customized and not be allowed to protrude from the glenoid vault. Initial fixation is the key to success and this design may fulfil this criterion, thus there would be a benefit in testing it.

Summary

The design has been included for completeness, however its glenoid fixation is of a lower standard than the Quad-Point TSR and the Hybrid-Screw TSR designs.

5.5 Summary

Between the Quad-Point TSR and the Hybrid-Screw TSR it is uncertain which of the two has a superior glenoid fixation. Using experimental methods one can successfully determine which is superior and during the testing the design may be optimized.

The Quad-Point TSR is the overall superior design, as the other glenoid fixation systems can be incorporated within the design. The anatomical design of the Quad-Point TSR results in many positives and very few negatives when compared with the reverse ball-in-socket design of the Hybrid-Screw TSR and the Central-Peg TSR.

Chapter 6

Conclusions

The two designs that stand out in the discussion are the Quad-Point TSR and the Hybrid-Screw TSR. Of these two designs the author believes the Quad-Point TSR is the superior joint replacement system for the following reasons; the position of the Quad-Point's rotational centre and the versatility of its screw placements.

6.1 Glenoid Fixation

Fixation to the glenoid is problematic in cases where constrained total shoulder systems are used. The fixation designs have the potential to succeed, however it is urged to proceed cautiously and use experimental technique to find an optimal solution.

6.2 Ball-in-Socket System

The ball-in-socket system provides the largest ROM for the amount of space it occupies. An alternative is to develop a dual spherical system, but this may prove unnecessary as the patient will not be mobile enough to utilize the extra ROM. The ROM generated by the split socket design is sufficient for this application.

The moment needed to induce plastic yield on the edge of the socket needs to be increased. This would be possible through a small amount of redesign. The overall performance of the socket is acceptable if the patient understands the prosthesis limitations and takes care of his/her shoulder. This is not the ideal solution, but a compromise of many contributing factors.

6.3 Humeral Fixation

The design of the humeral fixation is proven and should not be a cause of failure, unless the humeral fixation has been compromised during surgery or there is poor bone stock.

Chapter 7

Recommendations

It is recommended that the cementing screws used in the Hybrid-Screw TSR and the Central-Peg TSR should be angled as this would access a larger volume of bone for the purpose of fixation. Each cementing screw could also be tapered with flutes and this would improve cement fixation.

The size of the prostheses should be optimized using a *Sawbones* #1050 scapula (Appendix D). This inexpensive synthetic scapula model, would allow for more experimentation and in the long run would be beneficial in allowing the world orthopedic community to relate to the prosthesis size.

The length and diameter of the Central-Peg TSR uncemented stem (Fig. 4.11) may be too large. In order to produce optimal fixation the uncemented stem may have to be reduced in size.

It is possible to medialise the central axis of the humeral component, this will reduce the mechanical advantage of any muscle attached to the prothesis. The resulting benefit is that the anatomical volume that the prosthesis occupies, would be be reduced.

Instead of using domed cortical screws in the Quad-Point TSR design, a position locking cortical screw could be incorporated which has a 20 degree

window in which the screw can be positioned. Once the screw is in place a second screw component locks it in position. These systems are used in spinal orthopedic surgery. This addition would lock all the components together making the fixation more secure.

Chapter 8

Future Work

There is potential for future work on this project. The work described in this report is predominantly for the design phase of the project. There is still work to be done in the areas of prosthesis testing and the development of custom tooling needed to implant the prosthesis successfully.

8.1 Testing Glenoid Fixation

The design process of this thesis culminated in two extremely viable glenoid fixation designs. Now the performance of each design with respect to an existing standard needs to be quantified. *Depuy's* Delta® reverse shoulder replacement would be a good standard with which to compare results. The prosthesis has been on the market since 1991, and it is possible to obtain a used prosthesis for the purpose of reverse engineering.

In vivo studies are complex and there are ethical concerns, but the most glaring problem is subject variability. Cadaveric testing is possible but the testing would not be carried out on a fixed geometry as every scapula is unique. Complex FEA can be carried out incorporating bone remodeling. These models are computationally expensive and in some cases only give an insight into stress concentrations and bone remodeling patterns, not the

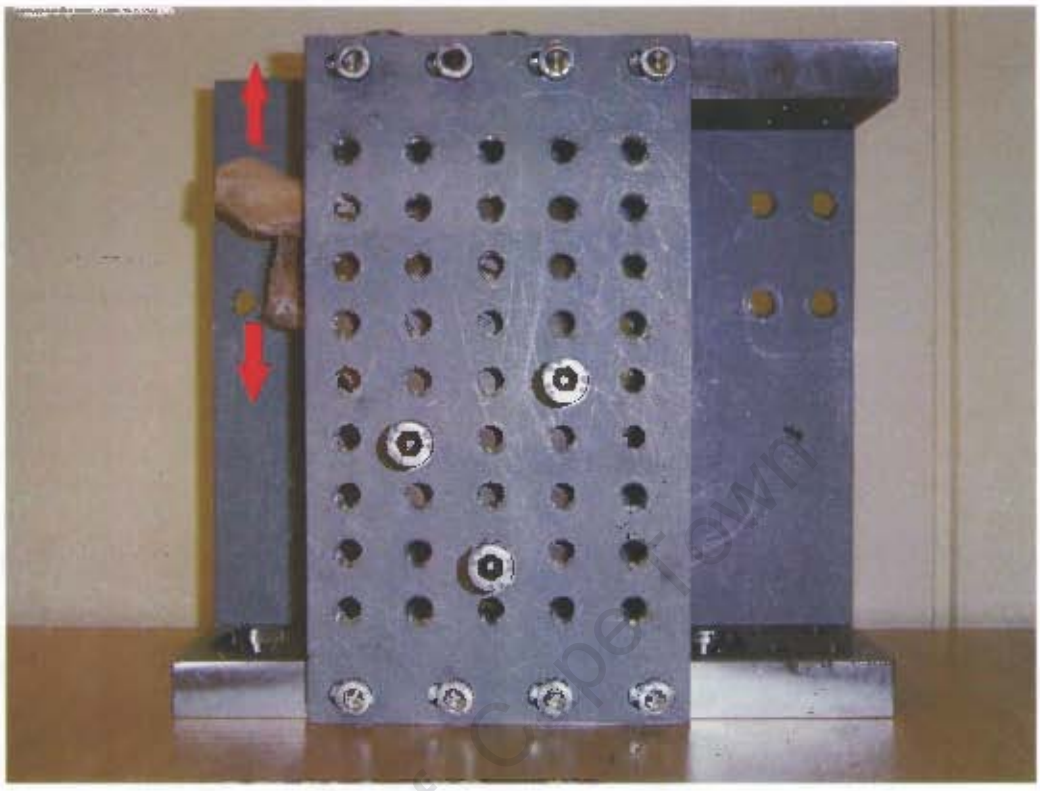

Figure 8.1: The scapula fixation test rig designed to mount onto a Zwick materials tester. The arrows show an inferior and a superior load on the glenoid.

loads at failure.

The author proposes the use of synthetic materials to simulate the scapula bone structure as this approach has been used to test implants in both synthetic femurs and tibias of the lower limb. *Sawbones Pacific Laboratories* produces both the femur and tibia commercially. Unfortunately they do not produce a synthetic scapula which simulates bone, but the company would however split the costs of manufacturing a mould for this purpose. Another alternative is to make one's own mould; all the materials required to do so are standard.

The author obtained ethics approval for the use of scapulae from unclaimed corpses at the Salt River Mortuary (Appendix D). It was important to be use un-embalmed bone as embalming chemicals destroy the natural properties of bone and for this reason only fresh corpses from the morgue could be used for testing. This facility was not utilized as there was a lack scapula available.

If these fixation experiments had been carried out, the results would have been beneficial in validating a synthetic bone model. A test rig was designed and built to clamp the scapulae in place on the Zwick tensile tester housed at the Material Engineering Department at the University of Cape Town (Fig. 8.1). All the drawings for the test rig can be found in Appendix E.

This is an exciting future project, since no papers have been found documenting initial fixation tests of a constrained total shoulder replacement. The author believes initial fixation strength combined with future bone ingrowth is the key to a successful constrained shoulder. Performing experiments designed to test initial fixation strength could lead to a superior solution.

8.2 Operating Tooling

The other important aspect of every prosthesis is the tooling which supports the prosthetic product. It ensures that the surgeon has a greater chance of inserting the prosthesis correctly. As there is so much variability in oncology cases, the surgeon may not use the designed tooling in every procedure, but it is still important to make sure that gaps in the prosthesis tooling are closed. This could be incorporated into an undergraduate project.

References

Ahir, S., Walker, P., Squire-Taylor, C., Blunn, G. and Bayley, J.: 2004, Analysis of glenoid fixation for a reversed anatomy fixed-fulcrum shoulder replacement, *Journal of Biomechanics* **37**, 1699–1708.

Aragon, P. and Hulbert, S.: 1972, Corrosion of ti-6al-4v in simulated body fluids and bovine plasma., *Journal of Biomedical Material Research.* **6**, 155–164.

Barrett, W., Franklin, J., Jackins, S., Wyss, C. and Matsen III, F.: 1987, Total shoulder arthroplasty, *Journal of Bone Joint Surgery* **69-A (6)**, 865–872.

Bayley, I. and Kessel, L. (eds): 1982, *Shoulder Surgery.*, Springer-Verlag: New York.

Boileau, P., Watkinson, D. J., Hatzidakis, A. M. and Balg, F.: 2005, Grammont reverse prosthesis: Design, rationale, and biomechanics, *Journal of Shoulder and Elbow Surgery* **14**(1S), 147S–161S.

Boyd, A., Thomas, W., Scott, R., Sledge, C. and Thornhill, T.: 1990, Total shoulder arthroplasty versus hemiarthroplasty., *Journal of Arthroplasty* **5 (4)**, 329–336.

Brostrom, L., Wallenstein, R., Olsson, E. and Anderton, D.: 1992, The kessel prosthesis in shoulder arthroplasty., *Clinical Orthopedics* **277**, 155.

Buchanan, S., Andrews, J. and Lemons, J.: 1978, Influence of carbon coupling on the corrosion susceptibility of cast surgical colbalt-chromium alloy., *Biomedical Material Research Symposium* **4**, 149–150.

Buechel, F., Pappas, M. and Depalma, A.: 1978, "floating socket" total shoulder replacement: Anotomical, biomechanical, and surgical rational., *Journal of Biomedical Material Research* **12**, 89–114.

Churchill, R. S., Brems, J. J. and Kotschi, H.: 2001, Glenoid size, inclination, and version: An anatomic study, *Journal of Shoulder and Elbow Surgery* **10 (4)**, 327–323.

Cofield, R.: 1977, Status of total shoulder arthroplasty., *Arch Surgery* **112**, 1088–1091.

Cofield, R.: 1983, Unconstrained total shoulder prostheses., *Clinical Orthopedics* **173**, 97.

Collins, D.: 1953, Structural changes around nails and screws in human bones., *Journal of Pathological Bacteriol.* **65**, 109–121.

Davis, A., Bell, R. and Goodwin, P.: 1994, Prognostic factors in osteosarcoma: A critical review., *Journal of Clinical Oncology* **12**, 423–431.

Davis, J., Burke, D., O'Conner, D. and Harris, W.: 1987, Comparison of the fatigue characteristics of centrifuged and uncentrifuged simplex-b bone cement., *Journal of Orthopedic Research* **5**, 366–371.

Evarts, C. (ed.): 1983, *Surgery of the musculoskeletal system*, Churchill Livingstone: New York.

Fenlin Jr, J.: 1975, Total glenohumeral joint replacement., *Orthopedic Clinic of North America* **67**, 565–583.

Field, L., Dines, D., Zabinski, S. and Warren, R.: 1997, Hemiarythroplasty of the shoulder for rotator cuff arythroplasty., *Journal of Shoulder and Elbow Surgery* **6**, 18–23.

Grover, H.: 1966, Metal fatigue in some orthopedic implants., *Journal of Material* **1**, 413–424.

Gupta, S., van der Helm, F. and van Keulen, F.: 2004, Stress analysis of cemented glenoid prostheses in total shoulder arthroplasty, *Journal of Biomechanics* **11**, 1777–1786.

Hench, L. and Ethridge, E.: 1982, *Biomaterials : An Interfacial Approach*, New York : Academic Press.

Heughan, C. and Hunt, T. K.: 1975, Some aspects of wound healing research: A review., *Canada Journal of Surgery* **18**, 118–126.

Iannotti, J., Gabriel, J., Schneck, S., B.G., E. and Misra, S.: 1992, The normal glenohumeral relationships., *Journal of Bone and Joint Surgery* **74A**, 491.

Kelly, I., Foster, R. and Fisher, W.: 1987, Neer total shoulder replacement in rheumatoid arthritis., *Journal of Bone and Joint Surgery* **69B**, 723–726.

Kölbel, R., Helbig, B. and Blauth, W. (eds): 1987, *Shoulder Replacement.*, Springer-verlag: New York.

Lautenschlager, E., Moore, B. and Schoenfeld, C.: 1974, Physical characteristics of setting of acrylic bone cements., *Biomedical Material Symposium* **5**, 185–196.

Lee, H. and Turner, D.: 1977, Temperature control of a bone cement by addition of a crystalline monomer, *Journal of Biomedical Material Research.* **11**, 671–676.

Leininger, R.: 1965, Plastics in surgical implants., *American Society of Testing Materials* .

Lisagor, B.: 1975, Corrossion and fatigue of surgical implants., *Standards News* **ASTM 3**, 20–24.

Lugli, T.: 1978, Atrificial shoulder joint by péan [1893]. the facts of an exceptional intervention and prosthetic method., *Clinical Orthopedics* **133**, 215–218.

McKee, G. K.: 1966, Developements in total hip joint replacement., *Proceedings - Institute of Mechanical Engineering* **181**, 85–89.

Poppen, N. K. and Walker, P. S.: 1976, Normal and abnormal motion of the shoulder., *Journal of Bone and Joint Surgery* **58A**, 195.

Post, M. and Haskell, S.S. Jablon, M.: 1980, Total shoulder replacement with a constrained prosthesis., *Journal of Bone and Joint Surgery* **62**, 327–335.

Rockwood Jr., C. A. and Matsen III, F. A. (eds): 1998a, *The Shoulder*, Vol. 1, 2nd edn, Saunders.

Rockwood Jr., C. A. and Matsen III, F. A. (eds): 1998b, *The Shoulder*, Vol. 2, 2nd edn, Saunders.

Scales, T., Winter, G. and Shirley, H.: 1970, Facrors influencing prosthetic procedures., *Proceedings Royal Society of Medicine* **63**, 1111.

Shigly, J. E. and Mischke, C. R.: 1989, *Mechanical Engineering Design*, 5th edn, McGraw-Hill.

Stewart, M. and Kelly, I.: 1997, Total shoulder replacement in rheumatoid disease., *Journal of Bone and Joint Surgery* **78-B(1)**, 68.

Watson, M. S. (ed.): 1990, *Surgical Disorders of the Shoulder.*, Churchhill Livingstone: Edinburgh.

Wilde, A., Borden, L. and Berms, J.: 1984, *Surgery of the Shoulder*, St. Louis: CV Mosby, chapter Experiences with the Neer total shoulder replacement, p. 224–228.

Wood, N., Kaminski, E. and Oglesby, R.: 1970, The significance of implant shape in experimental testing of biological materials. disc vs. rod., *Journal of Biomedical Material Research* **4**, 1–12.

Zadeh, H. and Calvert, P.: 1998, Recent advances in shoulder arthroplasty, *Current Orthopaedics* **12**, 122–134.

Zippel, J.: 1975, Luxationssichere schulterendoprosthese modell bme., *Z Orthopedics* **113**, 454–457.

Bibliography

Andrews, L. R., Cofield, R. H. and O'Driscoll, S. W.: 2000, Shoulder arthroplasty in patients with prior mastectomy for breast cancer, *Journal of Shoulder Elbow Surgery* **9 (5)**, 386–388.

Anglin, C., Tolhurst, P., Wyss, U. P. and Pichora, D. R.: 1999, Glenoid cancellous bone strength and modulus, *Journal of Biomechanics* **32**, 1091–1097.

Anglin, C., Wyss, U., Nyffeler, R. and Gerber, C.: 2001, Loosening performance of cemented glenoid prosthesis design pairs, *Clinical Biomechanics* **16**, 144–150.

Anglin, C., Wyss, U. P. and Pichora, D. R.: 2000, Mechanical testing of shoulder prostheses and recommendations for glenoid design, *Journal of Shoulder and Elbow Surgery* **9**(4), 323–331.

Büchler, P. and Farron, A.: 2004, Benefits of an anatomical reconstruction of the humeral head during shoulder arthroplasty: a finite element analysis, *Clinical Biomechanics* **19**, 16–23.

Cachia, V. V., Shumway, D., Culbert, B. and Padget, M.: 2003, Mechanical characteristics of the new bone-lok bi-cortical internal fixation device, *The Journal of Foot & Ankle Surgery* **42 (6)**, 344–349.

Collins, D. and Harryman, T.: 1997, Arthroplasty for arthritis and rotator cuff deficiency., *Orthopaedic Clinics of North America* **28 (2)**, 225.

Couteau, B., Mansat, P., Estivalezes, E., Darmana, R., Mansat, M. and Egan, J.: 2001, Finite element analysis of the mechanical behavior of a scapula implanted with a glenoid prosthesis, *Clinical Biomechanics* **16**, 566–575.

Egol, K. A., Kubiak, E. N., Fulkerson, E., Kummer, F. J. and Koval, K. J.: 2004, Biomechanics of locked plates and screws, *Journal of Orthopaedic Trauma* **18 (8)**, 488–493.

Greene, W. B. and Heckman, J. D.: 1994, *The clinical measurement of joint motion*, American Academy of Orthopaedic Surgeons.

Gupta, S., van der Helm, F. and van Keulen, F.: 2003, The possiblities of uncemented glenoid component – a finite element study, *Clinical Biomechanics* **19**, 292–302.

Hasan, S. S., Leith, J. M., Campbell, B., Kapil, R., Smith, K. L. and Matsen III, F. A.: 2002, Characteristics of unsatisfactory shoulder arthroplasties, *Journal of Shoulder and Elbow Surgery* **11 (5)**, 431–441.

Hempfing, A., Leunig, M., Ballmer, F. T. and Hertel, R.: 2001, Surgical landmarks to determine humeral head retrotorsion for hemiarthroplasty in fractures, *Journal of Shoulder and Elbow Surgery* **10 (5)**, 460–463.

Kaufler, T., Amis, A. and Emery, R.: 1998, Analysis of a glenoid component fixation designs in the rheumatoid scapula, *11th Conference of the ESB.*

Kelly, A.: 2003, *Design of a total shoulder/humerus replacement*, Master's thesis, University if Cape Town, Department of Mechanical Engineering.

Kelly, J. D. and Norris, T. R.: 2003, Decision making in glenohumeral arthroplasty, *The Journal of Arthroplasty* **18 (1)**, 75–82.

Kerner, J., Huiskes, R., van Lenthe, G., Weinans, H., van Rietbergen, B., Engh, C. and Amis, A.: 1999, Correlation between pre-operative periprosthetic bone density and post-operative bone loss in tha can be explained by strain-adaptive remodelling, *Journal of Biomechanics* **32**, 695–703.

Lacorix, D. and Prendergast, P.: 1998, 3d finite element analysis of of glenoid prosthesis for total shoulder arthroplasty, *11th Conference of the ESB.*

Lacroix, D. and Prendergast, P.: 1998, Stress analysis of glenoid component designs for shoulder arthroplasty., *Proceedings of the Institute of Mechanical Engineers: Engineering in Medicine* **Part H**, 211, 467.

Lewis, G., Fencl, R. M., Carroll, M. and Collins, T.: 2003, The relative influence of five variables on the in vitro wear rate of uncrosslinked uhmwpe acetabular cup liners, *Biomaterials* **24**, 1925–1935.

Lo, I. K., Bishop, J. Y. and Flatow, E. L.: 2003, Revison shoulder arthroplasty after failed total shoulder arthroplasty, *Operative Techniques in Orthopaedics,* **13 (4)**, 227–289.

Maloney, W. J.: 2002, Common threads in hip, knee, and shoulder arthroplasty, *The Journal of Arthroplasty* **17 No. 4 Suppl. 1**, 2.

Munnoch, D. A., Herbert, K. J., Morris, A. M. and Stevenson, J. H.: 1996, The deltoid muscle flap: anatomical studies and case reports, *British Journal of Plastic Surgery* **49**, 310–314.

Murphy, L. A., Prendergast, P. J. and Resch, H.: 2001, Structural analysis of an offset-keel design glenoid component compared with a center-keel design, *Journal of Shoulder and Elbow Surgery* **10 (6)**, 568–579.

Nagels, J., Stokdijk, M. and Rozing, P. M.: 2003, Stress shielding and bone resorption in shoulder arthroplasty, *Journal of Shoulder and Elbow Surgery* **12 (1)**, 35–39.

Nicholson, G. P.: 2003, Treatment of anterior superior shoulder iinstability with a reverse ball and socket prosthesis, *Operative Techniques in Orthopaedics* **13 (4)**, 235–241.

Nwakama, A. C., Cofield, R. H., Kavanagh, B. F. and Loehr, J. F.: 2000, Semiconstrained total shoulder arthroplasty for glenohumeral arthritis and massive rotator cuff tearing, *Journal of Shoulder and Elbow Surgery* **9 (4)**, 302–307.

Pearl, M. L., Kurutz, S., Robertson, D. D. and Yamaguchi, K.: 2002, Geometric analysis of selected press fit prosthetic systems for proximal humeral replacement, *Journal of Orthopaedic Research* **20**, 192–197.

Rittmeister, M. and Kerschbaumer, F.: 2001, Grammont reverse total shoulder arthroplasty in patients with rheumatoid arthritis and nonreconstructible rotator cuff lesions, *Journal of Shoulder and Elbow Surgery* **10 (1)**, 17–22.

Stein, H. L.: 1999, *Ultra High Molecular Weight Polyethylene (UHMWPE)*, ACMInternational.

Stoffel, K., Dieter, U., Stachowiak, G., Gächter, A. and Kuster, M. S.: 2003, Biomechanical testing of the lcp – how can stability in locked internal fixators be controlled?, *International Journal of the Care of the Injured* **34**, S–B11 – S–B19.

Tamai, K., Hamada, J., Ohno, W. and Saotome, K.: 2002, Surgical anatomy of multipart fractures of the proximal humerus, *Journal of Shoulder and Elbow Surgery* **11 (5)**, 421–427.

Torchia, M. E., Cofield, R. H. and Settergren, C. R.: 1997, Total shoulder arthroplasty with the neer prosthesis: long-term results, *Journal of Shoulder and Elbow Surgery* **6 (6)**, 495–505.

Ullman, D. G.: 1997, *The Mechanical Design Process*, 2nd edn, McGraw-Hill.

Viceconti, M., Muccini, R., Bernakiewicz, M., Balean, M. and Cristofolini, L.: 2000, Large sliding elements accurately predict levels of bone-implant micromotion relevant to ossoeintegration., *Journal of Biomechanics* **33**, 1611.

Viceconti, M., Olsen, S. and Burton, K.: 2005, Extracting clinically relevant data from finite element simulations, *Clinical Biomechanics* **20**, 451–454.

Wagner, M.: 2003, General principles for the clinical use of the lcp, *International Journal of the Care of the Injured* **34 (2)**, S–B31 – S–B42.

Warton, C.: 2002, The upper limb. Medical School in house anatomy text book.

Appendix A

Ball Neck Strength Calculations

Contents

A.1 Introduction **A1**
A.2 Method **A2**
A.3 Results **A2**
A.4 Conclusion **A4**

Figures

A.1 Ball and stem representations A3
A.2 Shear, moment, and deflection of beams A3
A.3 3D ABAQUS neck test model. A4

Tables

A.1 Results A4

A.1 Introduction

The $\varnothing 20mm$ Co-Cr-Mo ball that articulates with a UHMWPE socket is located at the end of a stem; the ball and stem are machined as one, Fig. A.1(a).

To create the largest window of mobility the neck of the stem is $\varnothing 6mm$. There was concern over its strength thus a simplified ABAQUS model was generated to calculate the structure's failure point, Fig. A.1(b). The results are given in Table A.1 and the ABAQUS model was verified using simple beam theory see Fig. A.2.

A.2 Method

The ABACUS model was created using 8-node linear brick elements and was loaded using a pressure distribution P, with the centre of pressure located $19mm$ from the encased border, Fig.A.1(b). A Young's Modulus of $200GPa$ and poisson's ratio of 0.3 were used. The model was progressively loaded until the Von Mises stress of an element reached the yielding point of the material; this was defined as $830MPa$ from *Biomaterials Ltd.* (Appendix D), Fig.A.3. The deflection of the beam at $19mm$ and the pressure distribution converted to force is given in Table A.1. A beam deflection calculation was then carried out using the force calculated in ABACUS, and the resulting deflection was then compared to the one generated by ABACUS. As the deflections are very similar to the ABACUS model we can safely say the model is accurate enough.

A.3 Results

Yielding of the Co-Cr-Mo was taken as the failure; this occurred at $2540N$, with a safety factor of 2 this becomes $1270N$. This is an extremely high load for a patient to place on their shoulder and would equate to carrying a $129kg$ load in one hand.

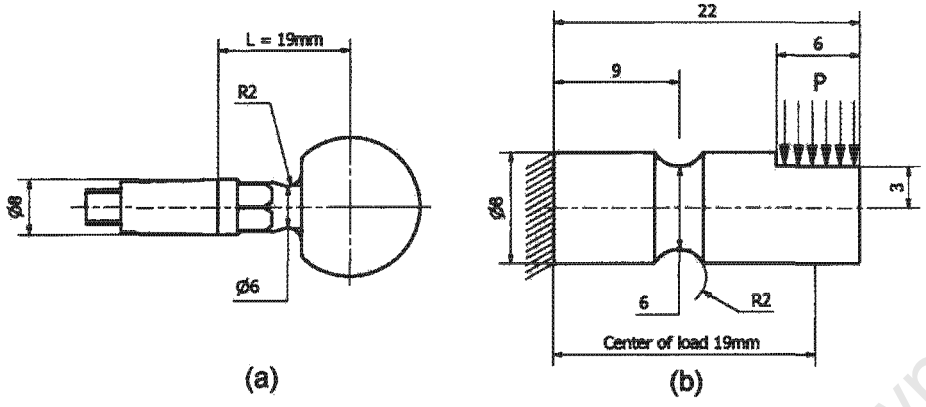

Figure A.1: Ball and stem representation: (a) ball and stem used in prosthesis, (b) the simplified ABACUS stem.

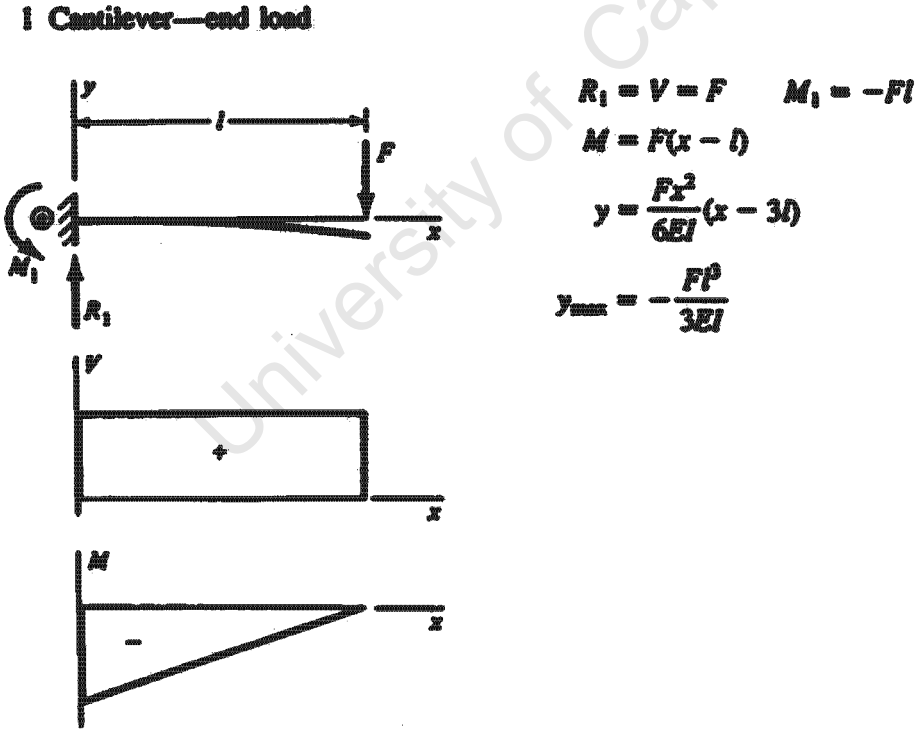

Figure A.2: Shear, moment, and deflection of beams (Shigly and Mischke, 1989, p.735).

Table A.1: Calculated displacements using beam theory and ABAQUS, round shafts of constant cross-section were used in the beam theory calculations.

Test Method	Force $[N]$	Displacement in y $[mm]$
Beam Theory $\varnothing 8mm$	2540	0.14
Beam Theory $\varnothing 7mm$	2540	0.25
ABAQUS	2540	0.25

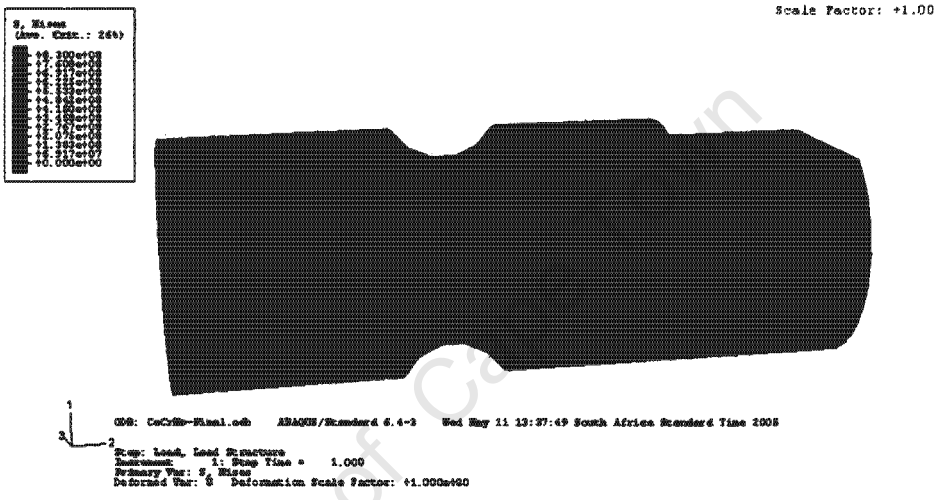

Figure A.3: 3D ABAQUS neck test model.

A.4 Conclusion

The $\varnothing 6mm$ Co-Cr-Mo neck will not fail under normal loading and with the high fatigue strength of Co-Cr-Mo and the relatively low loading that a shoulder joint undergoes with no rotator cuff or deltoid, fatigue is not a concern.

Tables

B.1 FEA dislocation forces B8

B.1 Introduction

This appendix report deals with the testing of a design concept for the link. The design is made up of a shallow socket into which a spherical ball is pressed. Once this is complete, the coupled socket and ball are then inserted into a rigid housing and locked in place by a wire fed into a machined groove (Fig. B.1). The housing constrains the socket and increases the force necessary to dislocate the ball.

There is a finite maximum retention force that a press fitted joint can achieve when working with a standard ball size. This maximum limit is set as a result of plastic deformity taking place in the socket as the ridged ball is initially pressed into the socket. The permanent plastic deformity that results is undesirable as it compromises the long term life of the joint. The other extremely important consideration is what will occur during the *in vivo* life span of the joint. Wear is a major concern as even a small amount of wear in the correct place will constitute an enormous increase in the risk of failure. The upper limb also provides a long lever arm which when loaded at its distal end creates a formidable moment on the shoulder joint and this has been the main cause of failure for previous constrained TSR designs (Zadeh and Calvert, 1998).

The main aim of this study is to find the maximum holding force of the discussed design and determine the design's controlling factors. The final

Appendix B

Press-Fit Socket Report

Contents

B.1 Introduction **B2**
B.2 Method **B3**
B.2.1 Interference Fit Calculations B4
B.2.2 FEA Model B5
B.2.3 Experimental Model B6
B.3 Results **B8**
B.3.1 FEA Results B9
B.3.2 Experimental Results B9
B.3.3 Comparison of Results B11
B.4 Discussion **B14**
B.5 Conclusions **B16**

Figures

B.1 Cross section of the ball, socket and housing. B3
B.2 Press-fit socket dimensions. B4
B.3 The FEA modeling set-up. B5
B.4 Zwick compression cradle. B6
B.5 The Zwick test set-up. B7
B.6 Socket FEA results B10
B.7 Displacement vs. reaction force on the ball. B11
B.8 Reaction force for both FEA and experimental results. . . B12
B.9 Comparison of break out force and push in force B13
B.10 Point of ball dislocation B14
B.11 The reaction force experienced on the FEA rigid ball. . . B15

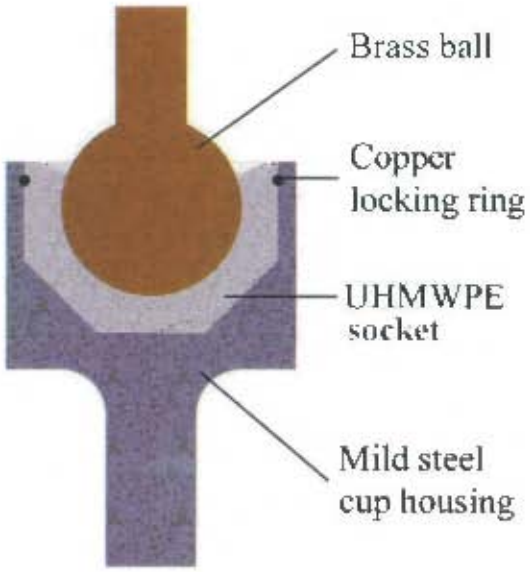

Figure B.1: Cross section of the ball-in-socket test joint held in the place by a wire locking ring and the rigid steel housing.

aim is to find a suitable linking component for use in a constrained shoulder joint that will fortify the oncologist's arsenal in facilitating limb salvage where muscle loss in the joint area is a major factor.

B.2 Method

As space constraints are one of the deciding factors in the design of a shoulder prosthesis, a $\varnothing 20mm$ diameter spherical ball was chosen as the test standard. This is the smallest commercially available Co-Cr-Mo ball for use in medical implants. The material used for the sockets was UHMWPE, as this is the only biologically compatible material suited for the design due to its good wear properties. The design was generated as follows; first rough calculations were carried out using interference fit theory (Shigly and Mischke, 1989) and then these values were used to formulate an analytical model using the Finite Element Analysis (FEA) package ABAQUS (HKS, USA). Computer

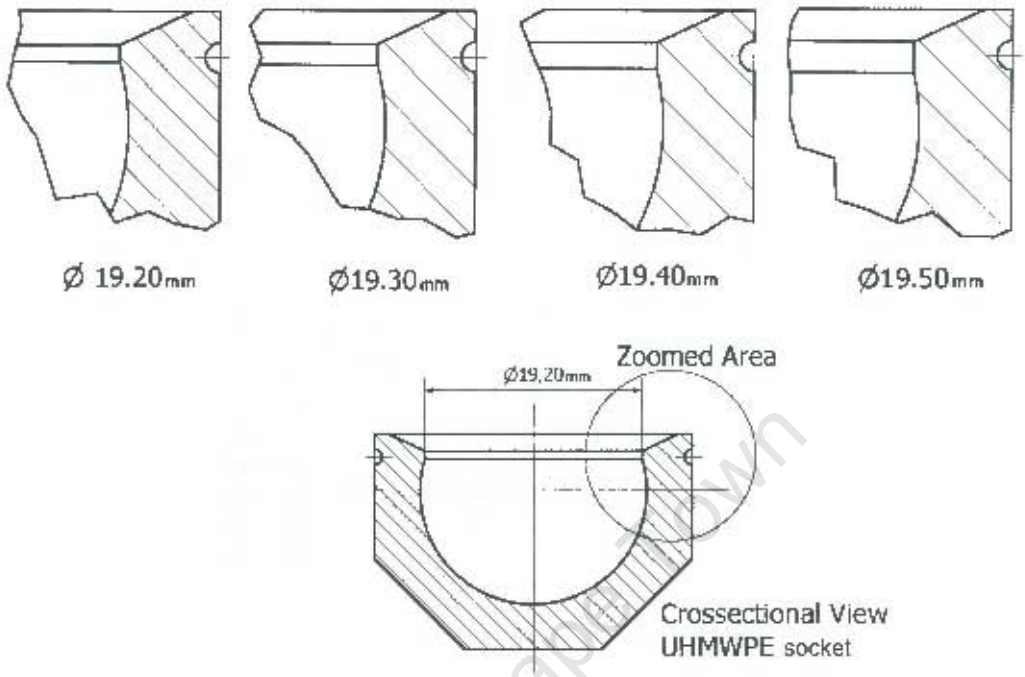

Figure B.2: The change in shape of the socket as the entry diameter increases.

simulations were carried out keeping the over-all dimensions of the socket constant, while changing the inlet diameter (Fig. B.2). This changed the degree of plasticity the socket undergoes until an entry diameter was found where the initial pressing in of the ball resulted in slight or zero residual stresses. The data from the FEA simulations was then used to design the sockets that were later experimentally tested on the Zwick tensile tester in the UCT Materials Engineering Department.

B.2.1 Interference Fit Calculations

When two cylindrical parts are assembled by shrinking or press-fitting one part upon another, a contact pressure is created between the two parts (Shigly and Mischke, 1989). The stresses resulting from the contact pressure can then be calculated using the equations found in Shigly and Mischke (1989), pg.62

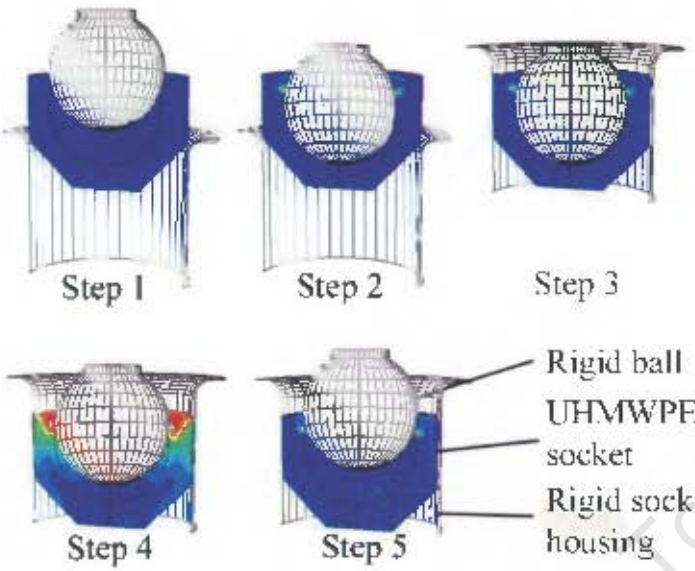

Figure B.3: The FEA modeling set-up.

& 63. It is assumed that the the socket and ball are cylinders. The results showed the UHMWPE would experience plasticity at an inner diameter of $\varnothing 19.40mm$. This information was then used in formulating the FEA model.

B.2.2 FEA Model

The model was made up of three components; a ball and housing both modelled as rigid and the socket modelled as UHMWPE, with a Young's modulus and Poisson's ratio of $0.8GPa$ and 0.25, respectively. The point at which the UHMWPE experienced plasticity was $22MPa$ (Hench and Ethridge, 1982). The system was modelled as quasi-static where no dynamic influences were taken into account. The analysis procedure can be seen in Fig. B.3 where the ball is pushed into the socket in Step 1. In Step 2 the rigid housing is moved up to incase the socket and finally in Step 3 the ball begins to dislocate. The points that were monitored on the model were the reaction force on the ball and the ball's position relative to the center of the socket. A temperature

(a) (b)

Figure B.4: Insertion of a ball into a socket using the Zwick compression cradle (a) and the set-up of an empty cradle on the Zwick (b).

variation was not modelled.

B.2.3 Experimental Model

Once the FEA model was complete, an inlet diameter range between $\varnothing 18.85mm$ and $\varnothing 19.55mm$ was selected for testing, as this would cover the range in which plasticity was taking place in the FEA model. This range would also give some extra room to explore what would happen when the UHMWPE was experiencing plasticity on the initial insertion of the ball.

The manufacture of the sockets proved to be difficult, as a high machining tolerance of five microns was necessary. This was achieved using the the HURCUS 2000 PC lathe, in the Department of Mechanical Engineering at UCT . A single extrusion of UHMWPE $\varnothing 30mm$ rod was used in the manufacture, a specially designed lathe cutter was also needed (Appendix E).

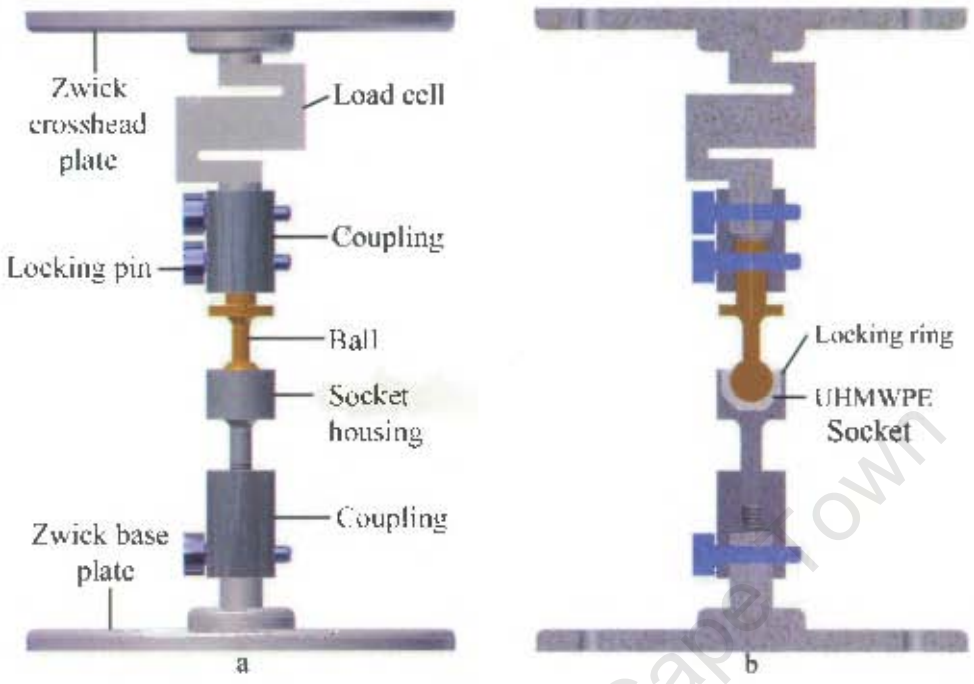

Figure B.5: The Zwick test set-up.

The cutter made it possible to produce the undercut on the socket and it was manufactured by *Schuurman Engineering* using wire erosion to achieve the high accuracy necessary. A $\varnothing 20.00mm$ spherical brass ball was also machined on the HURCUS 2000 PC lathe. Brass was the chosen material as it would be rigid enough for the testing and the softness of the brass would ease the manufacture process and facilitate the high tolerances necessary.

The testing was carried out in two stages during a single week to limit testing error. All tests were carried out on the Zwick tensile tester in the UCT Materials Engineering Department using the $10kN$ load cell. The test set-up consisted of a compression cradle for the insertion of the ball into a socket (Fig. B.4). The compression cradle allows the tester to be able to test in tensile mode at all times. Testing in compression is more complicated and can cause extraneous errors to creep into the data, especially when loads as

Table B.1: FEA dislocation forces

Inlet diameter $[mm]$	Dislocation force $[N]$
∅19.30	444
∅19.40	396
∅19.50	344

low as a $100N$ are being measured. The ball is dipped into saline solution prior to being inserted into the socket. This is to lubricate the system and prevent unnecessary shearing damage on the socket during insertion. Once the ball is inserted, the socket and ball link are removed from the compression cradle. The ball is then rotated in the socket to make sure that the inside of the socket is fully coated with saline solution as this replicates *in vivo* conditions. The ball-in-socket is then inserted into a mild steel housing, followed by the wire clip (Fig. B.5). The complete link system is then fitted to the Zwick using specifically designed couplings (Appendix E). The ball is then dislocated from the socket and the two measurements taken are the tensile force given by the load cell and the displacement of the Zwick cross head.

B.3 Results

The results showed a good correlation between the analytical FEA model and experimental data. There were however, marked differences in comparing the shape of curves. The experimental results will always be explained with regard to the FEA results as the FEA results have fewer external factors influencing the outcome. The external factors present in the experimental set-up are the test rig, friction and the presence of air.

B.3.1 FEA Results

The results showed a 300% increase in holding strength when the rigid housing was in place. Three simulations were carried out for the following inlet diameters: $\varnothing 19.30mm$, $\varnothing 19.40mm$ and $\varnothing 19.50mm$. The $\varnothing 19.40mm$ was the maximum calculated inlet diameter before plasticity occurred on insertion (Fig. B.2). There is $52N$ increase in the force necessary to dislocate the ball from the socket by decreasing the inlet diameter from $\varnothing 19.50mm$ to $\varnothing 19.40mm$ and another increase of $48N$ from $\varnothing 19.40mm$ to $\varnothing 19.30mm$ (see Table B.1). This is an almost linear trend for those three test points.

The visual analysis of an analytical model is very helpful in the design process, as long as the limitations and model are well understood. In Fig. B.6 one can see the lip of the socket undergoing plastic deformation at the central area where the socket has a light grey color. The image was captured for an inlet diameter of $\varnothing 19.40mm$ at the point of dislocation. A visual representation of the stress distribution throughout the socket is helpful in improving the design of socket shapes.

B.3.2 Experimental Results

The dislocation forces attained by the experimental results were in good correlation with the FEA simulations. The factor that created the dissimilarities in the curve shapes was the presence of air in the experimental set-up. Air trapped inside the socket during the insertion of the ball becomes pressurized, which increases the insertion force necessary and shifts the experimental curve down. While dislocating the ball, a vacuum is formed in the socket. This is shown in the experimental results by a dramatic increase in the reaction force in the first millimeter of the ball's displacement (Fig. B.8). The other factor creating differences in the results, is that in the FEA model the

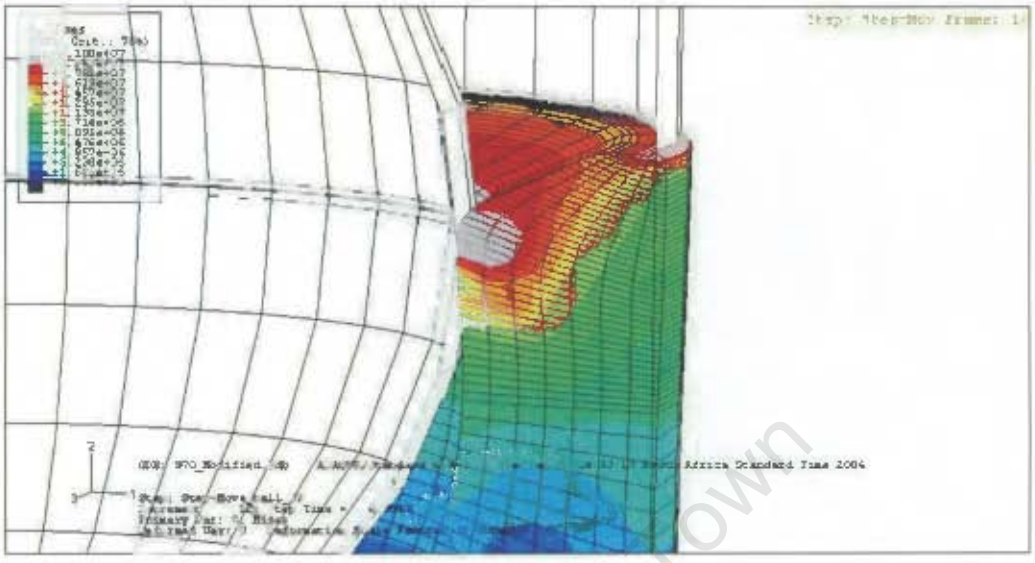

Figure B.6: A closer look at the sockets lip shows the FEA results as the ball experiences its maximum reaction force (generated in ABAQUS).

ball-in-socket is modelled as frictionless, whereas friction plays a role in the physical experiment. Nevertheless, the author does not believe friction is the primary contributing factor to the discrepancies between the FEA and physical results. Once the inlet diameter drops below $\varnothing 19.20mm$ there is a drop of between $100N$ and $50N$ in the reaction force during the first millimeter of displacement after which the normal shape of the curve resumes (Fig. B.7). This may be explained by the presence of a sheer plane occurring and giving way, creating a reduction in the reaction force. Once this has occurred, large scale plastic deformation takes place and the reaction force once again increases. This occurs due to the larger lip which would transfer the reaction force onto a hypothetical sheer plane lying on a $10mm$ radius taken from the centre of the socket.

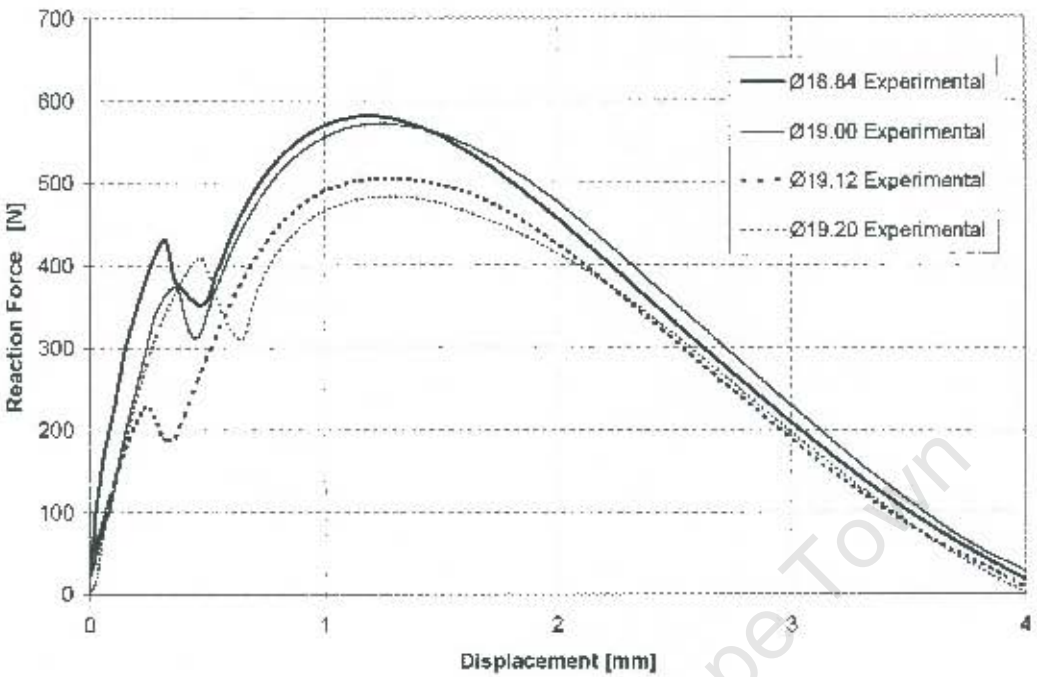

Figure B.7: The displacement of the ball vs. the reaction force experienced by the ball

B.3.3 Comparison of Results

When comparing the FEA and experimental data in Fig. B.8, there is a negative $100N$ reaction force on the ball in the FEA simulations, however, this is not present in the experimental simulation. The negative reaction force in FEA can only be from the reaction force the UHMWPE is applying on the ball due to the elastic energy it has gained during the dislocation step. The absence of this negative reaction force in the experimental results could be explained by the play in the test set-up. When the ball is in tension the play is taken up and does not influence the results, however, as the socket exerts a negative reaction force, only $2mm$ of play needs to exist in the system for the negative reaction force not to register on the load cell. The main concern in this experiment is the maximum reaction force on the ball during dislocation,

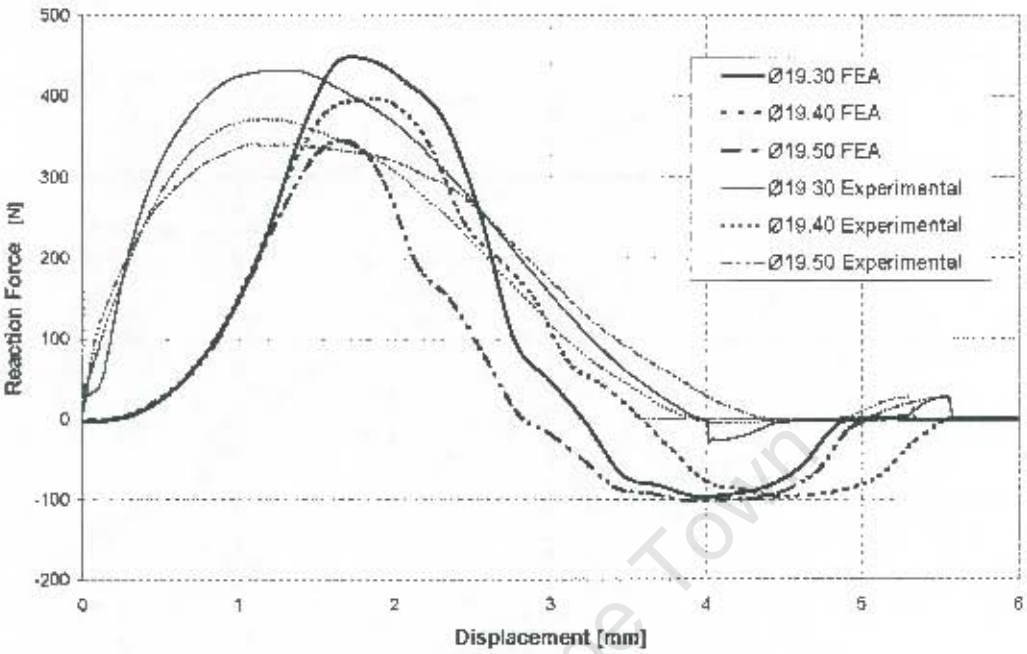

Figure B.8: Displacement vs. reaction force showing both FEA and experimental results.

thus no attempt was made to remove the play in the system and make the test set-up rigid.

The FEA data for the maximum reaction force during the break-out step lies within the experimental data as seen in Fig. B.9. This is an excellent validation of the FEA model. Due to the presence of air in the experimental set-up, the increased force necessary for the insertion step can be explained by a pressurized pocket of air forming in the UHMWPE socket. There is too little data present in the $\varnothing 18.85mm$ and $\varnothing 19.00mm$ range to make any conclusive assertions for the flattening of the maximum reaction force at dislocation.

The displacement the ball undergoes relative to the centre of the socket gives insight into the consistency of the experimental data, while not only looking

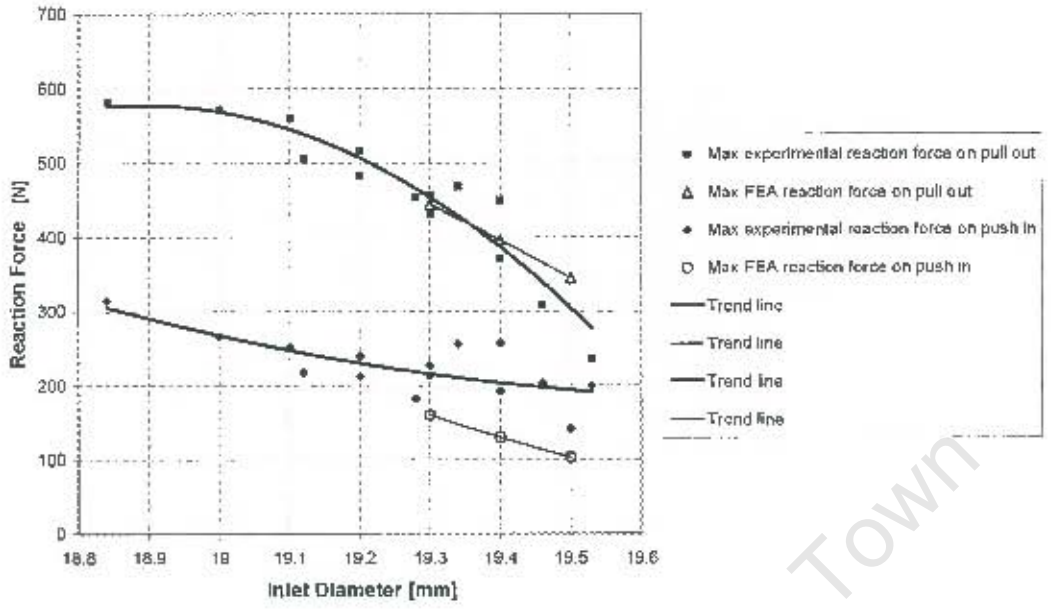

Figure B.9: Comparing the maximum reaction force during the dislocation of the ball, with the maximum force needed to push the ball into the socket.

at the maximum break out force. In Fig. B.10 one can see a consistent break out point at a mean displacement of $1.25mm$ from the center of the socket at entrance diameters below $\varnothing 19.30mm$. The scattering of the data for larger entrance diameters could be explained by the longer inlet wall produced at larger diameters see Fig. B.2. In the FEA simulation the ball dislocates consistently at a displacement of $1.75mm$ from the center of the socket. As there is a vacuum forming in the experimental socket, the break out point is not as distinct as the FEA break out points and in many instances is dragged out to about the same point as the FEA break out points as seen in Fig. B.8.

As the ball is pushed into the socket, the ball experiences a negative reaction force. There is a transition area where the force goes from positive to negative. This is the point at which the socket begins to pull the ball into the housing as the lip clips the ball into place and finally, the positive reaction force dissipates and goes to zero as the ball is centralized in the socket

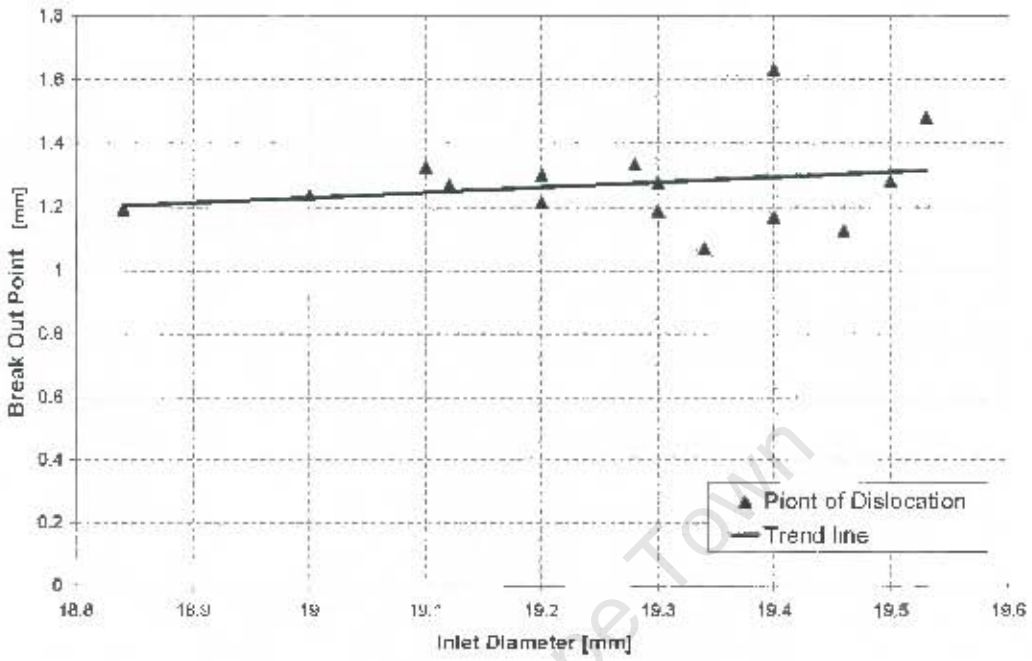

Figure B.10: The point at which dislocation takes place relative to the center of the ball vs the inlet diameter of the socket.

(Fig. B.11). The differences in the experimental data and the FEA model are hard to explain as there are many factors involved. The use of a compression cradle, the pocket of trapped air being pressurized in the socket and the play that is present in the test rig could all influence the outcome of the data in some way.

B.4 Discussion

When validating an FEA model in future, the model could include air. This is however, computationally expensive and time-consuming. The other alternative would be to drill a hole in the base of the socket and housing small enough not to influence the structural strength of either component and this would allow the air to escape with ease. An increase in the strength of a

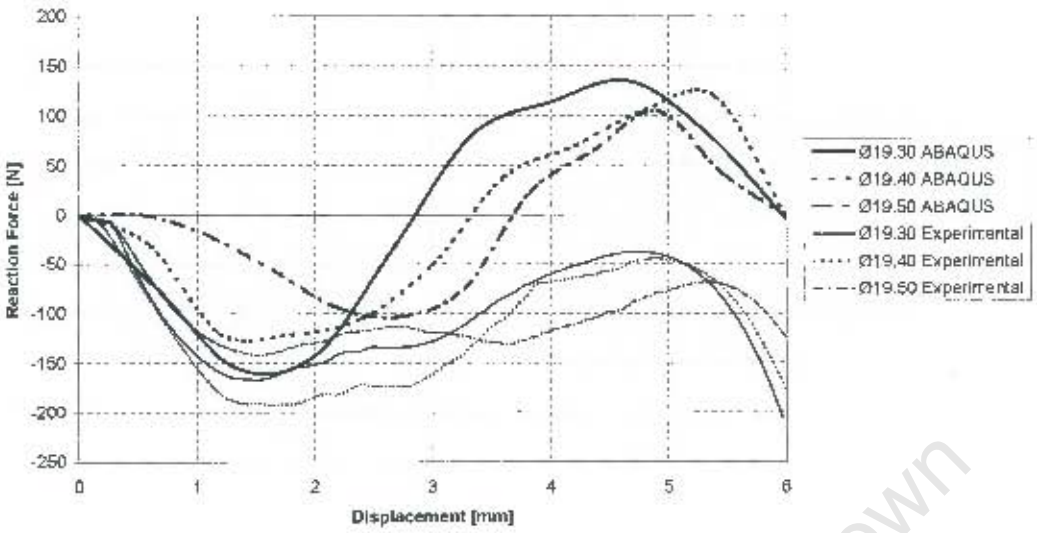

Figure B.11: The reaction force experienced on the FEA rigid ball.

press-fit socket can also be achieved by heating the UHMWPE socket before the insertion of the ball.

Temperature variation has not been taken into account as an internal prosthesis functions at the *in vivo* temperature of 37°C. The testing has been carried out at 21°C, thus the prosthesis would undergo a 16°C temperature rise under *in vivo* conditions. The thermal expansion may influence the results dramatically as the size of the lip only makes up 2% of the outside diameter of the socket. It is possible to model this change in temperature using FEA simulations and in the future redesign of the socket, this will be factored into the simulation. The dislocation due to a moment will also be calculated and accommodated for, as there is no need for the full mobility of a healthy anatomical shoulder as the muscle is not present to accommodate this movement.

B.5 Conclusions

The UHMWPE press-fit ball-in-socket does not have enough retaining force to be applied in a constrained total shoulder replacement. An alternative design is tested in Appendix C using FEA. The correlation between the FEA model and experimental results was extremely good, and future designs will be tested using only FEA.

Appendix C

Constrained Socket Report

Contents

C.1 Introduction **C2**
C.2 Method **C3**
C.2.1 Tensile Dislocation Models C3
C.2.2 Moment Dislocation Model C6
C.3 Results **C7**
C.4 Conclusions and Recommendations **C11**

Figures

C.1 Axisymmetric model at the start of the simulation. C2
C.2 *In vivo* temperature effects C4
C.3 Modeling of the locking clip C5
C.4 Axisymmetric temperature model with no stress C6
C.5 Plastic yielding in tension C8
C.6 Location of Node C and maximum deformation C8
C.7 3D tensile model C9
C.8 3D moment model showing pivoting C9
C.9 Point at which plastic yielding will take place in bending . C10

Tables

C.1 FEA models generated. C4
C.2 Material properties. C6

C.1 Introduction

In the previous press fit socket report it was concluded that a dislocation force of $400N$ was not sufficient for a constrained total shoulder replacement (TSR). A new concept was generated to increase the dislocation force, the idea was to split the UHMWPE socket in two halves with the Co-Cr-Mo ball being inserted from below instead of pressed in from above as seen Fig. C.1.

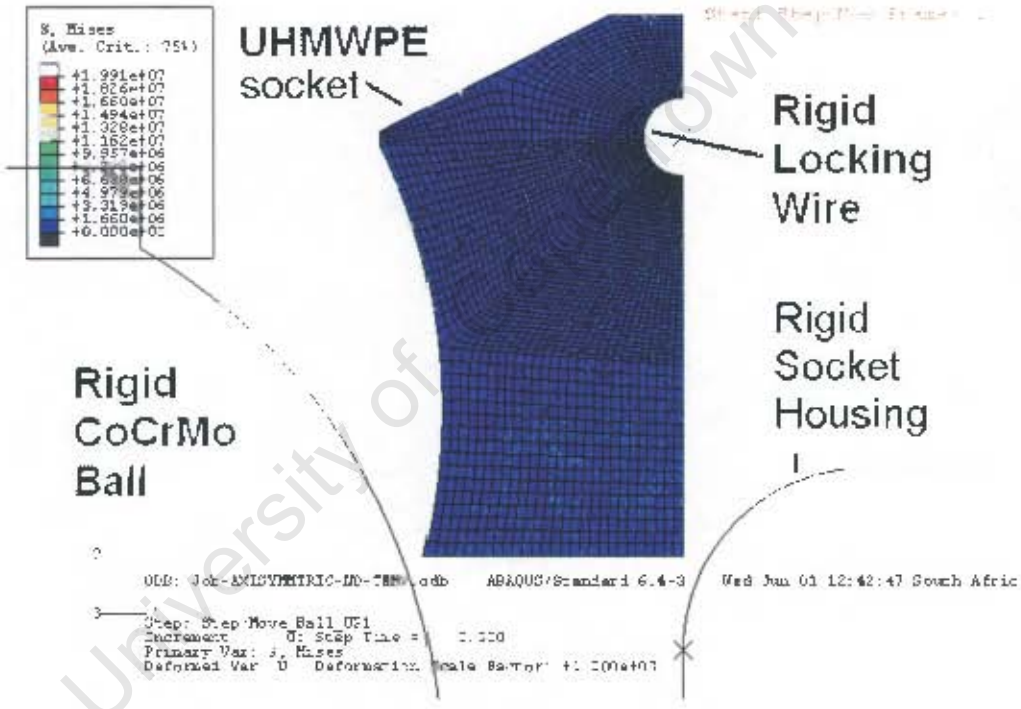

Figure C.1: Axisymmetric model at the start of the simulation.

In using this method one can increase the size of the lip and in so doing, increase the force needed to dislocate the ball. There are however drawbacks to using this design. The first being a reduction in the range of motion of the system and secondly, the split line creates a point of weakness at which wear could be increased on the UHMWPE socket. Appendix B compares experimental results with FEA models. One of the conclusions reached is

that the correlation between FEA and the experimental data is good and therefore it was decided to concentrate on the FEA modeling.

The new concept is modelled in both axisymmetric and solid FEA elements. The axisymmetric model incorporated the temperature increase due to the body being at 37°C. While the solid model was generated to simulate the ball-and-socket dislocating under a moment, as this is the most unstable condition to which the ball-and-socket is subjected. Moment dislocation can not be modelled using axisymmetric elements, as the problem is not symmetrical around the central axis. Using a solid model increases the complexity of the simulation and one must simplify the model, to reduce computational expense. All assumptions and simplifications are given in section C.2.

C.2 Method

The four models generated are listed in Table C.1. The effects of *in vivo* temperature on the system was modelled using a simple axisymmetric model. The result was a 2% increase in dislocation force needed to produce yielding in the UHMWPE socket. In Fig. C.2 the reaction force on the ball can be seen at a room temperature of 21°C and an *in vivo* temperature of 37°C simulation. Including temperature changes increases the complexity of the model and is unnecessary in this case as the influence of temperature on the dislocation force is only 2%. Thus temperature was neglected in subsequent solid models.

C.2.1 Tensile Dislocation Models

The material properties used for the models are given in Table C.2 and if more information is required, the material data sheets can be found in Appendix D.

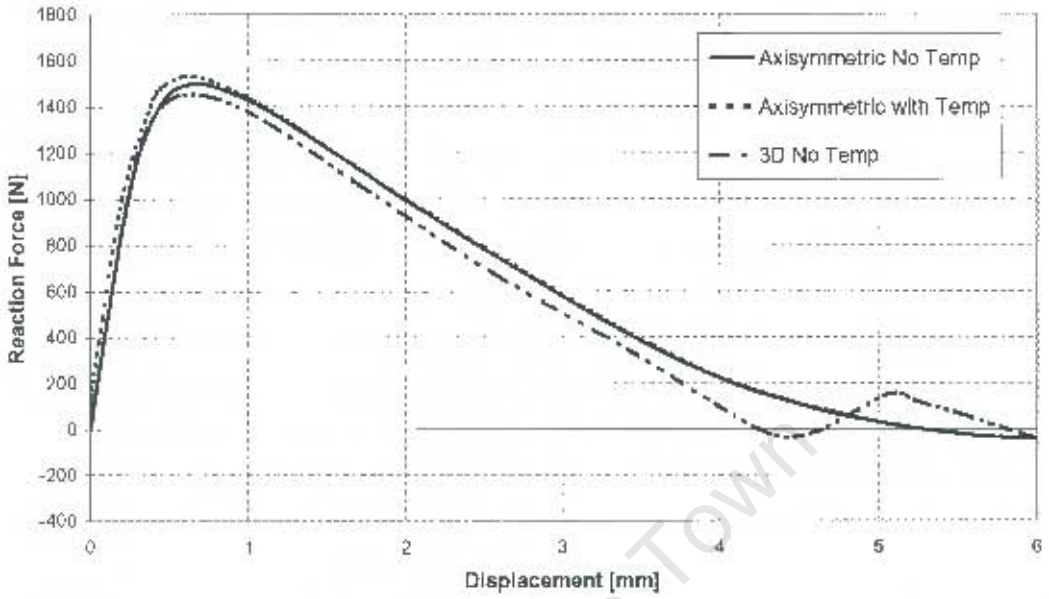

Figure C.2: *In vivo* temperature effects on a constrained UHMWPE socket.

As the computational cost of running the axisymmetric model was low, it was possible to model the interactions between the rigid locking wire and the UHMWPE socket as seen in Fig. C.3. The locking clip is made up of analytically rigid elements and its position is fixed. The interaction between the UHMWPE socket and the locking clip are modelled as frictionless, as this is the most severe condition the two could interact under; friction would add rigidity to the system. The simulation is made up of three steps: in step 1 the ball is inserted into the socket from below, in step 2 the housing is moved into position and locked, in step 3 the ball is dislocated by moving it

Table C.1: FEA models generated.

Model Type	System Modelled	Include Temperature Effects
Axisymmetric	Pull out	No
Axisymmetric	Pull out	Yes
3D Solid	Pull out	No
3D Solid	Roll Out	No

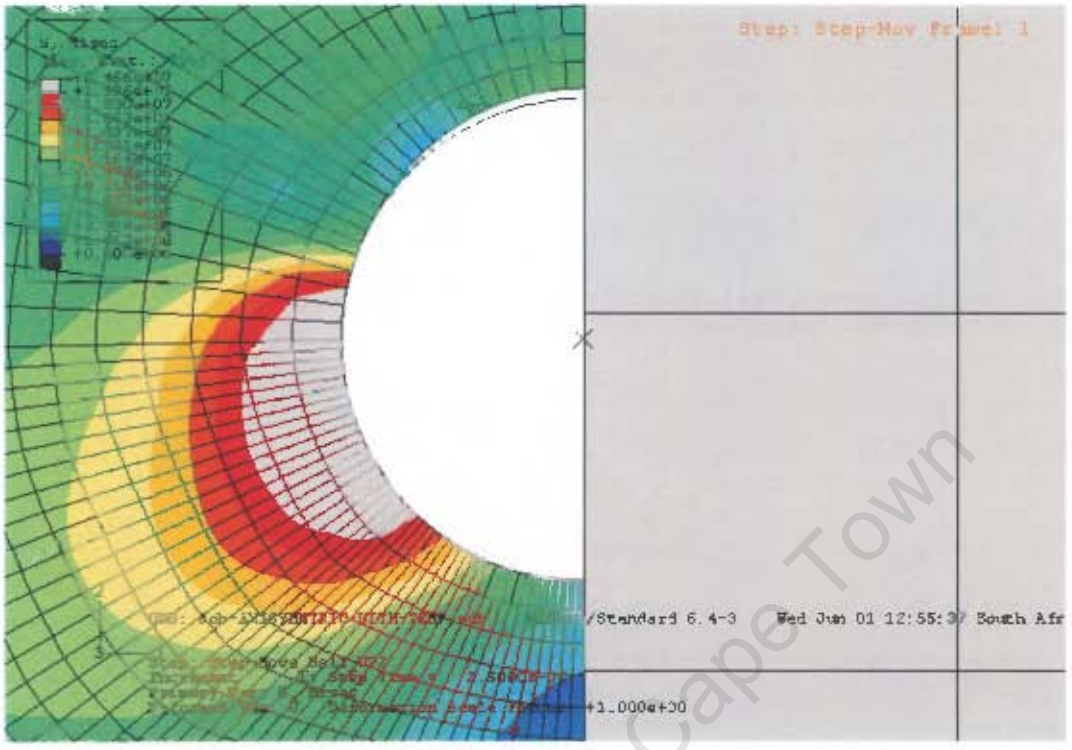

Figure C.3: Closer look at the modeling of the locking clip in the *in vivo* axisymmetric model.

vertically $6mm$ and during this linear motion the reaction force on the ball is calculated (Fig. C.4). The interaction between the housing surface and the socket is also modelled as frictionless contact, as is the interaction between the ball-and-socket.

An axisymmetric simulation carried out at room temperature was used to locate a nodal point in the socket where yielding of the material takes place first. Once this point was located, data was extracted from the nodal point. Using this information and the reaction force on the ball, one can determine at which reaction force yielding of the material takes place.

The solid model, used to simulate a dislocation under an applied moment, was also used to model dislocation of the ball and socket under tension.

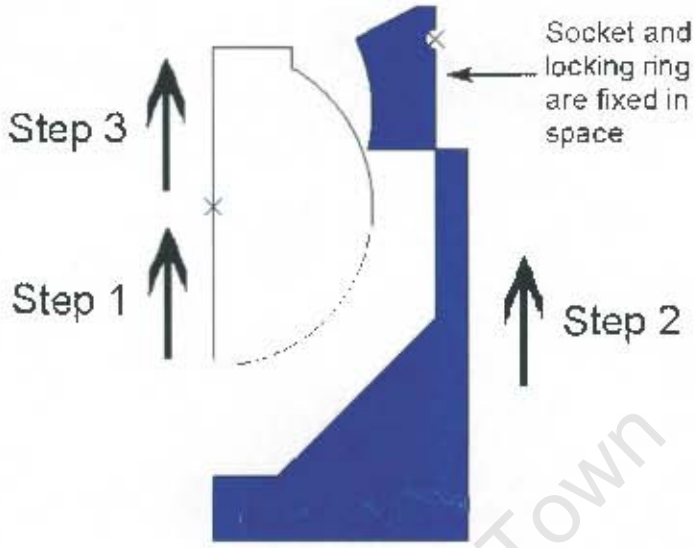

Figure C.4: Axisymmetric temperature model at the beginning of simulation.

Table C.2: Material properties.

Property	Units	UHMWPE	Ti6Al4V	CoCrMo
Density ρ	kg/m^3	930	4420	8500
Coefficient of expansion α	$m/m°C$	1.6×10^{-4}	-	-
Young's Modulus E	GPa	0.8	116	200
Possions Ratio ν	-	0.25	0.3	0.3
Proof stress σ_p	MPa	22	892	830

This was done to compare the solid model and the axisymmetric model as the latter had already been validated experimentally. The same interactions were used in both tension and moment dislocation simulations.

C.2.2 Moment Dislocation Model

To reduce the complexity of the moment dislocation model, the interaction between the rigid locking wire and the socket was not modelled. The simulation was also carried out in one step. The ball, housing and socket were all preassembled and the single step carried out was the ball being rotated $0.2 radians$. The ball was able to move vertically and laterally only; all other

degrees of motion were constrained. This limited to what point the ball could be dislocated as it would become a free body once it lost contact with the socket and the model would be come unstable. The interaction between the socket and ball, as well as the interaction between the housing and socket were modelled as hard frictionless contact. The lower outer wall of the top half of the UHMWPE cup was fixed to the housing. This was because the locking ring was not modelled.

C.3 Results

The split socket had a 125% increase in the force needed to produce yielding in the socket. Using Fig. C.5 the calculated force at which yield would take place was $900N$ in comparison to the press fit socket system which dislocated at $400N$. The constrained socket and press fit socket systems produce a 90° and 104° window of mobility respectively and the 13.5% reduction in mobility is the trade off for a larger dislocation force. Material yield took place at the same time around the locking ring and node C (Fig. C.6(a)). If friction was modelled, it is assumed that node C would be the first to experience yielding. In Fig. C.6(b) one can see what the final shape of a full dislocated socket looks like in a axisymmetric FEA model.

There were two points of interest on the moment model; the point where the stem contacts the rim of the socket Node B, and Node A where the ball pushes against the lip of the socket (Fig. C.7(a) and C.9(a)). Only $2.5Nm$ was needed to cause the UHMWPE to yield. Once the stem makes contact with the Ti-6Al-4V housing rim it begins to pivot on it (Fig. C.8(b)). Node A reaches plastic yield at $15Nm$ (Fig. C.9).

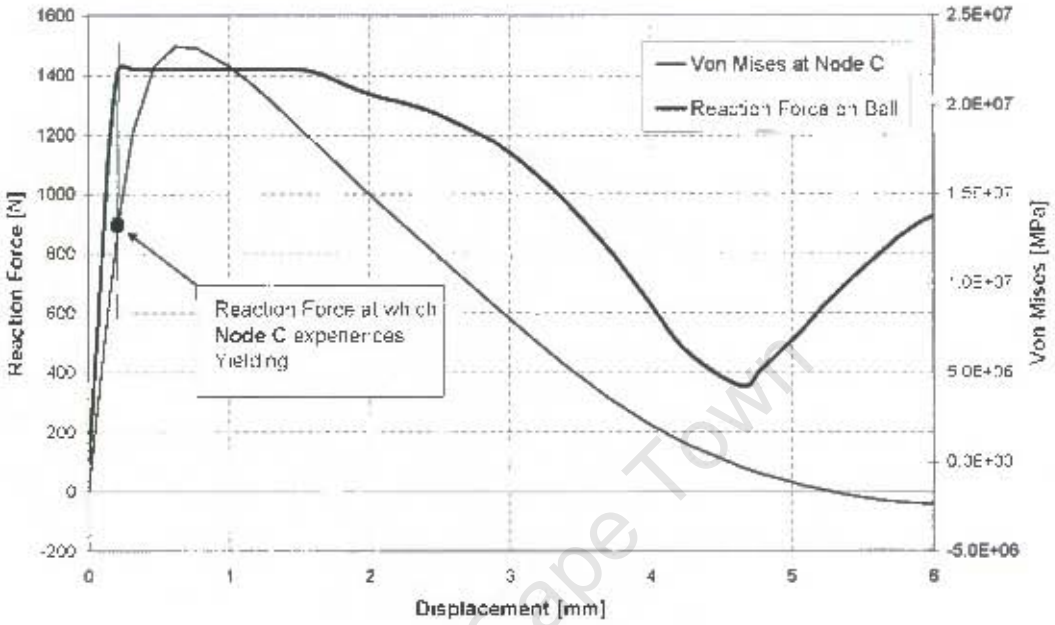

Figure C.5: Finding the tensile load at which Node C (Fig. C.6) experiences plastic yield.

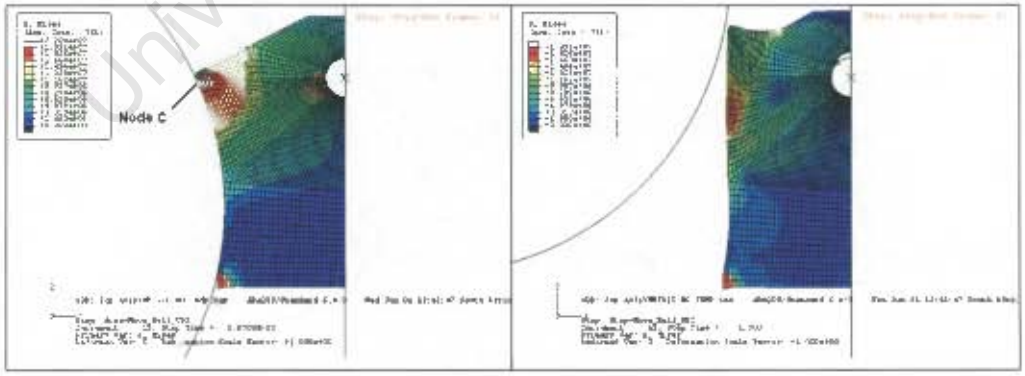

Figure C.6: Location of Node C (a) and Maximum deformation of the axisymmetric model (b).

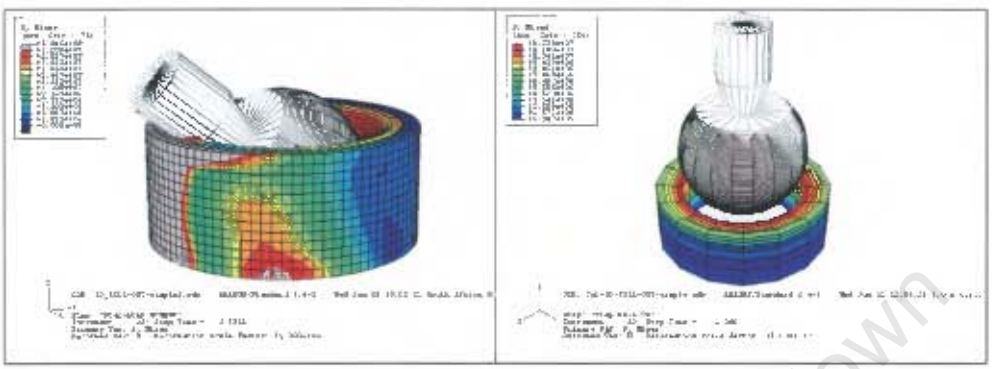

Figure C.7: 3D tensile model with residual Von Mises stresses shown (a) and 3D moment model (b).

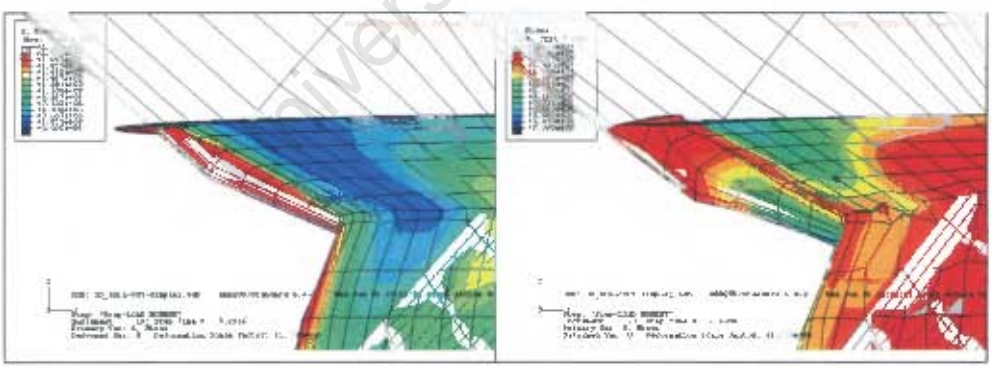

Figure C.8: 3D moment model showing pivoting on the edge of the Ti-6Al-4V housing, before pivot begins (a) and during pivoting (b).

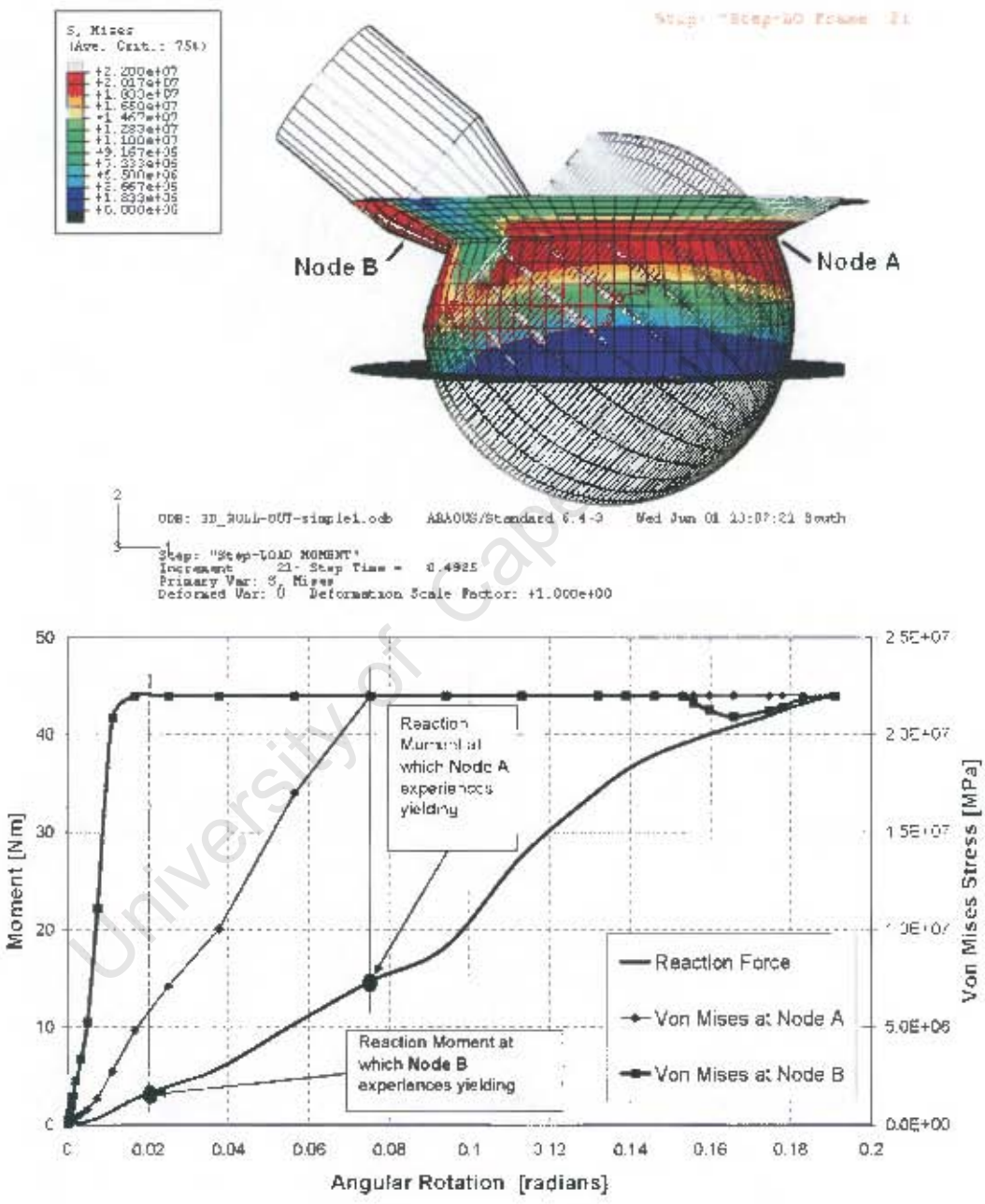

Figure C.9: Finding the moment load at which Nodes A & B experience plastic yield.

C.4 Conclusions and Recommendations

The split socket concept is an improvement on the press-fit concept, however the low moment of $15Nm$ needed to produce plastic yielding on the lip is worrying. Using a split socket it is possible to assemble a metal on metal prosthesis. This may solve the problem associated with UHMWPE and the low moment dislocation forces as a relatively small lip would produce a strong constrained link. However, there would be other concerns regarding impact wear on the lip and stem of the socket and ball, respectively .

Appendix D

Supporting Information

Contents

D.1 Letter of ethics approval D2
D.2 Delta brochure D4
D.3 Biomet Mosaic brochure D29
D.4 Biomet Bi-Polar brochure D35
D.5 Synthesis LCP Brochure D37
D.6 Sawbones catalogue D39
D.7 ASTM cortical screw standards D43
D.8 Material properties D47

UNIVERSITY OF CAPE TOWN

Research Ethics Committee
E53 Room 44.1, Old Main Building
Groote Schuur Hospital, Observatory, 7925
Queries : Xolile Fula
Tel : (021) 406-6492 Fax: 406-6411
E-mail : Xfula@curie.uct.ac.za

12 October 2004

REC REF: 360/2004

Mr GD Wessels
Mechanical Engineering
UCT

Dear Mr Wessels

THE USE OF HUMAN SCAPULAE IN THE TESTING OF PROSTHETIC JOINT FIXATION TO THE GLENOID

Thank you for submitting your study to the Research Ethics Committee for reviewal.

It is a pleasure to inform you that the Research Ethics Committee has formally approved the above mentioned study.
Please note that all tissue acquisition and control to be instituted by negotiating with Prof Lorna Martin and in keeping with statutory requirements of Law.

Please quote the REC. REF in all your correspondence

Yours sincerely

PROF. T. ZABOW
CHAIRPERSON

Surgical Technique

DELTA

DELTA CTA® REVERSE SHOULDER PROSTHESIS

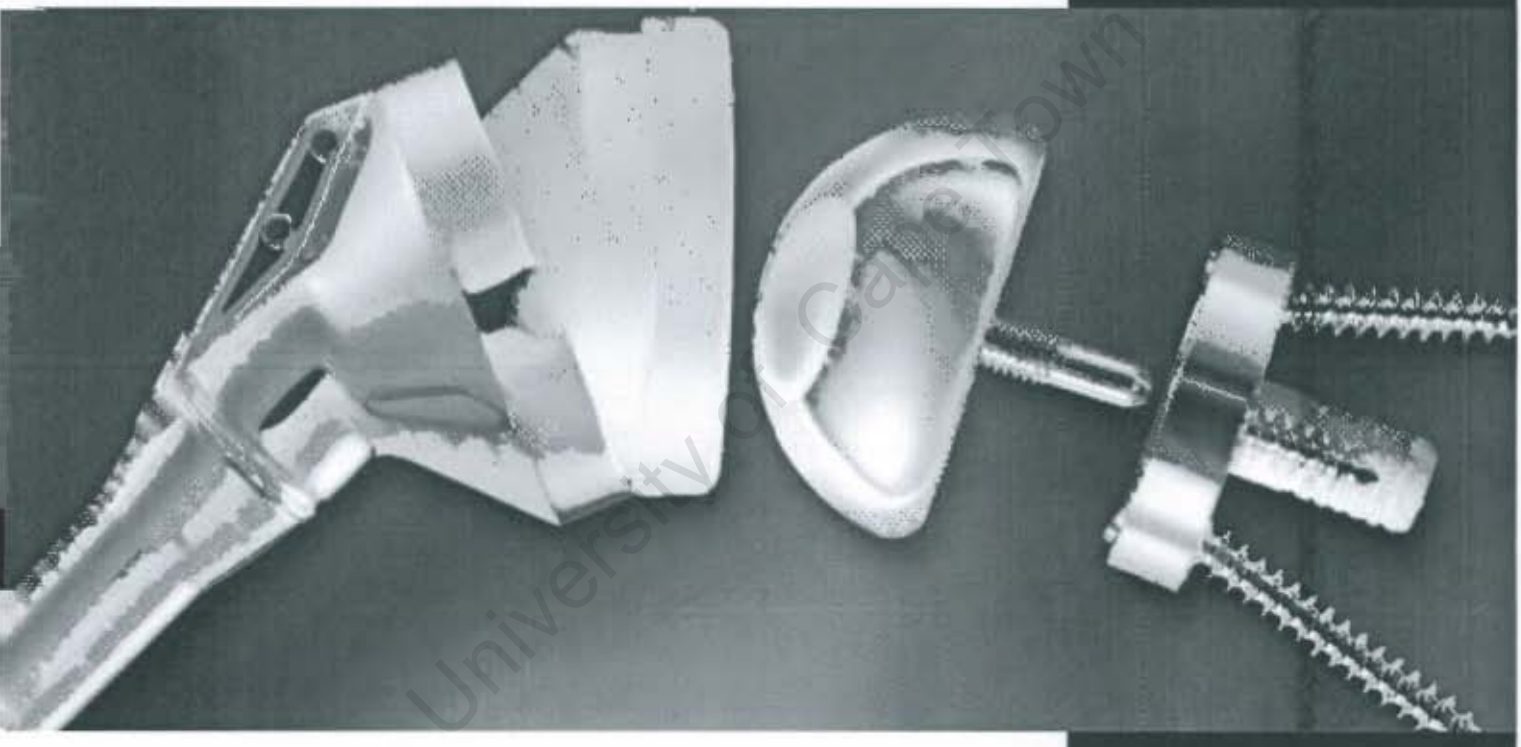

DePuy

a Johnson & Johnson company

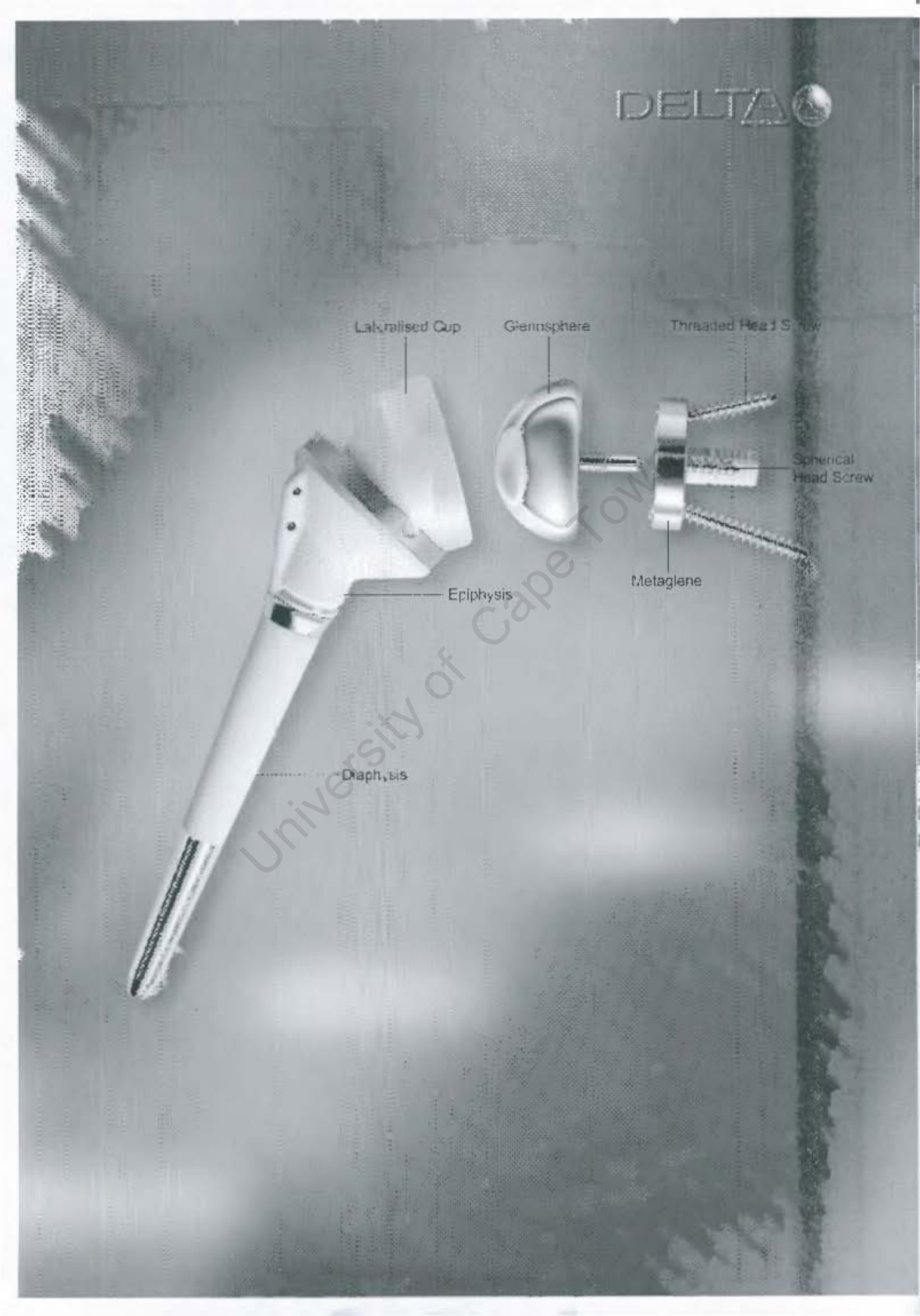

Contents

Surgical Steps	2
Introduction	3
Pre-operative Planning	4
Surgical Approach and Patient Positioning	4
Superior Lateral Approach	5
Humeral Head Resection	6
Humeral Reaming	7
Distal Humeral Reaming (Revision Surgery)	8
Proximal Reamer Guide Assembly	8
Proximal Humeral Reaming	9
Trial Humeral Implantation	10
Exposure of the Glenoid	10
Preparation of the Glenoid	11
Implantation of the Metaglene	12
Inferior and Superior Screw Placement	12
Anterior and Posterior Screw Placement	14
Trial Reduction	15
Glenosphere Placement	16
Humeral Implant Insertion	17
Hemi-arthroplasty	18
Closure	19
Post-operative Management	19
Ordering Information	20

Surgical Steps

Superior lateral approach

Resection of the humeral head

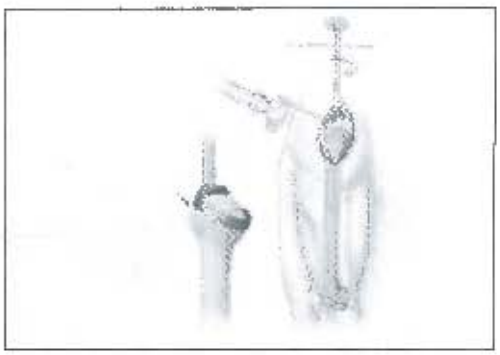

Diaphyseal preparation

Proximal reaming of the humerus

Preparation of the glenoid

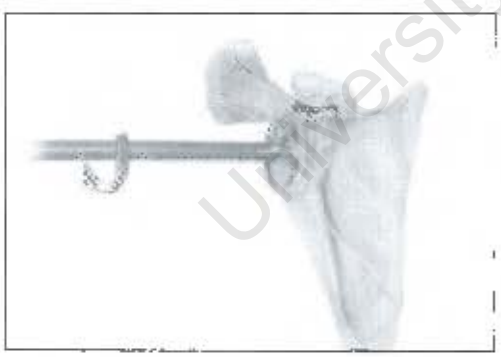

Insertion of the Metaglene

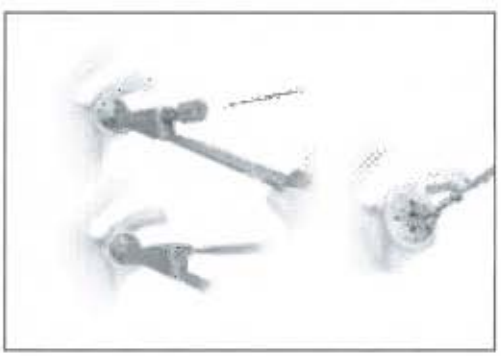

Glenosphere Placement

Insertion of the humeral Implant

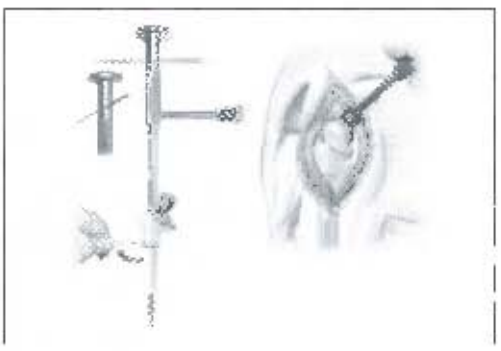

Introduction

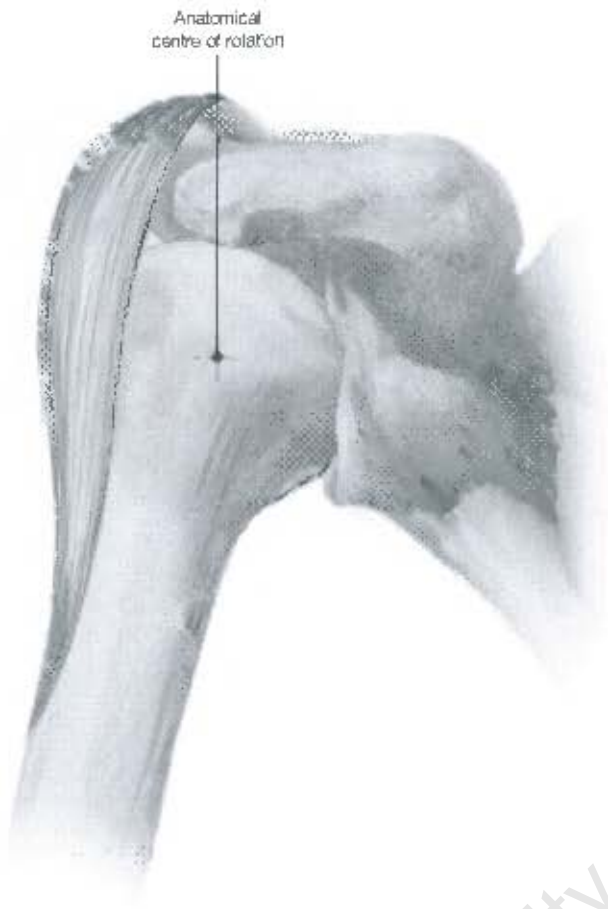

Figure 1

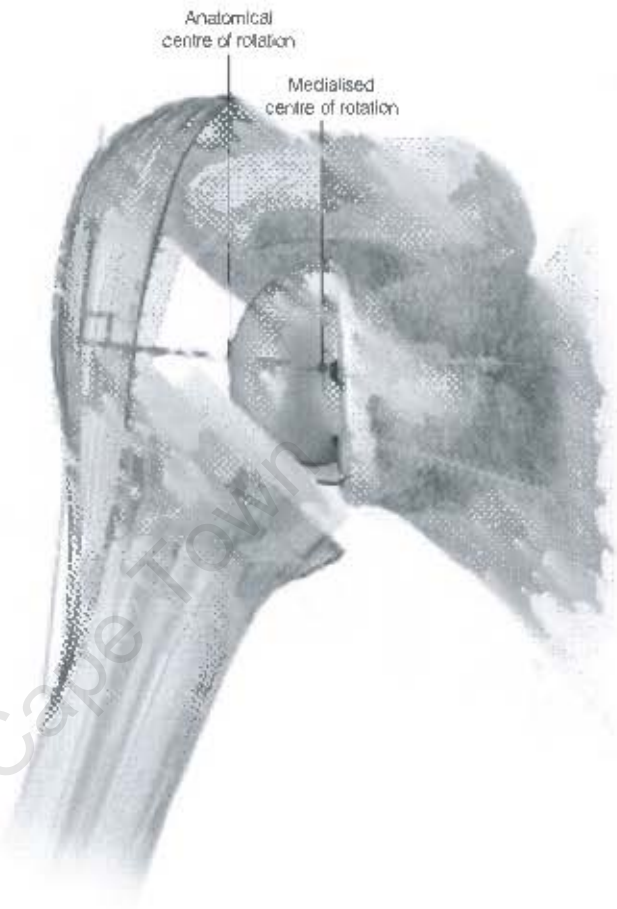

Figure 2

The Delta CTA™ Reverse Shoulder System is indicated for the treatment of glenohumeral arthritis when it is associated with irreparable rotator cuff damage and where conventional total shoulder arthroplasty may not be fully effective in restoring joint stability with an adequate range of movement. The design avoids high shear forces associated with unstable conventional or hemi-arthroplasty, that can cause the implant to wear and loosen.

The Delta CTA™ prosthetic geometry reverses the normal relationship between scapular and humeral components, moving the centre of rotation medially and distally to increase the lever arm length of the deltoid muscle (Figures 1 and 2).

This allows the three muscles in the deltoid group to compensate for rotator cuff deficiency, drawing the articulating surfaces together to stabilise the joint and allow as near normal function as possible.

Pre-operative Planning

Figure 3

An initial assessment is made of the bone in the superior and inferior aspects of the glenoid, using radiographic and CT imaging in order to determine the suitability of the patient for treatment. The size of the glenoid vault is assessed to ensure that all four metaglene screws can be placed within glenoid bone.

Pre-operative planning is also carried out, using AP and lateral shoulder radiographs of known magnification, and the available template to confirm the size and alignment of the implant (Figure 3).

Surgical Approach and Patient Positioning

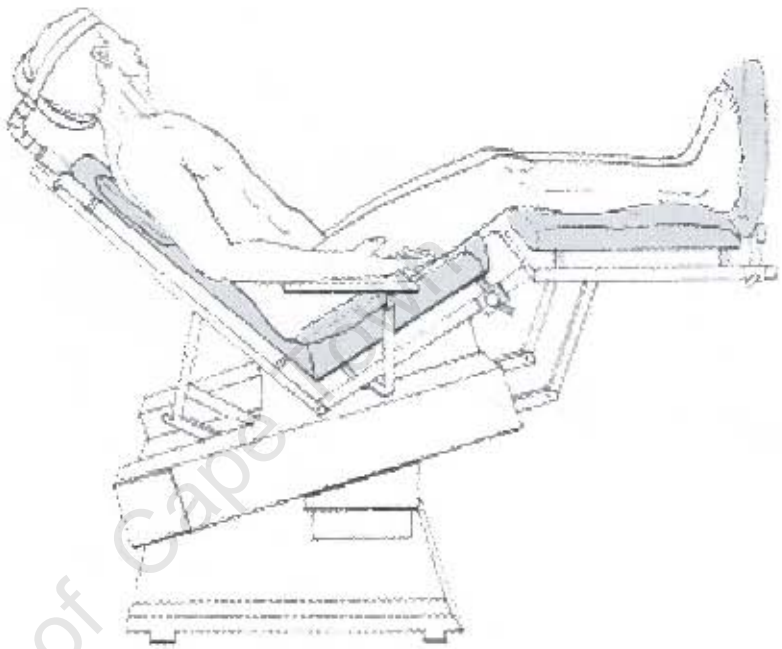

Figure 4

The patient should be in the deck chair position, with the affected arm completely free and resting on a support (Figure 4).

Superior Lateral Approach

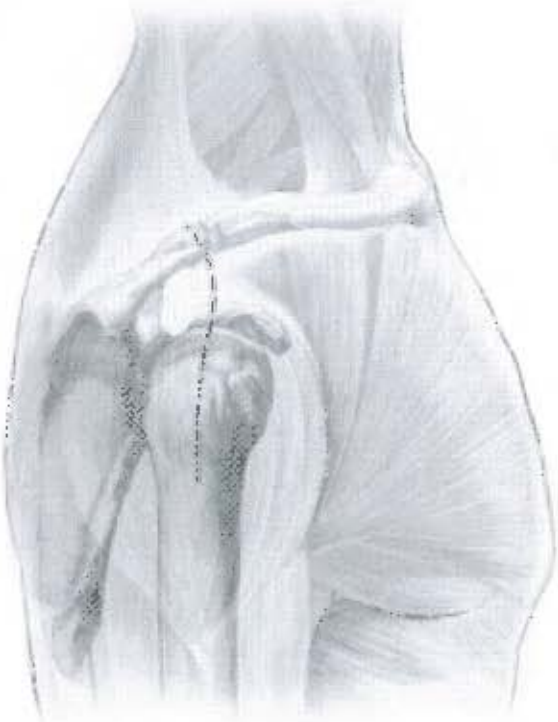

Figure 5

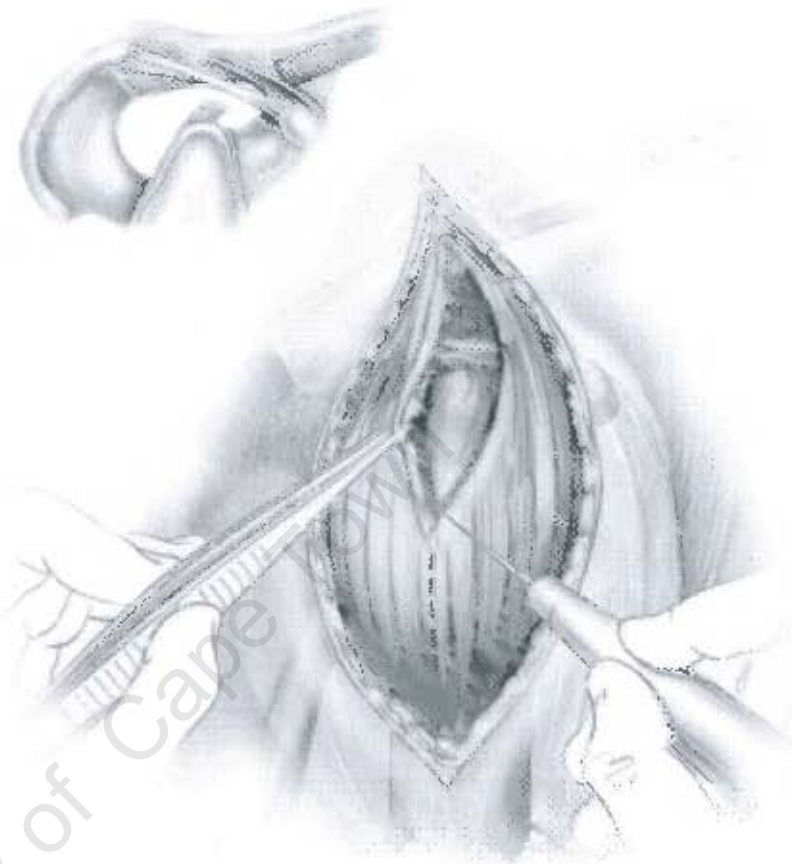

Figure 6

The quality and ease of implantation rely on a superior lateral approach (Figure 5). A delto-pectoral approach is also appropriate and the choice depends mainly on surgeon prefcrence and clinical parameters. Revision surgery for instance usually dictates a delto-pectoral approach as it allows for a longer humeral incision when faced with a difficult removal of the humeral stem. Used for classic rotator cuff repairs, the superior lateral approach allows a clear visualisation of the glenoid and therefore facilitates greatly the implantation of the glenoid components of the prosthesis.

The incision is started at the level of the AC joint, follows the anterior aspect of the acromion and finishes vertically downwards for 4 cm (Figure 6). Following subcutaneous dissection, the anterior and middle deltoid muscle bundles are separated opposite the lateral margin of the acromion, using blunt dissection (the dissection should not extend beyond 4 cm from the external aspect of the acromion in order to preserve the axillary nerve). When the subacromial bursa is visible, gentle longitudinal traction in line with the limb will allow a retractor to be placed in the subacromial space.

The anterior deltoid is released subperiosteally from its acromial insertion up to the AC joint.
The humeral head is then visible at the anterior edge of the acromion – the subacromial bursa is removed.
If necessary, exposure may now be improved by dividing the AC ligament and performing acromioplasty.
The limb is then externally rotated and the head is dislocated anterosuperiorly to facilitate positioning of the cutting guide. If the biceps is still present, it should be tenodenised in the bicipital groove. Retain the teres minor and infraspinatus when present.

Humeral Head Resection

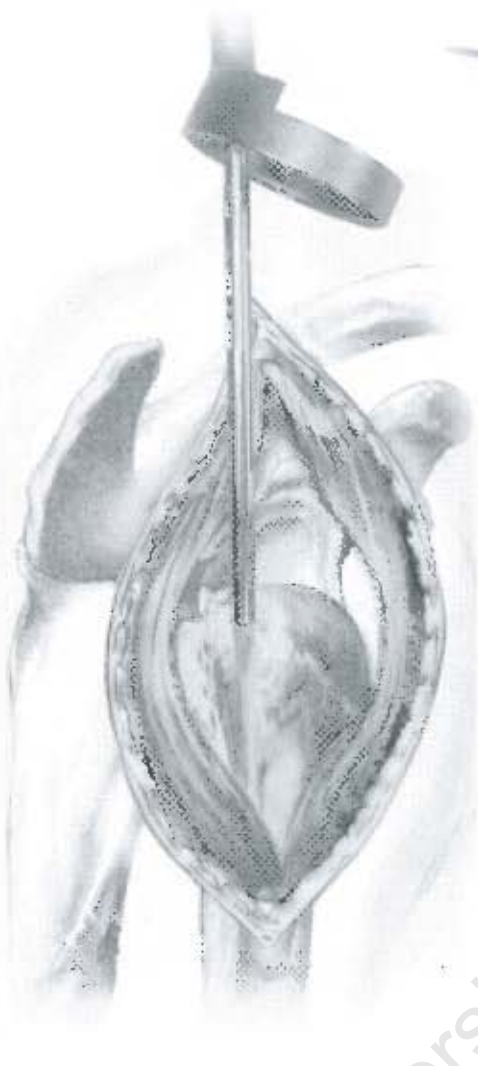

Figure 7

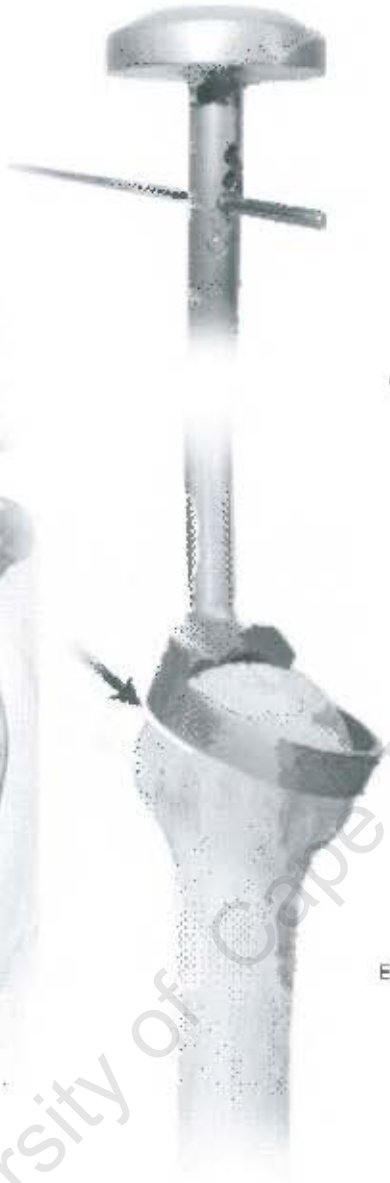

Figure 8A

Figure 8B

Figure 8C

An initial entry hole is made in the proximal humerus using an awl. The awl tip is centred over and in line with the long axis of the humerus, at the junction of the intratubercular groove and the articulating surface of the humeral head (Figure 7).

The orientation pin is then passed through the hole in the resection guide corresponding to the desired retroversion (Figure 8A). Preferably, this will be 0° since excessive retroversion will restrict joint rotation, especially in internal rotation. Retroversion is calculated with reference to the axis of the humeral epicondyles (Figure 8B).

The tip of the cutting guide is located in the entry hole and the guide is passed down the humeral canal until it rests on the humeral head. With the humeral resection guide rim located on the humeral head, the orientation pin is aligned with the transcondylar axis (Figure 8C).

Humeral Reaming

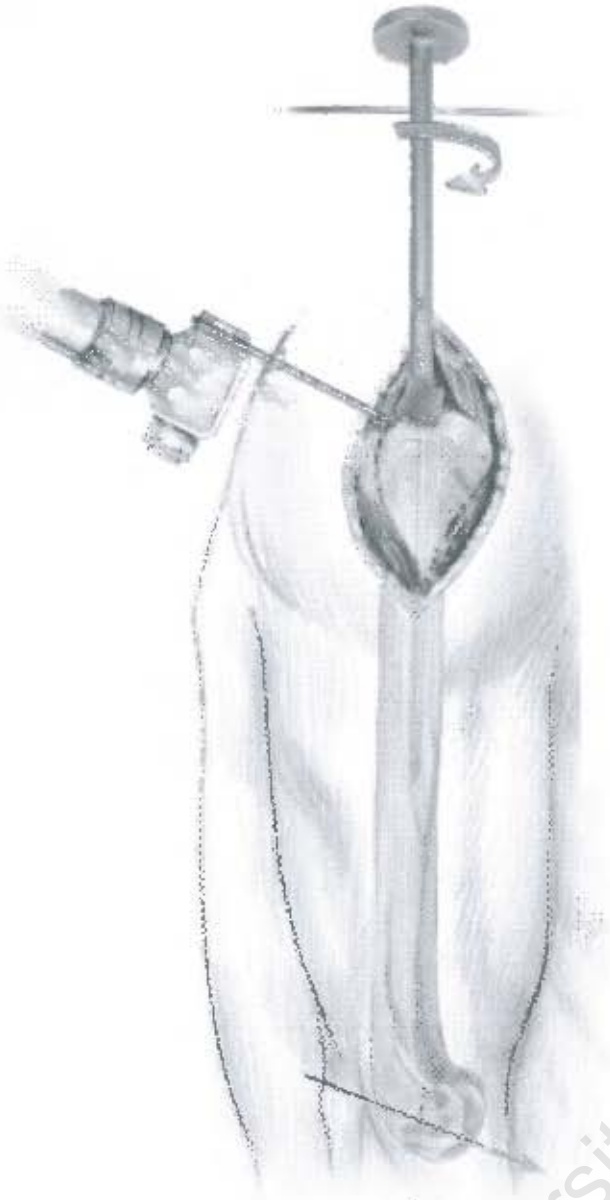

Figure 9

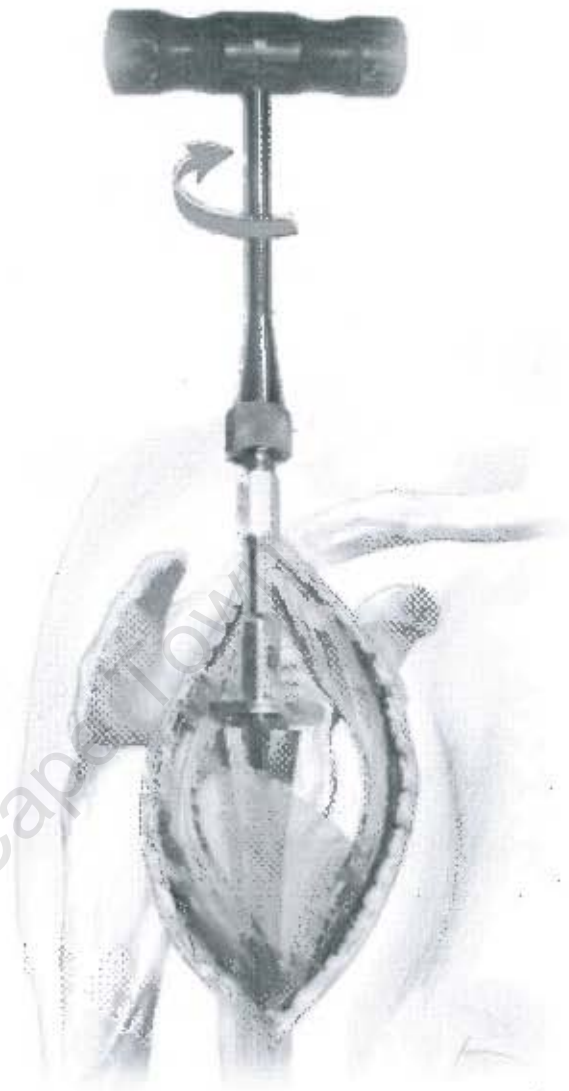

Figure 10

The humeral head resection is initiated in line with the inferior aspect of the humeral cutting guide (135°), the humeral cutting guide is removed and the resection completed (Figure 9). The initial resection removes a minimal amount of bone. More bone may be removed if necessary.

A forked retractor is passed under the scapula to lower the humerus. If this provides a clear sight of the glenoid surface, the resection level is correct. If not, a further resection may be carried out.

Starting with the smallest diameter distal reamer attached to the T-Handle, the distal humeral canal is reamed in line with the long axis of the humerus (Figure 10). The final reamer should not exceed the templated proximal diameter (up to size 4). Reaming stops when the flange of the reamer is level with the resection.

Power reaming should not be used to ream the humerus.

Distal Humeral Reaming (Revision Surgery)

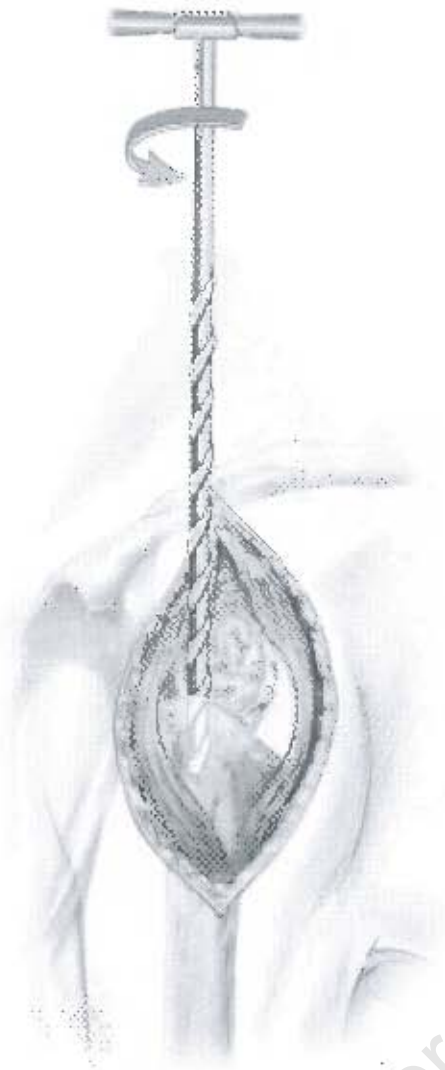

Figure 11

If a long stem is to be implanted, 150 mm and 180 mm diaphyseal revision reamers should be used in conjunction with the rigid reamers that are included within the Delta CTA™ revision instrumentation (Figure 11).

In addition to the reamers in the accompanying table, 5 mm and 6 mm diameter reamers are provided as start-up reamers.

Diaphyseal references	Reamer references
Size 1, length 150 mm (ref. DHR115H/DHC115B) Size 1, length 180 mm (ref. DHR118H/DHC118B)	7.5 mm diameter (ref. ALR 075)
Size 2, length 150 mm (ref. DHR215H/DHC215B) Size 2, length 180 mm (ref. DHR218H/DHC218B)	8 mm diameter (ref. ALR 008)
Size 3, length 150 mm (ref. DHR315H/DHC315B) Size 3, length 180 mm (ref. DHR318H/DHC318B)	9 mm diameter (ref. ALR 009)

Proximal Reamer Guide Assembly

Figure 12

The proximal reaming guide, 36 mm or 42 mm, corresponding to the templated epiphysis size, is screwed to the trial diaphyseal stem that matches the distal reamer diameter. The assembly is mounted on the humeral stem impactor and introduced in line with the long axis of the humerus (Figure 12).

Proximal Humeral Reaming

Figure 13

Figure 14

The orientation pin is passed through the hole in the impactor handle and the previously selected version angle is checked.

The assembly is impacted into the humeral canal until the appropriate mark (36 mm or 42 mm) on the impactor reaches the level of the resection (Figure 13).

Retroversion is again checked and the impactor is removed, leaving the reaming guide in place.

The appropriate size of proximal humeral reamer, (36.1, 36.2 or 42.2 mm) is mounted on the T-Handle.

The humerus is then reamed until the flange of the reamer is level with the osteotomy, and contact is made with cortical bone (Figure 14).

If necessary, the reaming guide can be inserted more deeply to ensure that the proximal reamer reaches the level of osteotomy.

Reaming is now complete and the reamer, reamer guide and trial stem are extracted from the humerus.

Trial Humeral Implantation

Figure 15

The trial epiphyseal component is attached to the trial diaphyseal stem, and the assembly is mounted onto the humeral stem impactor (Figure 15). It may be necessary to remove a wedge of cortical bone to accommodate the lateral fin on the epiphyseal component. The assembly is impacted into the humeral canal, ensuring the diaphyseal fin does not impinge upon the lateral cortex of the humerus. The humeral stem impactor is then removed, leaving the trial humeral components in place.

Exposure of the Glenoid

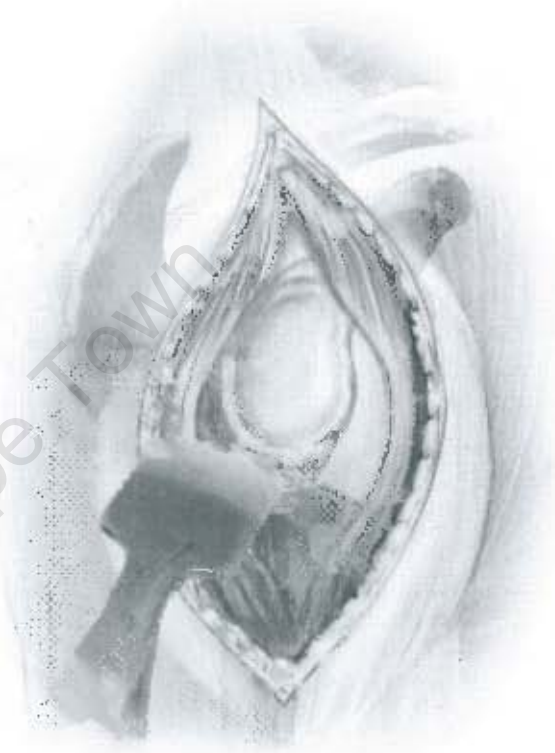

Figure 16

A forked retractor is positioned on the axillary margin of the scapula, under the inferior glenoid labrum, to reflect the humerus down or backward, depending on the approach taken. The labrum is excised and an extensive periglenoid capsulotomy is performed. Any peripheral osteophytes should be removed to restore the natural anatomic shape of the glenoid (Figure 16).

Preparation of the Glenoid

Figure 17A

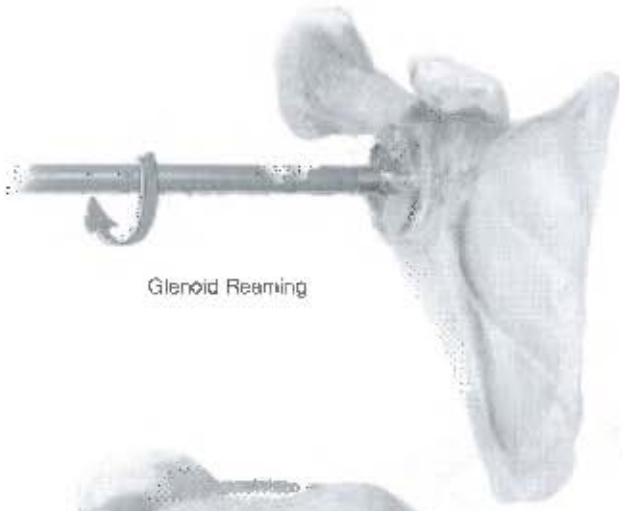

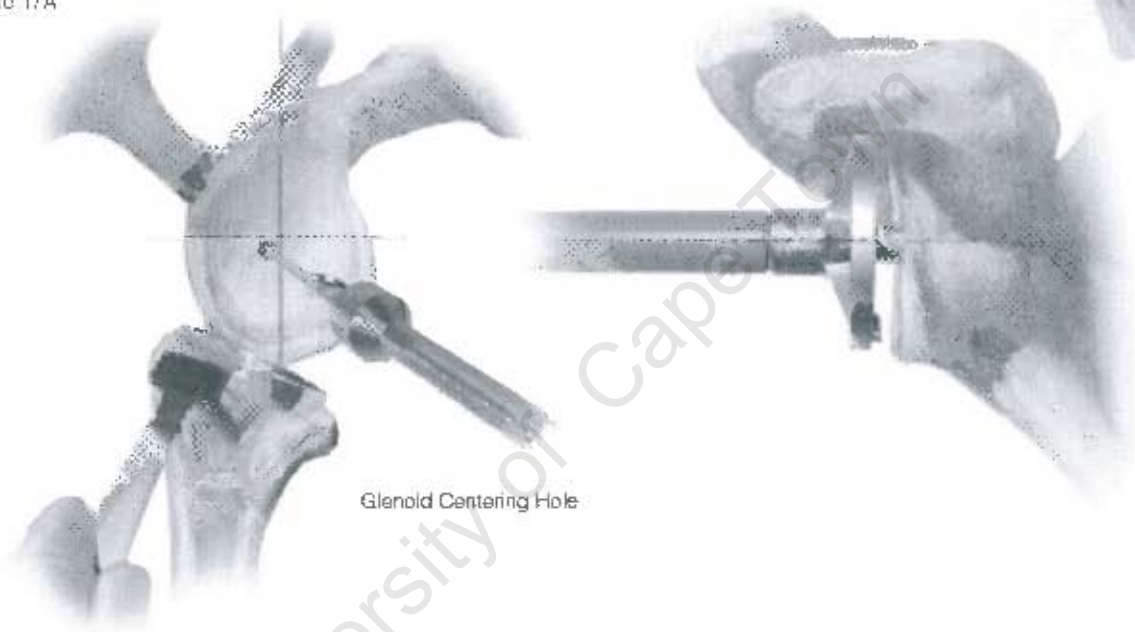

Figure 17B

Figure 18

The major and minor axes of the glenoid are then marked using diathermy. The 2.5 mm guide pin is attached to the power tool and an entry point is created just posterior and inferior to the intersection of the axes (Figure 17A). The location for this entry point may be checked using radiographic and CT imaging combined with X-ray templates. It should be as inferior as possible, while ensuring that sufficient space is available to place the inferior screw in cancellous bone for its entire length.

The cannulated stop drill is attached to the power source and the glenoid centering hole is completed over the guide pin (Figure 17B).

The glenoid reamer is attached to the power source and the reamer pilot shaft is introduced into the glenoid centring hole. In cases of osteoporotic bone, hand reaming should be used.

Ensure that the reamer is not in contact with bone before applying power since this may damage the glenoid.

The glenoid is then reamed until a smooth platform devoid of cartilage is created for the Metaglene, with sufficient depth to accommodate its peripheral rim (Figure 18). The depth should be checked before implantation of the prosthesis. If sufficient peripheral depth is not achieved, the glenosphere will not fully engage with the taper on the Metaglene, and further reaming should be carried out until the tray is fully seated.

Inferior and Superior Screw Placement

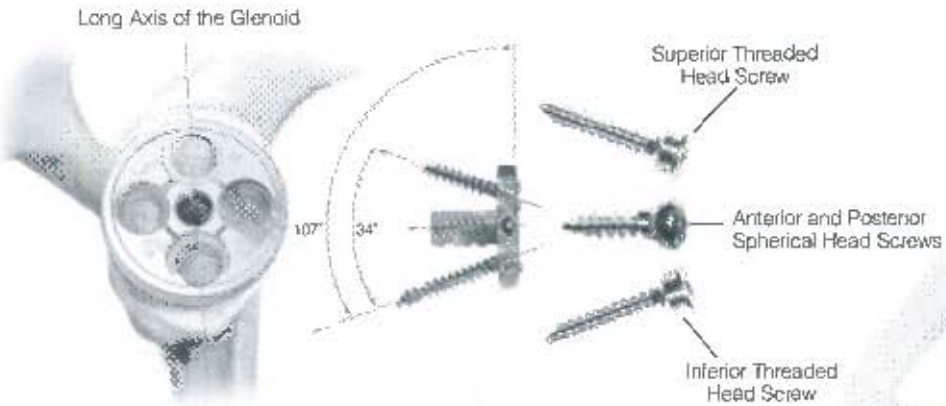

Figure 19

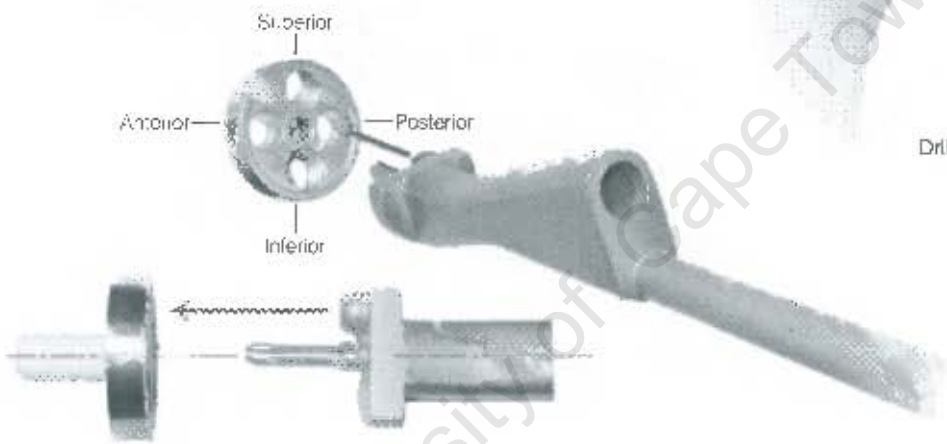

Figure 20

Figure 21
Drilling of Inferior Hole

The Metaglene is available in one size for both 36 mm and 42 mm Glenospheres and is implanted without cement. Initial, primary mechanical stability is provided by the 4.5 mm diameter screws. When correctly positioned, the angled, threaded screw holes in the Metaglene should be aligned superiorly and inferiorly on the glenoid (Figure 19). A revision Metaglene is available and may be selected for cases of severe erosion of the glenoid cavity rim.

The definitive Metaglene is attached to the holder, with the drill guide covering the inferior threaded screw hole on the implant. Check that the Metaglene is accurately seated on the holder.

The assembly is inserted into the prepared glenoid with the superior and inferior holes aligned with the long axis of the glenoid.

Caution: It is imperative to use the Metaglene holder to insert the inferior and superior screws. The 34° angle between these two screws is fixed and cannot be altered.

Once the Metaglene has been manually aligned, the holder is tapped firmly so that the tray is impacted flat onto the prepared surface of the glenoid.

It is important to ensure that the Metaglene is fully seated, flat on the prepared glenoid, before it is screwed into position.

A drill bush 2 or 2.5 mm in diameter, depending on the quality of bone, is then inserted into the drill guide. The corresponding long drill (A5273/A5274) is selected, passed through the bush, and the inferior fixation hole is drilled (Figure 21).

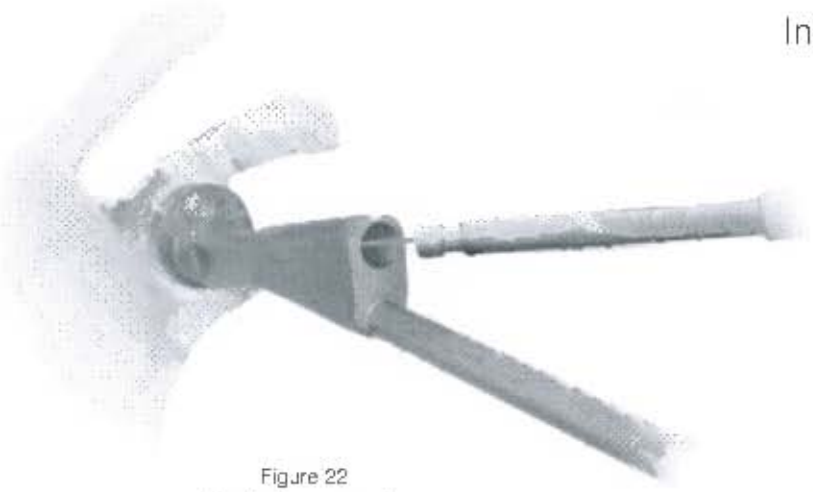

Figure 22
Depth Measurement

Figure 23
Screw Placement

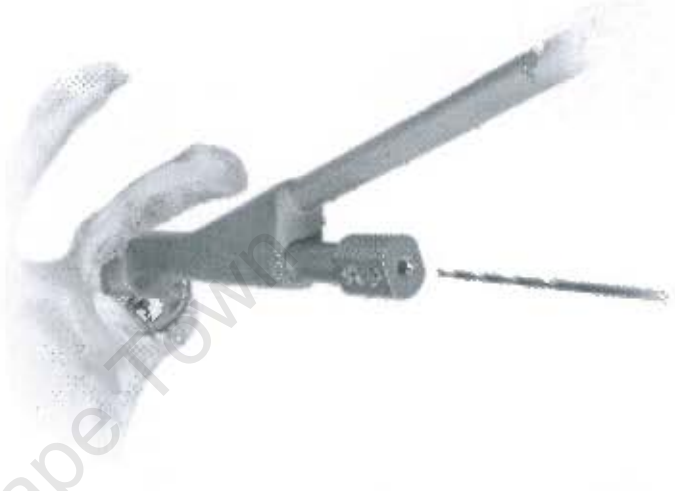

Figure 24
Drilling of Superior Hole

Laser etched depth markings on the long drills can help when choosing the most appropriate screw length.
A depth gauge is also provided. To use it, the drill bush should be removed to check the depth of the screw hole (Figure 22).
Threaded head screws must be used for the inferior and superior holes. The spherical head screws are designed for use only with anterior and posterior holes.

A threaded head screw of corresponding length to the measured depth is passed through the drill guide and screwed into the inferior fixation hole.
The screw should be fully tightened at this stage (Figure 23).

The Metaglene holder is then gently detached from the bearing tray and turned 180° to prepare the superior fixation hole in the same way as the inferior hole.
Its depth is measured and the appropriate threaded head screw is screwed into position (Figure 24), again ensuring it is fully tightened.

Anterior and Posterior Screw Placement

Figure 25
Anterior Hole Drilling

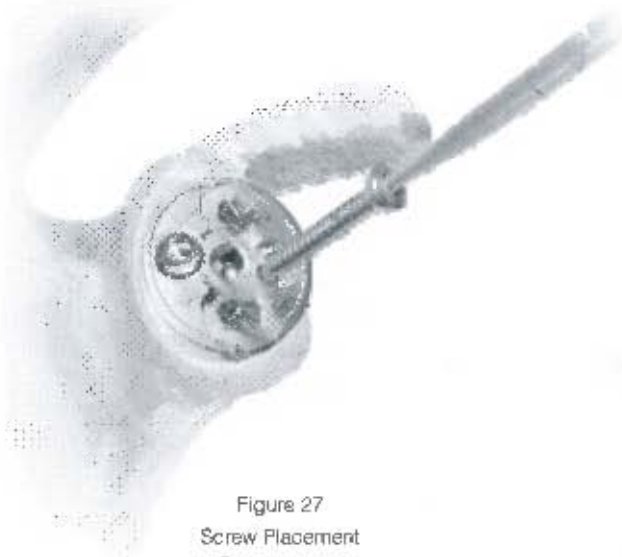

Figure 27
Screw Placement

Figure 26
Depth Measurement

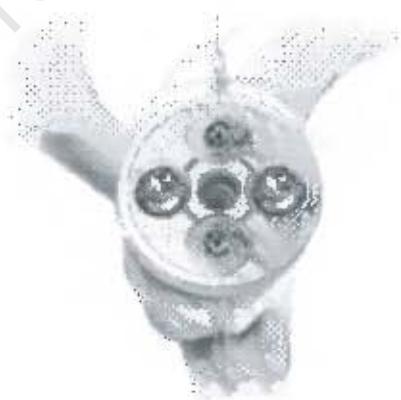

Figure 28
Final Screw Tightening

The Metaglene holder is removed and the free hand drill guide of appropriate size, 2.0 or 2.5 mm, is located in the anterior fixation hole. Both anterior and posterior screw positions allow angulation of ± 20 degrees. The drill guide is used to set the most appropriate angle to ensure that each screw is located in reliable bone stock (Figure 25). Preferential position is usually chosen by palpating the anterior and posterior aspects of the scapula as well as examining the X-rays and CT scans.

The anterior hole is drilled using the short drills with depth markings (MPG020/ MPG025). The drill guide is removed and the hole depth measured using the depth gauge (Figure 26).

A spherical head screw is introduced, and part tightened (Figure 27).
The same procedure is followed for the posterior screw. Both screws are then alternately fully tightened (Figure 28).

Trial Reduction

Figure 29

Figure 30

The appropriate trial glenosphere (36 mm or 42 mm) is attached to the Metaglene. The corresponding humeral cup trial is inserted into the humeral trial assembly. The shoulder is then reduced and assessed for a full range of movement.

Soft tissue tension is correct, when:

- The arm is pulled down and outward, approximately 5mm of humeral glenoid component separation is expected.
- The joint should remain stable when the arm is adducted, with no indication of subluxation. Only a small degree of superior lift-off is expected in extreme adduction (Figure 29). The lift-off will disappear during the arm elevation thanks to the deltoid contraction and the joint surface will be perfectly congruent (Figure 30).

To adjust joint tensioning, the lateralised cup is available in three thicknesses (+3 mm, +6 mm, +9 mm). If further soft tissue tension is required, a +9 mm metallic humeral spacer may be put in between the epiphysis and the cup. It should then be attached to the trial epiphyseal component, using the hexagonal head screwdriver. In case of muscular overtensioning, further humeral bone resection might be performed. Additional joint stability may be achieved by introducing a retentive, more constrained cup (+0 retentive, +6 retentive).

However those retentive cups should only be used in revision cases or to correct extreme instability. If the humeral cut is adequate, a lateralised cup will be sufficient in the majority of cases.

Glenosphere Placement

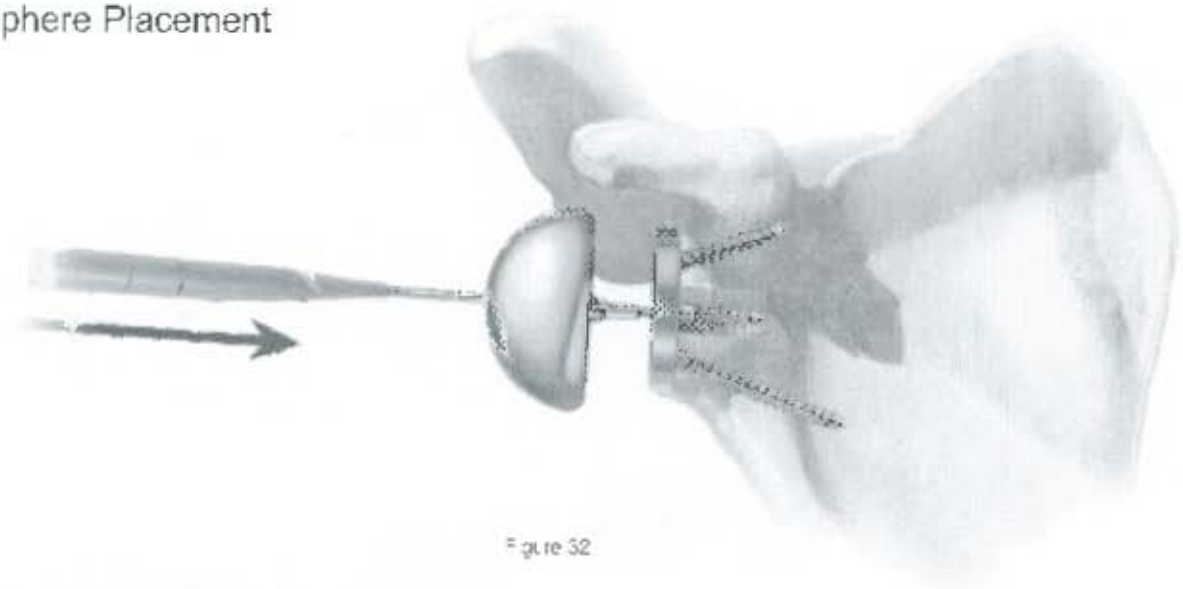

Figure 32

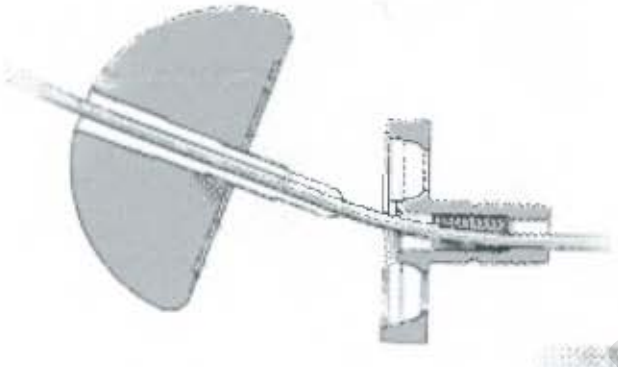

Figure 3

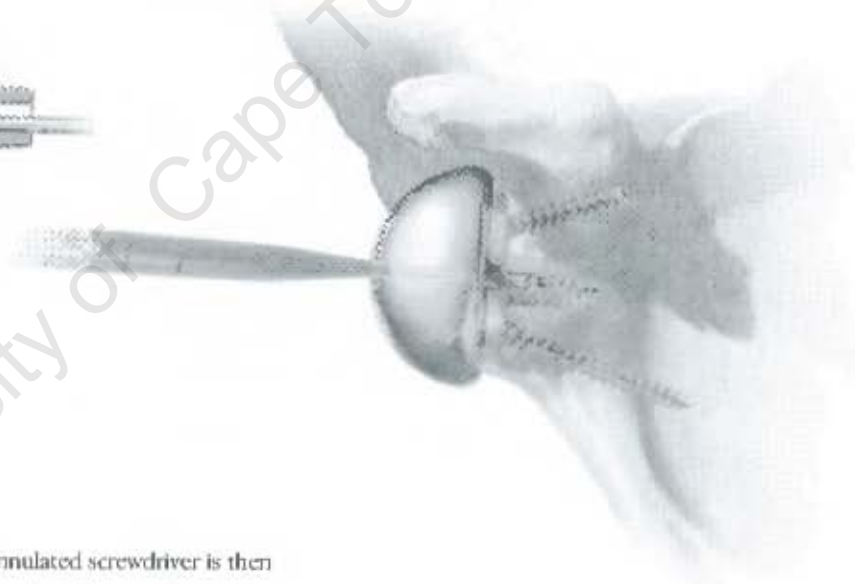

Figure 33

A 1.5 mm guide pin is inserted through the central hole of the Metaglene (Figures 31 & 32).

The 3.5 mm cannulated screwdriver is engaged in the definitive Glenosphere and guided over the 1.5 mm guide pin. After two or three turns, the cannulated screwdriver is disengaged and the glenoid bearing is checked to ensure that it is properly aligned.

The cannulated screwdriver is then re-engaged and the captive screw is tightened until the glenoid bearing closes on the taper of the bearing tray. Further impaction of the junction is then obtained by gently tapping the glenosphere using the glenosphere impactor and tightening again the glenosphere central screw.

Care should be taken to ensure that the glenoid bearing is fully locked onto the bearing tray (Figure 33).

Humeral Implant Insertion

Figure 34

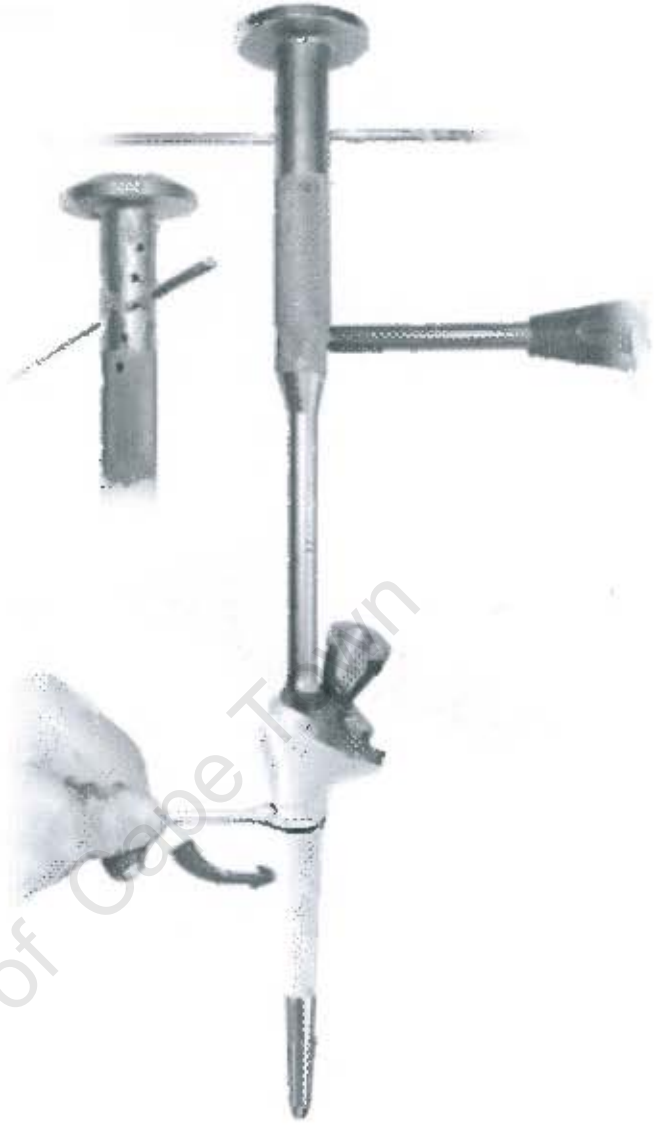

Figure 35

The trial humeral assembly is extracted from the humerus. The corresponding definitive humeral epiphyseal component is attached to the impactor (Figure 34). The definitive diaphyseal component is screwed to the epiphyseal component. The two components are then locked tight, using the wrench and driver (Figure 35). It is important to ensure the two components are tightly locked together to reduce the chance of post operative disassembly.

If cementless components are selected, the assembly is introduced in the appropriate retroversion and the assembly is impacted into the humeral canal.

If the implant is to be cemented, a synthetic cement restrictor or bone plug is introduced into the distal humeral canal to restrict the passage of cement. Cement is injected into the humeral canal and, when the cement is at its appropriate viscosity, the implant assembly is introduced in line with the long axis of the humerus and in the chosen version angle. Pressure is maintained on the introducer until the cement is fully polymerised.

Humeral Implant Insertion

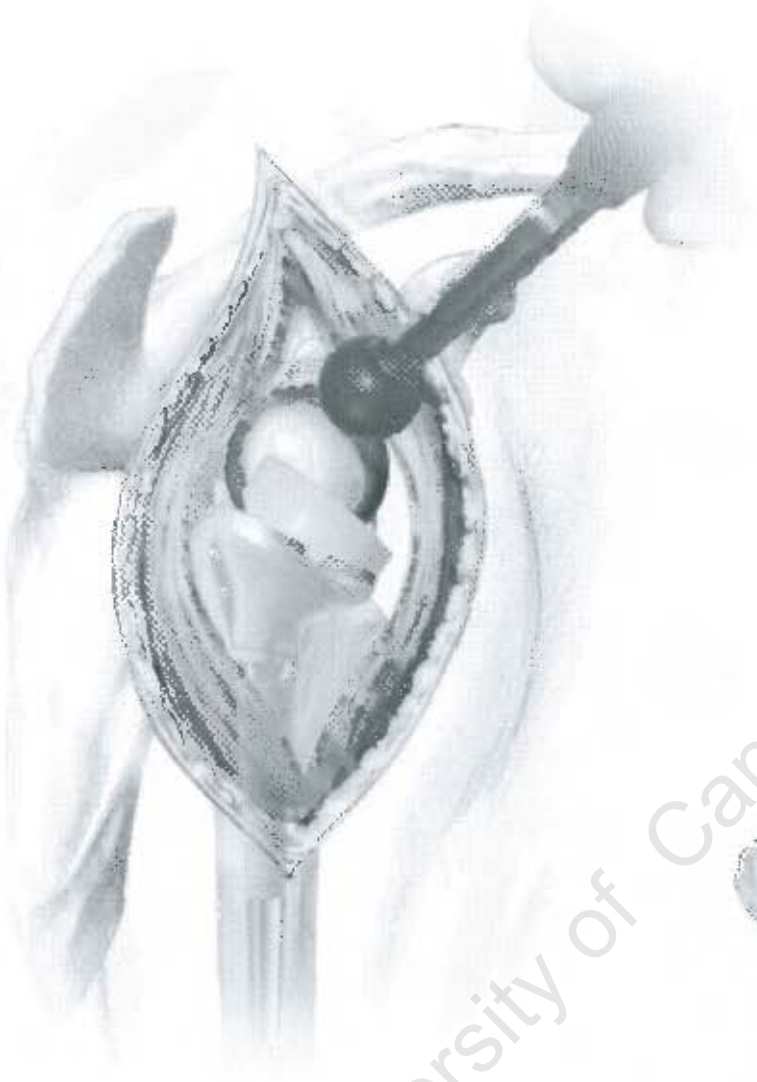

Figure 36

The definitive humeral cup is impacted using the cup impactor (Figure 36). The joint is reduced and a final assessment of joint stability and range of movement is carried out.

Hemi-arthroplasty

Figure 37

Figure 38

In cases of intra-operative fracture of the glenoid cavity, or revision of the Delta CTA™ glenoid, for example, a hemi-arthroplasty may be considered. Intermediate metallic heads are provided within the Delta CTA™ system to complete this procedure.
Two epiphyseal diameters, 36 and 42 mm, are available in standard and + 4 mm offset (Figure 37). The hemi heads can be assembled either directly onto the epiphysis or onto the metallic spacer. These should be introduced using the humeral head impactor (Figure 38).

Closure

Once the joint space is irrigated and cleared of debris, the anterior deltoid is firmly sutured at the fibrous acromial perimeter or using transosseous stitches. A drain is left in place.
Layered closure of the soft tissues normally leads to an adequate range of motion, without instability.

Post-operative Management

Appropriate post-operative physiotherapy is an important factor in the outcome of this procedure, since stability and mobility now depend on the deltoid alone. The physiotherapy programme, which should be planned to suit the individual patient, consists of two phases: early (6 weeks) and late.
Two days after the operation the patient can be mobile. This early phase is dedicated to gentle and gradual recovery of the passive range of shoulder motion: abduction of the scapula, anterior elevation and medial and lateral rotation. An abduction cushion may be used to relieve pressure on the deltoid.
Physiotherapy is mainly performed with the patient supine, passive and with both hands holding a bar that is manipulated by the contralateral hand, as described by Neer.

The patient is encouraged to use the affected arm to eat and write but should not raise the arm. In conjunction with these exercises for scapulohumeral recovery, it is important to strengthen muscle connection with the scapula in order to facilitate muscle and implant function. Passive exercise in the swimming pool is recommended as soon as scars begin to form.
After the sixth or seventh week, active strengthening movements may be gradually added to the programme. These exercises, which closely follow everyday activities, are performed in a sitting or standing position, using conventional methods, with isometric exercises and resistance movements becoming increasingly important.
A series of exercises for rhythmic stabilisation of the upper arm as well as eccentric working on lowering the arms complete the strengthening of the muscles. Physiotherapy should be performed over a period of at least six months.

Implants

EHC361B	Cemented Humeral Epiphysis, 36.1
EHC362B	Cemented Humeral Epiphysis, 36.2
EHC422B	Cemented Humeral Epiphysis, 42.2
EHR361H	Cementless Humeral Epiphysis, 36.1
EHR362H	Cementless Humeral Epiphysis, 36.2
EHR422H	Cementless Humeral Epiphysis, 42.2
DHC010B	85mm Cemented Humeral Diaphysis, Size 0
DHC110B	86mm Cemented Humeral Diaphysis, Size 1
DHC210B	88mm Cemented Humeral Diaphysis, Size 2
DHC310B	89mm Cemented Humeral Diaphysis, Size 3
DHC410B	94mm Cemented Humeral Diaphysis, Size 4
DHR000H	95mm Cementless Humeral Diaphysis, Size 0
DHR110H	96mm Cementless Humeral Diaphysis, Size 1
DHR210H	98mm Cementless Humeral Diaphysis, Size 2
DHR310H	99mm Cementless Humeral Diaphysis, Size 3
DHR410H	100mm Cementless Humeral Diaphysis, Size 4
4CHL336	Lateralised Humeral Cup, ø36, + 3 mm
4CHL636	Lateralised Humeral Cup, ø36, + 6 mm
4CHL936	Lateralised Humeral Cup, ø36, + 9 mm
4CHL342	Lateralised Humeral Cup, ø42, + 3 mm
4CHL642	Lateralised Humeral Cup, ø42, + 6 mm
4CHL942	Lateralised Humeral Cup, ø42, + 9 mm
4CHS036R	Medialised Retentive Humeral Cup, ø36, + 0 mm/ R
4CHS042R	Medialised Retentive Humeral Cup, ø42, + 0 mm/ R
4CHL636R	Lateralised Retentive Humeral Cup, ø36, + 6 mm/ R
4CHL642R	Lateralised Retentive Humeral Cup, ø42, + 6 mm/ R
RTH236	Humeral Spacer, ø36, + 9 mm
RTH242	Humeral Spacer, ø42, + 9 mm
THH036	Humeral Head, ø36, + 0 mm
THH436	Humeral Head, ø36, + 4 mm
THH042	Humeral Head, ø42, + 0 mm
THH442	Humeral Head, ø42, + 4 mm
MGC002H	Standard Metaglene
GSC236	Glenosphere Dia. 36 mm
GSC242	Glenosphere Dia. 42 mm
VFM4524	Metaglene Screws, Dia. 4.5 x 24 mm (Threaded Head)
VFM4530	Metaglene Screws, Dia. 4.5 x 30 mm (Threaded Head)
VFM4536	Metaglene Screws, Dia. 4.5 x 36 mm (Threaded Head)
VFM4542	Metaglene Screws, Dia. 4.5 x 42 mm (Threaded Head)
VFM4548	Metaglene Screws, Dia. 4.5 x 48 mm (Threaded Head)
VSM4518	Metaglene Screws, Dia. 4.5 x 18 mm (Spherical Head)
VSM4524	Metaglene Screws, Dia. 4.5 x 24 mm (Spherical Head)
VSM4530	Metaglene Screws, Dia. 4.5 x 30 mm (Spherical Head)
VSM4536	Metaglene Screws, Dia. 4.5 x 36 mm (Spherical Head)
VSM4542	Metaglene Screws, Dia. 4.5 x 42 mm (Spherical Head)

Humeral Preparation Instruments

GSH002	Humeral Resection Guide
ARR001	Orientation Pin
FPH361	Proximal Humeral Reamer, 36.1
FPH362	Proximal Humeral Reamer, 36.2
FPH422	Proximal Humeral Reamer, 42.2
FDH036N	Distal Humeral Reamer, Size 0, Dia. 36 mm
FDH136	Distal Humeral Reamer, Size 1, Dia. 36 mm
FDH236	Distal Humeral Reamer, Size 2, Dia. 36 mm
FDH336	Distal Humeral Reamer, Size 3, Dia. 36 mm
FDH436	Distal Humeral Reamer, Size 4, Dia. 36 mm
FDH142	Distal Humeral Reamer, Size 1, Dia. 42 mm
FDH242	Distal Humeral Reamer, Size 2, Dia. 42 mm
FDH342	Distal Humeral Reamer, Size 3, Dia. 42 mm
FDH442	Distal Humeral Reamer, Size 4, Dia. 42 mm
ITH003	Humeral Stem Impactor
EHF001	Forked Retractor
EHF002	Forked Retractor Large
GFP136	Proximal Reamer Guide, Dia. 36 mm
GFP142	Proximal Reamer Guide, Dia. 42 mm
IGF004	Reamer Guide Impactor/Extractor
CLE014	Diaphyseal Stem Locking Wrench
DHF010N	Humeral Diaphysis Trial, Size 0
DHF110	Humeral Diaphysis Trial, Size 1
DHF210	Humeral Diaphysis Trial, Size 2
DHF310	Humeral Diaphysis Trial, Size 3
DHF410	Humeral Diaphysis Trial, Size 4
EHF361	Humeral Epiphysis Trial, 36.1
EHF362	Humeral Epiphysis Trial, 36.2
EHF422	Humeral Epiphysis Trial, 42.2
RRH236	Humeral Spacer Trial, ø36, + 9 mm
RRH242	Humeral Spacer Trial, ø42, + 9 mm
A5469	Lateralised Humeral Cup Trial, ø36, + 3 mm
A5264	Lateralised Humeral Cup Trial, ø36, + 6 mm
A5468	Lateralised Humeral Cup Trial, ø36, + 9 mm
A5467	Lateralised Humeral Cup Trial, ø42, + 3 mm
A5261	Lateralised Humeral Cup Trial, ø42, + 6 mm
A5466	Lateralised Humeral Cup Trial, ø42, + 9 mm
A5265	Medialised Retentive Humeral Cup Trial, ø36, + 0 mm / R
A5262	Medialised Retentive Humeral Cup Trial, ø42, + 0 mm / R
A5263	Lateralised Retentive Humeral Cup Trial, ø36, + 6 mm / R
A5260	Lateralised Retentive Humeral Cup Trial, ø42, + 6 mm / R
TEH036	Humeral Head Trial, ø36, + 0 mm
TEH042	Humeral Head Trial, ø42, + 0 mm
TEH436	Humeral Head Trial, ø36, + 4 mm
TEH442	Humeral Head Trial, ø42, + 4 mm
















Glenoid Preparation Instruments

A5266	Guide Pin, Dia. 2.5 mm	
A5267	Cannulated Stop drill	
A5075	Glenoid Surfacing Rasp, Dia. 36 mm	
A5076	Glenoid Surfacing Rasp, Dia. 42 mm	
PAM001	T-Handle	
A5271	Drill Bush, Dia. 2.0 mm	
A5272	Drill Bush, Dia. 2.5 mm	
GPM020	Drill Guide, Dia. 2.0 mm	
GPM025	Drill Guide, Dia. 2.5 mm	
A5326	Long S/I Drill Bit, Dia. 2.0 mm (170 mm Length)	
A5327	Long S/I Drill Bit, Dia. 2.5 mm (170 mm Length)	
MPG020	Short A/P Drill Bit, Dia. 2.0 mm (100 mm Length)	
MPG025	Short A/P Drill Bit, Dia. 2.5 mm (100 mm Length)	
A5273	Glenosphere Trial, Dia. 36 mm	
A5274	Glenosphere Trial, Dia. 42 mm	
9E03011	3.5 mm Hex. Head Screwdriver, Cannulated	
A5307	Screw Depth Gauge	
PRT001	Standard Impactor Holder	
EPT001	Humeral Head Impactor	
EPC032	Humeral Cup Impactor	
A5074	1.5 mm Guide Wire	
A5268	Metaglene Holder	

Trays

A5807	Glenoid Tray Base
A5806	Glenoid Tray Insert
A5812	Glenoid Tray Lid
A5815	Glenoid Tray Screw Rack
A5809	Humeral Tray 1 Base
A5808	Humeral Tray 1 Insert
A5813	Humeral Tray 1 Lid
A5811	Humeral Tray 2 Base
A5810	Humeral Tray 2 Insert
A5814	Humeral Tray 2 Lid
A5819	Tray Insert for Cups

Delta CTA™ Revision

Implants

DHC115B	150 mm Revision Cemented Humeral Diaphysis, Size 1
DHC215B	150 mm Revision Cemented Humeral Diaphysis, Size 2
DHC315B	150 mm Revision Cemented Humeral Diaphysis, Size 3
DHC118B	180 mm Revision Cemented Humeral Diaphysis, Size 1
DHC218B	180 mm Revision Cemented Humeral Diaphysis, Size 2
DHC318B	180 mm Revision Cemented Humeral Diaphysis, Size 3
DHR115H	150 mm Revision Cementless Humeral Diaphysis, Size 1
DHR215H	150 mm Revision Cementless Humeral Diaphysis, Size 2
DHR315H	150 mm Revision Cementless Humeral Diaphysis, Size 3
DHR118H	180 mm Revision Cementless Humeral Diaphysis, Size 1
DHR218H	180 mm Revision Cementless Humeral Diaphysis, Size 2
DHR318H	180 mm Revision Cementless Humeral Diaphysis, Size 3
MRC002H	Revision Metaglene

Instruments

ETH001	Standard Humeral Prosthesis Extractor
MDE001	Extraction Rod
MAI001	Slap Hammer
ETH003	Stem Extractor
TEP035	3.5 mm Hex. Head Screwdriver
TEP025	2.5 mm Hex. Head Screwdriver
ALR005	Diaphyseal Reamer, Dia. 5 mm
ALR006	Diaphyseal Reamer, Dia. 6 mm
ALR075	Diaphyseal Reamer, Dia. 7.5 mm
ALR008	Diaphyseal Reamer, Dia. 8 mm
ALR009	Diaphyseal Reamer, Dia. 9 mm
DHF115	150 mm Long Humeral Diaphysis Trial, Size 1
DHF215	150 mm Long Humeral Diaphysis Trial, Size 2
DHF315	150 mm Long Humeral Diaphysis Trial, Size 3
DHF118	180 mm Long Humeral Diaphysis Trial, Size 1
DHF218	180 mm Long Humeral Diaphysis Trial, Size 2
DHF318	180 mm Long Humeral Diaphysis Trial, Size 3
A5288	Metaglene Extractor

Trays

A5280	Tray Base
A5281	Tray Insert
A5279	Lid

introduction

Complex revisions and salvage/oncology surgeries present unique challenges including reattaching soft tissues, properly tensioning the glenohumeral joint, and restoring joint function. The Mosaic™ System addresses these challenges with a three-piece modular humeral stem, providing the maximum amount of customization in a standard-line system.

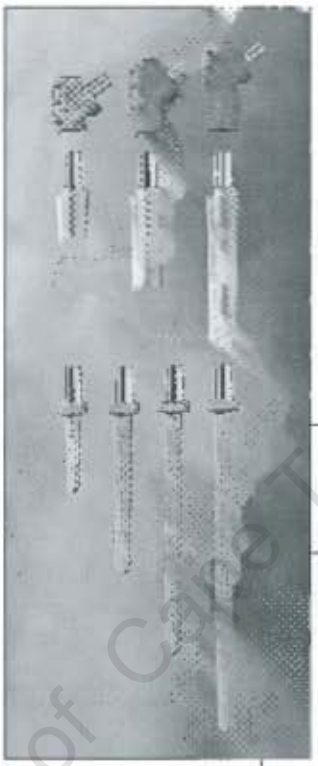

MOSAIC™

humeral replacement system

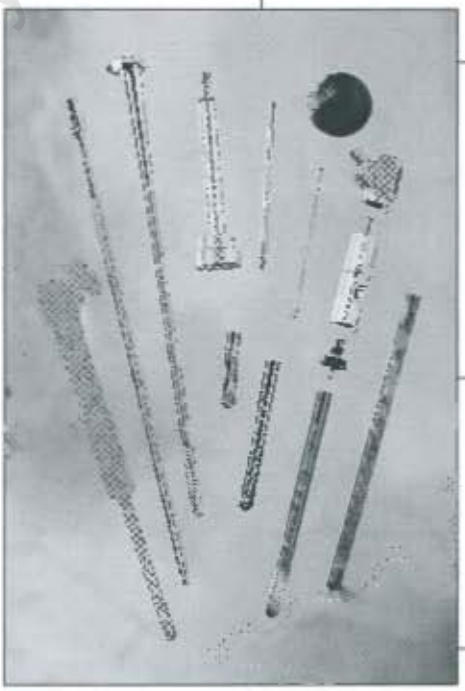

Unique instrumentation allows for an accurate resection level using a line-to-line trialing system with an integrated face reamer.

The Mosaic™ Humeral System was designed in conjunction with James Bruckner, M.D.

This technique is presented to demonstrate the surgical technique utilized by James Bruckner, M.D. Biomet, as the manufacturer of this device, does not practice medicine and does not recommend this or any other surgical technique for use on a specific patient. The surgeon who performs any procedure is responsible for determining and utilizing the appropriate products and techniques for each individual patient. Biomet is not responsible for selection of the appropriate surgical technique to be utilized for an individual patient.

surgical overview

step 1

Preoperatively plan using the x-ray templates, keeping in mind that the replacement range is 30–160mm in 10mm increments.

step 2

Perform a standard extensile oncologic approach to the proximal humerus and shoulder.

step 3

Mark the anterior location on the bone prior to resection. Using the metal template to see available resection lengths, resect the involved bone (Figure 1).

step 4

Ream the medullary canal with the tapered reamers (Figure 2) (1/2mm diameter increments with depth-gauge markers) to the desired diameter (6.5, 8.5, 10.5, or 12.5mm) and length (50, 100, 150, or 200mm) of intramedullary stem (Figure 2a).

The rasps (not shown) may be used to prepare the distal humerus for the anatomic taper of the intramedullary stem should it reach the distal humerus. These distal stem rasps have depth gauge markers as well as increment in diameter by 1mm (the implant increments by 2mm, so plan accordingly). When using a stem centralizer, ensure that the canal is prepared to be 2mm larger than the implant being used.

step 5

Choose the appropriately sized trial. Since all trials are sized identically with the corresponding implant, when allowing for a 2mm cement mantle, use the next size larger trial.

Screw the trial stem adapter onto the desired trial stem and place in the I/M canal (Figures 3 & 3a). If desired, the face reamer may be used over the trial adapter to correct any malalignment in the initial humeral resection (Figures 4 & 4a). Remove the face reamer and adapter for the next step.

step 6

Use the 3.5mm hex driver to attach the color-coded (Table 1) stem ledge to the corresponding trial stem (Figure 5).

Figure 1

Figure 2

Figure 2a

Figure 3

Figure 3a

Figure 4

Figure 4a

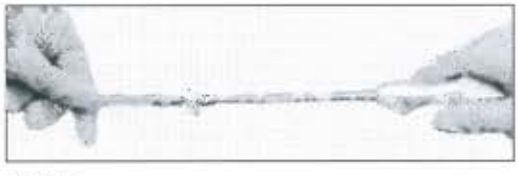

Figure 5

Diameter	Color
6.5mm	Silver
8.5mm	Gold
10.5mm	Black
12.5mm	Salmon
14.5mm	Gray

Table 1

step 7

Attach the desired segment trial to the stem trial assembly by using the thumb wheel (and breaker bar if necessary) (Figure 6). When using the optional soft tissue attachment sleeves, use the sleeve trials to determine the location of suture attachment sites. To do this, slide the sleeve trial over the segment trial until the distal ball plunger engages into the circumferential groove. Alignment indentations (every 45°) can be felt as the sleeve trial is turned on the segment trial. (These correspond to dimples on the final implant to easily replicate the trial orientation.)

Figure 6

step 8

Attach the desired proximal body trial to the stem or segment trial using the 3.5mm hex driver (Figure 7). On shorter resections, the segment will not be used. In these cases, the proximal body trial will be assembled directly to the stem trial.

Figure 7

Place an appropriately sized head trial on the proximal body trial assembly and perform a trial reduction (Figure 8).

Figure 8

Note: The dimple on the trial ledge indicates anterior orientation and is aligned with the anatomic taper at the distal end of the stem. When these are aligned with the anterior mark on the humerus, the implant is positioned at 40° retroversion. The corners on the 6.5mm and 8.5mm diameter ledges indicate +/- 10° while the corners on the 10.5mm and 12.5mm diameter ledges indicate +/- 5°.

step 9

Assemble the final implant to match the trial using the respective impactors to secure the taper junctions. *Locking screws are required at all taper junctions.* The small locking screw is used at the stem/segment junction and the large locking screw is used for the segment/proximal body junction (Figure 9). The small and large locking screws are packaged with each of the segments. When a segment is not used a Big Head/Small Thread locking screw unites the stem/proximal body junction (Figure 9a). This screw is packaged with each stem.

Figure 9

Figure 9a

Choose an appropriately sized stem centralizer and applicable cementing technique. *This device is intended for cemented applications only.*

features & benefits

Smooth, rounded suture holes on the proximal body

Eleven Bi-Angular™ head sizes

Titanium alloy porous coating promotes increased fixation and longevity

Three-piece modularity replaces 50 - 160mm in 10mm increments

Adjustable retroversion (40° +/- 10° for the 6.5mm and 8.5mm diameters and 40° +/- 5° for the 10.5mm and 12.5mm diameters)

Circumferential porous coating on the ledge of the intramedullary stem

Four intramedullary stem lengths (50, 100, 150 and 200mm) in four diameters (6.5, 8.5, 10.5 and 12.5mm) provide a total of 16 stem options

Anatomically tapered intramedullary stems better accommodate the distal humeral canal geometry

ordering information

Mosaic™ Proximal Body		
Part No.	Trials	Description
111000	405034	Standard
111001	405035	+10
111002	405036	+20

Mosaic™ Segment		
Part No.	Trials	Description
111003	405037	80mm
111004	405038	110mm
111005	405039	140mm

Mosaic™ Intramedullary Stem			
Part No.	Trials		Description
	Stem	Ledge	
111006	405005	405030	6.5 x 50mm
111007	405006	405030	6.5 x 100mm
111008	405007	405030	6.5 x 150mm
111009	405008	405030	6.5 x 200mm
111010	405009	405031	8.5 x 50mm
111011	405010	405031	8.5 x 100mm
111012	405011	405031	8.5 x 150mm
111013	405012	405031	8.5 x 200mm
111014	405013	405032	10.5 x 50mm
111015	405014	405032	10.5 x 100mm
111016	405015	405032	10.5 x 150mm
111017	405016	405032	10.5 x 200mm
111018	405017	405033	12.5 x 50mm
111019	405018	405033	12.5 x 100mm
111020	405019	405033	12.5 x 150mm
111021	405020	405033	12.5 x 200mm
–	405021	405029	14.5 x 50mm
–	405022	405029	14.5 x 100mm
–	405023	405029	14.5 x 150mm
–	405024	405029	14.5 x 200mm

Bi-Angular® Humeral Head		
Part No.	Trials	Description
114022	414422	40 x 15mm
114023	414423	40 x 19mm
114052	414415	44 x 15mm
114053	414419	44 x 19mm
114054	414423	44 x 23mm
114024	414424	48 x 19mm
114028	414428	48 x 23mm
114029	414421	48 x 27mm
114025	414420	52 x 19mm
114026	414426	52 x 23mm
114027	414427	52 x 27mm

Mosaic™ Stem Centralizer	
Part No.	Description
111022	6.3mm
111023	8.5mm
111024	10.5mm
111025	12.5mm

Trial Stem Adapter

405058

Face Reamer

405059

Humeral Head Driver

406514

T-Handle for Reamers

31-473620

3.5mm Hex Driver

CP460366	Short
32-471247	Long

Cylindrical Reamer

475801	6.5mm
475802	7.0mm
475803	7.5mm
475804	8.0mm
475805	8.5mm
475806	9.0mm
475807	9.5mm
475808	10.0mm
475809	10.5mm
475810	11.0mm
475811	11.5mm
475812	12.0mm
475813	12.5mm
475814	13.0mm
475815	13.5mm
475816	14.0mm
475817	14.5mm
475818	15.0mm
475819	15.5mm

Metal Resection Template

405051

X-Ray Templates

405000

Breaker Bar

405057

Extra Locking Screw Sets	
Part No.	Description
150481	Diaphyseal Big Head/ Small Thread
150475	

Rasp

405041	6.5mm
405042	7.5mm
405043	8.5mm
405044	9.5mm
405045	10.5mm
405046	11.5mm
405047	12.5mm
405048	13.5mm
405049	14.5mm

Taper Impactor

405052

Mosaic™/OSS Stem Impactor

405053

Taper Holder

405054

Mosaic™/OSS Stem Holder

405055

Mosaic™/OSS Proximal Body Inserter

405056

Taper Separator

32-471253

Loaner Sets

999285	Instruments
999585	Implants

Instrument Cases

595147	Hum. Resect & Reamers
595148	Rasp & Stem Trials
595149	Body/Seg/Sleeve/ Head Trials
595150	Impactors
595151	Miscellaneous Inst.

BIOMET ORTHOPEDICS, INC.
P.O. Box 587, Warsaw, IN 46581-0587 • 574.267.6639

web site: www.biomet.com • eMail: biomet@biomet.com
Form No. Y-BMT-7b6/02 1502/M

Bio-Modular®/Bi-Polar Shoulder Arthroplasty

Bi-Polar Features

- Concentric contact with shoulder cavity, both subacromial and glenoid.
- Potentially less glenoid-acromial wear due to bi-rotational head/shell motion.
- Enhanced tensioning of deltoid lever arm in rotator cuff deficient shoulders.

The Bi Polar numeral head is marketed for use in primary cases of non-inflammatory degenerative joint disease, rheumatoid arthritis, correction of severe functional deformity and fracture. The device is intended for use with a humeral stem inserted with bone cement. (USA)

[1]Data on file at Biomet, Inc.

Bio Modular is a registered trademark of Biomet, Inc.

BIOMET INC

Bi-Polar Hemi Arthroplasty

Prepare the humeral canal as specified in the Bio-Modular® Total Shoulder System technique (Y-BMI-260R). Position the trial head and shell components on the trial humeral stem or actual humeral stem implant to determine the proper neck length and shell size. The top of the head must project above the greater tuberosity to prevent tuberosity-acromial impingement. Adequate soft tissue tension must also be restored. However, the component should not set too proud or range of motion may be decreased, resulting in less than optimal contact between the Bi-Polar shell and the true glenoid.

Bi-Polar Head Assembly

Once the appropriate Bi-Polar head diameter and neck length have been established, final component assembly can now be performed as follows:

1. Insert the metal locking ring into the groove in the Bi-Polar shell. (This is usually pre-assembled.)
2. After thoroughly cleansing and drying the reverse morse taper, place the polyethylene locking ring over the collar of the stem, resting on the humeral resection line.
3. Place the 22.2mm inner Bi-Polar head through the polyethylene locking ring and into the reverse morse taper. Impact the head into the taper.
4. Place the polyethylene inner liner over the 22.2mm head.
5. Place the outer shell over the locking ring/inner liner assembly and snap together. The metal locking ring of the outer shell will snap into the outer groove on the polyethylene locking ring.
6. Should the prosthesis ever need to be removed, use the locking ring removal tool to disassemble the Bi-Polar components, and the removal ramp to disengage the modular head.

Reattach the subscapularis with non-absorbable sutures. Then externally rotate the arm to see at what degree of external rotation the suture line comes under tension. This will be the maximum amount of external rotation permitted during the first six weeks following surgery.

Close in a routine manner and apply a sling at the conclusion of the procedure.

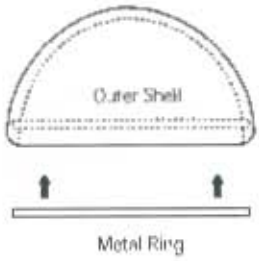

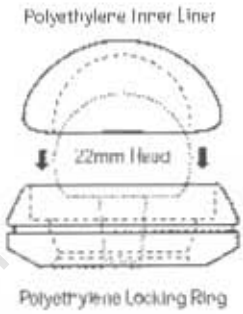

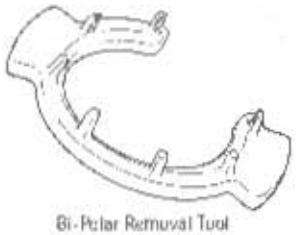

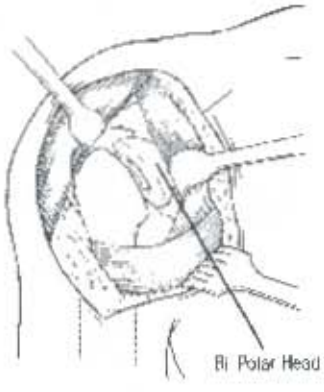

Bi-Polar Shell Components	
Part No.*	O.D./I.D.
113130	40 x 22.2mm
113131	44 x 22.2mm
113132	48 x 22.2mm
113133	52 x 22.2mm

*(Includes the polyethylene locking ring)

Metal Replacement Locking Rings for Bi-Polar Shells	
Part No.	Diameter
113170	40mm
113171	44mm
113172	48mm
113173	52mm

Bio-Modular®/Bi-Polar Modular Heads (Reverse Morse Taper)	
Part No.	Dia./Neck Length
113143	22.2mm / Standard
113144	22.2mm + 2
113145	22.2mm + 4

Bi-Polar Shell Trials
O.D./I.D. (mm)

408400	40 x 22.2mm
408402	44 x 22.2mm
408404	48 x 22.2mm
408406	52 x 22.2mm

Bio-Modular/Bi-Polar Modular Head Trials
Dia./Neck Length (mm)

408418	22.2mm / Standard
408420	22.2mm / + 2
408422	22.2mm / + 4

Bi-Polar Locking Ring Removal Tools
Dia. (mm)

408435	40mm
408436	44mm
408437	48mm
408438	52mm

Biomet, as the manufacturer of this device, does not practice medicine and does not recommend any particular surgical technique for use on a specific patient. The surgeon who performs any implant procedure is responsible for determining and utilizing the appropriate techniques for implanting the prosthesis in each individual patient. Biomet is not responsible for selection of the appropriate surgical technique to be utilized on an individual patient.

P.O. Box 587, Warsaw, IN 46581-0587 • 219.267.6639

web site: http://www.biomet.com • eMail: biomet@biomet.com

Form No. Y-BMT-618/003097/M

LCP: The Locking Compression Plate System

R. Frigg, A. Frenk, N.P. Haas & P. Regazzoni

Bone fractures lead to a complex tissue injury involving both the bone and the surrounding soft tissues. Treated in a conservative way, fractures often result in malalignment or non-unions as well as lead to stiffness of adjacent joints. To reduce the occurrence of these problems, open reduction and internal fixation of the bone can be carried out. The AO has developed these techniques and defined the basic principles of internal fixation. Anatomical reduction and stable internal fixation with plates and screws has been a very successful technique for the treatment of bone fractures.

Good bone healing can also result from relative stability, as known from conservative treatments, as well as from experience with intramedullary nails. The clinical outcome is dependent on obtaining correct length, axis and rotation of the fractured bone rather than on precise anatomical reduction and absolute stability. To achieve this, at the same time minimizing the amount of additional soft-tissue trauma, new surgical techniques for the treatment of multi-fragmented meta- and diaphyseal fractures with plates and screws were developed. These include the bridge-plating technique and the Minimally Invasive Plate Osteosynthesis (MIPO), and have been used with promising results [1–3].

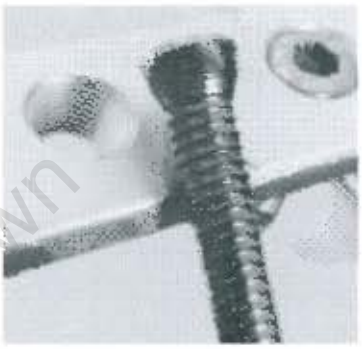

Fig. 2. LISS Plate and screw to show threaded hole/screw head.

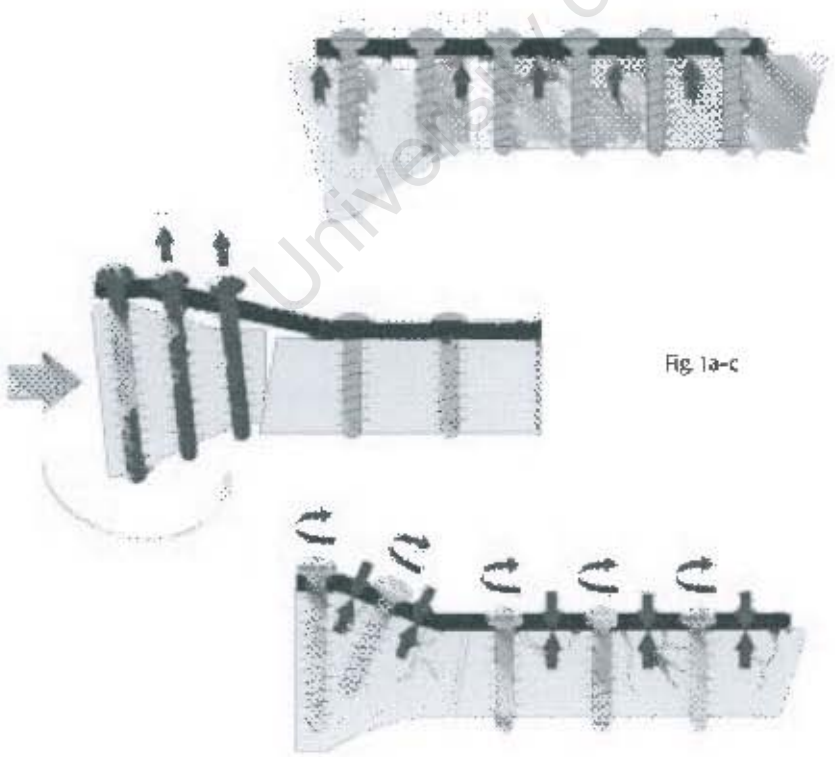

Fig. 1a–c

However, some problems in internal fixation with plates and screws remained unsolved. Three of those were implant related and, therefore, primarily technical issues: primary loss of reduction, secondary loss of reduction, and compression of the periosteum leading to a disturbance of the cortical blood supply, see Fig. 1a–c.

Plate and screws systems where the screw can be locked in the plate, so-called Locked Internal Fixators, were seen as a solution to these problems, Fig. 2. The plate and screws form one stable system and the stability of the fracture is dependant on the stiffness of the construct. No compression of the plate onto the bone is required, which reduces the risk of primary loss of reduction and preserves the bone blood supply. Locking the screw into the plate to ensure angular as well as axial stability eliminates the possibility for the screw to toggle, slide, or be dislodged and thereby strongly reduces the risk of postoperative loss of reduction. Based on the experiences gained with the PC-Fix system [4], the

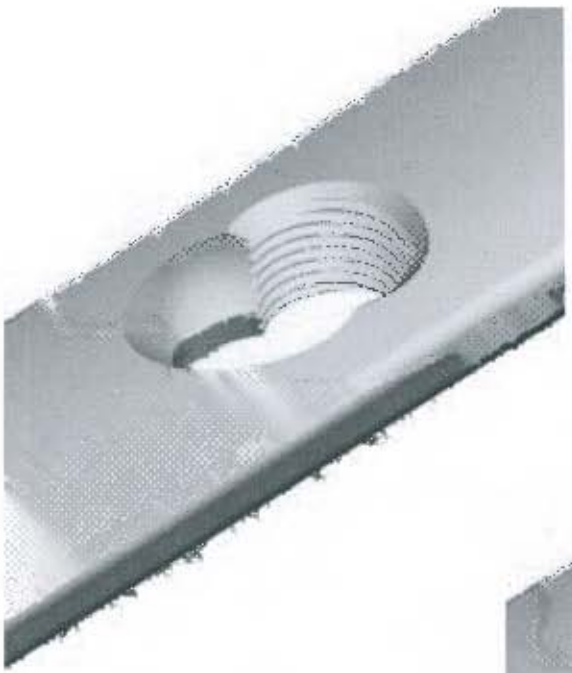

Fig. 3a–c. Combi-hole, Combi-hole with StandScrew, Combi-hole with Locking Head Screw

LISS DF and LISS PLT systems were developed and have shown very promising clinical results [5–7].

Several surgeons, in particular Prof. Dr. M. Wagner from Vienna, expressed the desire to have one plate system with the possibility for the surgeon to choose intraoperatively whether to use it with conventional screws, with locked screws, or with a combination of both. This problem was tackled by AO and led to the development of the Combination Hole of the Locking Compression Plate, see Fig. 3a–c. The first half of the hole comprises a Dynamic Compression Unit and is intended for a standard cortex or cancellous bone screw. As in a standard Dynamic Compression Plate, eccentric pre-drilling allows axial compression of the fracture to be achieved. Furthermore, the screw can be angulated, both laterally and longitudinally, respective to the plate axis. The threaded half of the hole is conical and permits the locking of the special Locking Head Screws (3.5 mm in diameter for the LCP small fragment set and 5.0 mm in diameter for the LCP large fragment set).

The AO Technical Commission decided in first phase to implement this idea on the large and small fragment plate systems, without modifying the overall design of the existing plates. This was very challenging—but successful—teamwork between the AO expert groups and Technical Commission, and the producers. The AOTK has approved both the LCP 4.5/5.0 large fragment system and LCP 3.5 small fragment system as standard products. A new milestone from the AO in the development of plates and screws for the new millennium!

SAWBONES®

a division of Pacific Research Laboratories, Inc.

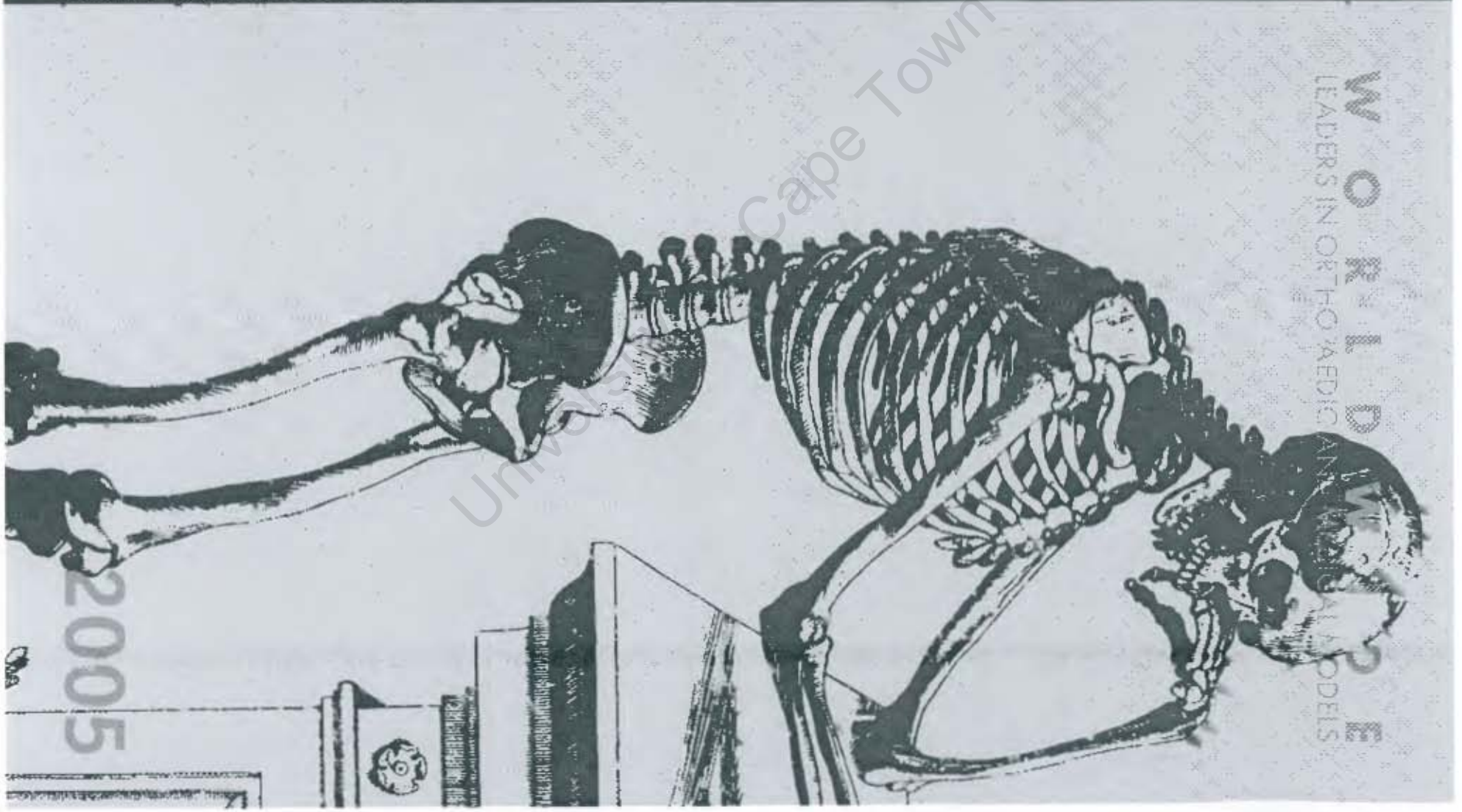

WORLDWIDE
LEADERS IN ORTHOPAEDIC ANATOMICAL MODELS

2005

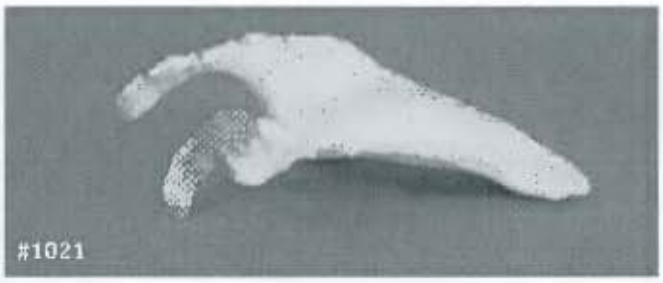

Scapula

Part #	Description	Price
1021	**Scapula:** Large left. Solid foam.	$11.50
1021-1	**Scapula:** Large left. Solid white plastic.	$31.00
1021-20	**Scapula:** Large right. Solid foam.	$11.50
1701-37	**Scapula:** Solid clear. Large left. Can be used for Product Display. See page 65 for details.	$77.75
1050	**Scapula:** Large left. With vise attachment block. Foam cortical shell.	$15.75
1050-1	**Scapula:** Large left. With vise attachment block. Foam cortical shell with neoprene capsule, clear glenoid rim and premolded anchor holes.	$43.00

Clavicle

Part #	Description	Price
1020	**Clavicle:** Length 16 cm. Large left. Solid foam.	$6.25
1020-20	**Clavicle:** Length 16 cm. Large right. Solid foam.	$6.25
1701-38	**Clavicle:** Solid clear. Large left. Can be used for Product Display. See page 65 for details.	$29.00

Humerus (Left Proximal Half)

Part #	Description	Price
1051	**Humerus:** Proximal half. Large left. Foam cortical shell with cancellous. Canal diameter 9 mm.	$9.50
1051-6	**Humerus:** Proximal half. Large left. Foam cortical shell with cancellous. Canal diameter 9 mm. With neoprene supraspinatus tendon.	$22.75
1051-7	**Humerus:** Proximal half. Large left. Foam cortical shell with cancellous. Canal diameter 9 mm. With clear insert and replaceable neoprene ligament (#1051-8).	$49.25

Models can be fractured or deformed to your specifications. Prices available upon request.

SAWBONES® WORLDWIDE
LEADERS IN ORTHOPAEDIC AND MEDICAL MODELS

COMPOSITE BONES

Composite Bones are designed to simulate the physical behavior of a human bone, providing an alternative for cadaver bones in testing and research. Mechanical behavior of the composite bone material falls within the range for cadaveric specimens. Composite bones have shown significantly lower variability in testing compared to cadaveric specimens for all loading regimens, offering a more reliable test bed[1,2]. Other advantages of testing with Composite Bones include unlimited sample sizes with no special handling or preservation requirements.

BIOMECHANICAL

3rd Generation Composite Bones

Sawbones 3rd Generation Composite Bone model natural cortical bone using a mixture of glass fibers and epoxy resin pressure injected around a foam core. The midshaft area has an intramedullary canal. Standard bone models are manufactured with a solid rigid polyurethane foam cancellous core material. The dense cell structure of the solid rigid polyurethane foam makes it slightly more uniform in properties. The bones can be manufactured using cellular rigid polyurethane foam upon special request. Cellular rigid polyurethane foam is visually more comparable to natural cancellous bone with cell size ranging from 0.5-1.0 mm. Both the solid rigid and cellular rigid polyurethane foams have 95% closed cell structure.

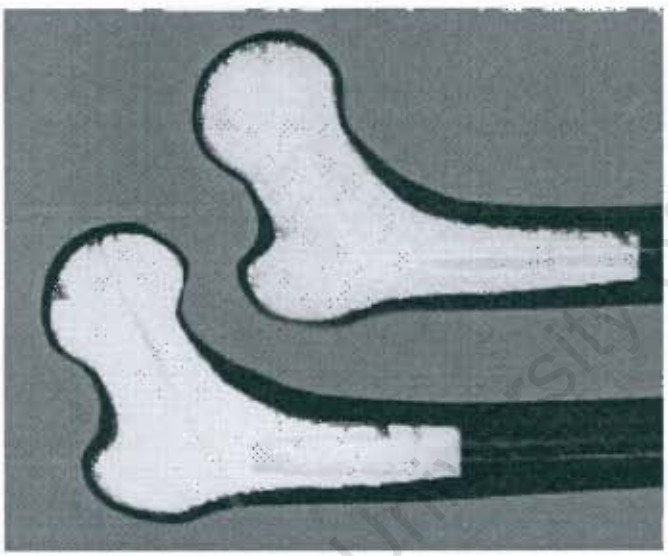

Average material properties:

Simulated Cortical Bone (E-Glass filled epoxy)

Density	Tensile		Compressive	
	Strength	Modulus	Strength	Modulus
(g/cc)	(MPa)	(MPa)	(MPa)	(MPa)
1.7	90	12,400	120	7,600

Simulated Cancellous Bone (Rigid polyurethane foam)

		Compressive	
	Density	Strength	Modulus
	(g/cc)	(MPa)	(MPa)
Solid	0.27	4.8	104
Cellular	0.32	5.4	137

Custom Bone Models

Custom bones and modifications are available upon request.

The 3rd Generation Composite Bone was developed to improve the composite bone physical behavior, increase anatomic detail in the cortical wall and ease manufacturing difficulties of the 2nd Generation bone. The 2nd generation bone will still be manufactured upon special request.

Supporting Composite Bone Data

For access to CAD models of some of our composite tibias and femurs, please see the following Web site.
www.cineca.it/hosted/LTM-IOR/back2net/ISB_mesh/isb_mesh.html

Substantial test data, regarding the mechanical validation of the femur and tibia models is available in the following documents.

1. Cristofolini, Luca (University of Bologna, Italy); Viceconti, Marco ; Cappello, Angelo and Toni, Aldo. **Mechanical validation of whole bone composite femur models.** *Journal of Biomechanics Vol. 29 (1996), 525-535.*
2. Cristofolini, Luca (University of Bologna, Italy) and Viceconti, Marco. **Mechanical validation of whole bone composite tibia models.** *Journal of Biomechanics Vol. 33 (2000), pp. 279-288.*
3. Heiner, Anneliese and Brown, Thomas. (University of Iowa, USA). **Structural properties of a new design of composite replicate femurs and tibias.** *Journal of Biomechanics Vol. 34 (2001), pp. 777-781.*

COMPOSITE BONES

SAWBONES WORLDWIDE
LEADERS IN ORTHOPAEDIC AND MEDICAL MODELS

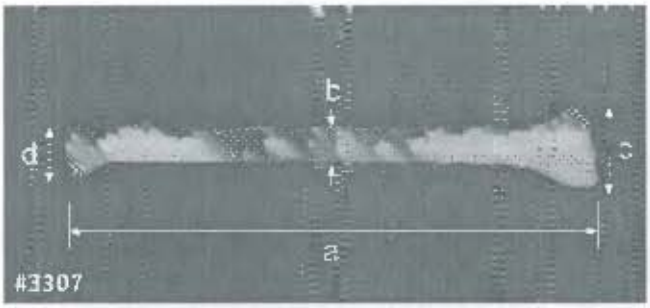

3rd Generation Composite Radius

Large, left. Dimensions: **a)** 250 mm; **b)** 16 mm; **c)** 35 mm; **d)** 27 mm; 5 mm canal

#3307 $106.00

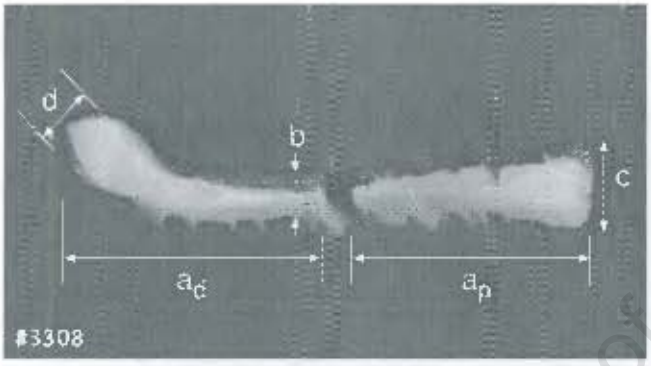

3rd Generation Composite Proximal & Distal Clavicle

Large, left. Dimensions: **a distal)** 95 mm; **a proximal)** 80 mm; **b)** 15 mm; **c)** 28 mm; **d)** 29 mm; no canal. Manufactured in two parts.

#3308 $93.25

3rd Generation Composite Hemi Pelvis & Sacrum

Large, left. Dimensions: **a)** 235 mm; **b)** 55 mm; **c)** 140 mm; **d)** 175 mm

#3305 **Hemi Pelvis** $138.75

#3305-2 **Sacrum** $130.00

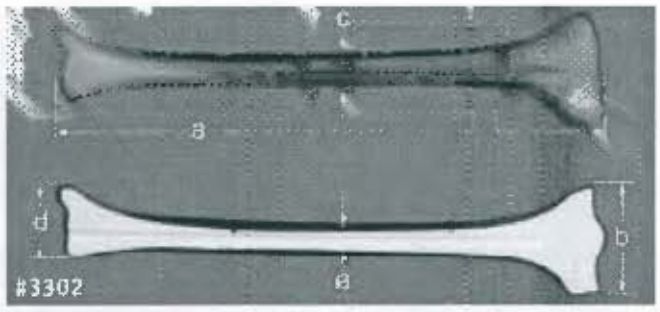

3rd Generation Composite Tibia

Medium, left. Dimensions: **a)** 375 mm; **b)** 74 mm; **c)** 22 mm; **d)** 52 mm; **e)** 9 mm canal

#3301 $106.00

Large, left. Dimensions: **a)** 405 mm; **b)** 84 mm; **c)** 28 mm; **d)** 58 mm; **e)** 10 mm canal

#3302 $106.00

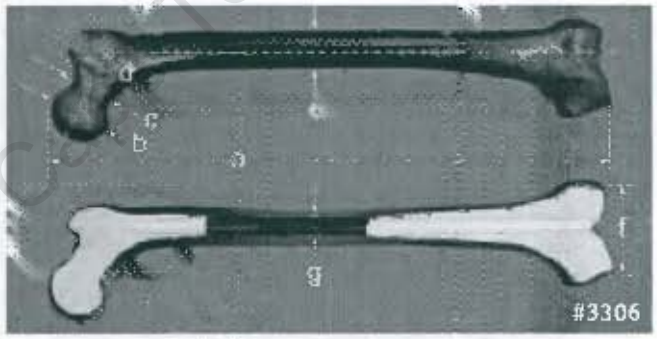

3rd Generation Composite Femur

Medium, left. Dimensions: **a)** 455 mm; **b)** 45 mm; **c)** 31 mm; **d)** 135°; **e)** 27 mm; **f)** 74 mm; **g)** 13 mm canal standard. Also available with 10 or 12 mm canal.

#3303 $106.00

Large, left. Dimensions: **a)** 485 mm; **b)** 52 mm; **c)** 37 mm; **d)** 120°; **e)** 32 mm; **f)** 93 mm; **g)** 16 mm canal standard. Also available with 10 or 12.8 mm canal.

#3306 $106.00

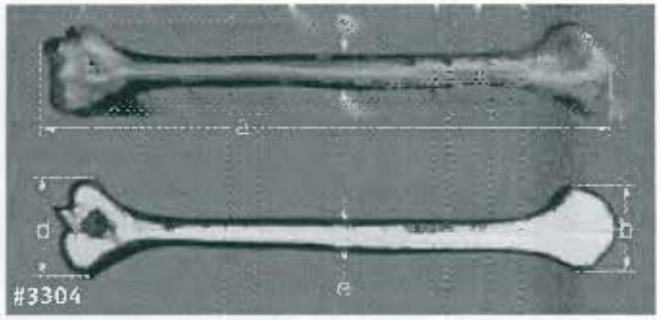

3rd Generation Composite Humerus

Large, left. a) 365 mm; **b)** 55 mm; **c)** 23 mm; **d)** 64 mm; **e)** 9 mm - canal tapers to 5.5 mm, 80 mm from the distal end.

#3304 $106.00

1993 ANNUAL BOOK OF ASTM STANDARDS

SECTION 13

Medical Devices

VOLUME

13.01 Medical Devices

Includes standards of the following committees:

F-4 on Medical and Surgical Materials and Devices
F-29 on Anesthetic and Respiratory Equipment
F-30 on Emergency Medical Services
F-31 on Health Care Services and Equipment
F-32 on Search and Rescue

Publication Code Number (PCN): 01-130193-54

ASTM 1916 Race Street, Philadelphia, PA 19103-1187 USA ■ (215) 299-5400 ■ TWX: 710-670-1037 ■ FAX: 215-977-9679

Designation: F 543 – 92

Standard Specification for Cortical Bone Screws[1]

This standard is issued under the fixed designation F 543; the number immediately following the designation indicates the year of original adoption or, in the case of revision, the year of last revision. A number in parentheses indicates the year of last reapproval. A superscript epsilon (ε) indicates an editorial change since the last revision or reapproval.

This specification has been approved for use by agencies of the Department of Defense and for listing in the DoD Index of Specifications and Standards.

1. Scope

1.1 This specification covers the acceptable materials, finish, identification, dimensions, and tolerances for metal cortical bone screws intended for use as surgical implants.

1.2 The values stated in U.S. customary units are to be regarded as the standard and SI (metric) equivalents approximate for Thread Types I, II, III, and IV. The values stated in SI units are to be regarded as the standard and U.S. customary equivalents approximate for Thread Type V.

2. Referenced Documents

2.1 *ASTM Standards:*

F 55 Specification for Stainless Steel Bar and Wire for Surgical Implants[2]

F 67 Specification for Unalloyed Titanium for Surgical Implant Applications[2]

F 75 Specification for Cast Cobalt-Chromium-Molybdenum Alloy for Surgical Implant Applications[2]

F 86 Practice for Surface Preparation and Marking of Metallic Surgical Implants[2]

F 90 Specification for Wrought Cobalt-Chromium-Tungsten-Nickel Alloy for Surgical Implant Applications[2]

F 116 Specification for Medical Screwdriver Bits[2]

F 117 Test Method for Driving Torque of Self-Tapping Medical Bone Screws[2]

F 136 Specification for Wrought Titanium 6Al-4V ELI Alloy for Surgical Implant Applications[2]

F 138 Specification for Stainless Steel Bar and Wire for Surgical Implants (Special Quality)[2]

3. Classification

3.1 This specification includes the following heads for bone screws:

3.1.1 *Type I*—Single recess oval head.

3.1.2 *Type II*—Cruciate recess oval head.

3.1.3 *Type III*—Slotted Phillips recess oval head.

3.1.4 *Type IV*—Phillips recess oval head.

3.1.5 *Type V*—Hexagonal recess oval head.

3.2 This specification includes the following threads for bone screws:

3.2.1 *Class A*—No. 4M bone screw thread.

3.2.2 *Class B*—No. 6M bone screw thread.

3.2.3 *Class C*—No. 6.5M bone screw thread.

3.2.4 *Class D*—No. 7M bone screw thread.

3.2.5 *Class E*—No. 8M bone screw thread.

3.2.6 *Class F*—Metric threads.

4. Material

4.1 Bone screws conforming to this specification shall be supplied from materials conforming to the following specifications: F 55, F 67, F 75, F 90, F 136, and F 138.

5. Dimensions and Tolerances

5.1 Bone-screw heads conforming to this specification shall be fabricated in accordance with the dimensions and tolerances shown in the respective figures indicated.

5.1.1 *Type I*—Fig. 1.

5.1.2 *Type II*—Fig. 2.

5.1.3 *Type III*—Fig. 3.

5.1.4 *Type IV*—Fig. 4.

5.1.5 *Type V*—Fig. 5.

5.2 Bone screw threads conforming to this specification shall be fabricated in accordance with the dimensions and tolerances shown in the tables indicated.

5.2.1 *Class A, B, C, D, and E*—Table 1.

5.2.2 *Class F*—Table 2.

5.3 *Tolerances:*

5.3.1 Unspecified tolerances for Figs. 1 through 5 are as follows:

Decimal ± 0.005 in. (0.13 mm)
Fraction ± 1/64 in. (0.4 mm)
Angle ± 2 deg
Metric ± 0.5 mm (0.019 in.)

6. Finish and Identification

6.1 Bone screws conforming to this specification shall be finished in accordance with Practice F 86.

6.2 Bone screws shall have no sharp exterior edges except where a sharp edge provides a functional purpose.

[1] This specification is under the jurisdiction of ASTM Committee F-4 on Medical and Surgical Materials and Devices, and is the direct responsibility of Subcommittee F04.21 on Osteosynthesis.

[1] Current edition approved Feb. 15, 1992. Published June 1992. Originally published as F 543 – 77. Last previous edition F 543 – 82.

[2] *Annual Book of ASTM Standards*, Vol 13.01.

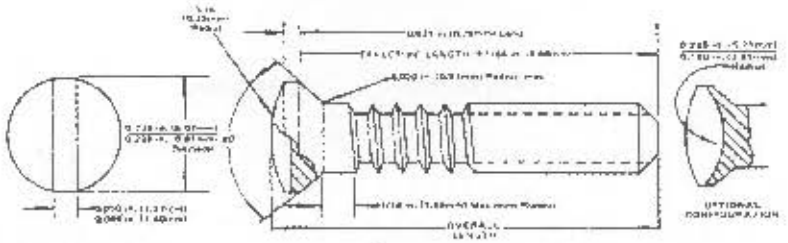

NOTE 1—*Slot Depth*—Slot shall penetrate to 30 % edge width (minimum) but shall not intersect below bottom of edge.
NOTE 2—All dimensions given shall apply equally to Class A, B, C, D, and E Bone screws.

FIG. 1 Oval Head Single Slot Recess Class A, B, C, D, and E Bone Screws

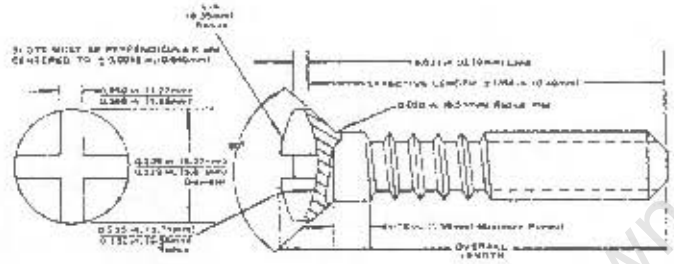

NOTE 1—Cruciate slot shall not intersect below bottom of edge.
NOTE 2—All dimensions given shall apply equally to Class A, B, C, D, and E Bone screws.
NOTE 3—Slot must be perpendicular to ±0.0015 in. (0.040 mm) and centered to ±0.010 in. (0.250 mm).

FIG. 2 Oval Head Cruciate Recess Class A, B, C, D, and E Bone Screws

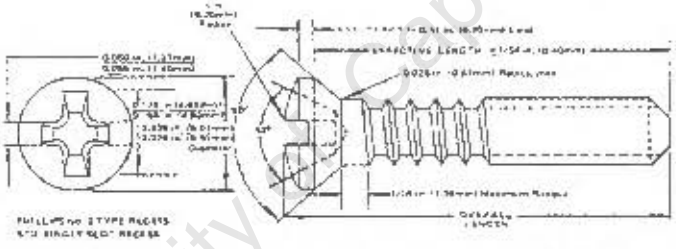

NOTE 1—*Slot Depth*—Single slot shall penetrate to 30 % edge width (minimum) but shall not intersect below bottom of edge.
NOTE 2—All dimensions given shall apply equally to Class A, B, C, D, and E Bone screws.

FIG. 3 Oval Head Slotted Phillips Recess Class A, B, C, D, and E Bone Screws

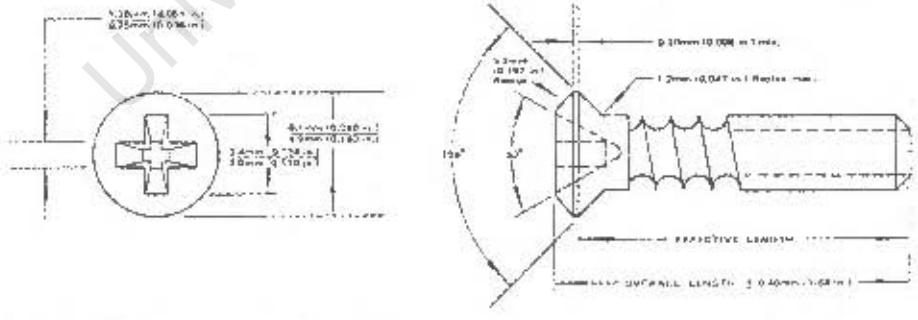

NOTE—All dimensions given shall apply equally to 2.7 mm, 3.5 mm, metric thread screws.

FIG. 4 Oval Head Phillips Recess 2.7 mm, 3.5 mm Bone Screws

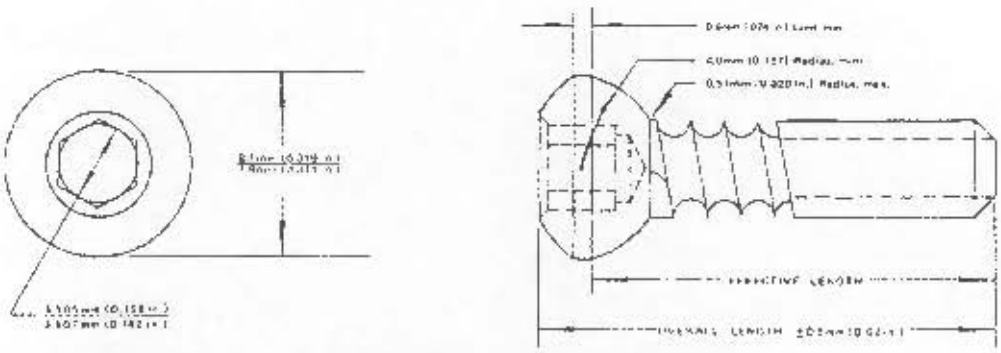

NOTE—Pilot hole shall not penetrate more than 83 % of head. Hex shall penetrate at least 50 % of the pilot hole.

FIG. 5 Oval Head Hexagonal Recess 4.5 mm

TABLE 1 Inch Threads—Dimensions and Tolerances (see Fig. 6)

Class	Size	Major Diameter		Minor Diameter		Threads per inch
		in.	mm	in.	mm	
A	4M	0.112	2.84	0.082	2.08	24
		0.110	2.79	0.080	2.03	
B	6M	0.140	3.56	0.104	2.64	20, 32
		0.134	3.40	0.098	2.49	
C	E 5M	0.146	3.71	0.106	2.69	20
		0.142	3.61	0.102	2.59	
D	7M	0.156	3.96	0.118	3.00	20
		0.152	3.86	0.112	2.84	
E	8M	0.166	4.22	0.127	3.23	20
		0.160	4.06	0.121	3.07	

TABLE 2 Metric Threads—Dimensions and Tolerances (see Fig. 6)

Size, mm	Major Diameter		Minor Diameter		Pitch, mm
	in.	mm	in.	mm	
2.7	0.110	2.80	0.083	2.10	
	0.102	2.60	0.067	1.70	1.0
3.5[A]	0.142	3.60	0.083	2.10	1.25
	0.134	3.40	0.075	1.90	1.75
3.5	0.142	3.60	0.095	2.45	1.25
	0.134	3.40	0.089	2.25	1.75
4.5	0.181	4.60	0.122	3.10	
	0.171	4.35	0.112	2.85	1.75

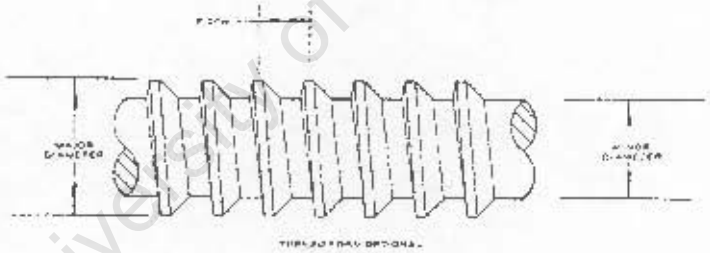

FIG. 6 Cortical Bone Screw Threads

Polyethylene

	PE-HWU	PE-HWST	PE-HML 500	PE-HMG 1000	PE-EL
Technical data Density, g/cm³, ISO 1183	0.95	0.95	0.95	0.93	0.99
Yield stress, MPa, DIN EN ISO 527	22	21	28	22	26
Elongation at yield, %, DIN EN ISO 527	9	9	8	10	7
Elongation at break, %, DIN EN ISO 527	300	500	300	350	60
Tensile-E-modulus, MPa, DIN EN ISO 527	800	800	850	800	1100
Impact strength, kJ/m², DIN EN ISO 179	without break	without break	without break	without break	without break
Notched impact strength, kJ/m², DIN EN ISO 179	12	13	50	without break	5
Ball indentation hardness, MPa, DIN EN ISO 2039-1	40	43	45	40	50
Shore hardness, D, ISO 868	63	62	66	64	63
Average thermal coefficient of elongation, K⁻¹, DIN 53752	1.8×10^{-4}	1.8×10^{-4}	1.8×10^{-4}	1.8×10^{-4}	1.8×10^{-4}
Thermal conductivity, W/m·K, DIN 52612	0.38	0.38	0.38	0.38	0.38
Fire behaviour, DIN 4102	normal inflamable	normal inflamable	normal inflamable	normal inflamable	normal inflamable
Dielectric strength, kV/mm, IEC 243-1	47	50	44	44	–
Surface resistance, Ohm, DIN IEC 167	10^{14}	10^{14}	10^{14}	10^{14}	$\leq 10^{8}$
Temperature range, °C	+30 up to +80	+50 up to +80	–100 up to +80	–260 up to +80	–20 up to +80
Chemical resistance	highly resistant to many acids, alkalis and solvents				
Physiologically acceptable acc. to BgVV[1] and FDA[2] (USA)	yes	yes	yes	yes (in colour natural)	no
Fabrication					
Welding	yes	yes	yes	possible	possible
Glueing, glassfibre reinforcing	only after preparatory treatment				
Lacquering, printing	only after preparatory treatment				
Warm bending	good	good	possible	limited	possible
Properties and applications	especially for outdoor use UV-stabilised, good thermoformable, particularly for the use in container and apparatus building as well as in the thermoforming sector	physiologically acceptable, particularly for applications in the food industry	high molecular weight, abrasion resistant, good sliding properties, particularly for applications in the conveyor industry as well as in machine and apparatus building	highest molecular weight, good abrasion resistance, good sliding properties, for the use in the conveyor industry, particularly in silo and bunker building	electrically conductive, for outdoor use UV-stabilised, particularly for the use in container and apparatus building in the explosion proofing sector

[1] Federal Health Institute for the protection of consumers and veterinary medicine
[2] Food and Drug Administration

INSPECTION CERTIFICATE
ABNAHMEPRÜFZEUGNIS
CERTIFICAT DE RÉCEPTION

BIOMATERIALS® LIMITED

CUSTOMER: FÜR FA/CLIENT

UNIVERSITY OF CAPE TOWN
MECHANICAL ENGINEERING DEPARTMENT
ROUNDEBOSCH 7701
SOUTH AFRICA

BECKLANDS CLOSE
BAR LANE INDUSTRIAL ESTATE
ROECLIFFE, BOROUGHBRIDGE
NORTH YORKSHIRE.
YO51 9NR

Form No 7 – 3 (3) | Issue No: 1 | Cert No:45677 | Date: 18/07/2003

YOUR ORDER NUMBER IHRE BESTELL NR VOTRE COMMANDE	DATE: DATUM DATE	DELIVERY NOTE No: ZUR LIEFERUNGSCHEIN-NR A QUOI VA SI D'EXPEDITION	DATE: DATUM DATE	OUR REFERENCE: UNS KOMM-NR NOTRE REFERENCE
F560534	27.03.03	97	15.07.03	W.O:10596

PRODUCT: ERZEUGNISFORM PRODUIT	6/4 TITANIUM ALLOY ELI SURGICAL IMPLANT GRADE	SPECIFICATION: LIEFERBEDINGUNGEN CONDITION DE LIVRAISON	ASTM F136-98 BS 7252-ISO 5832-3 1997

ITEM: POS POSTE	QUANTITY: ANZAHL NOMBRE	DIMENSIONS (mm): ABMESSUNGEN DIMENSIONS	WEIGHT: MASSE MASSE (KG)	CAST: SCHMELZEN NR COULEE NR	CONDITION: LIEFERZUSTAND ETAT DE LIVRAISON
1	3 OFF	20 MM DIAMETER X 1000 MM		CU71728	ANNEALED GROUND

CHEMICAL COMPOSITION / CHEMISCHE ZUSAMMENSETZUNG / COMPOSITION CHIMIQUE

ITEM: POS POSTE	CAST: SCHMELZEN NR COULEE NR	Al	V	Fe	C	N	O	H
1	CU71728	6.12	4.20	0.17	0.01	0.005	0.185	0.003

MECHANICAL PROPERTIES / MECHANISCHE PRÜFUNG / CARACTERISTIQUES MECANIQUES

ITEM: POS POSTE	TEST No: PRÜB NR EPROUVETTE No	Rp.2 PROOF STRESS 0.2%ONDERDE LIMITE ELASTIQUE CONVENTIONNELLE	R el YIELD STRENGTH STRECKGRENZE LIMITE ELASTIQUE APARENTE	Rm TENSILE STRENGTH ZUGFESTIGKEIT RESISTANCE A LA TRACTION	A ELONGATION % BRUCHDEHNUNG ALLONGEMENT	Z RED OF AREA % BRUCH SCHNURUNG STRICTION	HARDNESS HÄRTE DURETE	IMPACT VALUE KERBSCHLAGARBEIT RESILIENCE
1		892		975	17.0	46		

REMARKS: BEMERKUNGEN / REMARQUES
GRAIN SIZE: 10
MICRO TEST: PASS
BETA TRANSUS: 965/970°C

WE HERBY CERTIFY, THAT THE WHOLE OF THE SUPPLIES DETAILED ABOVE COMPLY WITH THE TERMS OF THE ORDER CONTRACT AND UNLESS OTHERWISE STATED ARE COVERED BY THE SOURCE'S CERTIFICATE OF CONFORMITY WITH FULL LOT TRACEABILITY IN ACCORDANCE WITH OUR QUALITY SYSTEM REQUIREMENTS. MANUFACTURED, TESTED AND INSPECTED IN ACCORDANCE WITH OUR QUALITY SYSTEM REQUIREMENTS

ON BEHALF OF HEYMARK METALS LTD

APPROVED SIGNATORY

Heymark Metals is a NQA registered BS EN ISO 9002 company
Certificate number 7772

INSPECTION CERTIFICATE
ABNAHMEPRÜFZEUGNIS
CERTIFICAT DE RÉCEPTION

BIOMATERIALS®
LIMITED

CUSTOMER: FÜR FA/CLIENT

UNIVERSITY OF CAPE TOWN
MECHANICAL ENGINEERING DEPARTMENT
ROUNDEBOSH 7701
SOUTH AFRICA

BECKLANDS CLOSE
BAR LANE INDUSTRIAL ESTATE
ROECLIFFE, BOROUGHBRIDGE
NORTH YORKSHIRE.
YO51 9NR

Tel: +44 (0) 1423 323388
Fax: +44 (0) 1423 326888

Form No 7 – 3 (4) Issue No: 1 Cert No:45683 Date: 21/07/2003

YOUR ORDER NUMBER IHRE BESTELL NR VOTRE COMMANDE	DATE: DATUM DATE	DELIVERY NOTE No: ZUR LIEFANZEIGEN-NR A L'AVIS D'EXPEDITION	DATE: DATUM DATE	OUR REFERENCE: UNS KOMM-NR NOTRE REFERENCE
F560534	27.03.03	97	15.07.03	W.O:10596

PRODUCT: COBALT CHROME MOLY
ERZEUGNISFORM
PRODUIT

SPECIFICATION: ASTM F1537
LIEFERBEDINGUNGEN
CONDITION DE LIVRAISON

ITEM: POS POSTE	QUANTITY: ANZAHL NOMBRE	DIMENSIONS (mm): ABMESSUNGEN DIMENSIONS	WEIGHT: MASSE MASSE (Kg)	CAST: SCHMELZEN NR COULEE NR	CONDITION: LIEFERZUSTAND ETAT DE LIVRAISON
7	2 OFF	19.05 MM DIAMETER X 1000 MM		H51094	WARM WORKED, GROUND

CHEMICAL COMPOSITION CHEMISCHE ZUSAMMENSETZUNG / COMPOSITION CHIMIQUE

ITEM: POS POSTE	CAST: SCHMELZEN NR COULEE NR	C	Mn	P	S	Si	Cr	Mo	N	Ni	Fe	W	Co
7	H51094	0.043	0.48	0.002	0.0004	0.38	27.59	5.67	0.18	0.17	0.32	<0.05	BAL

MECHANICAL PROPERTIES / MECHANISCHE PRÜFUNG CARACTÉRISTIQUES MÉCANIQUES

ITEM: POS POSTE	TEST No: PRÜF NR EPROUVETTE No	Rp.2 PROOF STRESS DEHN GRENZE LIMITE ELASTIQUE CONVENTIONNELLE	R el YIELD STRENGTH STRECKGRENZE LIMITE ELASTIQUE APPARENTE	Rm TENSILE STRENGTH ZUGFESTIGKEIT RESISTANCE A LA TRACTION	A ELONGATION % BRUCHDEHNUNG ALLONGEMENT	Z RED OF AREA % BRUCHEINSCHNÜRUNG STRICTION	HARDNESS HÄRTE DURETE	IMPACT VALUE KERBSCHLAGARBEIT RESILIENCE
		N/mm²		N/mm²			RC	
7		830		1260	42.0	27.0	35.5-36.5	

REMARKS: BEMERKUNGEN / REMARQUES
GRAIN SIZE: 10

WE HERBY CERTIFY, THAT THE WHOLE OF THE SUPPLIES DETAILED ABOVE COMPLY WITH THE TERMS OF THE ORDER CONTRACT AND UNLESS OTHERWISE STATED ARE COVERED BY THE SOURCE'S CERTIFICATE OF CONFORMITY WITH FULL LOT TRACEABILITY IN ACCORDANCE WITH OUR QUALITY SYSTEM REQUIREMENTS. MANUFACTURED, TESTED AND INSPECTED IN ACCORDANCE WITH OUR QUALITY SYSTEM REQUIREMENTS

ON BEHALF OF HEYMARX METALS LTD

APPROVED SIGNATORY
Biomaterials® is a NQA registered BS EN ISO 9002 company
Certificate number 7772

Appendix E

Drawings

E.1 Equipment

Drawing Number	Drawing Title	Part Description
Equipment-01-01	UHMWPE Socket Cutter	UHMWPE Socket Cutter
Equipment-02-00	Tension Test Set-up	Assembly
Equipment-02-01	Zwick Couplings	Compression Coupling
Equipment-02-02	Zwick Couplings	Top Tension Coupling
Equipment-02-03	Zwick Couplings	Lower Tension Coupling
Equipment-02-04	Test Housing for Socket	Test Housing for Socket
Equipment-02-05	Zwick Test Ball	Zwick Test Ball
Equipment-02-06	Socket Locking Ring	Socket Locking Ring
Equipment-02-07	Press-fit Test Socket	Press-fit Test Socket
Equipment-03-00	Scapula Test Rig	Assembly
Equipment-03-01	Scapula Test Rig	Rig Base
Equipment-03-02	Scapula Test Rig	Rig Large Side
Equipment-03-03	Scapula Test Rig	Rig Small Side
Equipment-03-04	Scapula Test Rig	Rig Top
Equipment-03-05	Scapula Test Rig	Rig Top Slider
Equipment-03-06	Scapula Test Rig	Rig Supraspinous Bar
Equipment-03-07	Scapula Test Rig	Allen M10x70mm Ball
Equipment-03-08	Scapula Test Rig	Rig Top Slider Nut
Equipment-03-09	Scapula Test Rig	Rig Side Clamp Face
Equipment-03-10	Scapula Test Rig	Rig 90 Foot
Equipment-03-11	Scapula Test Rig	Rig Compression Foot
Equipment-03-12	Scapula Test Rig	Allen M8x70mm Ball

E.2 Full Designs

Drawing Number	Drawing Title	Part Description
Full-01-00	Hybrid-Screw TSR	Assembly
Full-01-01	Hybrid-Screw TSR	Glenoid Fixation Plate
Full-01-02	Hybrid-Screw TSR	Ball and Tapered Stem
Full-01-03	Hybrid-Screw TSR	Cemented Glenoid Peg
Full-01-04	Hybrid-Screw TSR	Coracoid Plate
Full-01-05	Hybrid-Screw TSR	UHMWPE Socket Bottom
Full-01-06	Hybrid-Screw TSR	UHMWPE Socket Top
Full-01-07	Hybrid-Screw TSR	Socket Locking Clip
Full-01-08	Hybrid-Screw TSR	Coracoid Screw
Full-01-09	Hybrid-Screw TSR	Peg Stop Rotation
Full-01-10	Hybrid-Screw TSR	Humeral Housing
Full-01-11	Hybrid-Screw TSR	Humeral Stem Extension
Full-01-12	Hybrid-Screw TSR	Humeral Stem
Full-02-00	Central-Peg TSR	Assembly
Full-02-01	Central-Peg TSR	Glenoid Central Peg
Full-03-00	Quad-Point TSR	Assembly
Full-03-01	Quad-Point TSR	Housing
Full-03-02	Quad-Point TSR	Coracoid Plate
Full-03-03	Quad-Point TSR	Coracoid Plate Screw
Full-03-04	Quad-Point TSR	Ball and Stem
Full-03-05	Quad-Point TSR	Humeral Component
Full-03-06	Quad-Point TSR	Ball Locking Screw

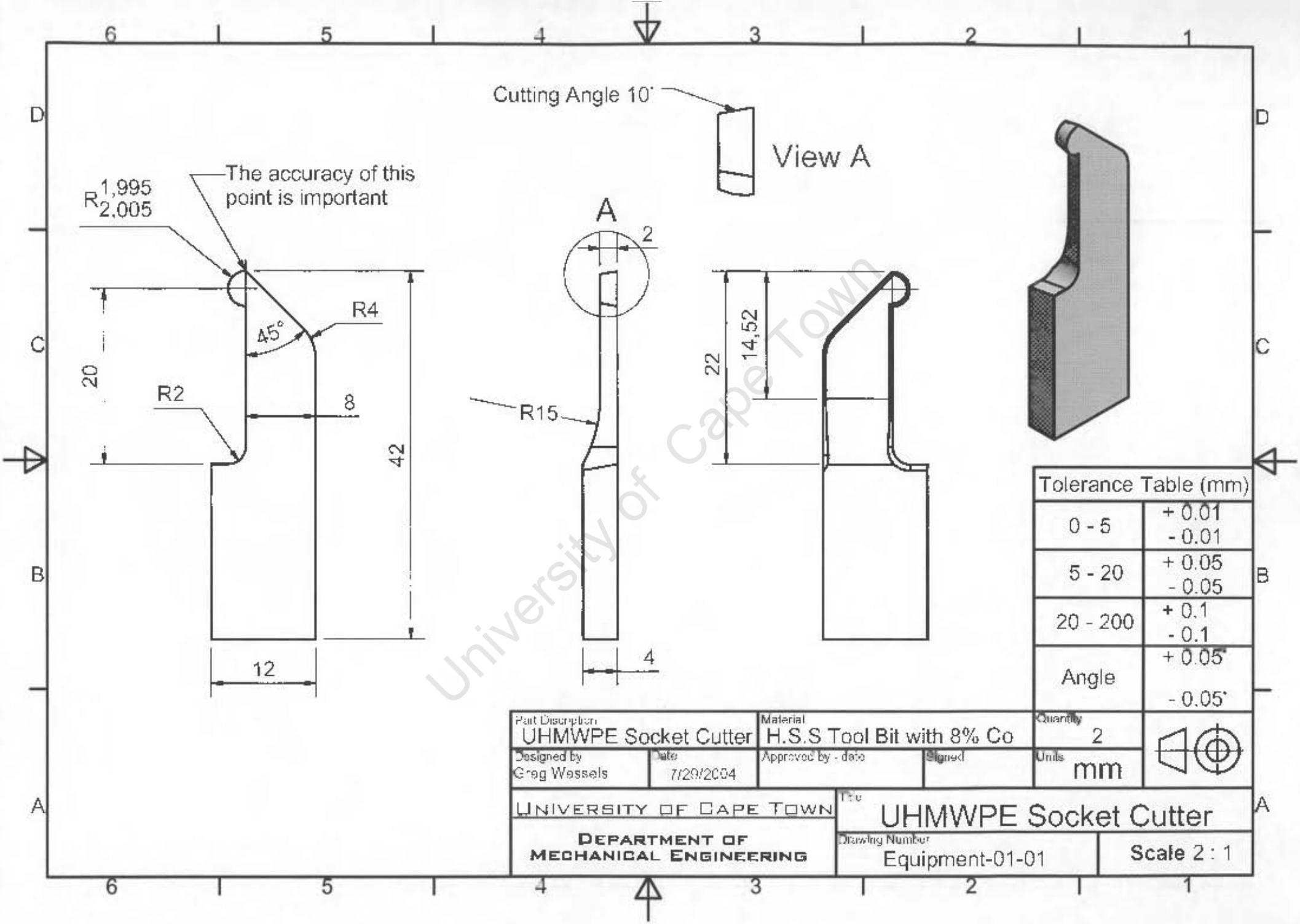

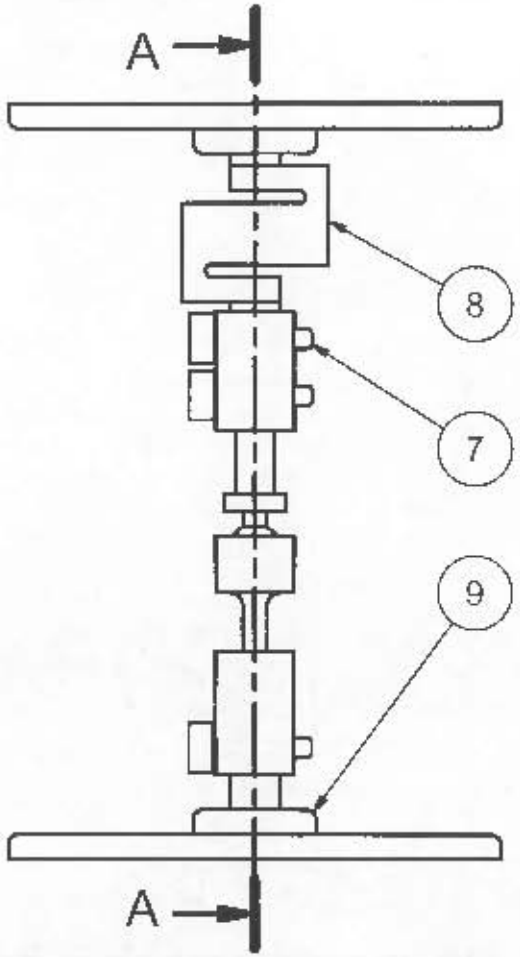

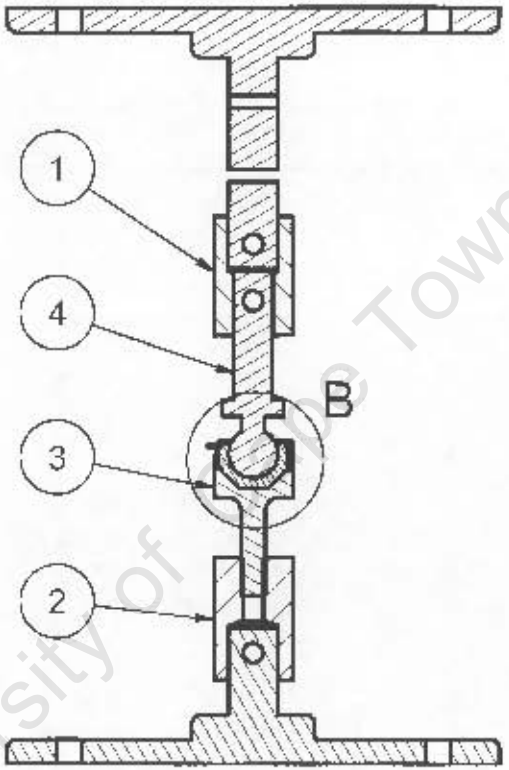

Section on A-A

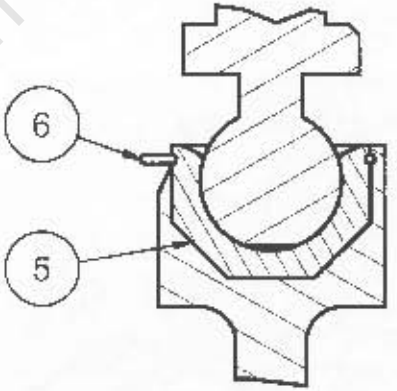

View B (1 : 1)

No#	Part Discription	Items	Drawing No#
1	Top Tension Coupling	1	Equ-02-02
2	Lower Tension Coupling	1	Equ-02-03
3	Test Housing for Socket	1	Equ-02-04
4	Zwick Test Ball	1	Equ-02-05
5	Press-fit Test Socket	1	Equ-02-07
6	Socket Locking Ring	1	Equ-02-06
7	Zwick Pin	3	No Drawing
8	Zwick Load Cell	1	No Drawing
9	Zwick Base Plate	1	No Drawing

Part Discription: Assembly

Material: Brass, Steel, UHMWPE

Quantity: 1

Designed by: Greg Wesse s

Date: 4/7/2005

Approved by: date

Signed

Units: mm

UNIVERSITY OF CAPE TOWN

DEPARTMENT OF MECHANICAL ENGINEERING

Title: Tension Test Set-up

Drawing Number: Equipment-02-00

Scale 3 : 1

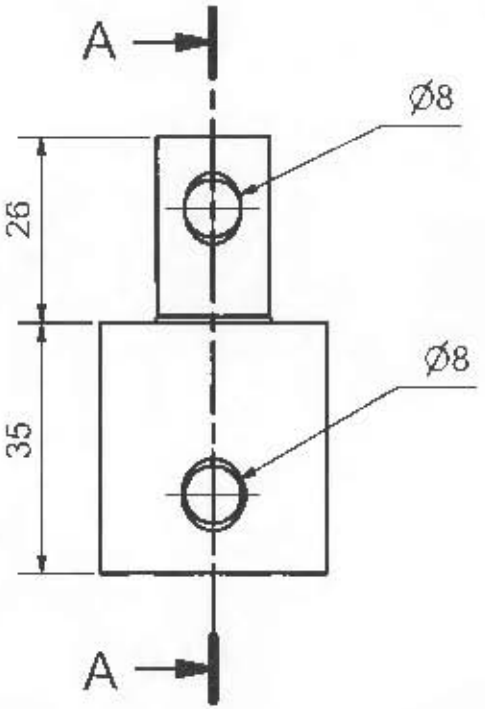

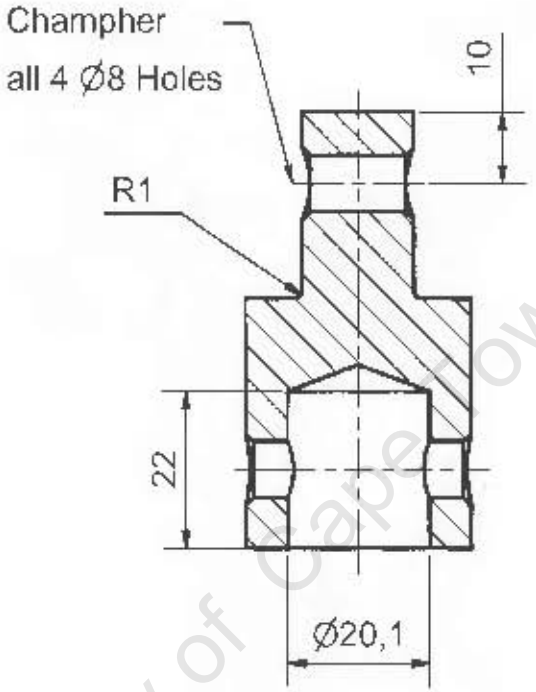

Section on A-A

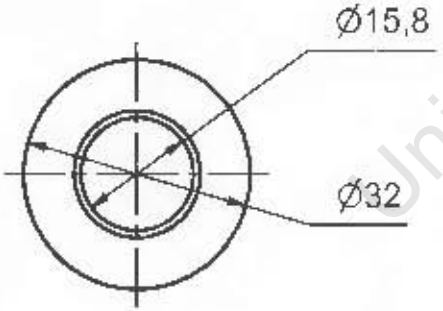

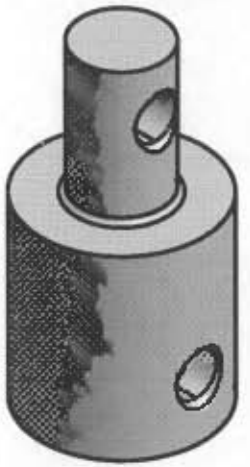

Tolerance Table (mm)	
0 - 5	+ 0.01 - 0.01
5 - 20	+ 0.05 - 0.05
20 - 200	+ 0.1 - 0.1
Angle	+ 0.05° - 0.05°

Part Discription: Compression Coupling		Material: Mild Steel		Quantity: 2	
Designed by: Greg Wessels	Date: 7/29/2004	Approved by - date	Signed	Units: mm	
University of Cape Town		Title: Zwick Couplings			
Department of Mechanical Engineering		Drawing Number: Equipment-02-01		Scale 1 : 1	

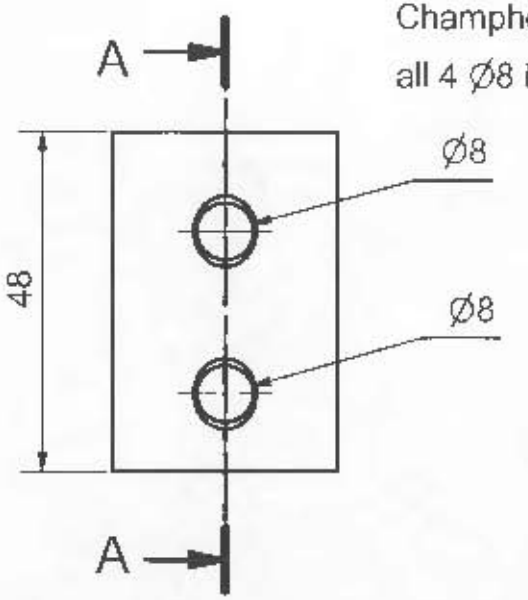

Champher
all 4 Ø8 Holes

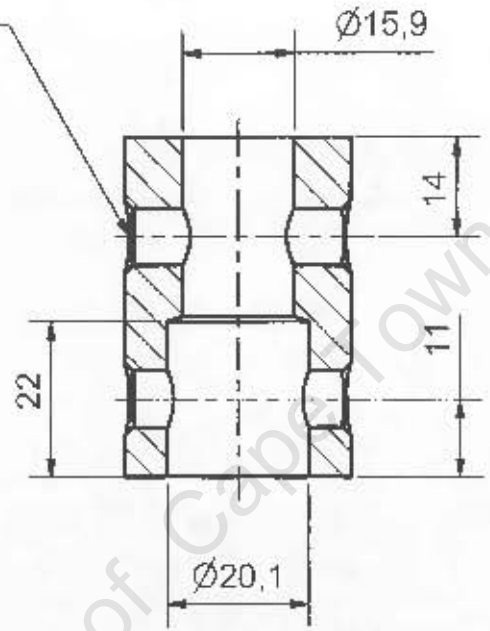

Section on A-A

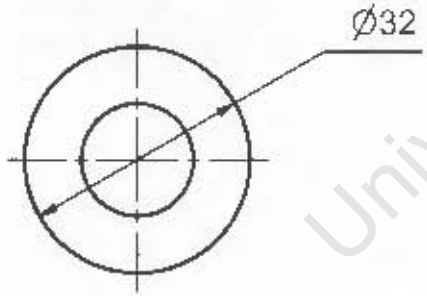

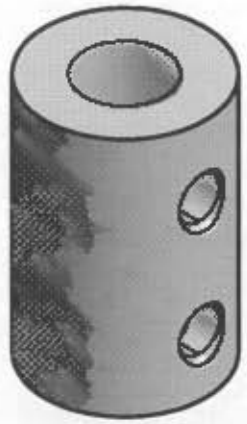

Tolerance Table (mm)	
0 - 5	+ 0.01 - 0.01
5 - 20	+ 0.05 - 0.05
20 - 200	+ 0.1 - 0.1
Angle	+ 0.05° - 0.05°

Part Discription: Top Tension Coupling		Material: Mild Steel		Quantity: 1	
Designed by: Greg Wessels	Date: 7/29/2004	Approved by - date	Signed	Units: mm	
UNIVERSITY OF CAPE TOWN		Title: Zwick Couplings			
DEPARTMENT OF MECHANICAL ENGINEERING		Drawing Number: Equipment-02-02		Scale 1 : 1	

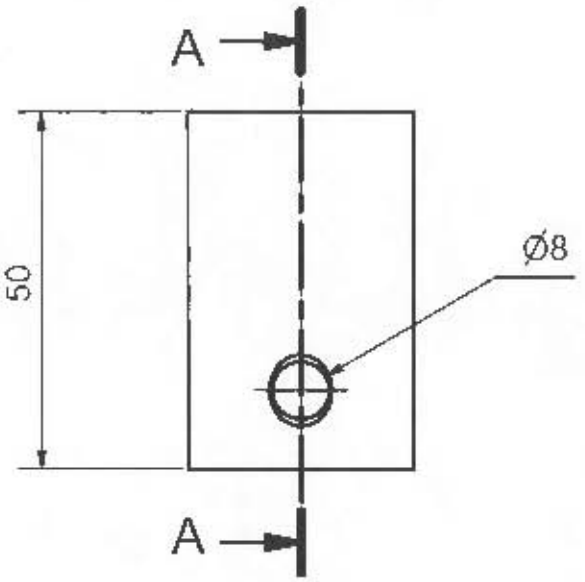

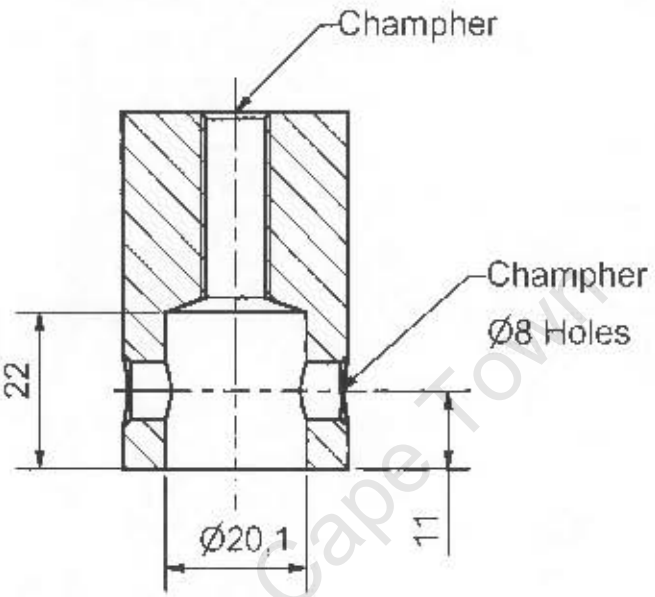

Section on A-A

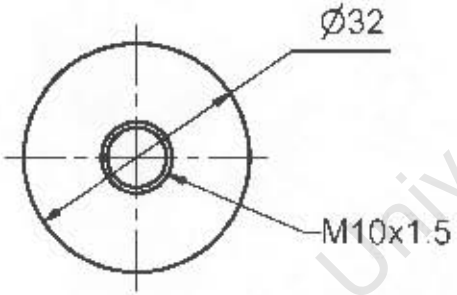

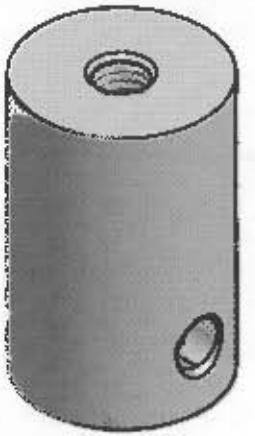

Tolerance Table (mm)	
0 - 5	+ 0.01 - 0.01
5 - 20	+ 0.05 - 0.05
20 - 200	+ 0.1 - 0.1
Angle	+ 0.05° - 0.05°

Part Description: Lower Tension Coupling		Material: Mild Steel		Quantity: 1	
Designed by: Greg Wessels	Date: 7/29/2004	Approved by - date	Signed	Units: mm	
UNIVERSITY OF CAPE TOWN DEPARTMENT OF MECHANICAL ENGINEERING		Title: Zwick Couplings			
		Drawing Number: Equipment-02-03		Scale 1 : 1	

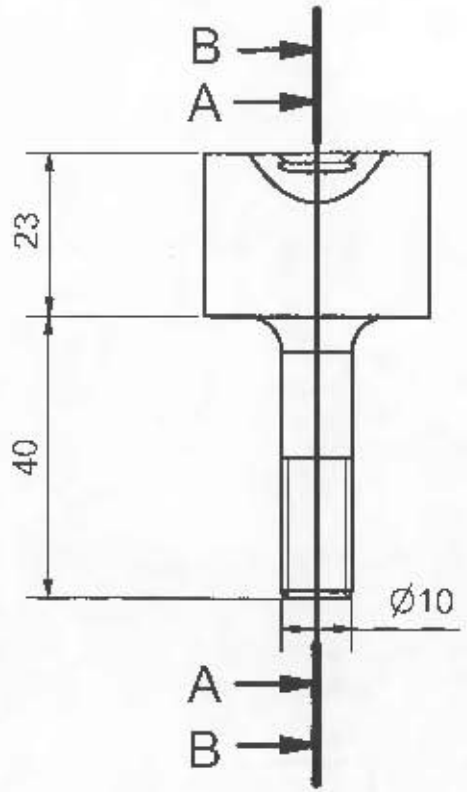

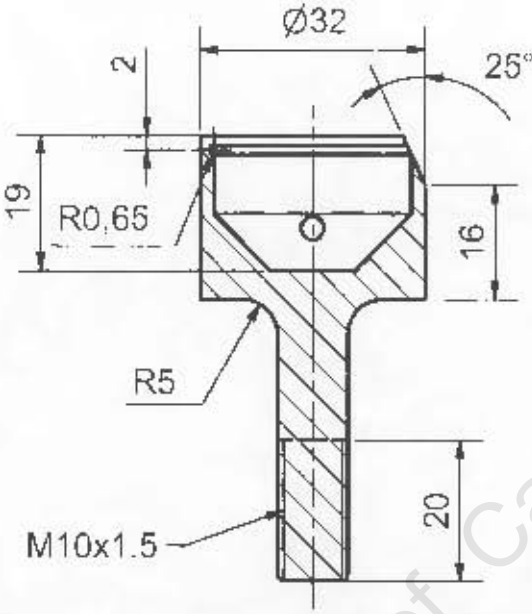

Section on A-A

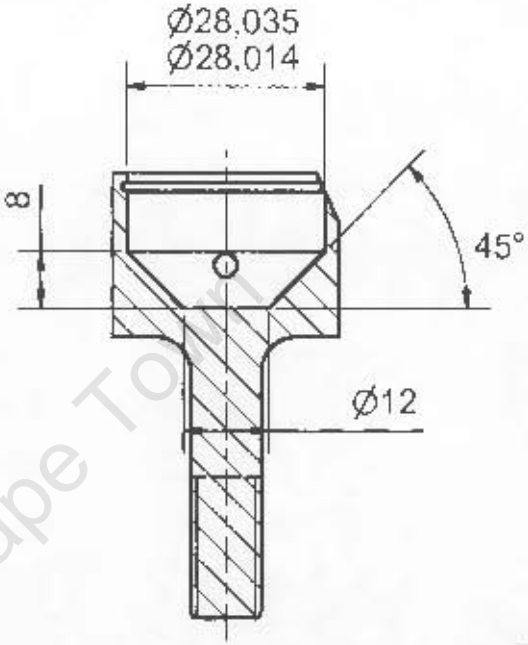

Section on B-B

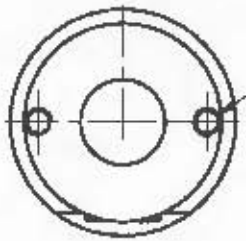

Tolerance Table (mm)	
0 - 5	+ 0.005 - 0.005
5 - 20	+ 0.01 - 0.01
20 - 200	+ 0.05 - 0.05
Angle	+ 0.05° - 0.05°

Part Description: Test Housing for Socket		Material: Mild Steel		Quantity: 1	
Designed by: Greg Wessels	Date: 5/17/2004	Approved by - date:	Signed	Units: mm	
University of Cape Town		Title: Test Housing for Socket			
Department of Mechanical Engineering		Drawing Number: Equipment-02-04		Scale 1 : 1	

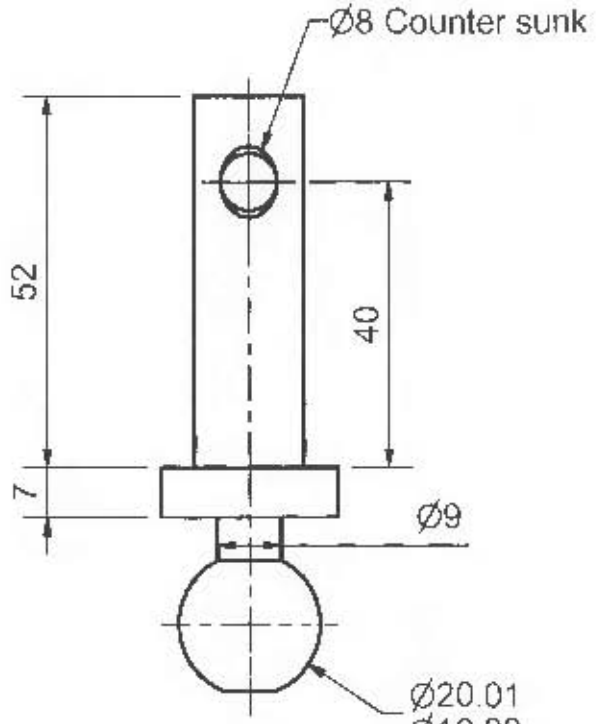

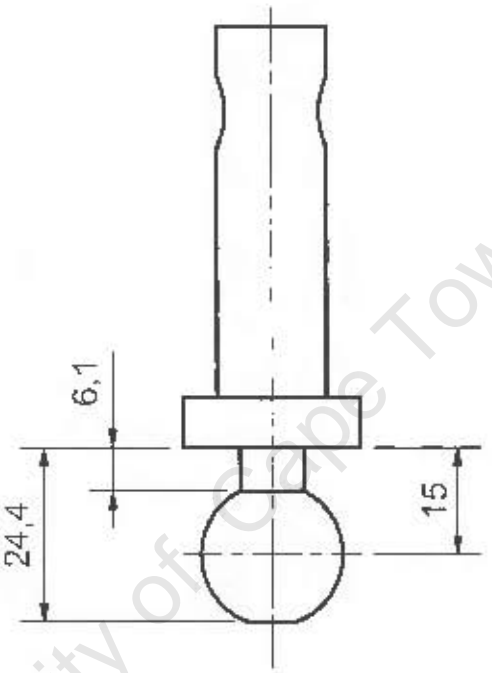

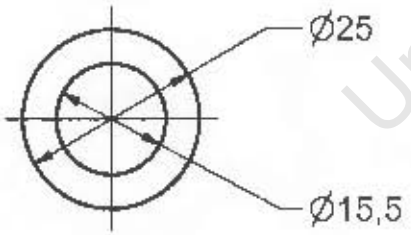

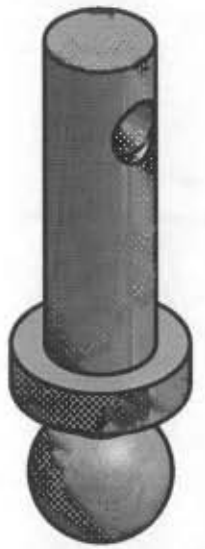

Tolerance Table (mm)	
0 - 5	+ 0.01 - 0.01
5 - 20	+ 0.05 - 0.05
20 - 200	+ 0.1 - 0.1
Angle	+ 0.05° - 0.05°

Part Discription: Zwick Test Ball		Material: Brass		Quantity: 1	
Designed by: Greg Wessels	Date: 7/29/2004	Approved by - date	Signed	Units: mm	
University of Cape Town Department of Mechanical Engineering		Title: Zwick Test Ball			
		Drawing Number: Equipment-02-05		Scale 1 : 1	

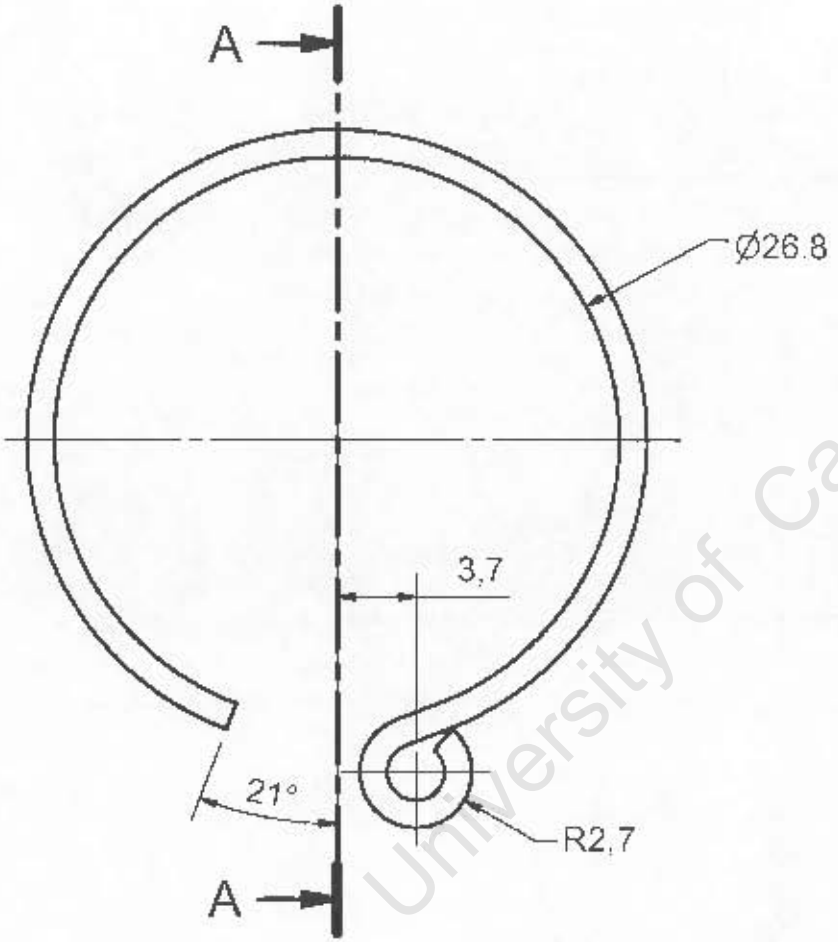

Section on A-A

Tolerance Table (mm)	
0 - 5	+ 0.01 - 0.01
5 - 20	+ 0.05 - 0.05
20 - 200	+ 0.1 - 0.1
Angle	+ 0.05° - 0.05°

Part Discription: Socket Locking Ring		Material: Copper		Quantity: 1	
Designed by: Greg Wessels	Date: 4/7/2005	Approved by - date	Signed	Units: mm	

UNIVERSITY OF CAPE TOWN

DEPARTMENT OF MECHANICAL ENGINEERING

Title: Socket Locking Ring

Drawing Number: Equipment-02-06

Scale 3 : 1

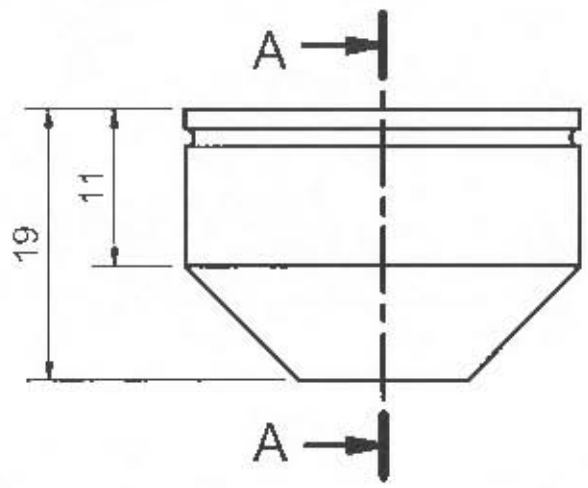

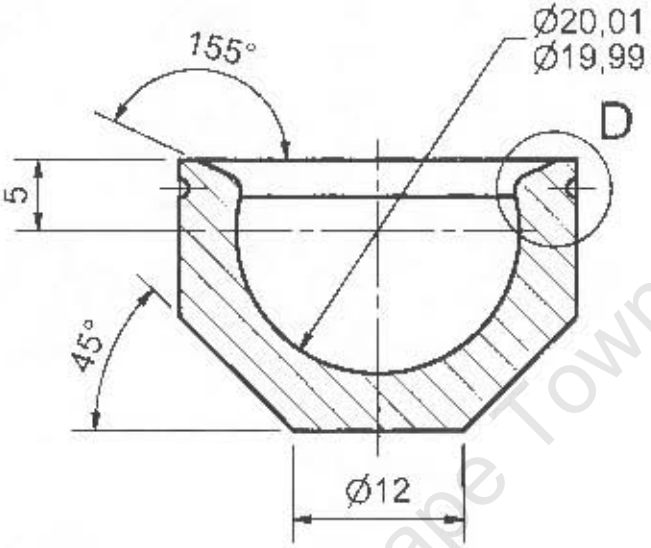

Section on A-A

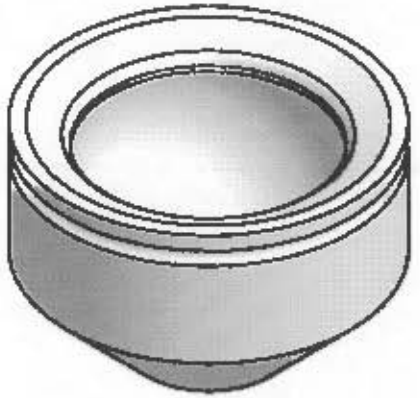

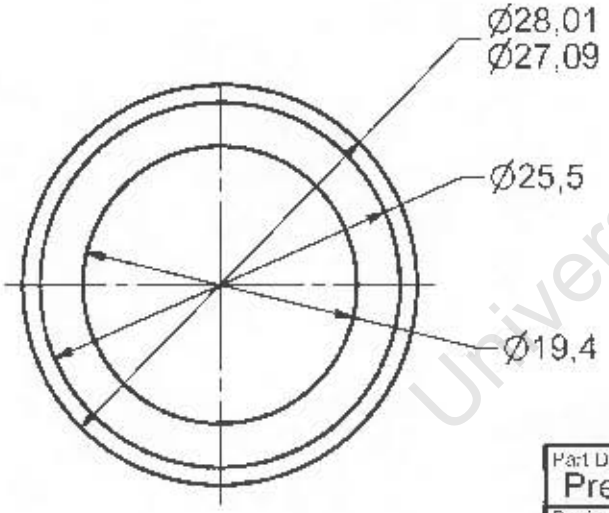

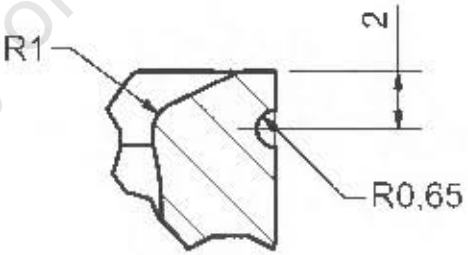

View D

Tolerance Table (mm)	
0 - 5	+ 0.01 - 0.01
5 - 20	+ 0.05 - 0.05
20 - 200	+ 0.1 - 0.1
Angle	+ 0.05° - 0.05°

Part Discription: Press-fit Test Socket		Material: UHMWPE		Quantity: 1	
Designed by: Greg Wessels	Date: 4/7/2005	Approved by: date	Signed	Units: mm	
University of Cape Town Department of Mechanical Engineering		Title: Press-fit Test Socket			
		Drawing Number: Equipment-02-07		Scale: 2:1	

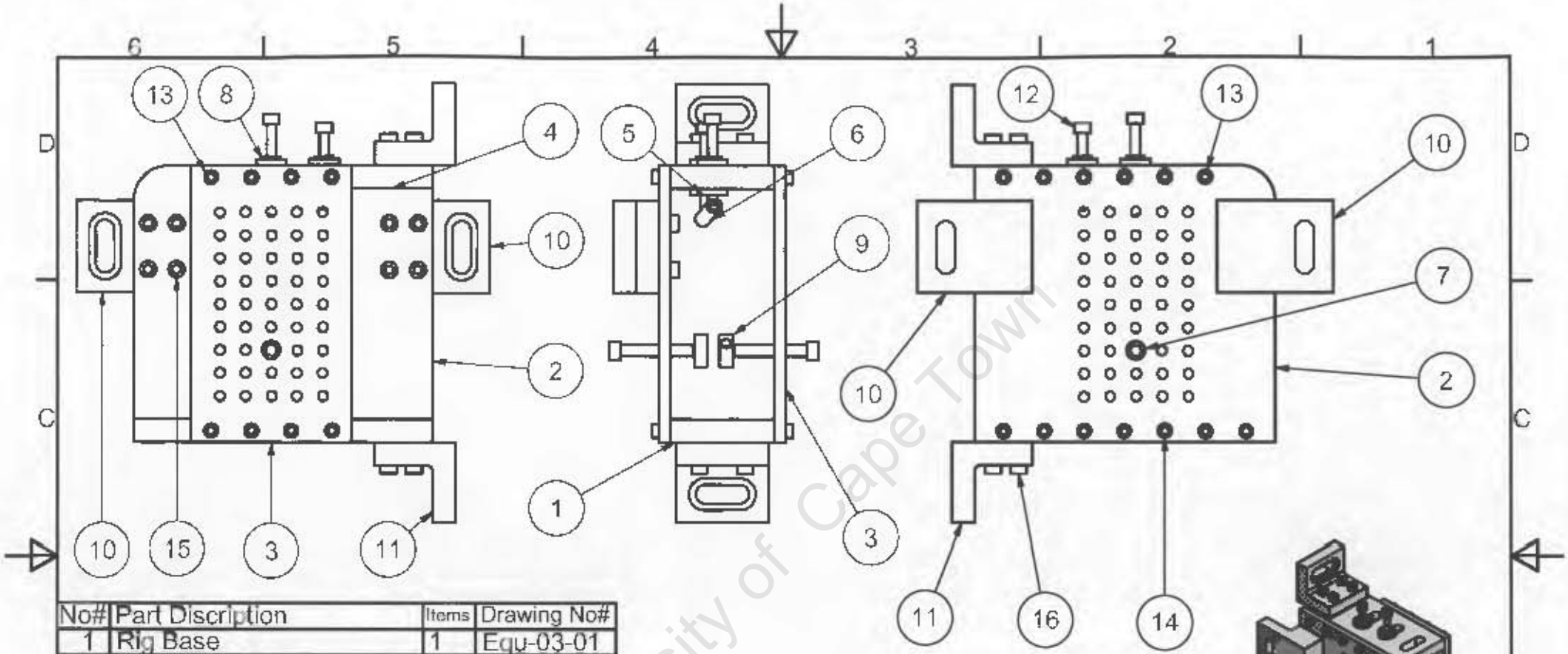

No#	Part Discription	Items	Drawing No#
1	Rig Base	1	Equ-03-01
2	Rig Large Side	1	Equ-03-02
3	Rig Small Side	1	Equ-03-03
4	Rig Top	1	Equ-03-04
5	Rig Top Sliders	2	Equ-03-05
6	Rig Supraspinous Bar	1	Equ-03-06
7	Allen M10 x 70mm Ball	12	Equ-03-07
8	Rig Top Slider Nut	2	Equ-03-08
9	Rig Side Clamp Face	6	Equ-03-09
10	Rig 90 Feet	2	Equ-03-10
11	Rig Compression Feet	2	Equ-03-11
12	Allen M8 x 70mm Ball	2	Equ-03-12
13	Allen Screw M8 x 25mm	10	No Drawing
14	Allen Screw M8 x 30mm	11	No Drawing
15	Allen Screw M10 x 35mm	8	No Drawing
16	Allen Screw M10 x 40mm	8	No Drawing

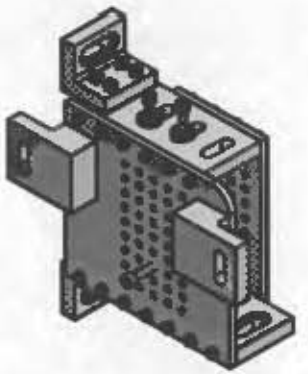

Scale 1 : 8

Part Discription	Material	Quantity
Assembly	Stainless Steel 316	1

Designed by	Date	Approved by - date	Signed	Units
Greg Wessels	7/29/2004			mm

UNIVERSITY OF CAPE TOWN

DEPARTMENT OF MECHANICAL ENGINEERING

Title: Scapula Test Rig

Drawing Number: Equipment-03-00

Scale 2 : 9

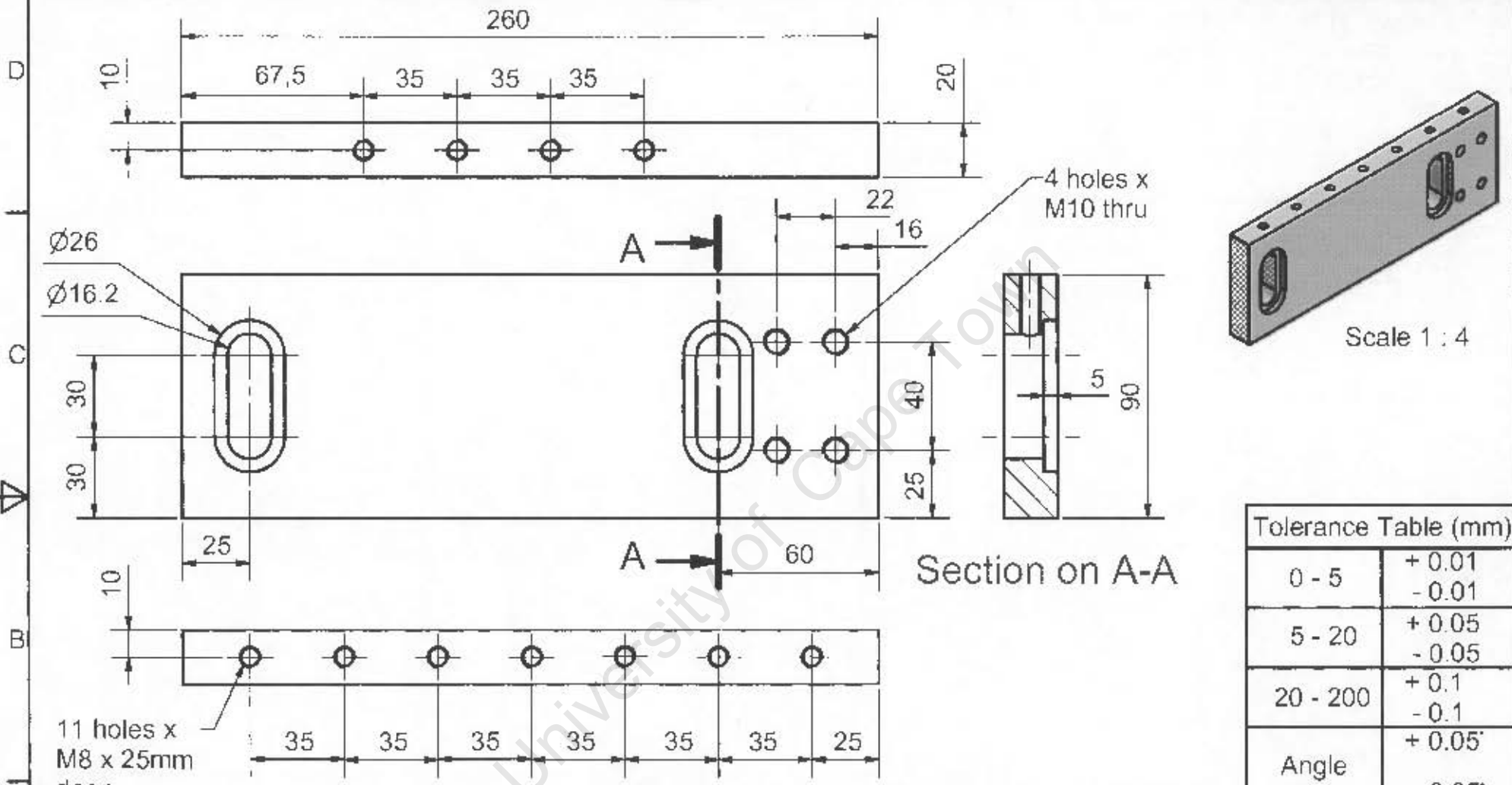

Scale 1 : 4

Tolerance Table (mm)	
0 - 5	+ 0.01 - 0.01
5 - 20	+ 0.05 - 0.05
20 - 200	+ 0.1 - 0.1
Angle	+ 0.05° - 0.05°

Part Description: Rig Base		Material: Stainless Steel 316		Quantity: 1	
Designed by: Greg Wessels	Date: 7/29/2004	Approved by: date	Signed	Units: mm	
University of Cape Town Department of Mechanical Engineering		Title: Scapula Test Rig			
		Drawing Number: Equipment-03-01		Scale 1 : 2	

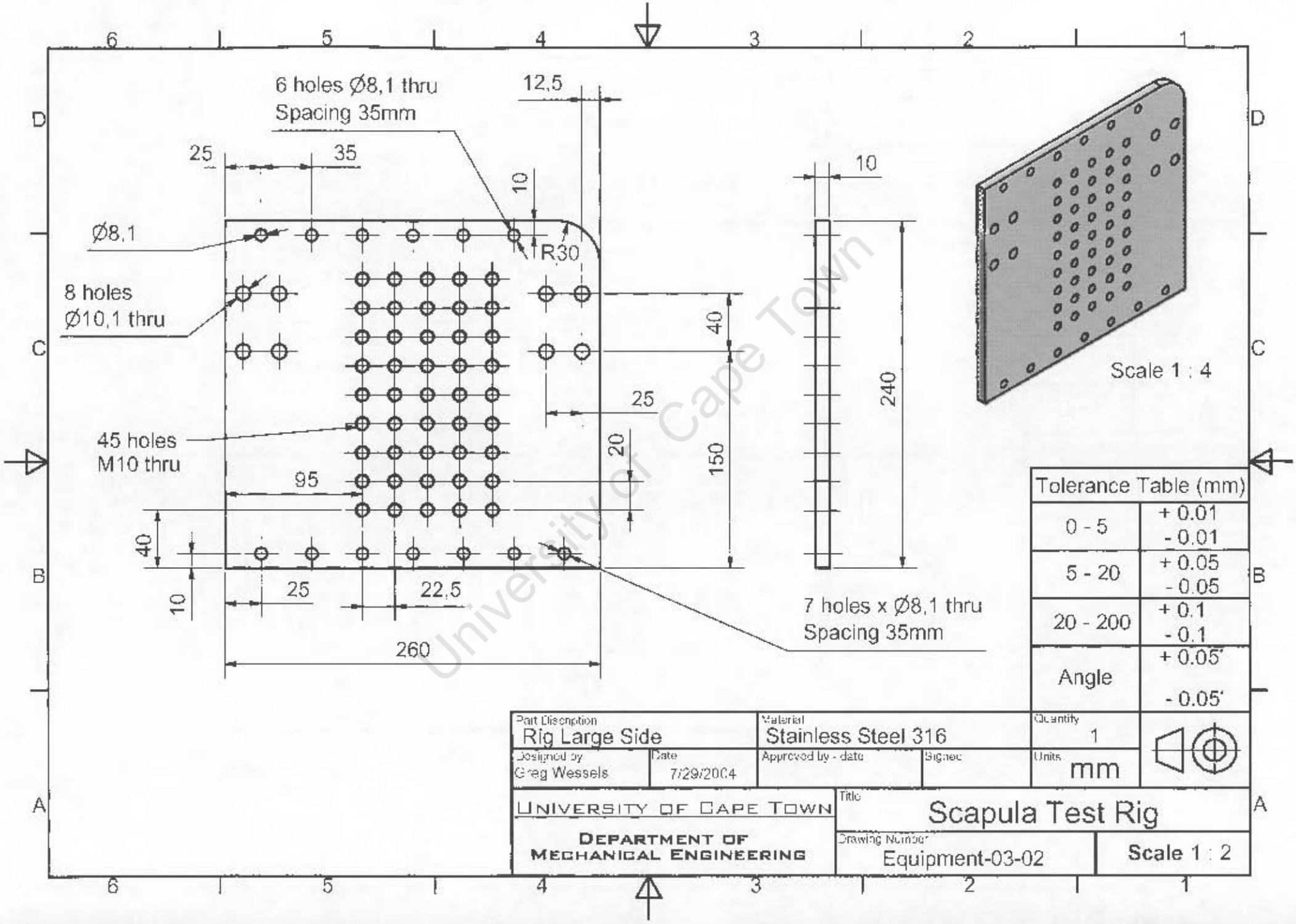

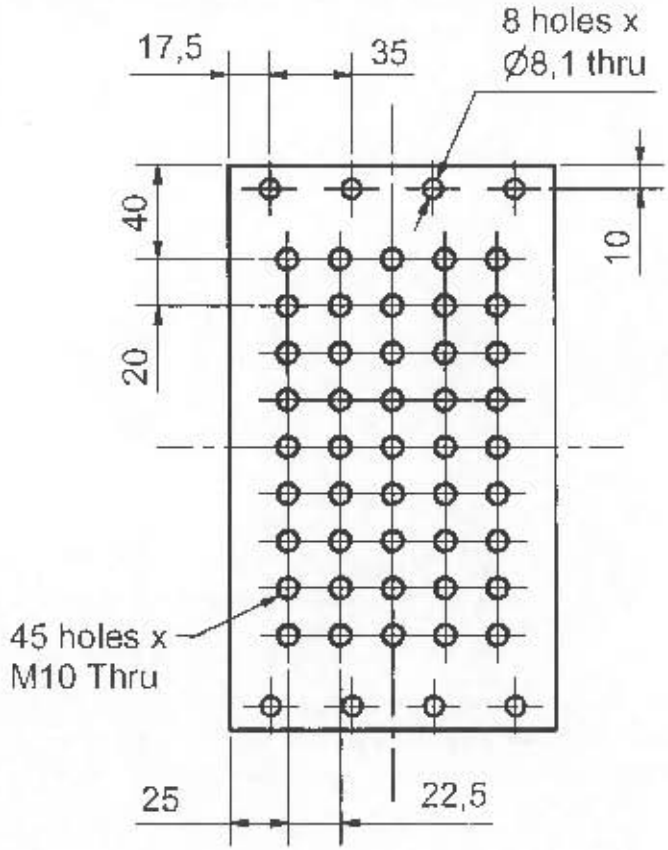

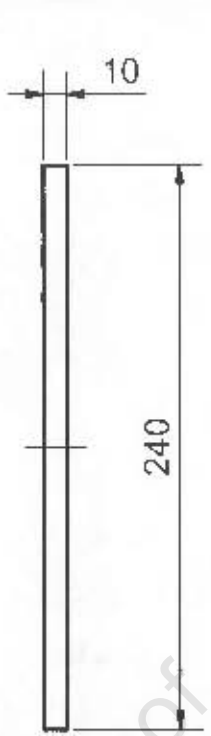

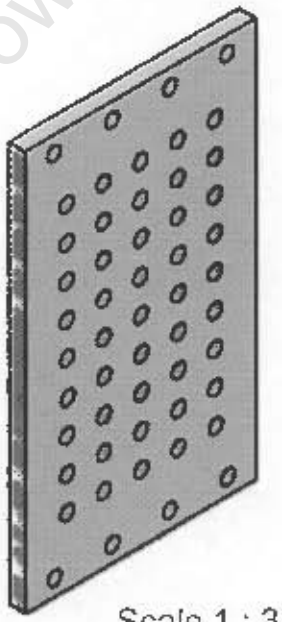

Scale 1 : 3

Tolerance Table (mm)	
0 - 5	+ 0.01 - 0.01
5 - 20	+ 0.05 - 0.05
20 - 200	+ 0.1 - 0.1
Angle	+ 0.05° - 0.05°

Part Description: Rig Small Side		Material: Stainless Steel 316	Quantity: 1
Designed by: Greg Wessels	Date: 7/29/2004	Approved by - date:	Signed:
			Units: mm

UNIVERSITY OF CAPE TOWN

DEPARTMENT OF MECHANICAL ENGINEERING

Title: Scapula Test Rig

Drawing Number: Equipment-03-03

Scale 1 : 3

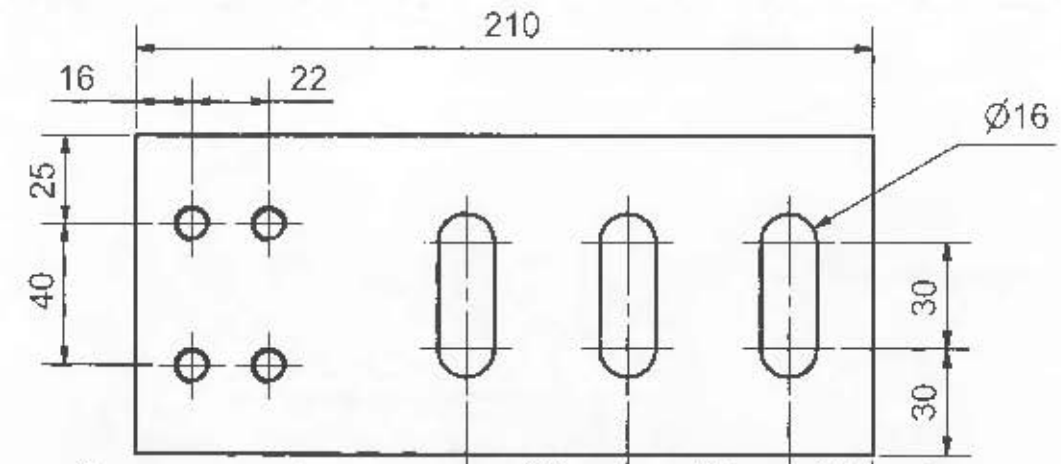

Section on A-A

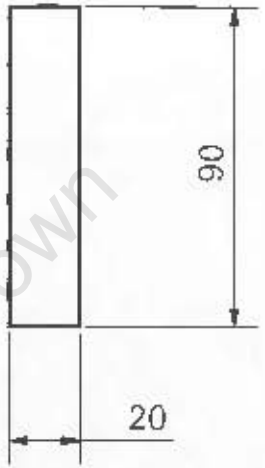

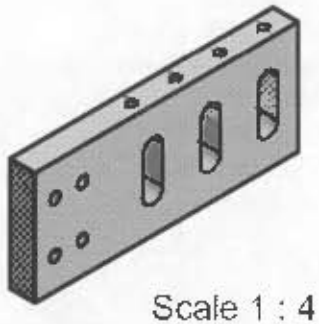

Scale 1 : 4

Tolerance Table (mm)	
0 - 5	+ 0.01 - 0.01
5 - 20	+ 0.05 - 0.05
20 - 200	+ 0.1 - 0.1
Angle	+ 0.05° - 0.05°

Part Description: Rig Top		Material: Stainless Steel 316		Quantity: 1	
Designed by: Greg Wessels	Date: 7/29/2004	Approved by - date:	Signed	Units: mm	
UNIVERSITY OF CAPE TOWN		Title: Scapula Test Rig			
DEPARTMENT OF MECHANICAL ENGINEERING		Drawing Number: Equipment-03-04		Scale 1 : 2	

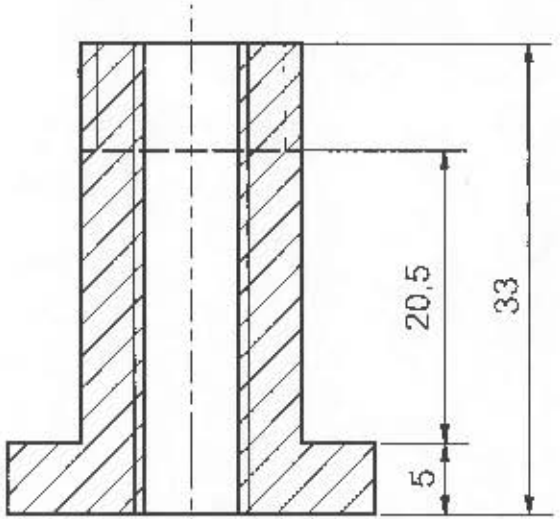

Section on A-A

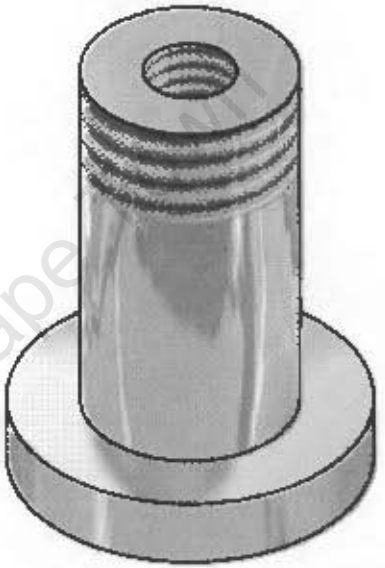

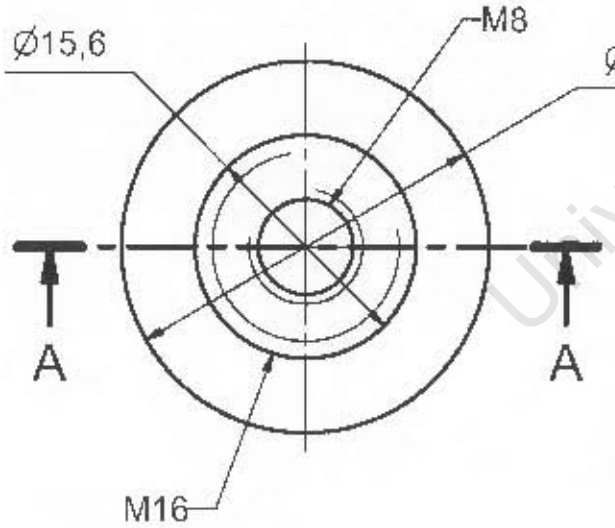

Tolerance Table (mm)	
0 - 5	+ 0.01 - 0.01
5 - 20	+ 0.05 - 0.05
20 - 200	+ 0.1 - 0.1
Angle	+ 0.05° - 0.05°

Part Description: Rig Top Slider		Material: Stainless Steel 316		Quantity: 2	
Designed by: Greg Wessels	Date: 7/29/2004	Approved by - date	Signed	Units: mm	
University of Cape Town		Title: Scapula Test Rig			
Department of Mechanical Engineering		Drawing Number: Equipment-03-05		Scale 2 : 1	

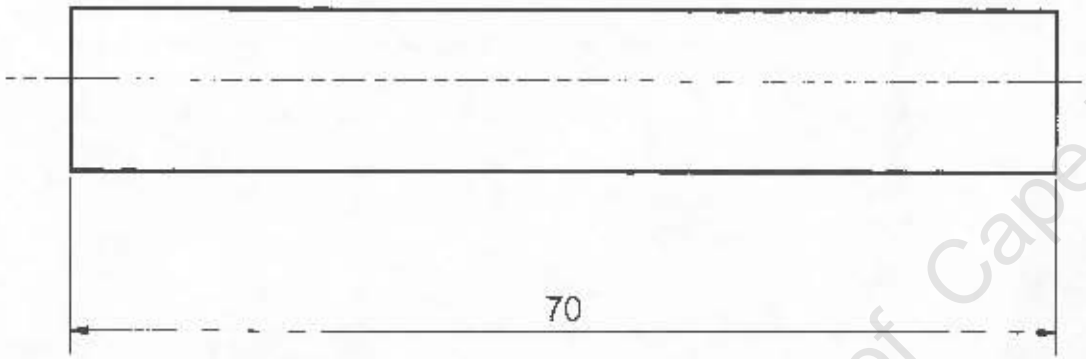

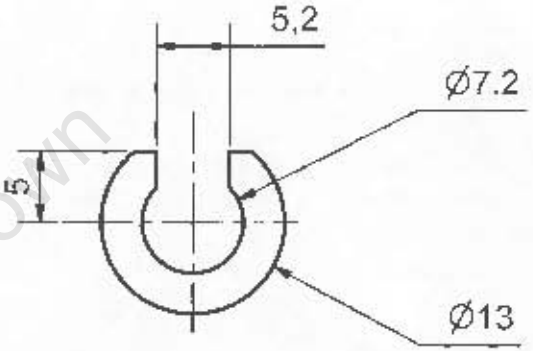

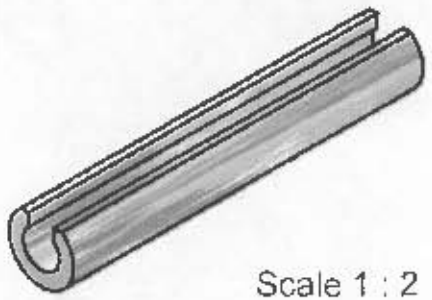

Scale 1 : 2

Tolerance Table (mm)	
0 - 5	+ 0.01 - 0.01
5 - 20	+ 0.05 - 0.05
20 - 200	+ 0.1 - 0.1
Angle	+ 0.05° - 0.05°

Part Description: Rig Supraspinous Bar		Material: Stainless Steel 316		Quantity: 1	
Designed by: Greg Wessels	Date: 7/29/2004	Approved by: cate	Signed:	Units: mm	
UNIVERSITY OF CAPE TOWN		Title: Scapula Test Rig			
DEPARTMENT OF MECHANICAL ENGINEERING		Drawing Number: Equipment-03-06		Scale 1 : 1	

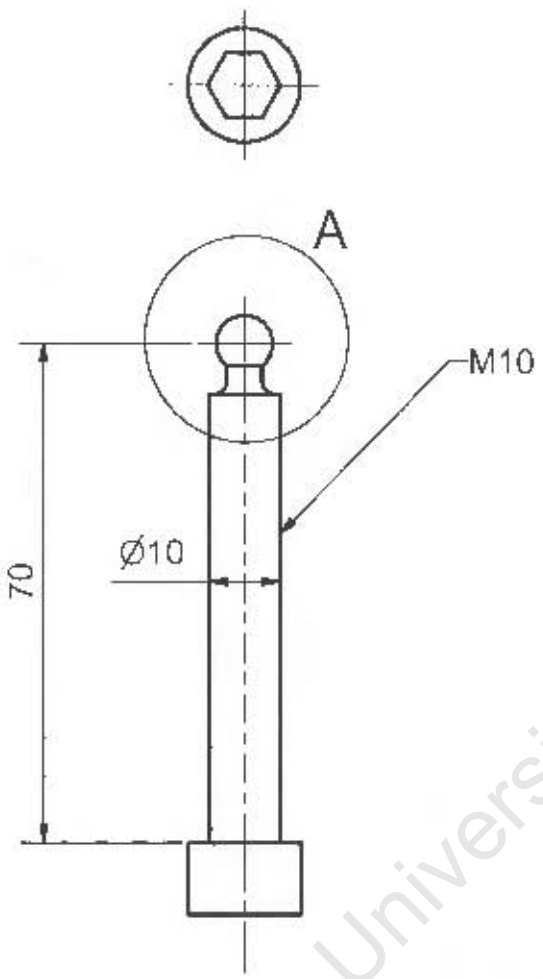

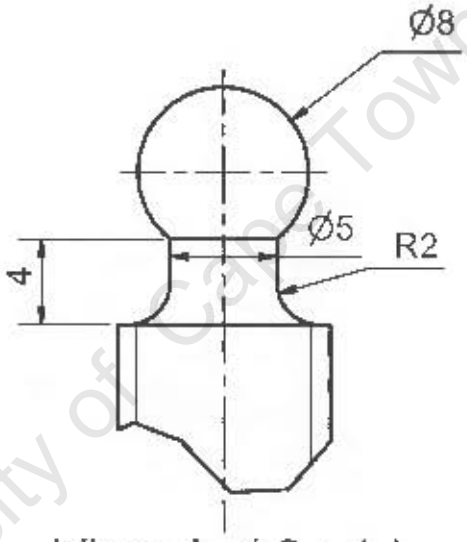

View A (3 : 1)

Tolerance Table (mm)	
0 - 5	+ 0.01 - 0.01
5 - 20	+ 0.05 - 0.05
20 - 200	+ 0.1 - 0.1
Angle	+ 0.05° - 0.05°

Part Discription: Allen M10 x 70mm Ball		Material: Stainless Steel 316		Quantity: 12	
Designed by: Greg Wessels	Date: 7/29/2004	Approved by - date	Signed	Units: mm	
University of Cape Town		Title: Scapula Test Rig			
Department of Mechanical Engineering		Drawing Number: Equipment-03-07		Scale 1 : 1	

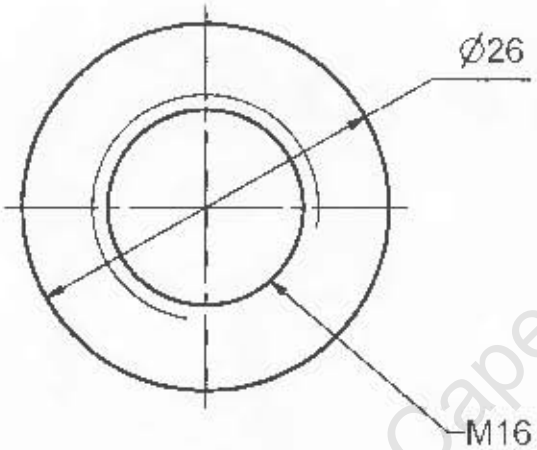

Tolerance Table (mm)	
0 - 5	+ 0.01 - 0.01
5 - 20	+ 0.05 - 0.05
20 - 200	+ 0.1 - 0.1
Angle	+ 0.05° - 0.05°

Part Description: Rig Top Slider Nut		Material: Stainless Steel 316		Quantity: 2	
Designed by: Greg Wessels	Date: 7/29/2004	Approved by - date:	Signed	Units: mm	
UNIVERSITY OF CAPE TOWN		Title: Scapula Test Rig			
DEPARTMENT OF MECHANICAL ENGINEERING		Drawing Number: Equipment-03-08		Scale 2 : 1	

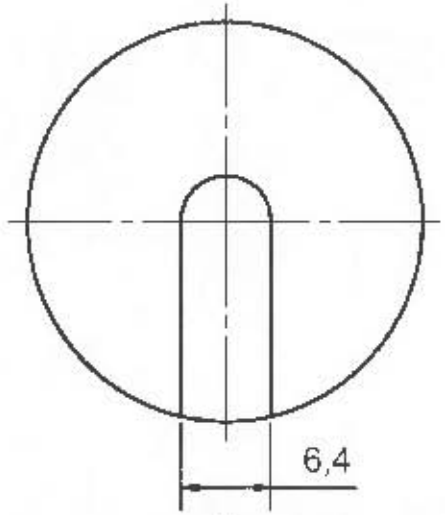

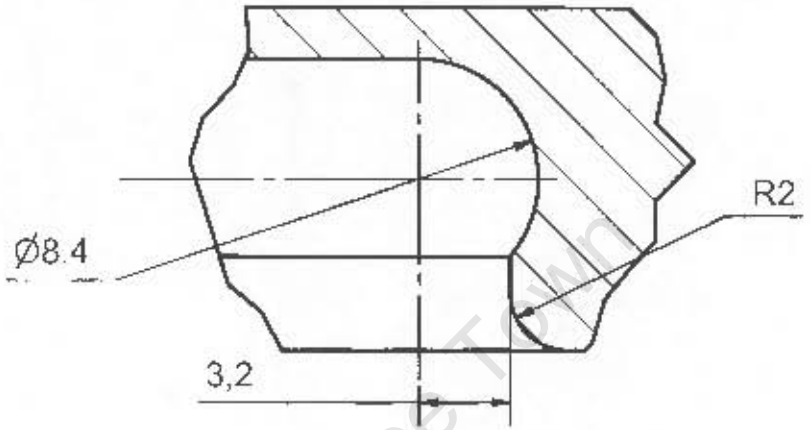

View B (4 : 1)

Scale 1 : 1

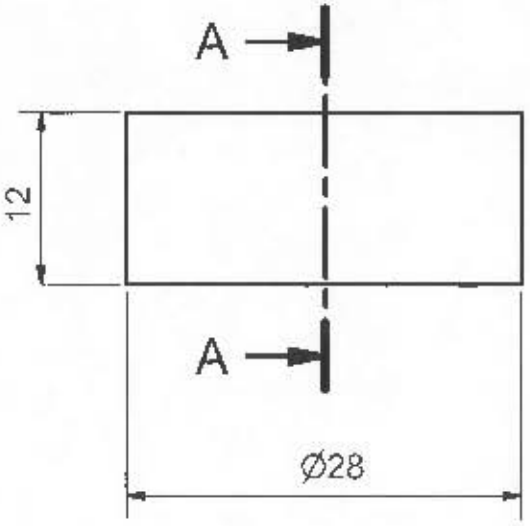

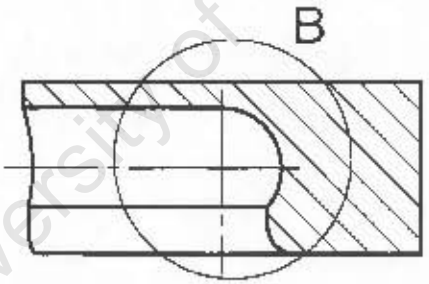

Section on A-A

Tolerance Table (mm)	
0 - 5	+ 0.01 - 0.01
5 - 20	+ 0.05 - 0.05
20 - 200	+ 0.1 - 0.1
Angle	+ 0.05° - 0.05°

Part Description: Rig Side Clamp Face		Material: Stainless Steel 316		Quantity: 6	
Designed by: Greg Wessels	Date: 7/29/2004	Approved by: date	Signed	Units: mm	
University of Cape Town Department of Mechanical Engineering		Title: Scapula Test Rig			
		Drawing Number: Equipment-03-09		Scale 2 : 1	

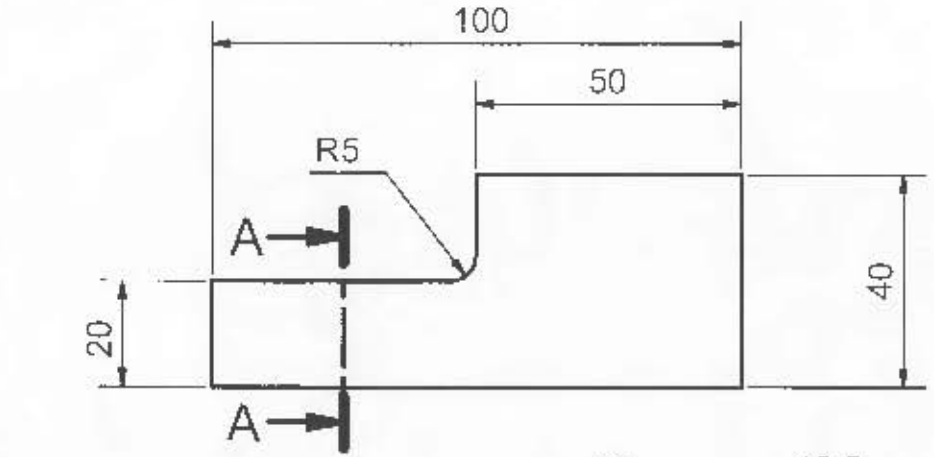

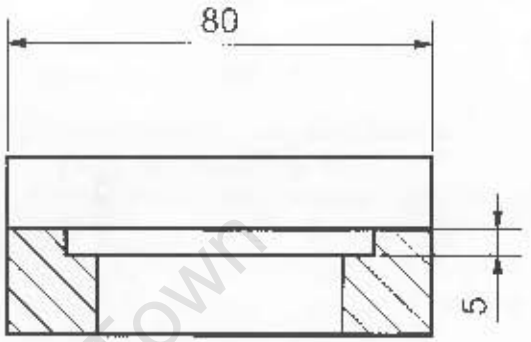

Section on A-A

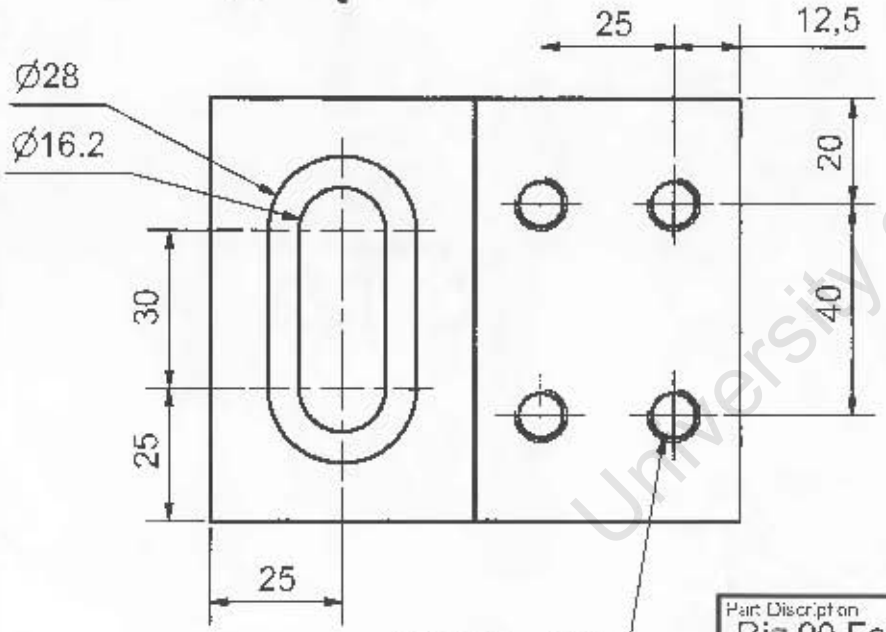

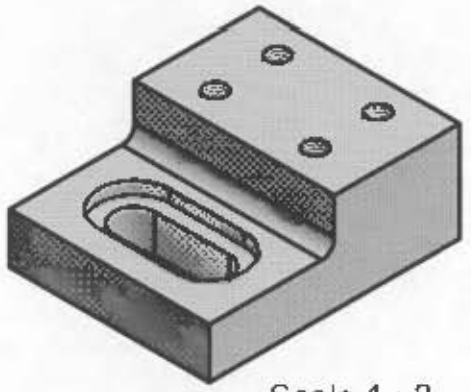

Scale 1 : 2

Tolerance Table (mm)	
0 - 5	+ 0.01 - 0.01
5 - 20	+ 0.05 - 0.05
20 - 200	+ 0.1 - 0.1
Angle	+ 0.05° - 0.05°

Part Description: Rig 90 Foot		Material: Stainless Steel 316		Quantity: 2	
Designed by: Greg Wessels	Date: 7/29/2004	Approved by - date	Signed	Units: mm	

UNIVERSITY OF CAPE TOWN

DEPARTMENT OF MECHANICAL ENGINEERING

Title: Scapula Test Rig

Drawing Number: Equipment-03-10

Scale 1 : 1

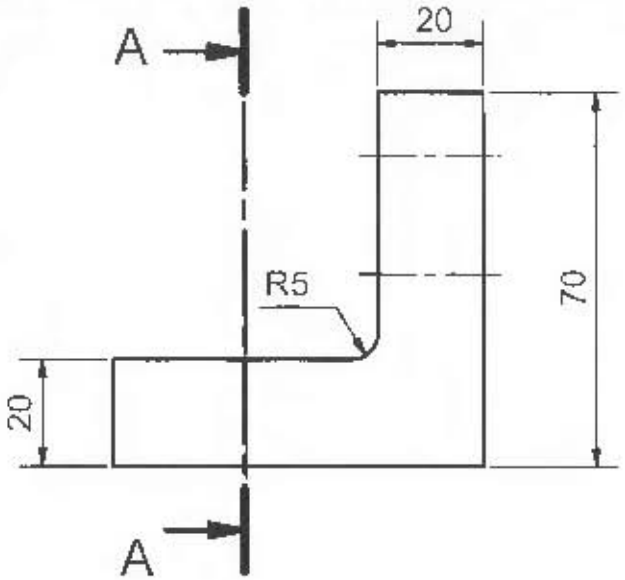

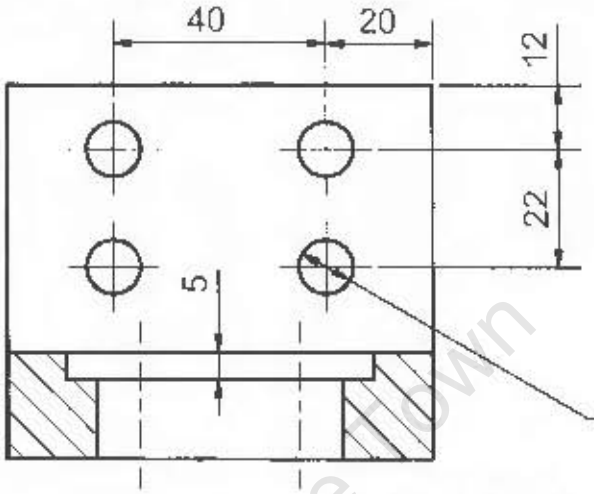

Section on A-A

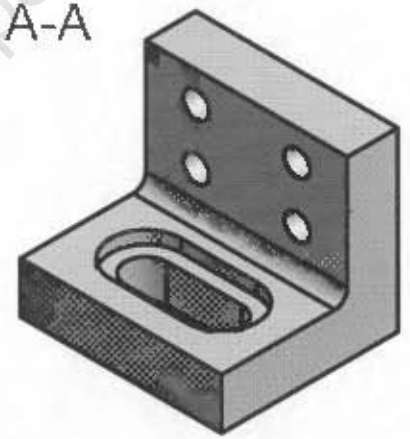

Scale 1 : 2

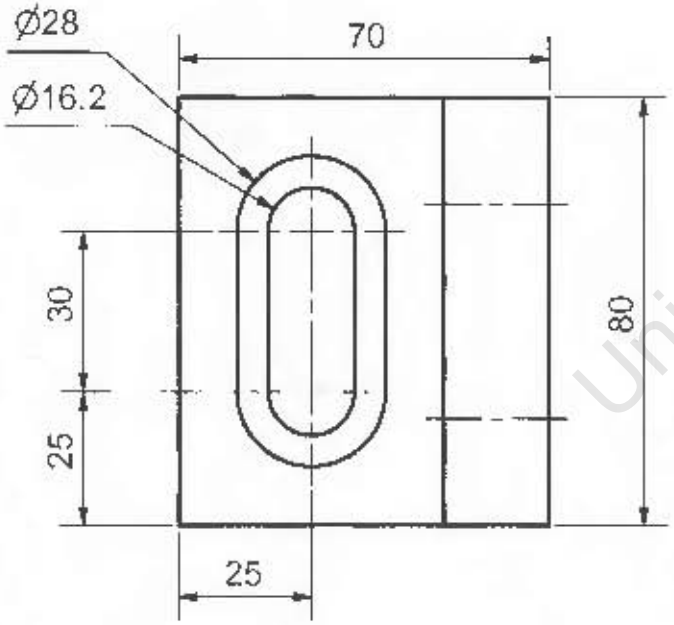

Tolerance Table (mm)	
0 - 5	+ 0.01 - 0.01
5 - 20	+ 0.05 - 0.05
20 - 200	+ 0.1 - 0.1
Angle	+ 0.05° - 0.05°

Part Description: Rig Compression Foot		Material: Stainless Steel 316		Quantity: 2	
Designed by: Greg Wessels	Date: 7/29/2004	Approved by: date	Signed	Units: mm	
University of Cape Town		Title: Scapula Test Rig			
Department of Mechanical Engineering		Drawing Number: Equipment-03-11		Scale 3 : 4	

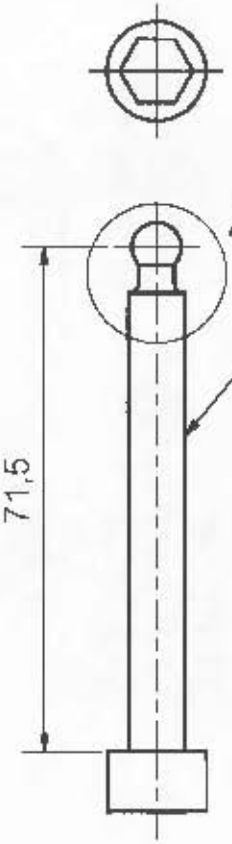

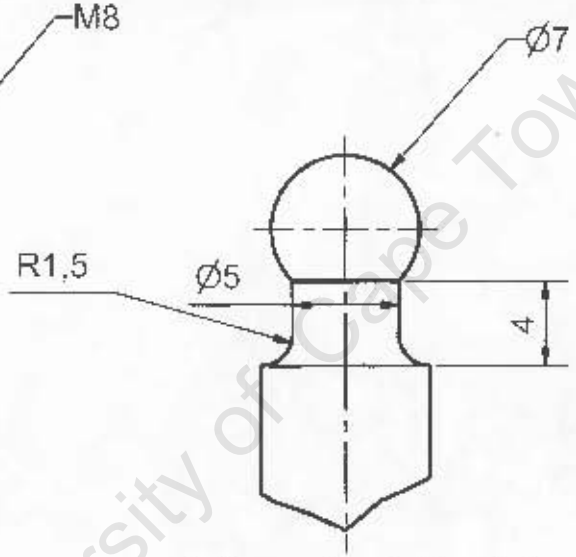

View A (3 : 1)

Tolerance Table (mm)	
0 - 5	+ 0.01 - 0.01
5 - 20	+ 0.05 - 0.05
20 - 200	+ 0.1 - 0.1
Angle	+ 0.05° - 0.05°

Part Description: Allen M8 x 70mm Ball		Material: Stainless Steel 316		Quantity: 2	
Designed by: Greg Wessels	Date: 7/29/2004	Approved by: date	Signed	Units: mm	
UNIVERSITY OF CAPE TOWN		Title: Scapula Test Rig			
DEPARTMENT OF MECHANICAL ENGINEERING		Drawing Number: Equipment-03-12		Scale 1 : 1	

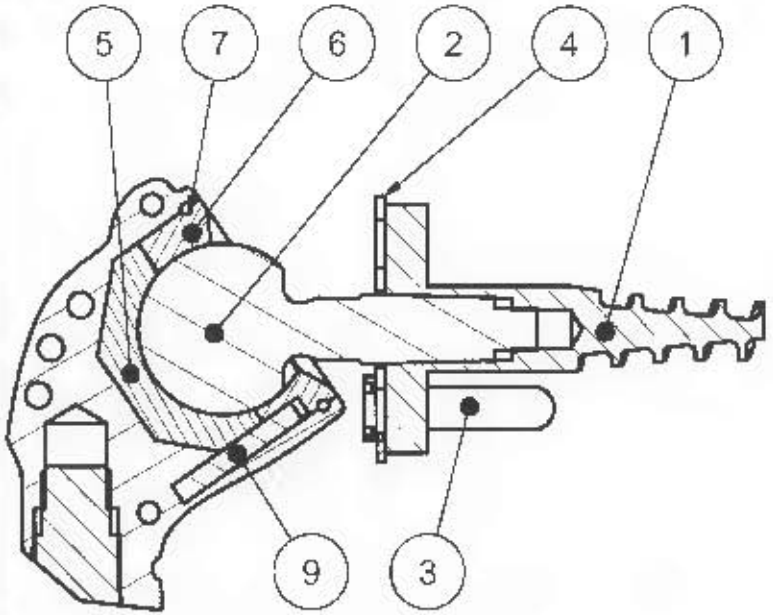

View B (1.20 : 1)

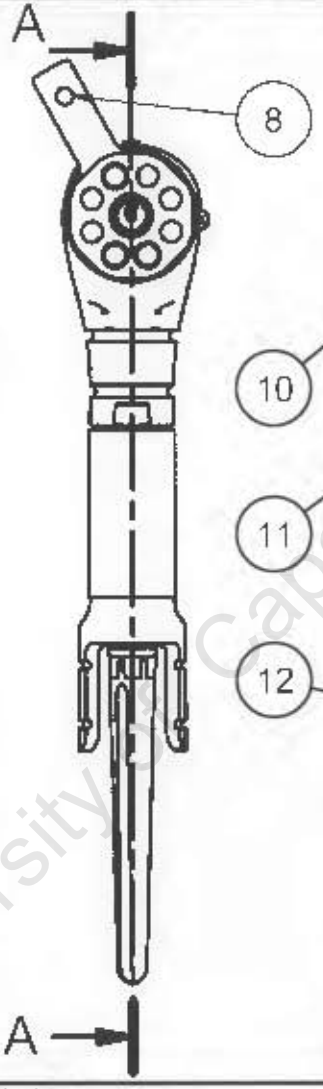

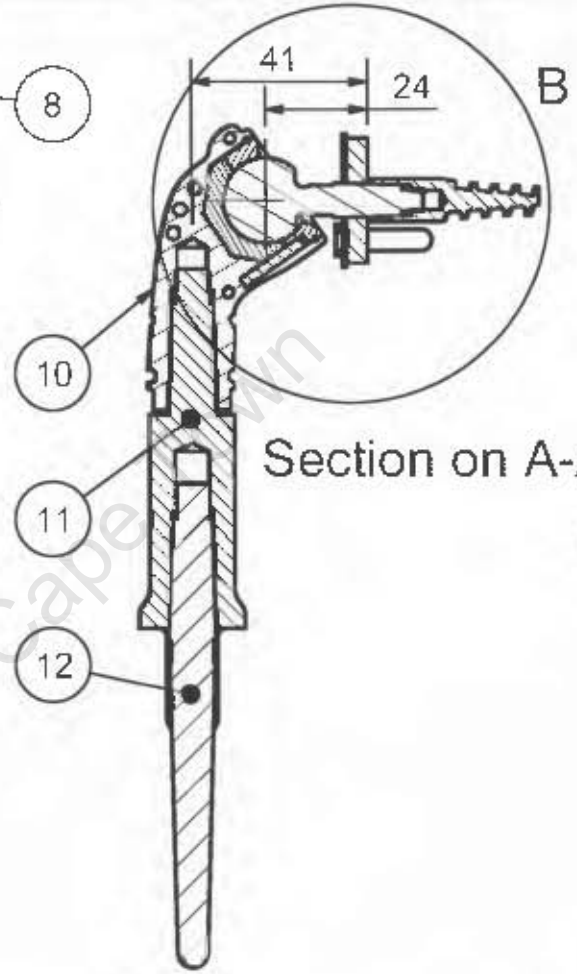

Section on A-A

No#	Part Discription	Items	Drawing No#
1	Glenoid Fixation Plate	1	Full-01-01
2	Ball and Tapered Stem	1	Full-01-02
3	Cemented Glenoid Peg	3	Full-01-03
4	Coracoid Plate	1	Full-01-04
5	UHMWPE Socket Bottom	1	Full-01-05
6	UHMWPE Socket Top	1	Full-01-06
7	Socket Locking Clip	1	Full-01-07
8	Coracoid Screw	1	Full-01-08
9	Peg Stop Rotation	1	Full-01-09
10	Humeral Housing	1	Full-01-10
11	Humeral Stem Extension	1	Full-01-11
12	Humeral Stem	1	Full-01-12

Part Discription: Assembly		Material: Co-Cr-Mo, Ti, UHMWPE		Quantity: 1
Designed by: Greg Wessels	Date: 4/26/2005	Approved by - date:	Signed:	Units: mm

UNIVERSITY OF CAPE TOWN

DEPARTMENT OF MECHANICAL ENGINEERING

Title: Hybrid-Screw TSR

Drawing Number: Full-01-00

Scale 1:1.66

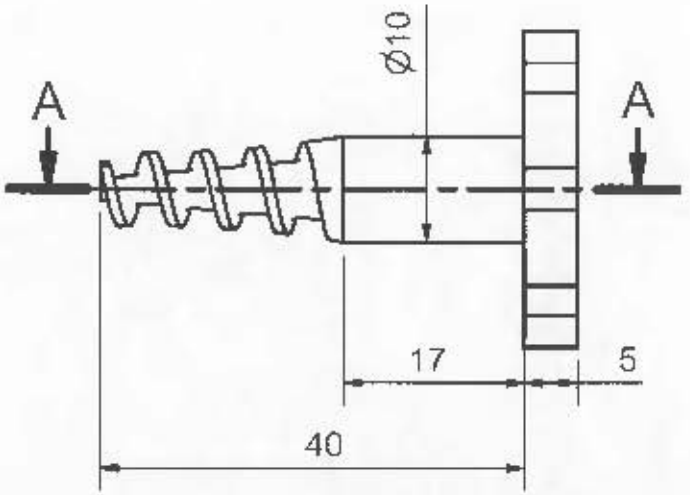

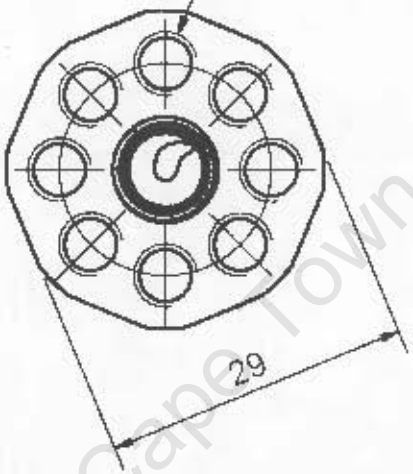

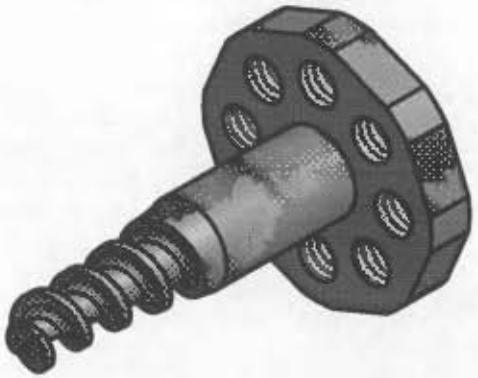

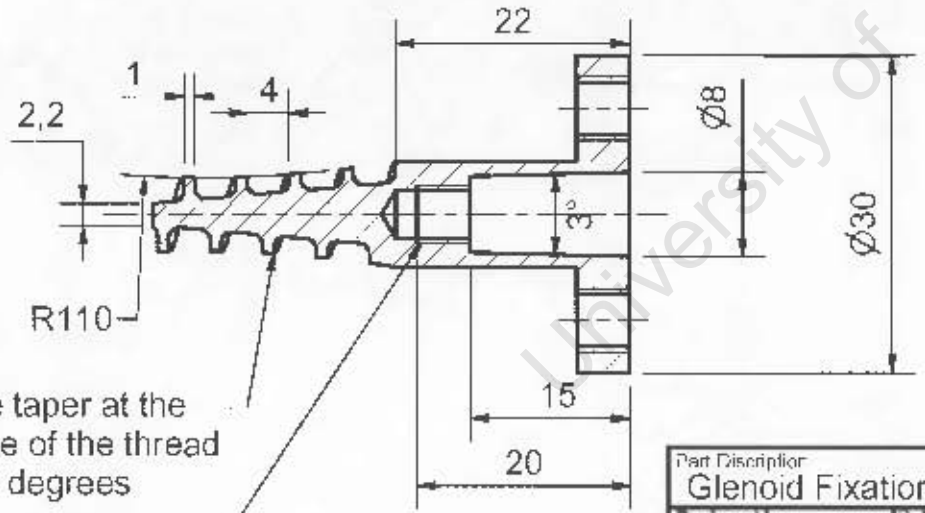

Section on A-A

Tolerance Table (mm)	
0 - 5	+ 0.01 - 0.01
5 - 20	+ 0.05 - 0.05
20 - 200	+ 0.1 - 0.1
Angle	+ 0.05° - 0.05°

Part Description: Glenoid Fixation Plate		Material: Ti-6Al-4V		Quantity: 1	
Designed by: Greg Wessels	Date: 4/7/2005	Approved by - date	Signed	Units: mm	
UNIVERSITY OF CAPE TOWN		Title: Hybrid-Screw TSR			
DEPARTMENT OF MECHANICAL ENGINEERING		Drawing Number: Full-01-01		Scale 1.5:1	

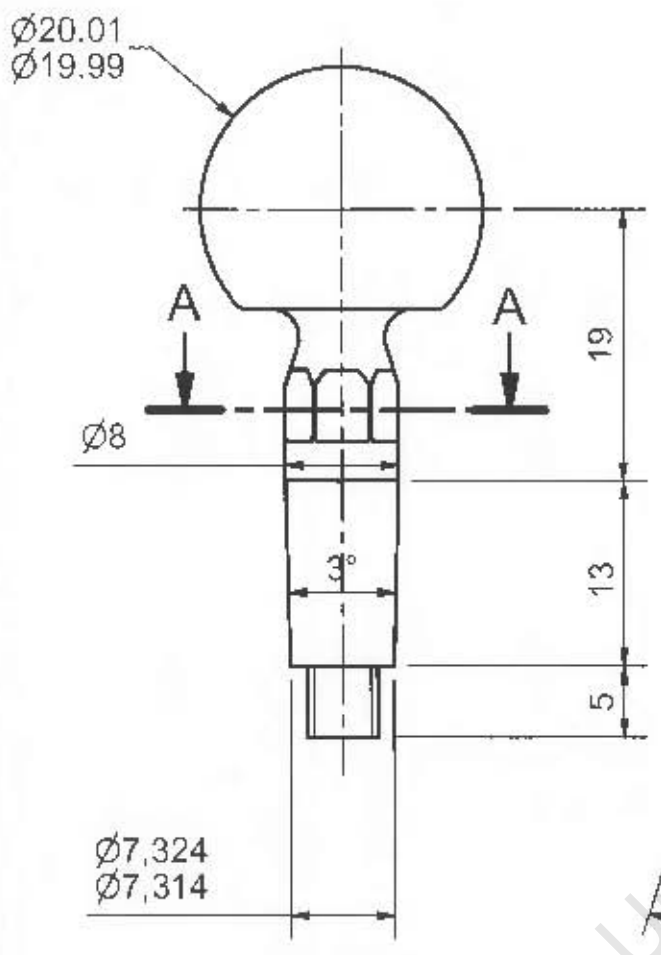

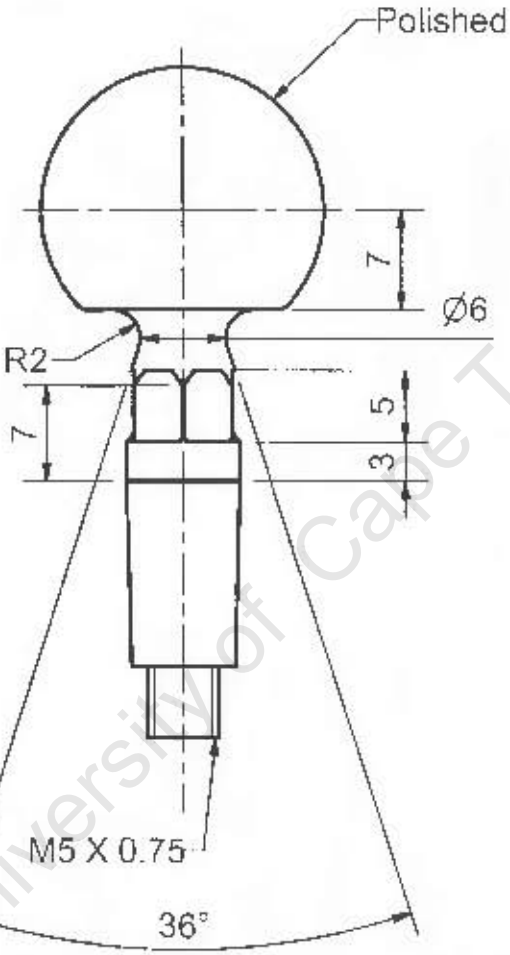

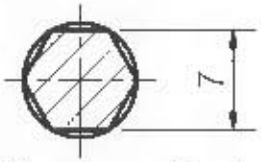

Section on A-A

Tolerance Table (mm)	
0 - 5	+ 0.01 - 0.01
5 - 20	+ 0.05 - 0.05
20 - 200	+ 0.1 - 0.1
Angle	+ 0.05° - 0.05°

Part Discription: Ball and Tapered Stem		Material: Co-Cr-Mo		Quantity: 1	
Designed by: Greg Wessels	Date: 4/7/2005	Approved by - date	Signed	Units: mm	
University of Cape Town		Title: Hybrid-Screw TSR			
Department of Mechanical Engineering		Drawing Number: Full-01-02		Scale 2 : 1	

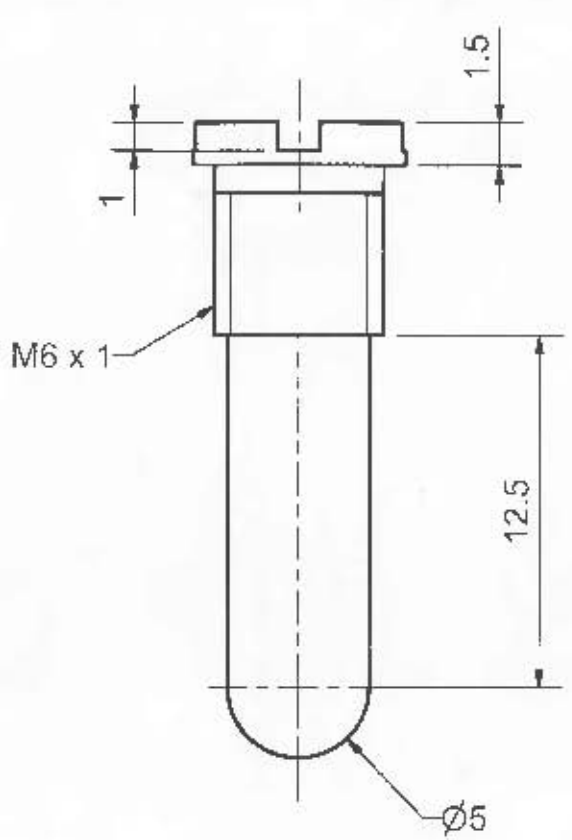

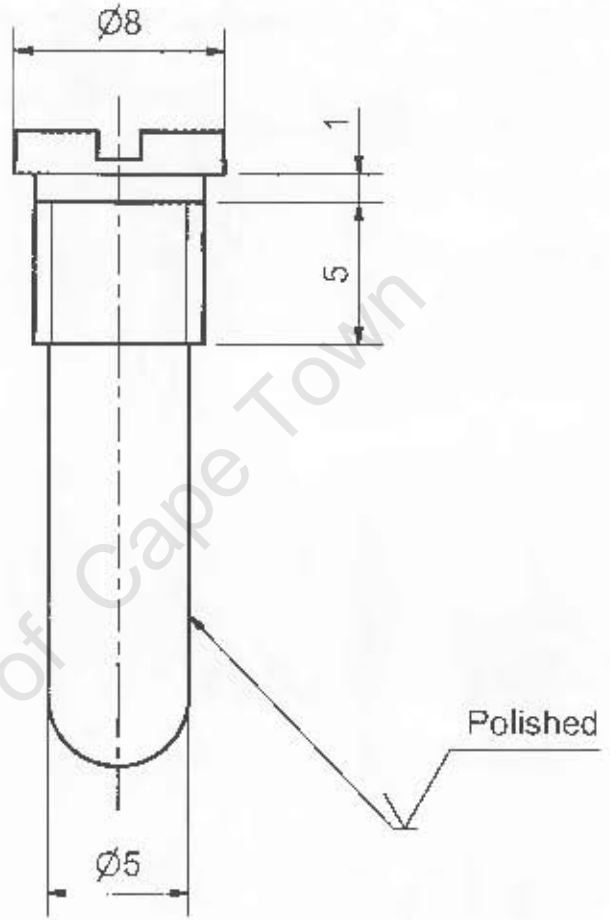

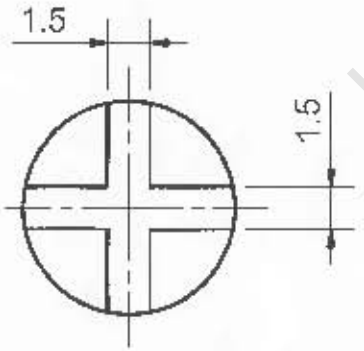

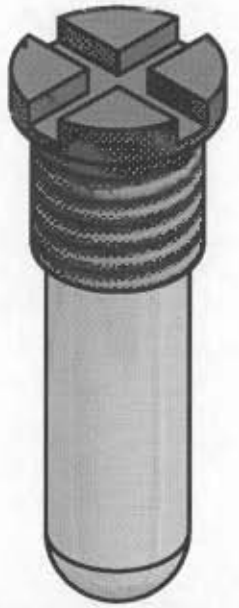

Tolerance Table (mm)	
0 - 5	+ 0.01 - 0.01
5 - 20	+ 0.05 - 0.05
20 - 200	+ 0.1 - 0.1
Angle	+ 0.05° - 0.05°

Part Description: Cemented Glenoid Peg		Material: Ti-6Al-4V		Quantity: 3	
Designed by: Greg Wessels	Date: 4/7/2005	Approved by: date	Signed	Units: mm	
University of Cape Town		Title: Hybrid-Screw TSR			
Department of Mechanical Engineering		Drawing Number: Full-01-03		Scale 4 : 1	

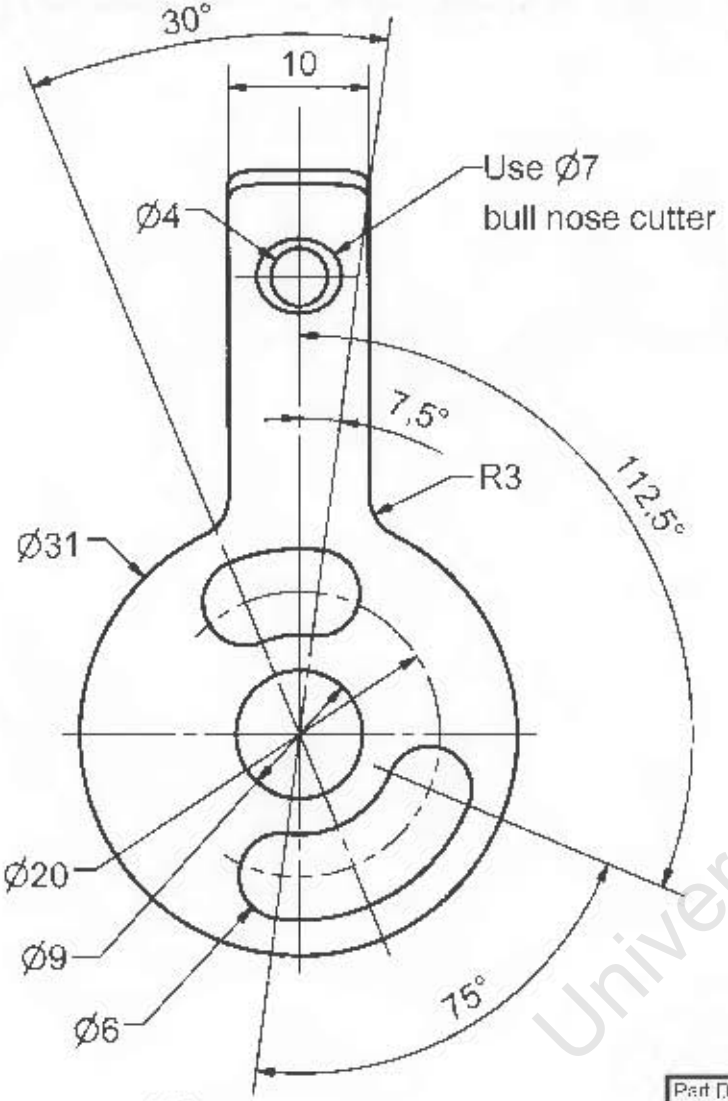

Tolerance Table (mm)	
0 - 5	+ 0.01 - 0.01
5 - 20	+ 0.05 - 0.05
20 - 200	+ 0.1 - 0.1
Angle	+ 0.05° - 0.05°

Part Description: Coracoid Plate		Material: Ti-6Al-4V		Quantity: 1	
Designed by: Greg Wessels	Date: 4/7/2005	Approved by - date:	Signed:	Units: mm	
University of Cape Town		Title: Hybrid-Screw TSR			
Department of Mechanical Engineering		Drawing Number: Full-01-04		Scale 2 : 1	

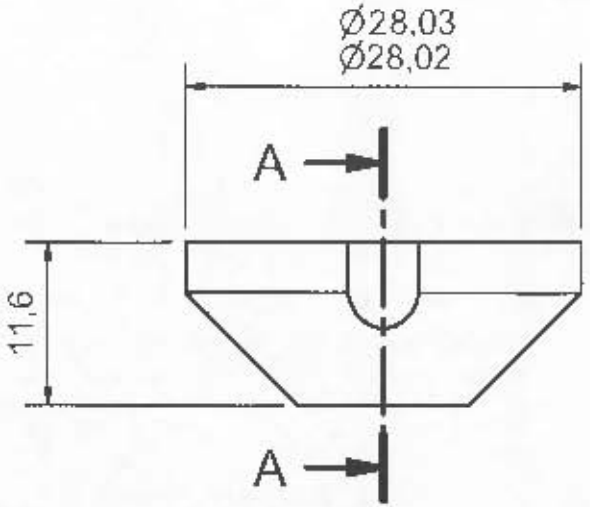

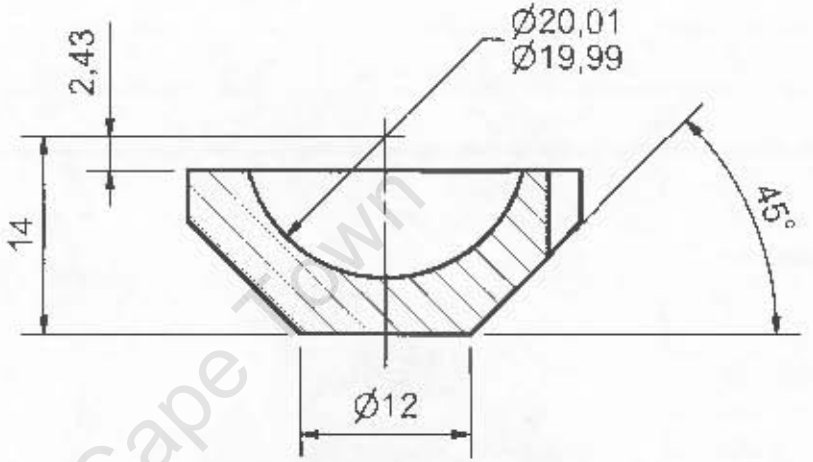

Section on A-A

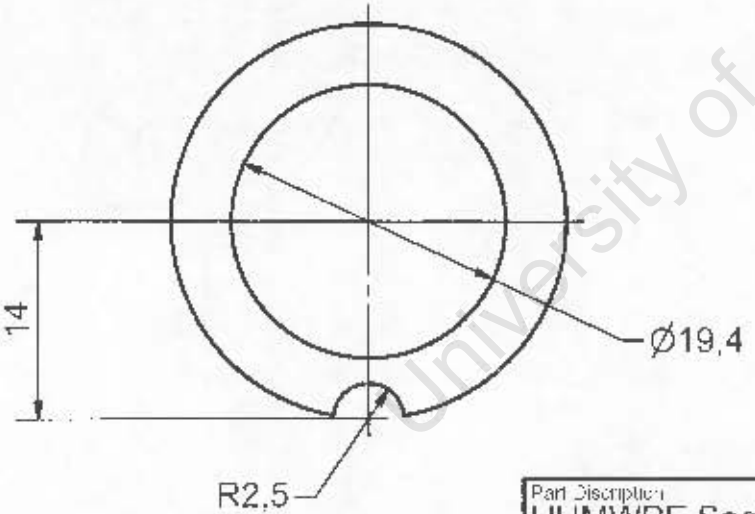

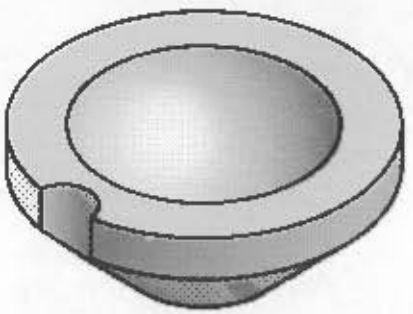

Tolerance Table (mm)	
0 - 5	+ 0.01 - 0.01
5 - 20	+ 0.05 - 0.05
20 - 200	+ 0.1 - 0.1
Angle	+ 0.05° - 0.05°

Part Description: UHMWPE Socket Bottom		Material: UHMWPE		Quantity: 1	
Designed by: Greg Wessels	Date: 4/7/2005	Approved by - date:	Signed	Units: mm	
University of Cape Town		Title: Hybrid-Screw TSR			
Department of Mechanical Engineering		Drawing Number: Full-01-05		Scale 2 : 1	

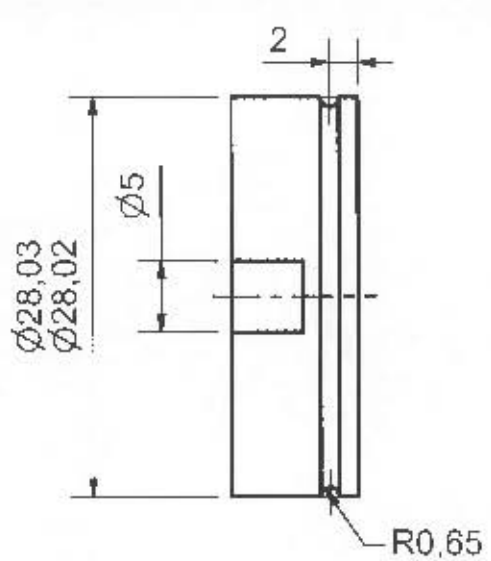

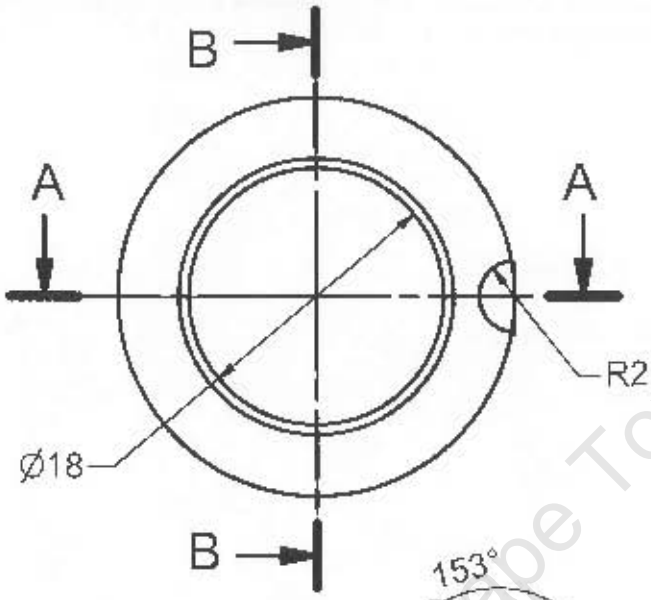

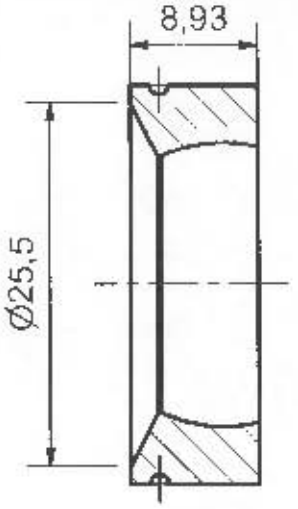

Section on B-B

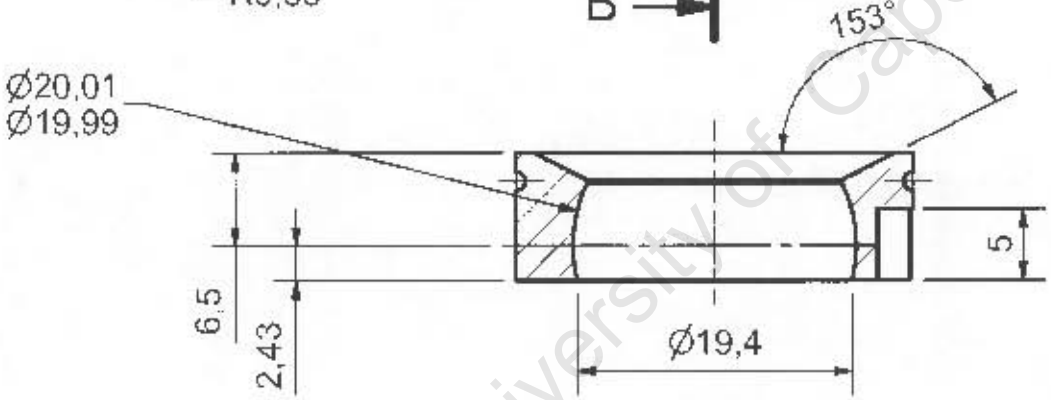

Section on A-A

Scale 1 : 1

Tolerance Table (mm)	
0 - 5	+ 0.01 - 0.01
5 - 20	+ 0.05 - 0.05
20 - 200	+ 0.1 - 0.1
Angle	+ 0.05° - 0.05°

Part Description: UHMWPE Socket Top		Material: UHMWPE		Quantity: 1	
Designed by: Greg Wessels	Date: 4/7/2005	Approved by - date	Signed	Units: mm	
University of Cape Town Department of Mechanical Engineering		Title: Hybrid-Screw TSR			
		Drawing Number: Full-01-06		Scale 2 : 1	

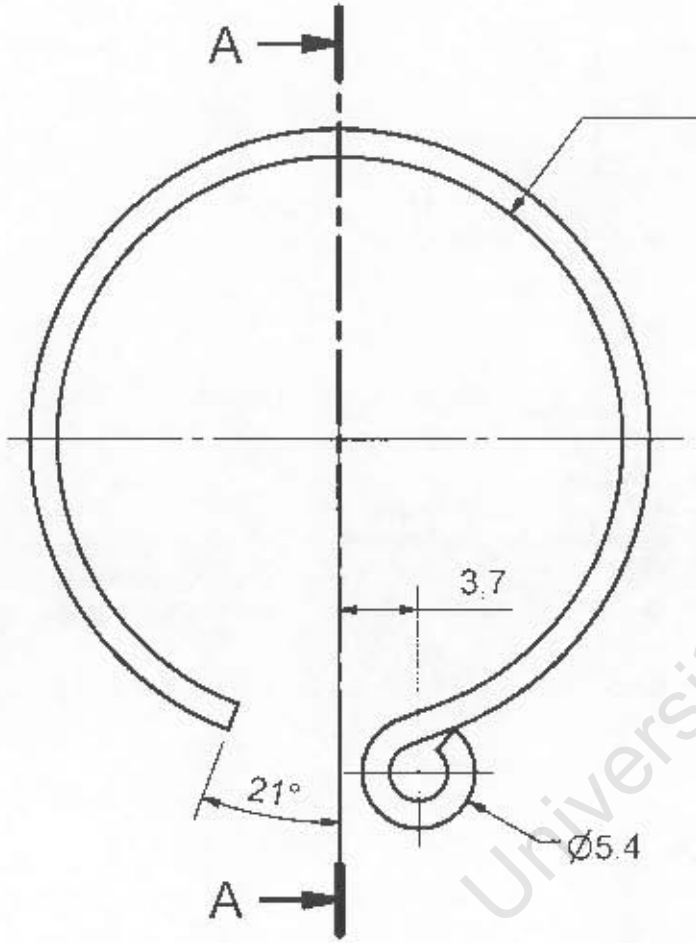

Section on A-A

Tolerance Table (mm)	
0 - 5	+ 0.01 - 0.01
5 - 20	+ 0.05 - 0.05
20 - 200	+ 0.1 - 0.1
Angle	+ 0.05° - 0.05°

Part Discription: Socket Locking Clip		Material: Ti-6Al-4V		Quantity: 1	
Designed by: Greg Wessels	Date: 4/7/2005	Approved by - date	Signed	Units: mm	

UNIVERSITY OF CAPE TOWN

DEPARTMENT OF MECHANICAL ENGINEERING

Title: Hybrid-Screw TSR

Drawing Number: Full-01-07

Scale 3 : 1

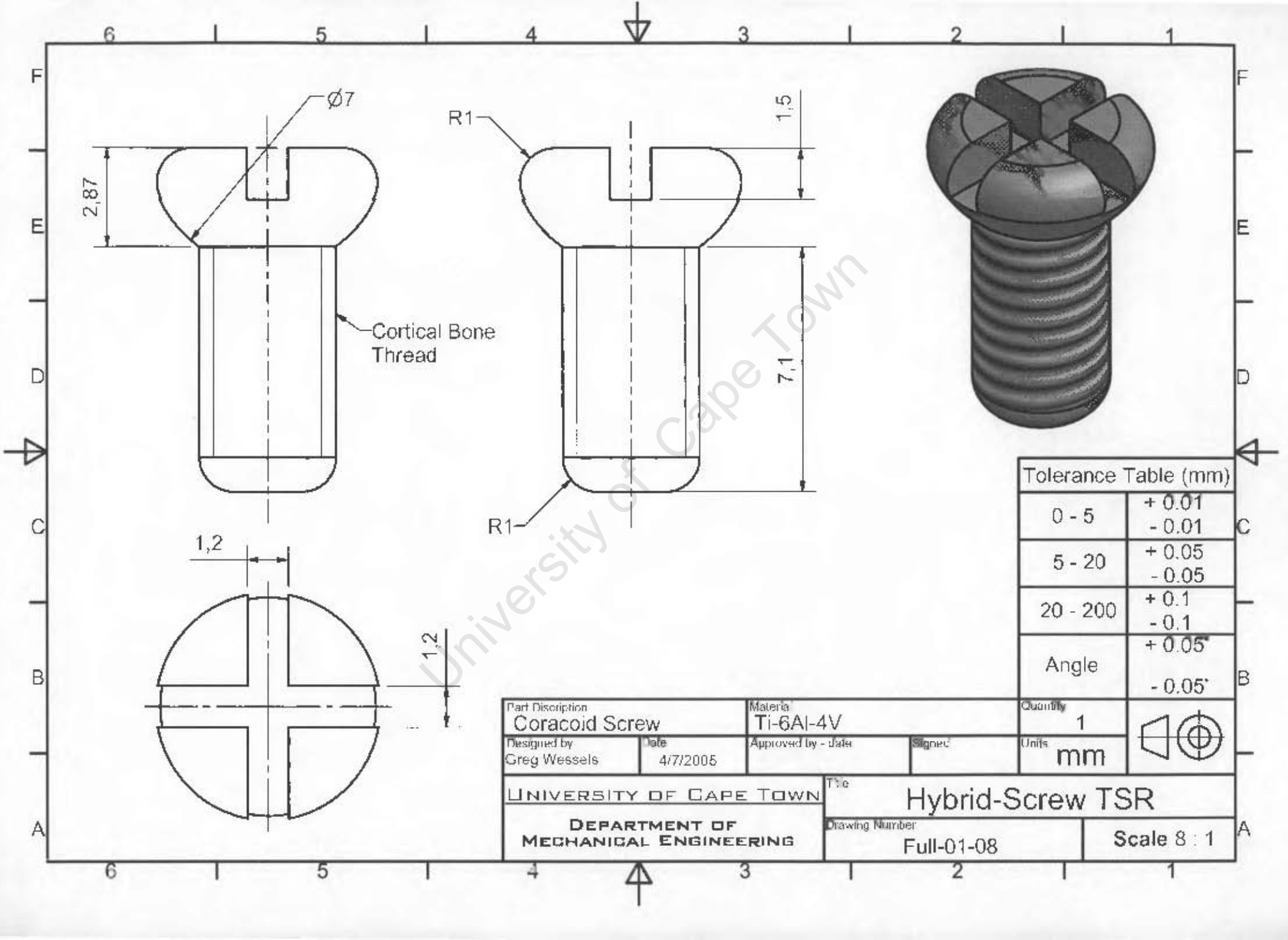

Tolerance Table (mm)	
0 - 5	+ 0.01 - 0.01
5 - 20	+ 0.05 - 0.05
20 - 200	+ 0.1 - 0.1
Angle	+ 0.05° - 0.05°

Part Discription: Coracoid Screw	Material: Ti-6Al-4V		Quantity: 1	
Designed by: Greg Wessels	Date: 4/7/2005	Approved by - date:	Signed:	Units: mm
University of Cape Town Department of Mechanical Engineering	Title: Hybrid-Screw TSR			
	Drawing Number: Full-01-08		Scale 8 : 1	

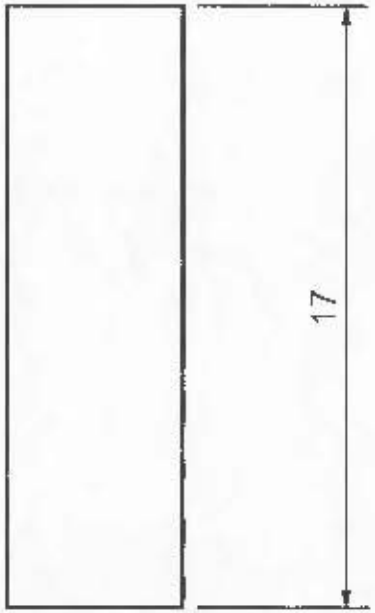

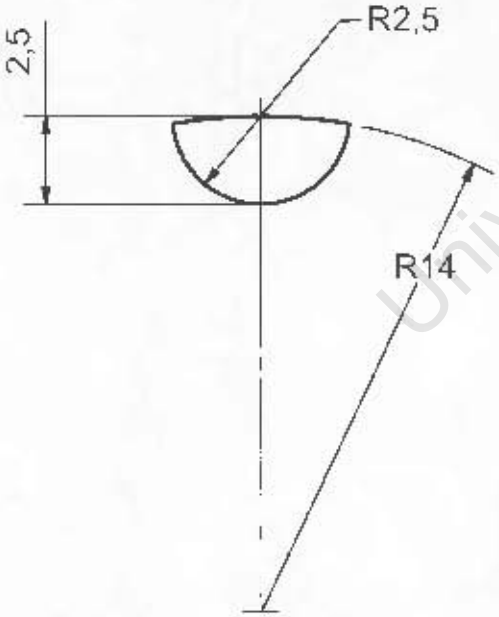

Tolerance Table (mm)	
0 - 5	+ 0.01 - 0.01
5 - 20	+ 0.05 - 0.05
20 - 200	+ 0.1 - 0.1
Angle	+ 0.05° - 0.05°

Part Discription: Peg Stop Rotation		Material: Ti-6Al-4V		Quantity: 1	
Designed by: Greg Wessels	Date: 4/7/2005	Approved by - date	Signed	Units: mm	
University of Cape Town		Title: Hybrid-Screw TSR			
Department of Mechanical Engineering		Drawing Number: Full-01-09		Scale 5 : 1	

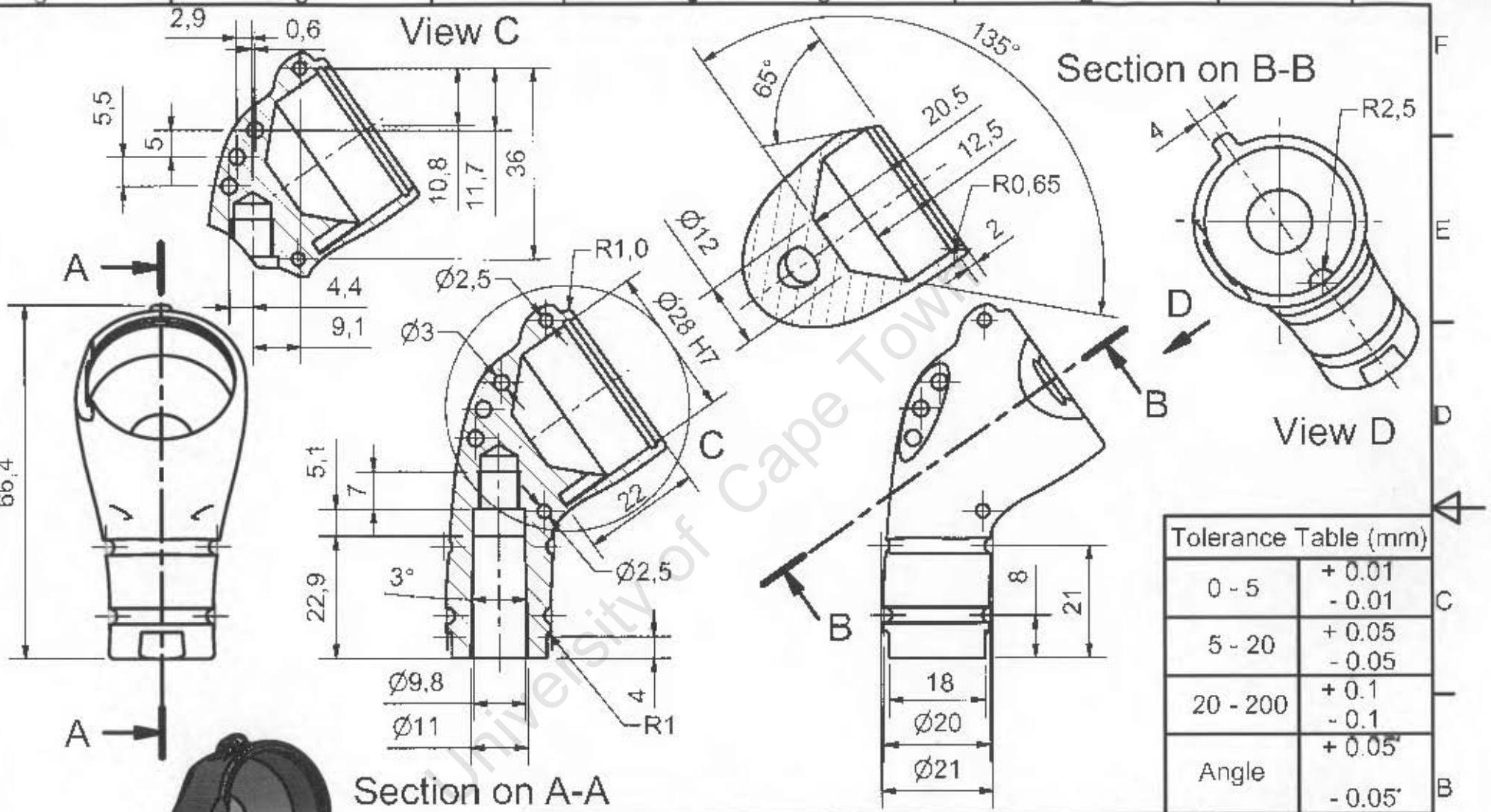

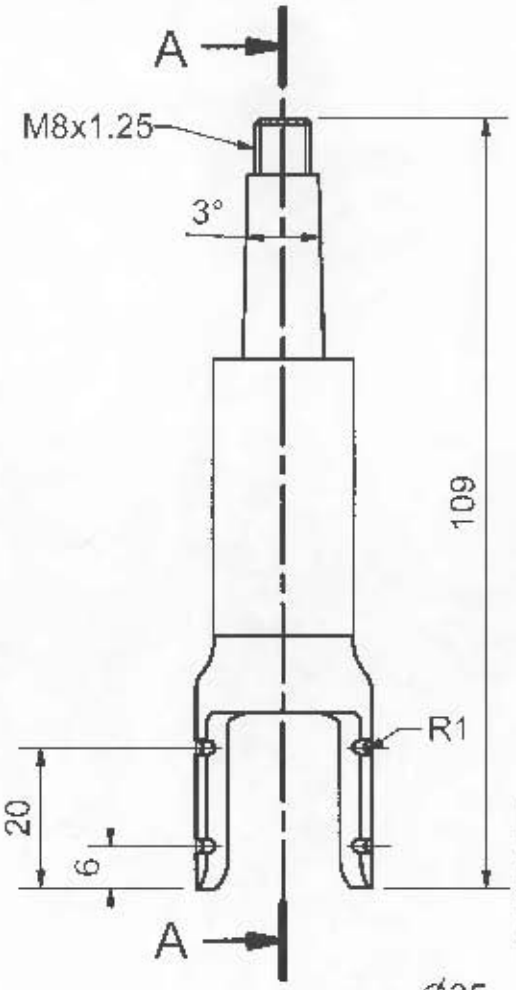

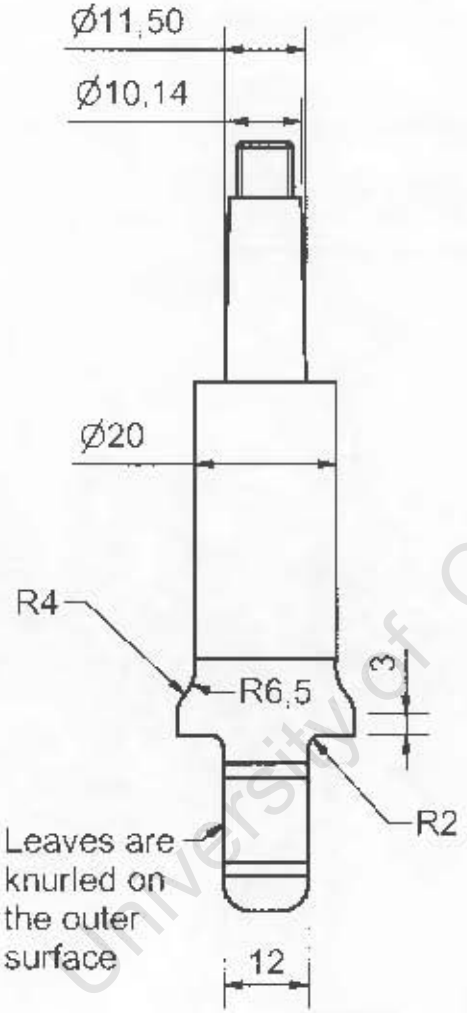

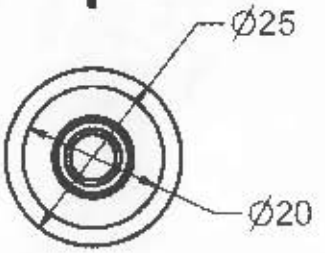

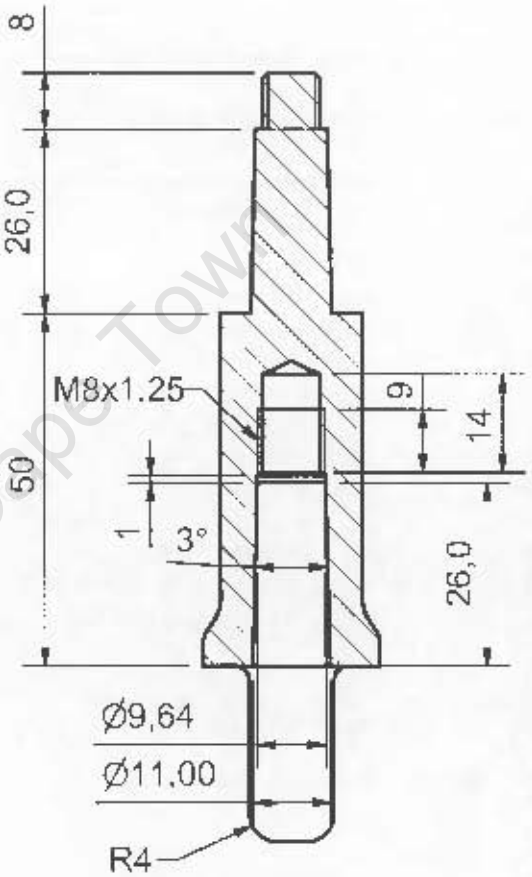

Section on A-A

Scale 1 : 1.25

Tolerance Table (mm)	
0 - 5	+ 0.01 - 0.01
5 - 20	+ 0.05 - 0.05
20 - 200	+ 0.1 - 0.1
Angle	+ 0.05° - 0.05°

Part Discription: Humeral Stem Extension		Material: Ti-6Al-4V		Quantity: 1	
Designed by: Greg Wessels	Date: 4/7/2005	Approved by: date	Signed	Units: mm	
UNIVERSITY OF CAPE TOWN		Title: Hybrid-Screw TSR			
DEPARTMENT OF MECHANICAL ENGINEERING		Drawing Number: Full-01-11		Scale: 1:1	

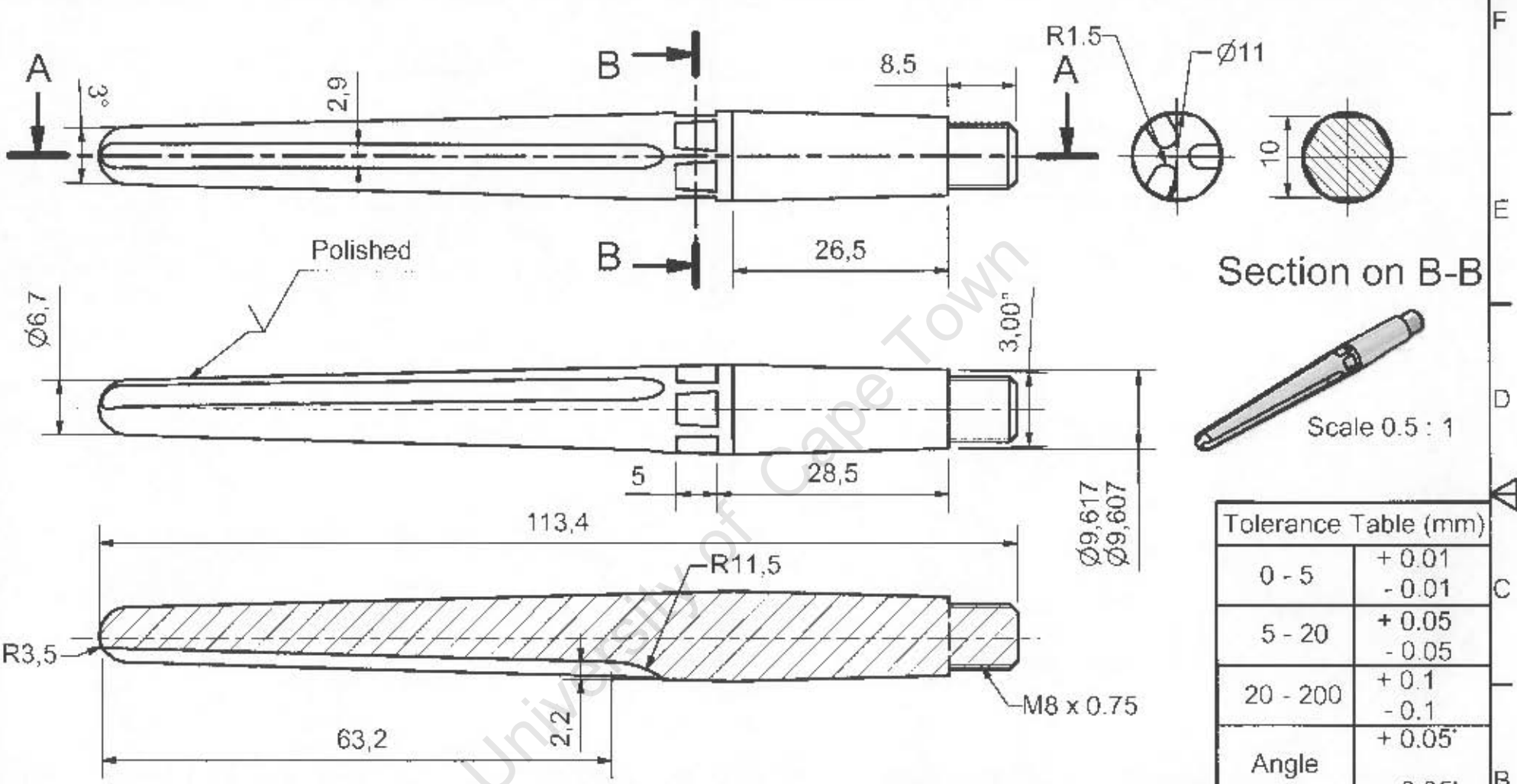

Tolerance Table (mm)	
0 - 5	+ 0.01 - 0.01
5 - 20	+ 0.05 - 0.05
20 - 200	+ 0.1 - 0.1
Angle	+ 0.05° - 0.05°

Part Discription: Humeral Stem		Material: Ti-6Al-4V		Quantity: 1	
Designed by: Greg Wesse s	Date: 4/7/2005	Approved by - date:	Signed:	Units: mm	
UNIVERSITY OF CAPE TOWN DEPARTMENT OF MECHANICAL ENGINEERING		Title: Hybrid-Screw TSR			
		Drawing Number: Full-01-12		Scale 1.5 : 1	

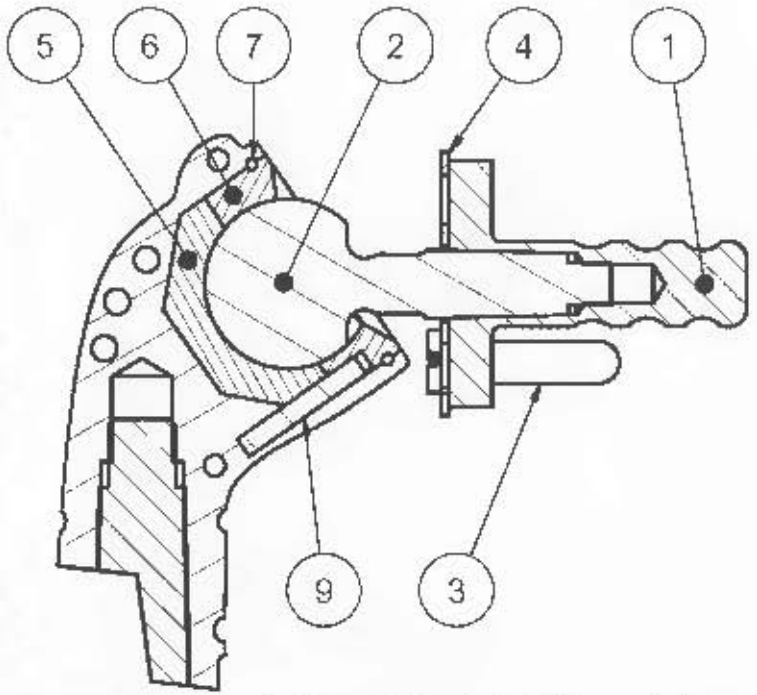

View B (1.20 : 1)

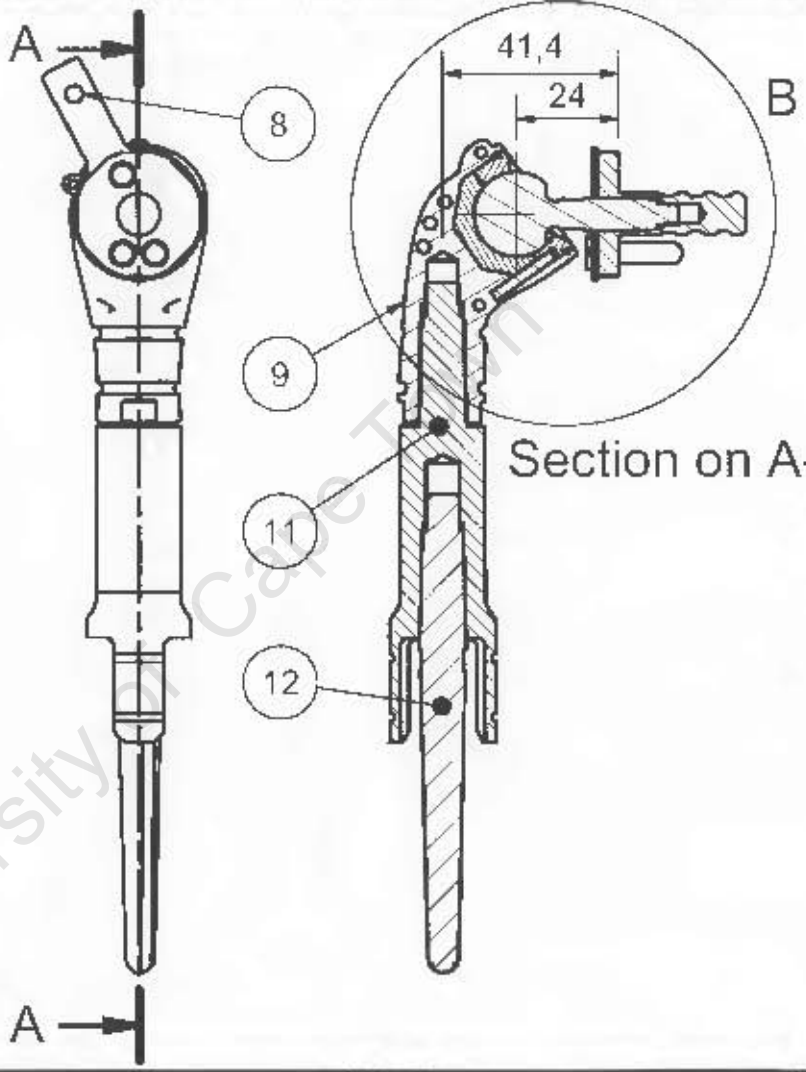

Section on A-A

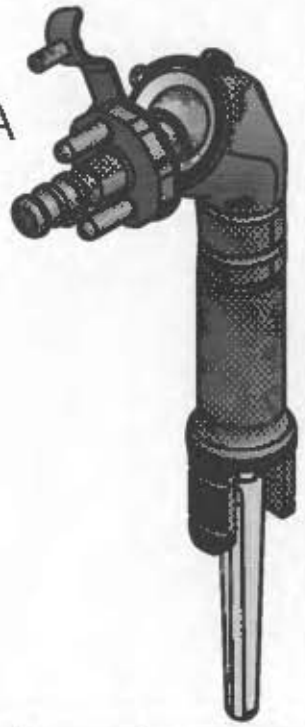

No#	Part Discription	Items	Drawing No#
1	Glenoid Central Peg	1	Full-02-01
2	Ball and Tapered Stem	1	Full-01-02
3	Cemented Glenoid Peg	3	Full-01-03
4	Coracoid Plate	1	Full-01-04
5	UHMWPE Socket Bottom	1	Full-01-05
6	UHMWPE Socket Top	1	Full-01-06
7	Socket Locking Clip	1	Full-01-07
8	Coracoid Screw	1	Full-01-08
9	Peg Stop Rotation	1	Full-01-09
10	Humeral Housing	1	Full-01-11
11	Humeral Stem Extension	1	Full-01-10
12	Humeral Stem	1	Full-01-12

Part Discription: Assembly		Material: Co-Cr-Mo, Ti, UHMWPE		Quantity: 1
Designed by: Greg Wessels	Date: 4/26/2005	Approved by - date:	Signed:	Units: mm

UNIVERSITY OF CAPE TOWN
DEPARTMENT OF MECHANICAL ENGINEERING

Title: Central-Peg TSR

Drawing Number: Full-02-00

Scale 1:1.66

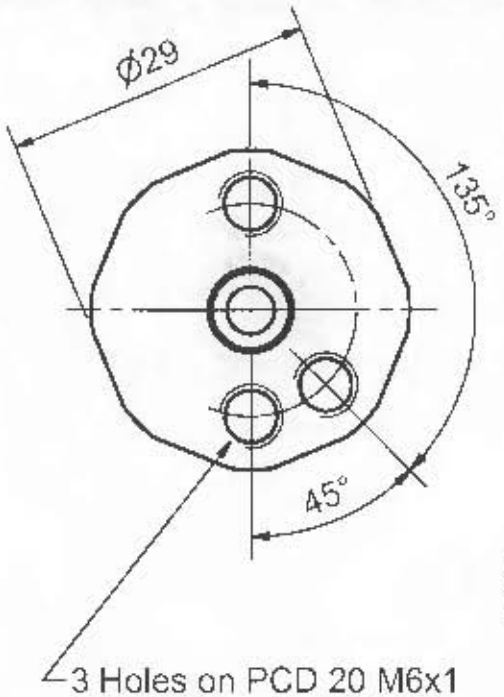

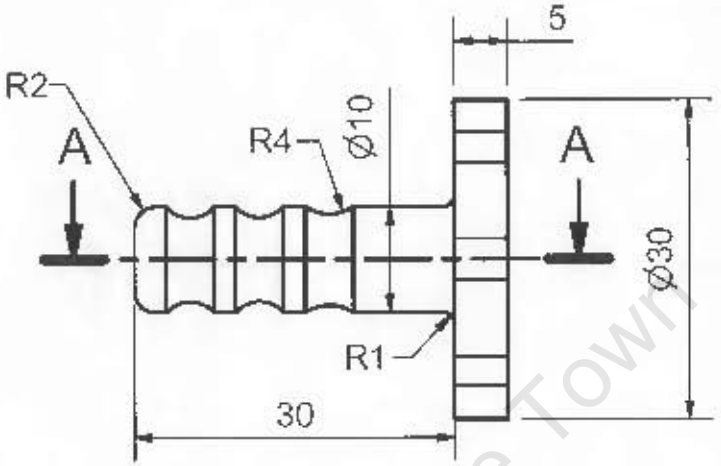

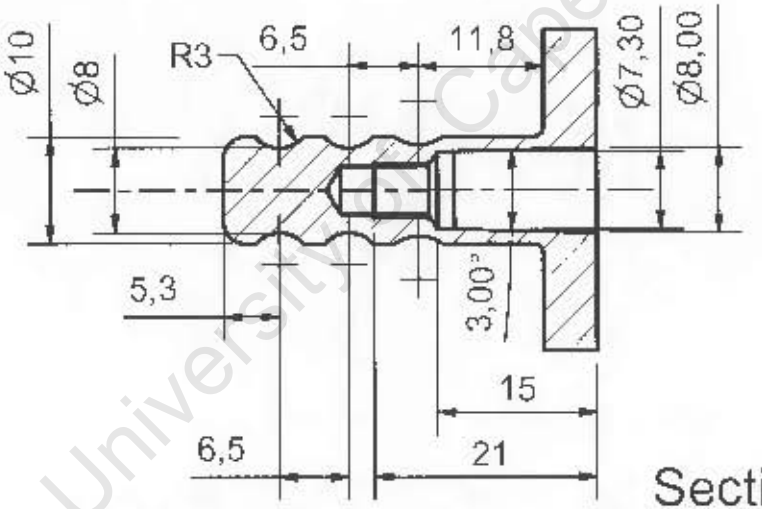

Section on A-A

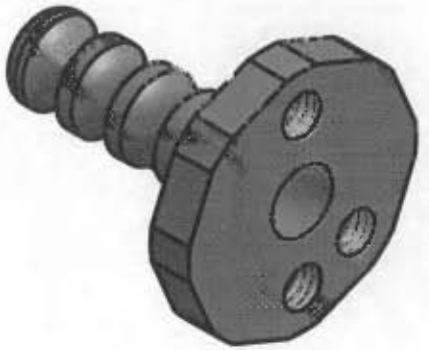

Tolerance Table (mm)	
0 - 5	+ 0.01 - 0.01
5 - 20	+ 0.05 - 0.05
20 - 200	+ 0.1 - 0.1
Angle	+ 0.05° - 0.05°

Part Description: Glenoid Central Peg		Material: Ti-6Al-4V		Quantity: 1	
Designed by: Greg Wessels	Date: 4/7/2005	Approved by - date	Signed	Units: mm	
UNIVERSITY OF CAPE TOWN		Title: Central-Peg TSR			
DEPARTMENT OF MECHANICAL ENGINEERING		Drawing Number: Full-02-01		Scale 1.5:1	

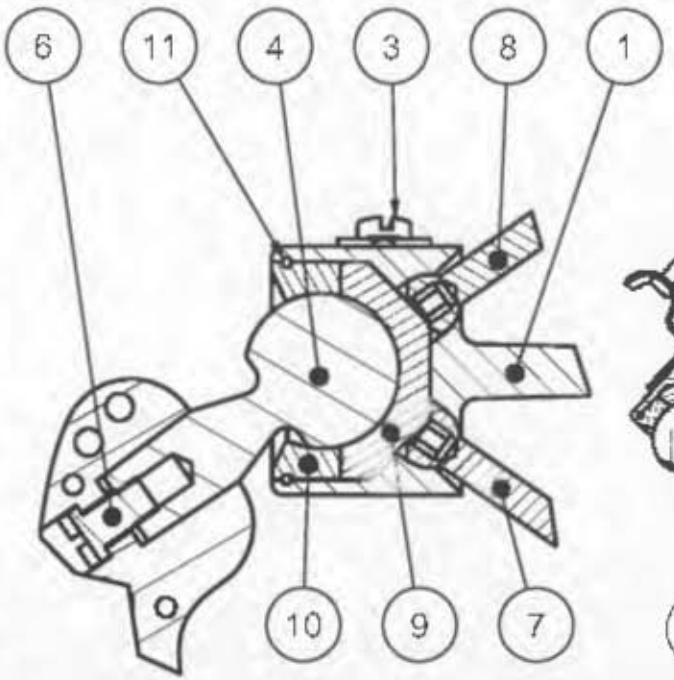

View B

Section on C-C

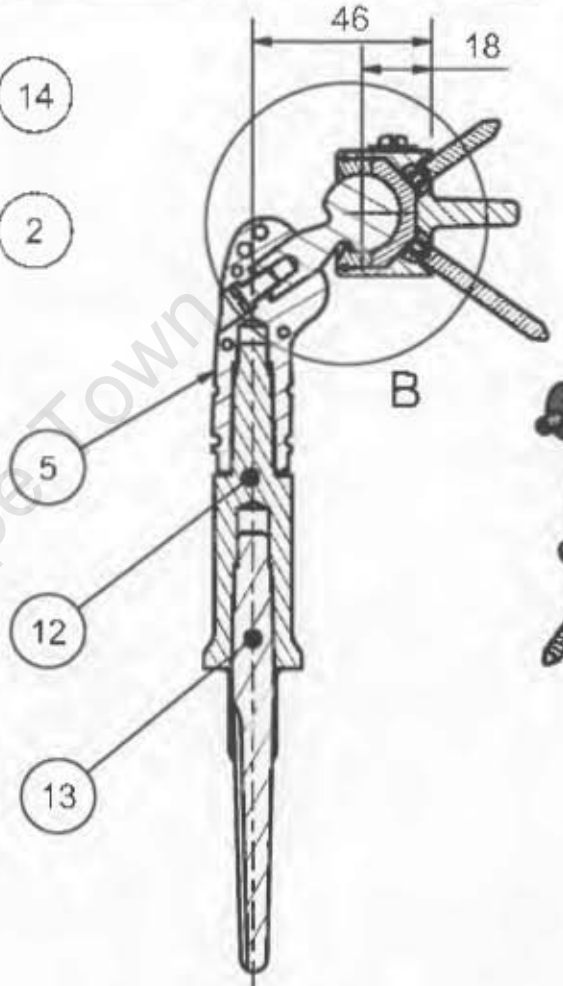

Section on A-A

No#	Part Discription	Items	Drawing No#
1	Housing	1	Full-03-01
2	Coracoid Plate	1	Full-03-02
3	Housing Screw	2	Full-03-03
4	Ball and Stem	1	Full-03-04
5	Humeral Component	1	Full-03-05
6	Ball Locking Screw	1	Full-03-06
7	40mm Cortical Screw	1	ASTM
8	30mm Cortical Screw	1	ASTM
9	UHMWPE Socket Bottom	1	Full-01-05
10	UHMWPE Socket Top	1	Full-01-06
11	Socket Locking Clip	1	Full-01-07
12	Humeral Stem Extension	1	Full-01-11
13	Humeral Stem	1	Full-01-12
14	Coracoid Screw	1	Full-01-08
15	Peg Stop Rotation	1	Full-01-09

Part Discription: Assembly		Material: Co-Cr-Mo, Ti, UHMWPE		Quantity: 1
Designed by: Greg Wessels	Date: 4/26/2005	Approved by: date	Signed	Units: mm

UNIVERSITY OF CAPE TOWN

DEPARTMENT OF MECHANICAL ENGINEERING

Title: Quad-Point TSR

Drawing Number: Full-03-00

Scale 1:1.66

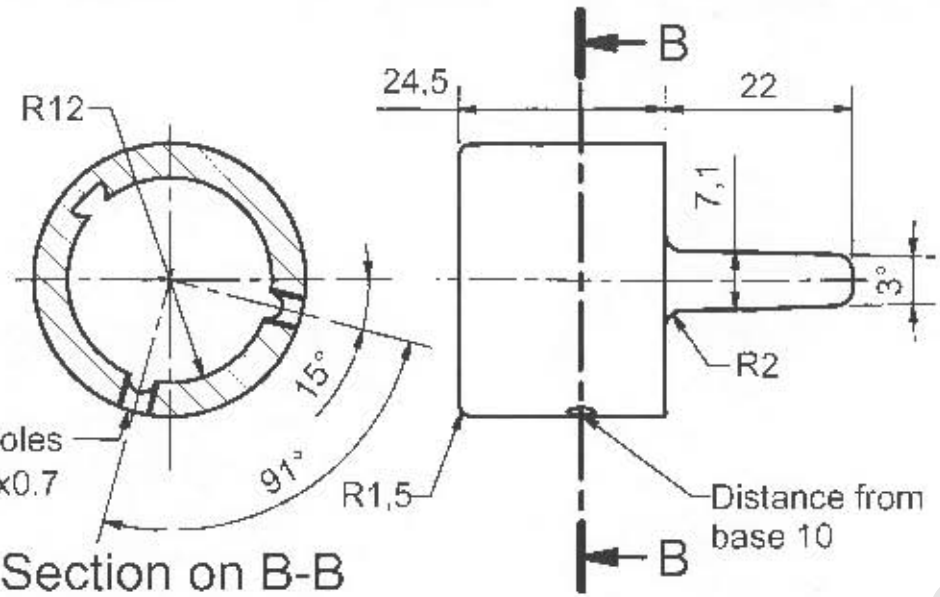

Section on B-B

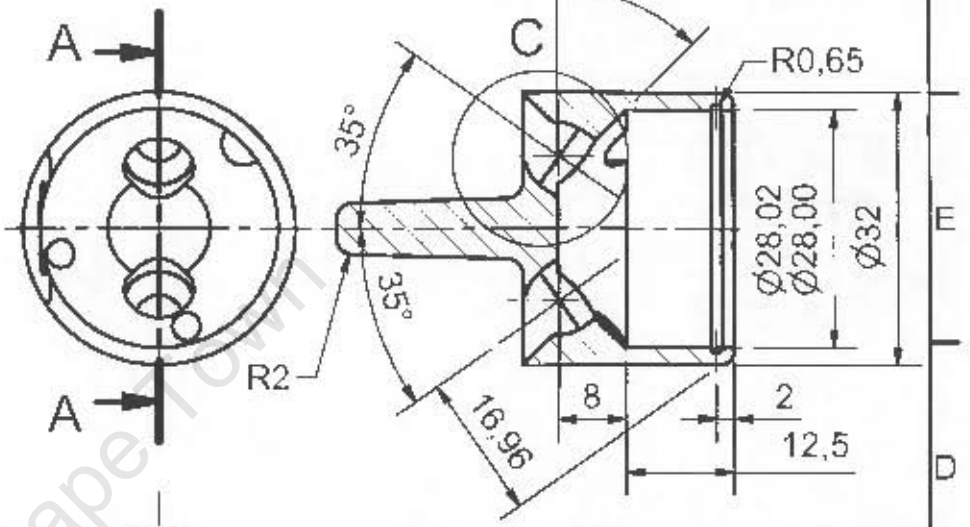

Section on A-A

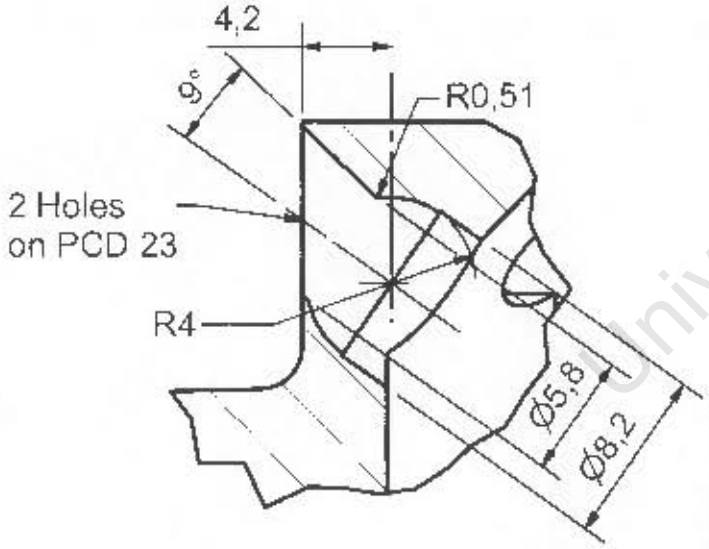

View C (3 : 1)

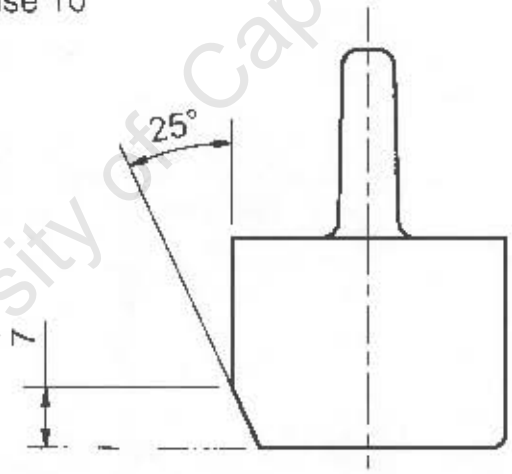

Scale 1 : 2

Tolerance Table (mm)	
0 - 5	+ 0.01 - 0.01
5 - 20	+ 0.05 - 0.05
20 - 200	+ 0.1 - 0.1
Angle	+ 0.05° - 0.05°

Part Discription: Housing		Material: Ti-6A-I4V		Quantity: 1	
Designed by: Greg Wesse s	Date: 4/7/2009	Approved by: date	Signed	Units: mm	

UNIVERSITY OF CAPE TOWN

DEPARTMENT OF MECHANICAL ENGINEERING

Title: Quad-Point TSR

Drawing Number: Full-03-01

Scale 1.5:1

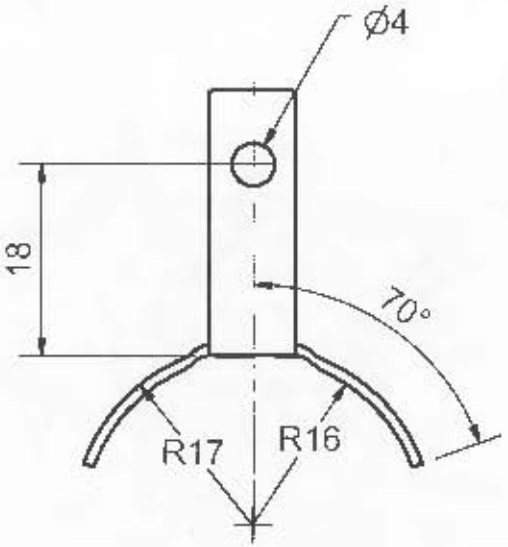

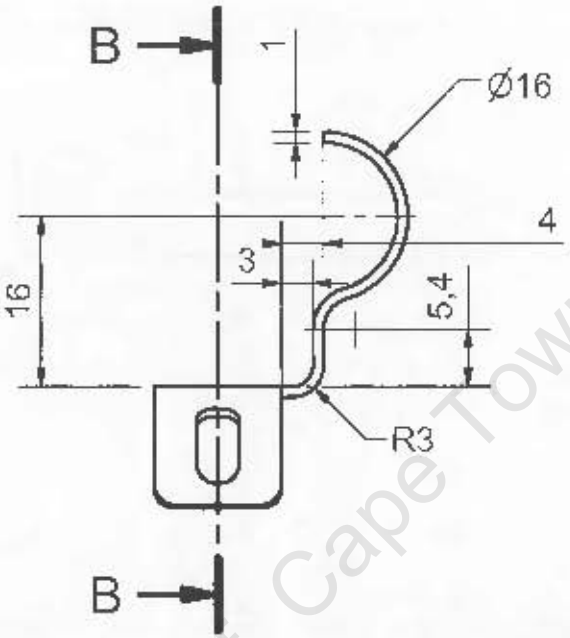

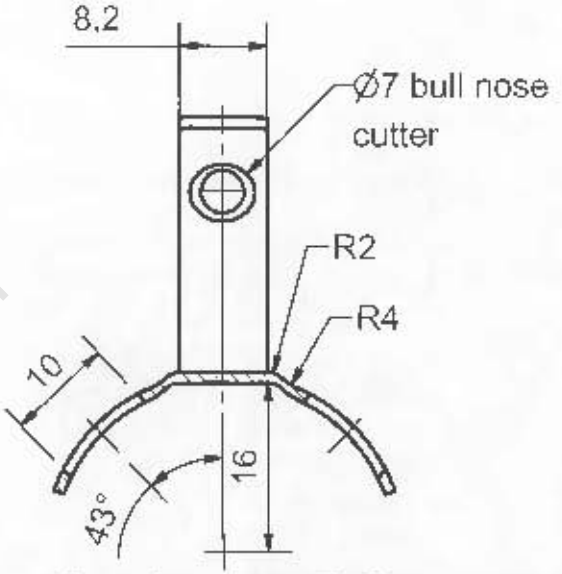

Section on B-B

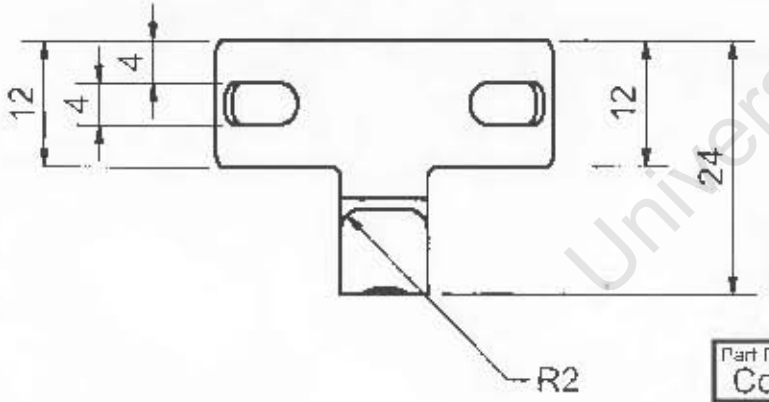

Tolerance Table (mm)	
0 - 5	+ 0.01 - 0.01
5 - 20	+ 0.05 - 0.05
20 - 200	+ 0.1 - 0.1
Angle	+ 0.05° - 0.05°

Part Discription: Coracoid Plate		Material: Ti-6Al-4V		Quantity: 1	
Designed by: Greg Wessels	Date: 4/7/2005	Approved by: date	Signed	Units: mm	

UNIVERSITY OF CAPE TOWN

DEPARTMENT OF MECHANICAL ENGINEERING

Title: Quad-Point TSR

Drawing Number: Full-03-02

Scale 1.5:1

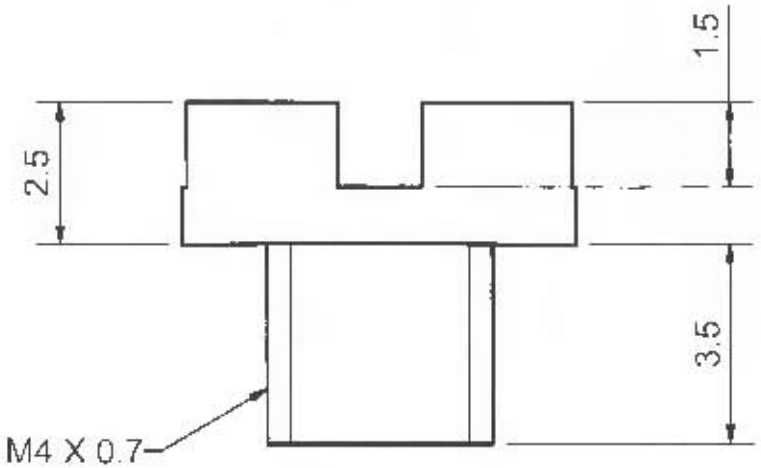

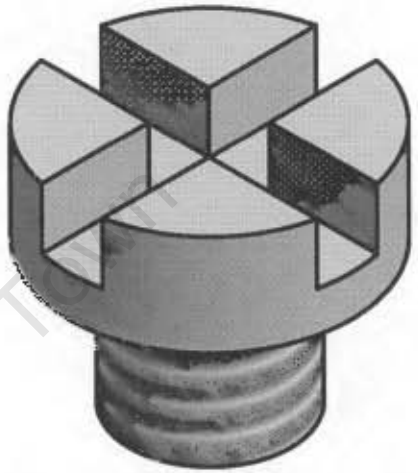

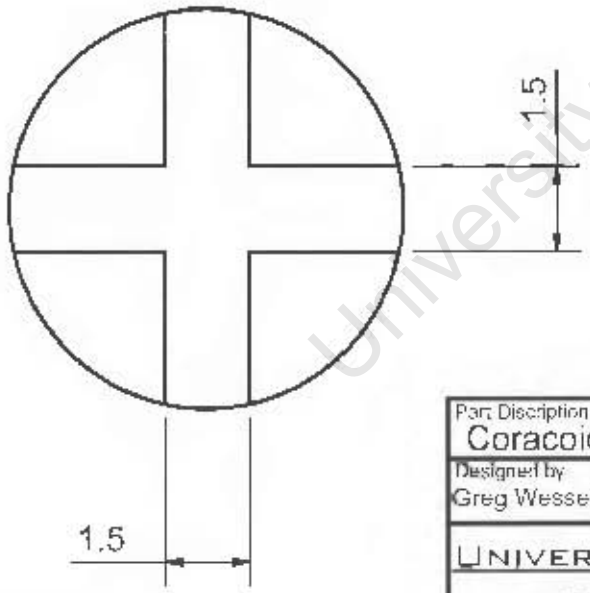

Tolerance Table (mm)	
0 - 5	+ 0.01 - 0.01
5 - 20	+ 0.05 - 0.05
20 - 200	+ 0.1 - 0.1
Angle	+ 0.05° - 0.05°

Part Description: Coracoid Plate Screw		Material: Ti-6Al-4V		Quantity: 2	
Designed by: Greg Wessels	Date: 4/7/2005	Approved by - date:	Signed:	Units: mm	
University of Cape Town		Title: Quad-Point TSR			
Department of Mechanical Engineering		Drawing Number: Full-03-03		Scale 8 : 1	

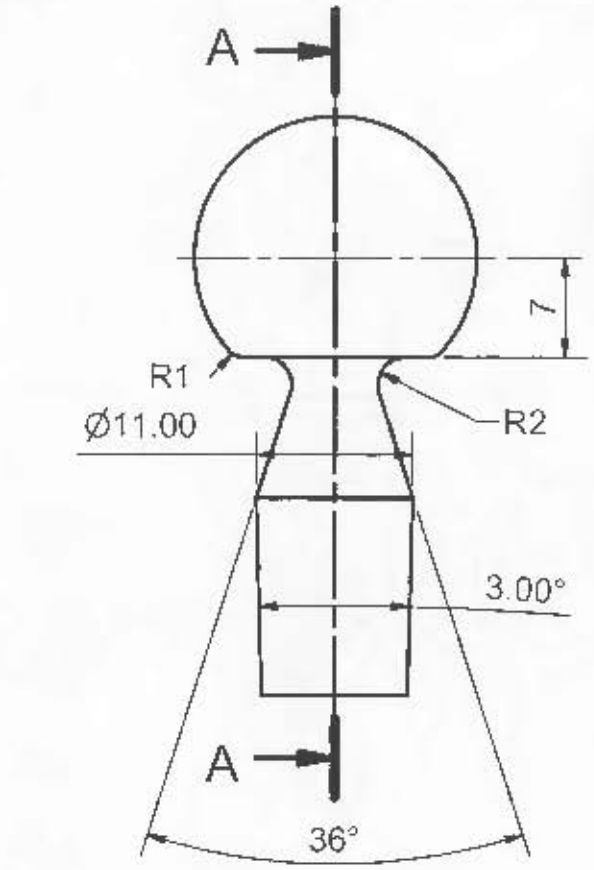

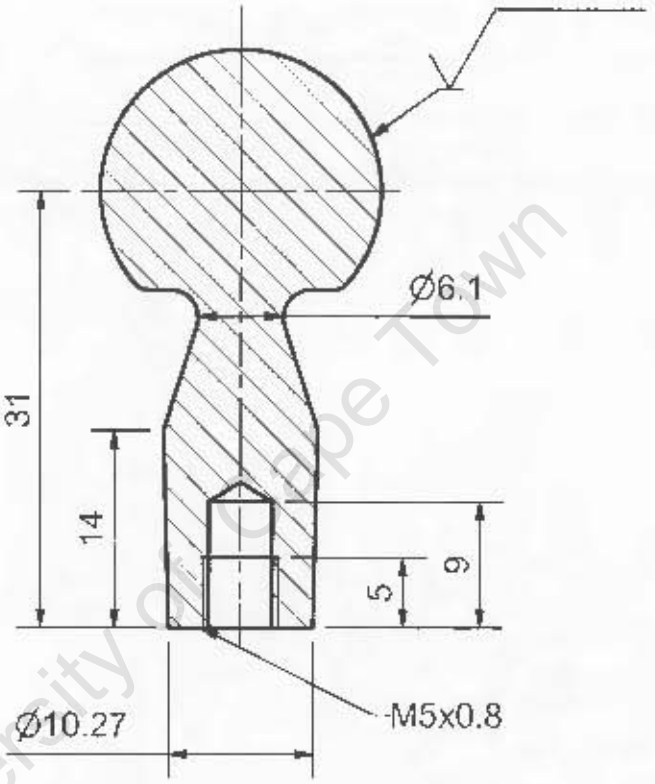

Section on A-A

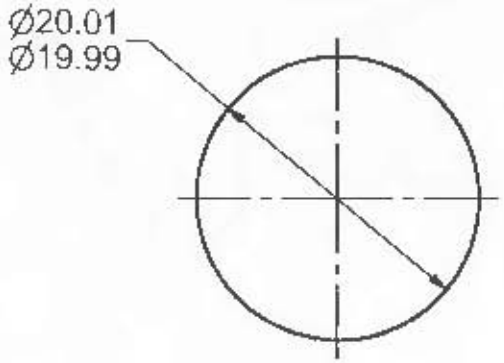

Tolerance Table (mm)	
0 - 5	+ 0.01 - 0.01
5 - 20	+ 0.05 - 0.05
20 - 200	+ 0.1 - 0.1
Angle	+ 0.05° - 0.05°

Part Discription: Ball and Stem		Material: Co-Cr-Mo		Quantity: 1	
Designed by: Greg Wessels	Date: 4/7/2005	Approved by: date	Signed	Units: mm	
University of Cape Town		Title: Quad-Point TSR			
Department of Mechanical Engineering		Drawing Number: Full-03-04		Scale 2 : 1	

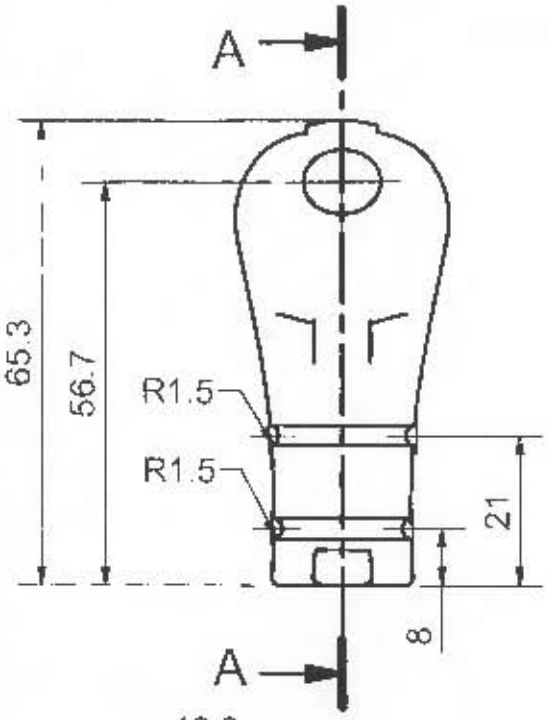

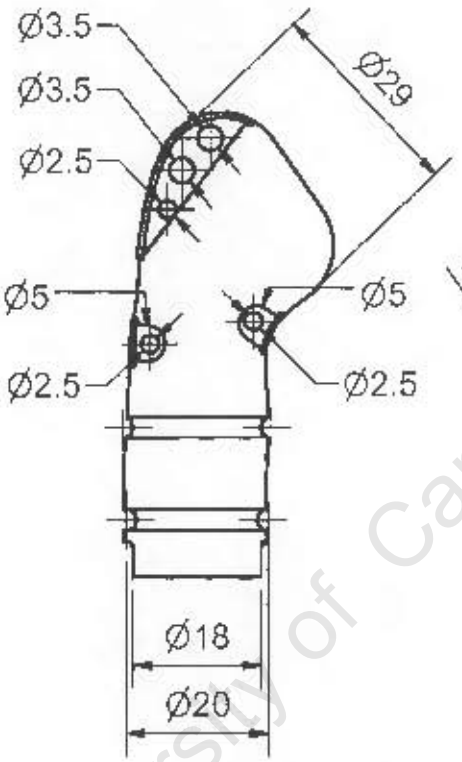

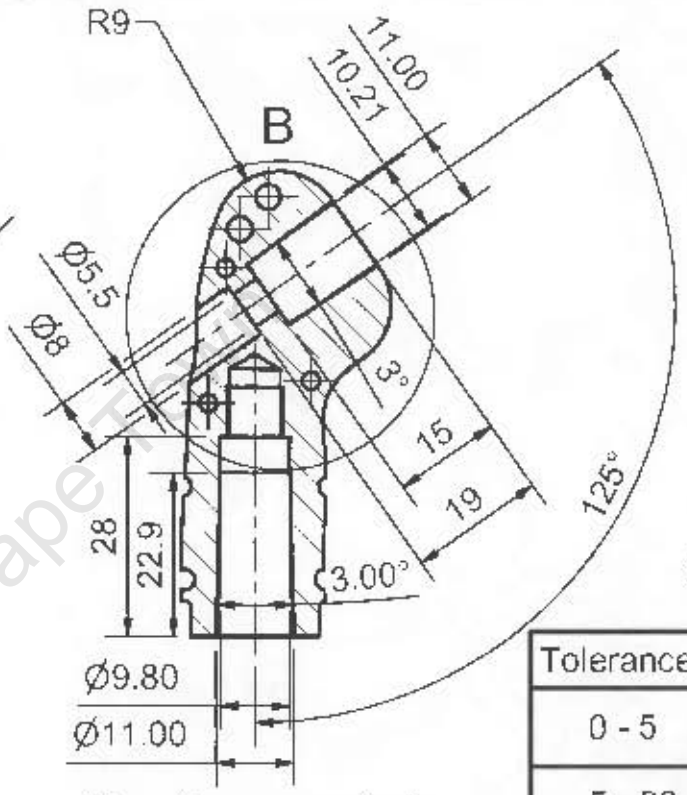

Section on A-A

Scale 1 : 2

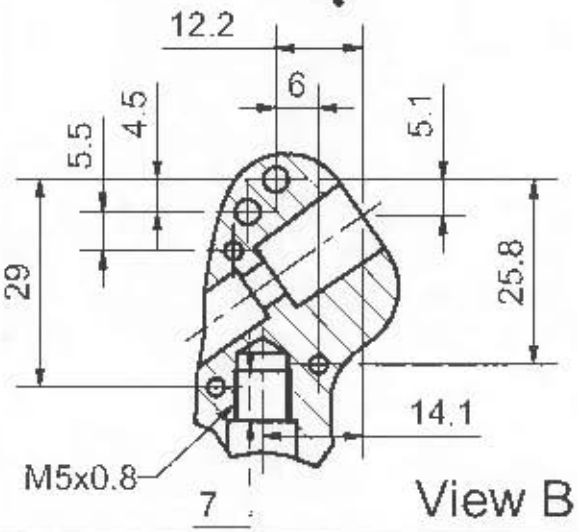

View B

Tolerance Table (mm)	
0 - 5	+ 0.01 - 0.01
5 - 20	+ 0.05 - 0.05
20 - 200	+ 0.1 - 0.1
Angle	+ 0.05° - 0.05°

Part Discription: Humeral Component		Material: Ti-6Al-4V		Quantity: 1	
Designed by: Greg Wessels	Date: 4/7/2005	Approved by - date	Signed	Units: mm	
UNIVERSITY OF CAPE TOWN DEPARTMENT OF MECHANICAL ENGINEERING		Title: Quad-Point TSR			
		Drawing Number: Full-03-05		Scale 1 : 1	

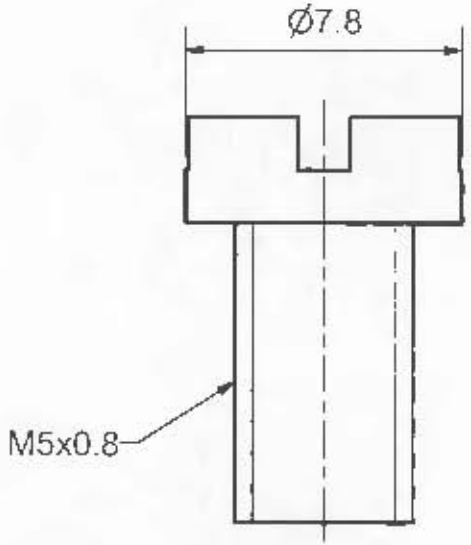

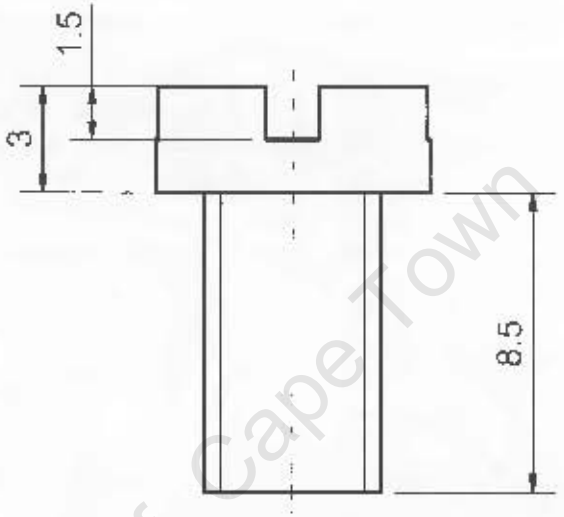

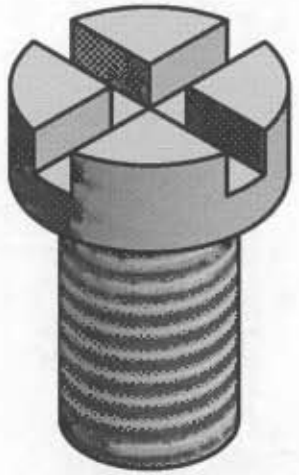

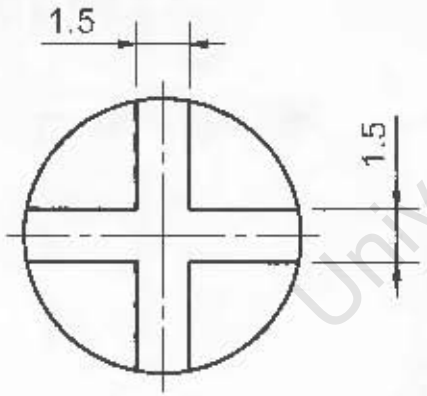

Tolerance Table (mm)	
0 - 5	+ 0.01 - 0.01
5 - 20	+ 0.05 - 0.05
20 - 200	+ 0.1 - 0.1
Angle	+ 0.05° - 0.05°

Part Description: Ball Locking Screw		Material: Ti-6Al-4V		Quantity: 1	
Designed by: Greg Wessels	Date: 4/7/2005	Approved by: date	Signed	Units: mm	
University of Cape Town Department of Mechanical Engineering		Title: Quad-Point TSR			
		Drawing Number: Full-03-06		Scale 5 : 1	